

Ground source energy in crystalline bedrock - increased energy extraction by using hydraulic fracturing in boreholes

Randi Kalskin Ramstad

November 2004

Department of Geology and Mineral Resources Engineering
Faculty of Engineering Science and Technology
Norwegian University of Science and Technology

Dissertation submitted of the requirements for the Norwegian academic degree
Doktor ingeniør

Summary

The use of improved equipment and methodology can result in considerable reductions in the drilling costs for medium- to large sized ground source heat pump system in crystalline bedrock. The main point has been to use special techniques within hydraulic fracturing to create a larger heat exchange area in the bedrock, and thus a greater energy extraction per borehole. The energy extraction is based on circulating groundwater.

Stimulation with hydraulic fracturing is a well known technique in order to improve borehole yields for drinking water-, oil-, and geothermal purposes. A procedure for injection of propping agents in selected borehole sections, and custom-made equipment for hydraulic fracturing in crystalline bedrock, a double packer, have been developed in this study. The propping agents are likely to ensure a permanent improvement of the hydraulic conductivity in a long-run perspective.

In addition to a pre-test, a comprehensive test programme has been performed at each of the two pilot plants at Bryn and at the former property of Energiselskapet Asker og Bærum (EAB) in Bærum municipality outside Oslo, Norway. A total of 125 stimulations with hydraulic fracturing using water-only and hydraulic fracturing with injection of sand have been performed in 9 boreholes. Test pumping and geophysical logging (temperature, electrical conductivity, gamma radiation, optical televiewer and flow measurements) have been carried out in order to document the effect of the hydraulic fracturing.

The pilot plants at Bryn and EAB, where the ground source heat pump systems are based on circulating groundwater, have demonstrated the short-period energy extraction, limitations and opportunities of the concept for hydraulic fracturing and increased energy extraction in different geological and hydrogeological areas. The bedrock at Bryn and EAB is characterized as a low-metamorphic sandstone and a nodular limestone, respectively. At Bryn, the five boreholes were organised with a central borehole encircled by four satellite boreholes 13 metres away from the central borehole. The central borehole at EAB was flanked with two boreholes 16 and 20 metres away. In operation mode, groundwater was pumped from the satellite boreholes, heat exchanged, and re-injected into the groundwater magazine via the central borehole. Routine operation of the plants has not yet been initiated.

The main findings from this study can be summarized as follows:

- Hydraulic fracturing with water-only results in an overall increase in water yield for the hard rock borehole.
- Hydraulic fracturing with injection of sand as propping agent also leads to an increased water yield.
- The use of sand as propping agent seems to be more required in fractures with high counter pressure, in this study higher than approximately 40 bars, compared with fractures with lower counter pressure. The particle size of the sand should also be adjusted to the appearing counter pressure, and injection of coarser sand is recommended in fractures with lower counter pressures.
- Comparing the results from the hydraulic fracturing performed at Bryn and EAB shows that the pressure levels, required to create new fractures, varied

considerably. The maximum pressures present at Bryn were higher than the corresponding pressures at EAB. At Bryn 70% (44 out of 63) of the pressure-time curves from the hydraulic fracturing with water-only were interpreted as initiation or reopening of fractures, while the number for EAB was 97% (36 out of 37). The lower degree of fracturing at Bryn is likely to be a result of high rock stresses and high tensile strength of the bedrock, also confirmed by the results from the rock stress measurements performed at Bryn. Considering the bedrock at EAB, characterized as nodular limestone, the tensile strength is assumed to be less than the values for the low-metamorphic sandstone present at Bryn.

- The infiltration rate in the central boreholes is a critical factor for the energy extraction and a successful operation of ground source heat pump systems based on circulating groundwater. Results from the short-period circulation tests accomplished at Bryn and EAB show that the infiltration rate in the central borehole at Bryn (approximately 2500 litres/hour) was too low to obtain a satisfactory operation of the plant, while the infiltration rate at EAB (14000 litres/hour) was sufficient to achieve profitability. Under the actual conditions, a reduction in the construction costs, i.e. the drilling costs, for a conventional ground source heat pump system with single U-collectors in vertical boreholes, of more than 50% were achieved for the pilot plant at EAB when the energy extraction from water is more than 105 MWh. The large difference in the infiltration rate between Bryn and EAB was probably related to: (1) Large initial differences in the borehole yield prior to hydraulic fracturing (<560 litres/hour at Bryn and >6300 litres/hour at EAB). Nodular limestone generally has high permeability, while compact sandstone rocks are expected to have low permeability. (2) Hydraulic fracturing was most successful at EAB. (3) The higher rock stress level present at Bryn compared to EAB will increase the tendency to tighten the opened fractures, even the fractures with injected sand.
- The FEFLOW-modelling of the pilot plant at Bryn and EAB emphasized the important relation between the available heat exchange area in the bedrock, the thermal conductivity of the bedrock, and the energy potential.
- The increased borehole yields achieved by hydraulic fracturing in this study, and the improved, reliable and cost-effective hydraulic fracturing techniques in crystalline bedrock, will probably increase the interest for groundwater as a domestic water supply for small- to medium sized water works.

Acknowledgements

The present thesis has been carried out at the Department of Geology and Mineral Resources Engineering at the Norwegian University of Science and Technology (NTNU) and at the Geological Survey of Norway (NGU). Releasing financial support was provided by Energiselskapet Asker og Bærum, the Norwegian Well Drillers Association and the Research Council of Norway.

I am deeply thankful to:

My supervisors Bernt Olav Hilmo and Bjørge Brattli for invaluable guidance at different stages in the work.

The initiator of the project, the consultant, the ultimate field co-worker and colleague Helge Skarphagen for his active participation and never ending support, coffee cups and discussions.

The project group which has consisted of, in addition to the three persons mentioned above, Espen Hiorth and Jan Håbrekke (Brønnteknologiutvikling AS), Arne Myrvang and Lisbeth Alnæs (SINTEF, Rock- and Soil Mechanics) and Kjell Køber (Energiselskapet Asker og Bærum).

The contact person in Bærum municipality Vidar Haugen for organizing the sites for the pilot plants.

Knut Ellingsen, Harald Elvebakk, Leif Furuhaug, Øystein Jæger, Janusz Koziel, Bjørn Larsen, Kirsti Midttømme, Frank Sivertsvik, Gaute Storrø, Are Sjøreng and Geir Viken at NGU and Even Brekke (NTNU), Rune Helgesen (Geoenergi AS) and Tor Simon Pedersen (NVE) who has carried out or assisted the different kinds of fieldwork.

Arne Solli and Ola Sæther at NGU for helping me with the interpretation of the optical televiewer- and water chemistry data, respectively.

Jan Cramer for reading the thesis and correcting my english.

The NTNU-students Jo Svenningsson Nordstrand and Tormod Spangelo for providing me valuable data and knowledge.

Brødrene Myhre AS and Båsum Boring for practical help and kind service.

Therese Scheldt, ex-colleague at NTNU, for professional advices and fruitful discussions.

The Organisation for Doctoral Candiates of Applied Earth Sciences for organizing inspiring social events.

Marianne, Lise and Olav for their hospitality.

My father and brother Elling for kindly lending me different kinds of useful tools and a handy car for the fieldwork.

My mother and father for support through many years.

And finally, the boys in my life, Håkon and Øystein for good help, love and lots of fun.

Trondheim 9th of November 2004

Table of contents

1	Introduction	1
1.1	Project idea	1
1.2	Hypotheses	2
1.3	Organisation of thesis	3
2	Background, methods and equipment	4
2.1	Hydraulic fracturing	4
2.1.1	Hydraulic fracturing in hard rock water wells - Previous work	4
2.1.2	Hydraulic fracturing for the utilization of low-geothermal energy	8
2.1.3	Rock stresses influencing the fracture orientation	11
2.1.4	Rock stress measurements	12
2.1.5	Important rock properties	15
2.1.6	Hydraulic fracturing with water - how to do it	16
2.1.7	Hydraulic fracturing with injection of sand	17
2.1.8	Measurements of water- and packer pressures	19
2.2	Equipment development	20
2.2.1	Double packer - FrakPak - AIP 410-550	20
2.2.2	High-pressure tank for the injection fluid	21
2.2.3	Injection packer for the central borehole	22
2.2.4	Air pressure mixer	22
2.3	Geophysical logging equipment	23
2.3.1	Optical televiewer	23
2.3.2	Temperature, electric conductivity and natural gamma (TCN-log)	25
2.3.3	Impeller flowmeter probe	25
2.4	Testing of borehole yield	26
2.4.1	Equipment for test pumping	26
2.4.2	Different kinds of test pumping: Ordinary, columnar- and sectional	28
2.4.3	Sink- and rise tests: Theory	29
2.4.4	Estimation of water yield	30
2.5	Water quality in ground source heat pump systems based on circulating groundwater	32
2.6	Laboratory methods	33
2.6.1	Water analysis	33
2.6.2	XRF-, XRD- and petrographical analysis	35
2.7	Measuring the terrain level	36
2.8	Thermal response test	37
3	Research areas	40
3.1	Lade - investigations, geology and borehole facts	41
3.2	Bryn - investigations, geology and borehole facts	42
3.3	EAB - investigations, geology and borehole facts	47
4	Investigations performed	49
4.1	Laboratory test - mixing of thickener and water	49
4.2	Lade	50
4.2.1	Test pumping, water analysis and geophysical logging	50
4.2.2	Hydraulic fracturing with water-only	50
4.2.3	Hydraulic fracturing with injection of sand	51
4.2.4	Measuring changes in the terrain	52
4.3	Bryn	52
4.3.1	Drilling and XRF-, XRD- and thin-section analysis of drill cuttings	52
4.3.2	Test pumping, water analysis and geophysical logging	52
4.3.3	Rock stress measurements	53
4.3.4	Hydraulic fracturing with water-only	54
4.3.5	Hydraulic fracturing with injection of sand	55
4.3.6	Levelling	57
4.3.7	Thermal response test	58
4.3.8	Test run of the pilot plant	58
4.4	EAB	60

4.4.1	Test pumping, water analysis, flow measurements and geophysical logging	60
4.4.2	Hydraulic fracturing with injection of sand	60
4.4.3	Levelling	62
4.4.4	Thermal response test	63
4.4.5	Test run of the pilot plant	63
4.5	Modelling of energy potentials	64
4.5.1	Software presentation - FEFLOW and HFM	64
4.5.2	Comparison of the FEFLOW- and HFM software at Bryn	67
4.5.3	FEFLOW-modelling of the energy potentials at Bryn and EAB	69
5	Results	73
5.1	Lade	73
5.1.1	Borehole yields, possible water inlets and groundwater quality	73
5.1.2	Geophysical logging	76
5.1.3	Hydraulic fracturing with water-only	76
5.1.4	Hydraulic fracturing with injection of sand	77
5.1.5	Changes in the terrain level	78
5.2	Bryn	79
5.2.1	Drilling and XRD-, XRF- and thin-section analysis of drill cuttings	79
5.2.2	Borehole yields and groundwater level disturbances	82
5.2.3	Changes in the borehole yield caused by hydraulic fracturing	91
5.2.4	Rising curves	94
5.2.5	Groundwater chemistry	98
5.2.6	Rock stresses	100
5.2.7	Borehole conditions - degree of fracturing, temperature, conductivity and radioactivity ...	101
5.2.8	Identification of possible new water inlets in the boreholes	108
5.2.9	Hydraulic fracturing with water-only	111
5.2.10	Hydraulic fracturing with injection of sand	120
5.2.11	Terrain level changes	122
5.2.12	Thermal response	123
5.2.13	Effect extraction from the pilot plant	125
5.2.14	Recommended alternative use of the boreholes at Bryn	127
5.3	EAB	128
5.3.1	Borehole yields and groundwater chemistry	128
5.3.2	Flow patterns	131
5.3.3	Borehole conditions - degree of fracturing, temperature, conductivity and radioactivity ...	131
5.3.4	Identification of possible new water inlets in the boreholes	134
5.3.5	Hydraulic fracturing with injection of sand	136
5.3.6	Terrain level changes	140
5.3.7	Thermal response	140
5.3.8	Effect extraction from the pilot plant	142
5.3.9	Changes in the borehole yield caused by hydraulic fracturing with injection of sand	144
5.3.10	Recommended use of the boreholes at EAB	144
5.4	Modelled energy potential	145
5.4.1	Comparison of FEFLOW and HFM at Bryn	145
5.4.2	Modelled energy potentials at Bryn and EAB	147
5.5	Comparison of the pressure levels from hydraulic fracturing	152
5.6	Method development	154
5.6.1	Double packer - FrakPak - AIP 410-550	154
5.6.2	Hydraulic fracturing with water-only	155
5.6.3	Hydraulic fracturing with injection of sand	156
5.6.4	Experiences with the optical televiewer	157
6	Economy	159
6.1	A simple economical analysis	159
6.1.1	Construction costs	160
6.1.2	Estimation of energy extraction from groundwater	160
6.1.3	Calculation of effective borehole metres using EED	162
6.1.4	Profitable pilot plant at EAB?	164
6.1.5	Profitable pilot plant at Bryn? - Theoretical considerations	166
6.1.6	Construction costs at varying effect extractions at Bryn and EAB	168
6.2	Energy efficiency - energy extraction per meter borehole	168

7	Discussion	170
7.1	Cost reductions by the use of improved equipment and methodology	170
7.2	Hydraulic fracturing and geological conditions	170
7.3	Sufficient infiltration capacity and distributed circulation of groundwater?	171
7.3.1	Hydraulic communication - preferred borehole configurations	171
7.3.2	Identification of water inlets	173
7.4	Need of sand as propping agents?	174
7.5	Suggestions for further work	176
8	Summary and conclusions.....	178
9	References	180
	Appendix.....	1
1	Rise data from Bryn after hydraulic fracturing with water-only	1
2	Rise data from Bryn after hydraulic fracturing with injection of sand	9
3	Fracture analysis - histograms and stereograms	20

Chapter 1 Introduction

The project *Ground source energy from crystalline bedrock - increased energy extraction by using hydraulic fracturing in boreholes* was initiated in 1999. The main objective was to develop equipment and methodology in order to achieve a 50% reduction in the drilling costs for medium- to large sized ground source heat pump system in crystalline bedrock. The drilling costs often amounts to somewhere between 30-40% of the total construction costs for conventional ground source heat plants with vertical collectors in crystalline bedrock (Skarphagen et al., 1999). This project introduced an alternative concept where the energy extraction is based on pumped groundwater from a permeable bedrock, artificially made by hydraulic fracturing. Hydraulic fracturing creates fractures in the bedrock, increases the heat exchange area between the groundwater and the bedrock, and consequently the energy extraction per borehole as well. The short-period energy extractions, limitations and opportunities of the method were tested out in two pilot plants at Bryn and at the former property of Energiselskapet Asker og Bærum (EAB), respectively. The results from the short-period testing will form the basis for the long-term operation of the pilot plants probably utilized as both heat- and cooling storages for the nearby buildings connected to the two plants in the future.

Joint venture partners in the project, with a budget of approximately 5 millions NOK, has been the Geological Survey of Norway (NGU), Brønnteknologiutvikling AS (BTU), the Norwegian University of Science and Technology (NTNU), Energiselskapet Asker og Bærum (now Viken Nett AS), the Research Council of Norway, SINTEF Civil and Environmental Engineering, department of Rock and Soil Mechanics, and the Norwegian Well Drillers Association.

1.1 Project idea

The project idea introduces an alternative concept for the use of ground source heat pump system based on circulating groundwater in crystalline bedrock. The plant consists of five boreholes where a central borehole is surrounded by four satellite boreholes (figure 1–1). This configuration was expected to ensure the best hydraulic communication and the largest heat exchange area between the boreholes. In operation mode, the groundwater is pumped from the four satellite boreholes to the heat exchanger, where the energy extraction takes place. Afterwards the groundwater is reinjected into the magazine through the central borehole. A successful reinjection and circulation of the groundwater requires good hydraulic communication between the boreholes. Since most boreholes in crystalline bedrock have a modest yield, creating a fractured and conductive bedrock by performing hydraulic fracturing in several levels in each borehole is thought of as beneficial. A fractured and permeable bedrock will work as a huge heat exchanger for the circulating groundwater, and the energy extraction per borehole meter is likely to be higher for this special kind of plant compared with conventional ground source heat pump system with collectors in vertical boreholes. Here, the energy extraction from the surrounding bedrock of the borehole is collected by the circulating water-antifreeze solution in the closed collector.

The water quality is important for a successful operation of ground source heat pump systems based on circulating groundwater, and has to be examined thoroughly. Particularly substances which can cause precipitation (iron, manganese and carbonates), silting and corrosion is of major concern (paragraph 2.5).

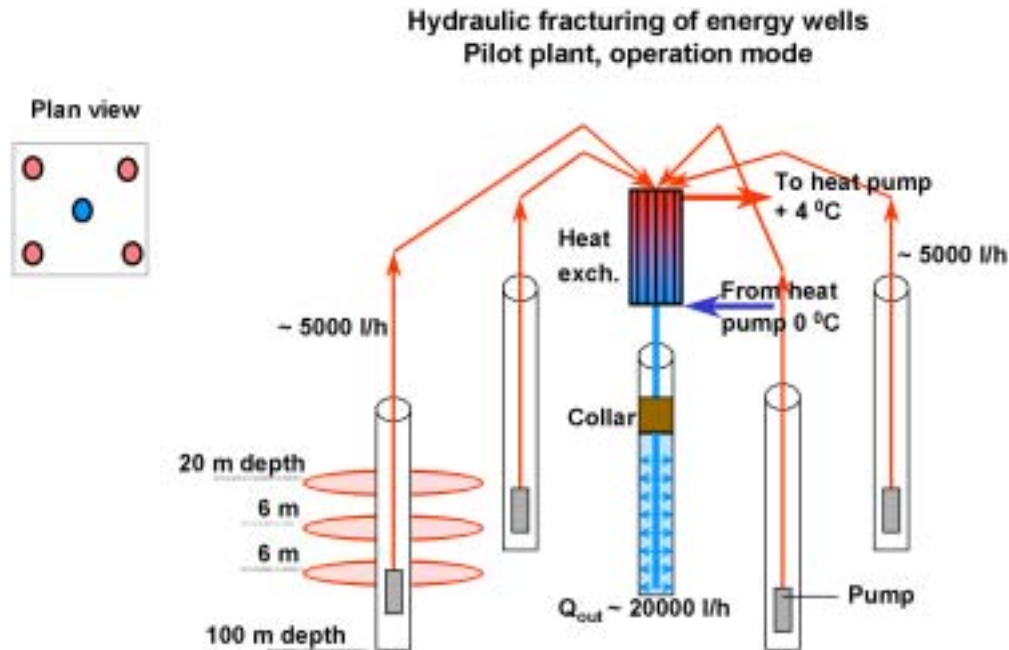


Figure 1–1: Principle drawing showing the special kind of ground source heat pump system based on circulating groundwater (Skarphagen et al., 1999). In operation mode, the groundwater is pumped from the four satellite boreholes to the heat exchanger where the energy extraction takes place. Afterwards the groundwater is re-injected into the magazine through the central borehole. Hydraulic fracturing at several levels in each borehole increases the hydraulic conductivity and the heat exchange area in the bedrock.

1.2 Hypotheses

The aim of this work has been to test the following hypotheses:

- 1) The development of suitable and reliable equipment and methodology for hydraulic fracturing with injection of propping agents will reduce the drilling costs for medium- to large sized ground source heat pump systems in crystalline bedrock by up to 50%.
- 2) Independent of the geological conditions, a complete fracturing is expected to take place using the developed and improved equipment and methodology for hydraulic fracturing of boreholes located in crystalline bedrock.
- 3) Sectional hydraulic fracturing in several levels in each borehole will ensure a distributed circulation of the groundwater and a sufficient infiltration capacity of the infiltration borehole in the ground source heat pump system based on groundwater.
- 4) Hydraulic fracturing using injection of propping agents will cause a further improvement of the borehole yields compared to those yields achieved by hydraulic fracturing with water-only.

1.3 Organisation of thesis

Chapter 1 gives a brief introduction to the project idea and the aim and hypotheses of this study. Chapter 2 focuses on the methods and equipment employed in the study with special emphasis on the theoretical and practical aspects concerning hydraulic fracturing as a technique. Chapter 2 also provides a short description of the newly developed equipment suited for hydraulic fracturing applications. Chapter 3 and 4 introduce the research areas at Lade, Bryn and EAB and summarizes the laboratory- and field investigations performed in connection with the testing of the equipment and methodology at the three sites. The testing is described in chronological order and reflects the different stages in the study. The last part of chapter 4 deals with the modelling of the pilot plants at Bryn and EAB, while the results from the investigations and the modelling are presented in chapter 5. Some economical considerations, evaluating the profitability of a ground source heat system based on circulating groundwater versus a conventional ground source heat system with vertical collectors, are presented in chapter 6. Finally, a discussion of relevant results for the evaluation of the hypotheses and summary and conclusions are presented in chapter 7 and 8, respectively.

Chapter 2 Background, methods and equipment

2.1 Hydraulic fracturing

2.1.1 Hydraulic fracturing in hard rock water wells - Previous work

A comprehensive study of the effectiveness of fracture stimulation for increasing borehole yield in Newfoundland in Canada are reported by Gale and MacLeod (1995). Extensive hydrogeological and geophysical tests were performed before and after hydraulic stimulation in six drilled bedrock, low- to moderately yielding (<5 litres/minute), boreholes at six different geographic and geologic locations. Sectional hydraulic fracturing in three or four levels in each well, using water pressures in the range of 2-10 MPa (20-100 bars), made the borehole yield increase 30 to 910%. A closer look at the pressure and flow curves plotted against time, revealed a possible relation between pressure, flow rate and borehole yield. While the limited data base prevents Gale and MacLeod (1995) from drawing general conclusions, it would appear that the higher the injection pressure required to maintain maximum flow rate, the lower the absolute increase in the well yield. Similarly, large increases in borehole yield appear to be correlated with strong backflows of cloudy and sediment laden water when the injection cavities were opened to the atmosphere after stimulation. The term maximum flow rate describes the relatively large flow rate into the rock formation right after initiation or reopening of a fracture.

A ranking of the borehole stimulation potential in order to increase the borehole yield as a function of rock type, based on the results from the six boreholes, is cited in table 2-1.

Table 2-1: Borehole stimulation potential by Gale and MacLeod (1995).

Rock type	Stimulation potential
siliceous siltstone	very good
sandstone-conglomerate	good
shale/siltstone/sandstone	good
shale	moderate
volcanic	moderate

Geophysical logging of the boreholes using a TV-camera, turned out to provide essential guidance in selecting the intervals to be stimulated and identifying the locations for the packer seals. However, the TV-logs did not show any obvious changes in fracture apertures that were produced by hydraulic fracturing (Gale and MacLeod, 1995).

In order to check the long-term yield of the boreholes after hydraulic fracturing, a retest of the borehole yield was performed in one of the six boreholes eight weeks after the first post-stimulation test. Even though this borehole showed a minor increase in the borehole yield, the remaining question after this study is whether or not propping agents are required to keep the fractures open. Gale and MacLeod (1995), in a review of

previous work, claim that the literature does not show any consistent experience in the use of propping agents to maintain borehole yields once the borehole has been stimulated. Attempts to follow the oil and gas industry approach and use large quantities of sand have not yielded consistent results.

In the previous work-section, Gale and MacLeod (1995) refer to 30 to 60 minutes and 1000 litres, to be the minimum length of time and volume required to propagate the fracture or increase the fracture interconnection within the bedrock. Further, there appears to be a strong bias in favour of using a double packer assembly rather than a single packer unit for hydraulic stimulations of boreholes in fractured rocks.

In a study of hydraulic fracturing performed in low yielding boreholes in the crystalline basement rocks of Masvingo Province, Zimbabwe, reported by Herbert et al. (1993), 12 boreholes were stimulated with hydraulic fracturing using a single- or double packer unit. In 50% of the cases the borehole yield was increased by an average of 80% in the range of 10 to 240%. As a single-borehole test at Marabamba, a small amount of single-sized, 0.5 mm sand, was introduced into the injected water when stimulating an already identified water entry at 26 meters depth. Using a double packer unit, hydraulic fracturing with water-only reaching a water pressure of 25 bars, had been performed at this level in advance. A following generator failure made further hydraulic fracturing impossible. After hydraulic fracturing with water-only, the yield had increased by 23%, while the injection of sand caused an overall increase of 3%. In other words, the injection of sand caused a reduction in the borehole yield compared to the results from hydraulic fracturing with water-only.

Hydraulic fracturing with water-only has been performed in a large number of low yielding boreholes in different geological and geohydrological regimes in South Africa (Less and Anderson, 1993). Results from the Swartwater study area (10 holes) indicate that the scientifically sited boreholes, sited in order to intersect geological features such as faults or contacts et cetera, are the most likely to have improved yields after hydraulic fracturing. In the case of random site selection, 47% (79 out of 170) of all boreholes treated, responded positively.

Since many of the selected boreholes were old and no information was available, routinely geophysical logging and test pumping were performed to supply the information required to ensure the most effective hydraulic fracturing. Less and Anderson (1993) report that identifying the position of any fractures or fracture zones were very important for positioning the packers. The on-site time required to perform the hydraulic fracturing procedure, including pre- and post-test pumping and four packer settings, and by using new equipment and experienced personnel is limited to maximum 12 hours. The hydraulic fracturing unit is capable of generating 130 kW. According to equation 2.1, energy consumption is a product of flow rate and pressure (Less and Anderson, 1993).

$$\text{Energy (kW)} = \text{flow rate (l/s)} \times \text{pressure (MPa)} \quad [2.1]$$

Herrick (2000) presents the general experience with hydraulic fracturing from the water well contractors working in hard rock formations in the US. Employing hydraulic fracturing, using either a single- or double packer unit, has for many contractors reduced

the drilling depth. Mostly, the borehole yield is sufficient when combining drilling down to 250 feet (76 meters) with hydraulic fracturing. Depending on formation and equipment, borehole pressures are typically ranging from 500 to 5000 psi (34.5-345 bars). The demand for hydraulic fracturing services is usually in low-yielding boreholes and the availability of a detailed borehole log or accurate borehole history, especially for old boreholes, is a great help in determining whether or not to use the technique. Adequate lateral distances from other boreholes, usually at least 200 feet (61 meters), are always considered when selecting new borehole sites for hydraulic fracturing in hard rock areas.

Banks and Robbins (2002) emphasize that the best hydraulic fracturing rigs have a dual pump system. One pump applies a high pressure to initiate the fracture, while the secondary pump has a high volume capacity, injecting large flows of water to propagate the fracture as far as possible. Further, hydraulic fracturing at shallow depths (<25-30 meters) runs the risk of creating fractures to the surface, which would be vulnerable to contamination and thus should be avoided.

Baski Incorporation in the US is a well known manufacturer of a wide range of inflatable packers, including those for hydraulic fracturing. In a correspondence regarding hydraulic fracturing and the use of propping agents, Henry A. Baski (2001) in Baski Inc., says: "To the best of my knowledge, propping agent-fracturing technology in hard rock has not been developed".

The Australian Water Resources Council by Williamson and Woolley (1980) in Smith (1989) report of hydraulic fracturing tests in three new boreholes. The boreholes were located at, and referred to as Young, Collinga and Temora, where the bedrock consists of granodiorite, quartz schist, and phyllite and quartzite respectively. Two phases of fracturing were planned: (1) Hydraulic fracturing with water-only, followed by (2) a Revert (Johnson, organic polymer drilling fluid) -sand treatment. The stimulation in each borehole was focused at one section of 4 or 5 meters, located at depths where an existing fracture already was identified by using a borehole TV.

In phase one, performing hydraulic fracturing with water-only, the pressure rose up to 32 and 43 bars at Young and Collinga, and the borehole yields were increased. At the Temora site nothing virtually happened. Williamson and Woolley (1980) concluded that the pressure and flow were probably not sufficient to make a difference. The borehole TV survey at Young showed no visible sign of new fracturing except for a chip out of the borehole wall.

Phase two at Young where performed as follows: (a) 1800 litres 58-sec (Marsh funnel) Revert, (b) 1800 litres Revert and sand (114-sec, 25 g/litres of sand), and (c) 1800 litres Revert. Breaker chemical was pumped in with the Revert to accelerate its breakdown. The same phase two procedure was performed at Collinga and Temora, but coarser sand was selected.

For all boreholes, the yield was reduced after phase two treatments, probably caused by plugging attributed to sand or Revert breakdown products. Rapid and severe biofouling was observed at Young and Collinga, but not Tamara, and may have been a contributing factor to the reduced yield. Working with phase two, the Revert-sand mixture treatments, continuously pumping was not possible due to the lack of fluid capacity. Consequently the Revert-sand mixture had to be mixed and then pumped into

the borehole section which may have caused an incomplete distribution of organic polymer breaker in the Revert-sand mixture.

Finally, Williamson and Woolley (1980) recommend that:

- 1) Hydraulic fracturing with water-only should be used, as no improvements could be accomplished by using the viscous fluid-propping agent mixture.
- 2) If propping agents are used, the grains should be relatively coarse.
- 3) Hydraulic fracturing is most effective for wells yielding less than 0.25 litres/second.

The “Manual of Hydraulic Fracturing for Well Stimulation and Geologic Studies”, prepared for the National Well Water Association in the U.S by Smith (1989), is a comprehensive summary of procedures, equipment and geologic aspects related to hydraulic fracturing stimulations.

Smith (1989) states that the need for propping agents in the groundwater industry is in dispute. The success or failure of the use of propping agents in many situations probably depends on a variety of factors like: (a) the tectonic tension in the rock and its tensile strength, (b) fracture geometry, (c) selection of the right propping agent, (d) correct placement of the propping agents, and (e) successful development of the borehole after fracturing. The use of propping agents in the groundwater industry varies. In general the consensus seems to be that propping agents should only be used where necessary, for instance in situations where induced fractures are likely to squeeze shut (Smith, 1989).

Choosing the right size, type and volume of propping agents seems to be a subject of experimentation. Hard sand or plastic beads, as coarse as possible for instance 30-50 mesh (0.6-0.3 millimetres), are recommended by the groundwater industry contractors. Compared with the oil business, the use of coarser and less propping agents are recommended. Propping sand should be pumped in with heavily chlorinated water or suspended in heavily chlorinated borehole water (Smith, 1989). The injection of propping agents can be done by leading pressurized fluid into the propping agents chamber and thus the mixture is pressed into the fracture ahead of the fluid (figure 2-1). The transport fluid for the propping agents can either be viscosifiers as organic or synthetic polymers together with a chemical breaker, or clean water.

In most applications, the water pressure required to clean, open or initiate fractures is reported to be between 500 and 2000 psi (34.5 and 138 bars), with 3000 psi (207 bars) required for very hard rock and deeper wells (Macaulay, 1987; Baski, 1987; Waltz, 1988; in Smith 1989).

Hydro-Frac Equipment Schematic

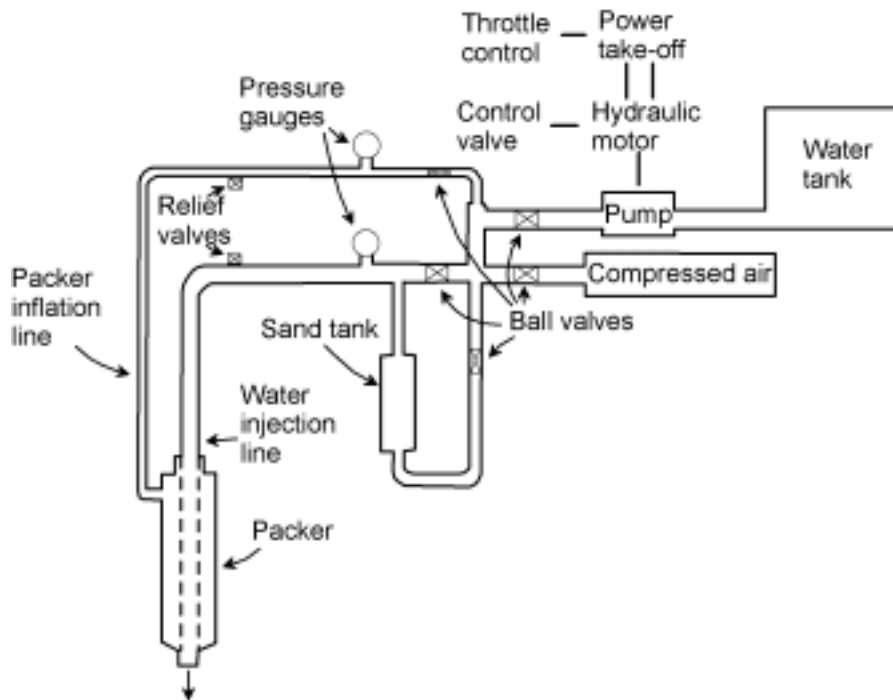


Figure 2–1: Schematic illustration of the hydraulic fracturing system including the injection of propping agents (based on Smith, 1989).

2.1.2 Hydraulic fracturing for the utilization of low-geothermal energy

Experimental studies concerning the HYDROCK-concept has been performed in hard rock (granite) boreholes at Rixö, Sweden (Larson et al., 1983; Sundquist and Wallroth, 1990). The HYDROCK-concept describes a ground source heat pump system in crystalline bedrock where circulating water extracts energy from several fracture planes created by hydraulic fracturing (figure 2–2). The HYDROCK-plant requires good hydraulic conductivity in the fracture planes interconnecting the infiltration- and pumping boreholes. Ideally, the HYDROCK store should be built in homogenous isotropic rocks although a moderate fabric can be accepted. Another ideal situation would be anisotropic, layered/banded rock which will easily split along planes of weakness when fractured (Hellström and Larson, 2001).

Hydraulic fracturing in two non-fracture sections at 44.0 and 32.5, each of 1.0 meter, was performed in the central borehole at Rixö. During hydraulic fracturing, pressure levels reached 10.5 and 22 MPa (105 and 220 bars), respectively. The use of a casing cutter at the 44.0 level before hydraulic fracturing, certainly reduced the water pressure necessary to achieve fracturing and caused a horizontal fracture. The borehole yield increased from 8.5 to 16.5 litres/minute. A variable hydraulic communication with three encircled boreholes, six and ten meters away from the central borehole, was observed and indicates an asymmetric fracture initiation (Sundquist and Wallroth, 1990). A pumping capacity of 55 litres/minute prevented an effective fracture propagation. Only

the new fracture at 44.0 meters depth was large enough to be detected by borehole TV-logging after hydraulic fracturing.

Injection tests were performed in the stimulated sections at 44.0 and 32.5 meters depth in two stages. In stage one, after some injections the flow and pressure were steady at 0.92 litres/second and 2.2-2.5 MPa (22-25 bars), respectively. The injection tests were resumed in stage two where, in order to maintain the same flow rate (0.92 litres/second), the pressure rose up to 18-22 MPa (180-220 bars). The pressure rise from stage one to two can be explained by the appearance of high friction losses in the created fractures. The permeability of the newly, created fractures are calculated to be 30 times lower than the natural fracture located at 66 meters depth (Sundquist and Wallroth, 1990).

For further studies, Sundquist and Wallroth (1990) suggest that fractures with high hydraulic conductivity and minor leakages can be created by using high flow rates (>10 litres/second) when performing hydraulic fracturing, and/or by pumping spacing materials into the created fracture. A high viscosity fluid is required to pump spacing materials, for instance sand.

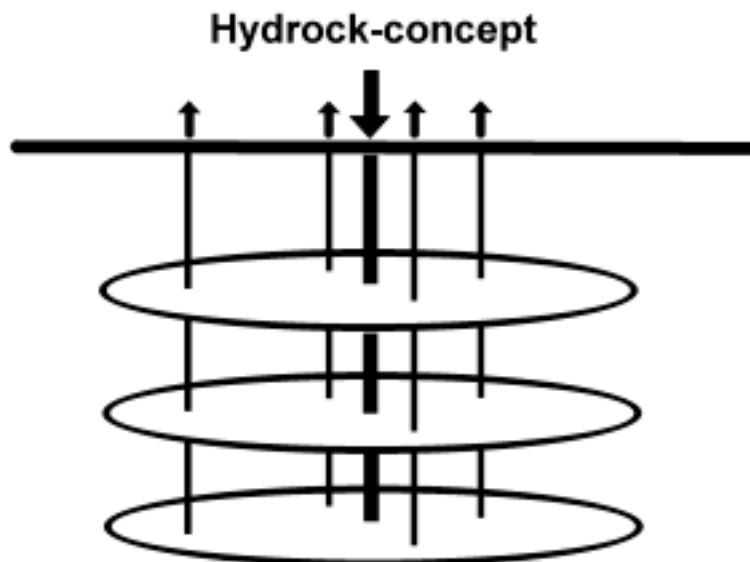


Figure 2–2: A schematic illustration of the basic principles in the HYDROCK- concept. Three circular fracture planes perforated by a central borehole and four satellite boreholes (modified after Hellström and Larson, 2001).

Hydraulic- and explosive fracturing has been performed in the swedish study “Fracturing of a pilot plant for borehole heat storage in rock at Luleå, Sweden”, reported by Nordell et al. (1984). The small-scale pilot plant for heat supply and -extraction consists of 19 boreholes, which are 21 meters deep and 52 millimetres in diameter. The boreholes are positioned as triangles where the distance is 1.3 meters among themselves (figure 2–3). The main purpose of the project was to achieve a lasting increase of the hydraulic conductivity by doing hydraulic and explosive fracturing in the bottom of the boreholes. Having a high conductivity, the heat store can be operated without expensive borehole installations.

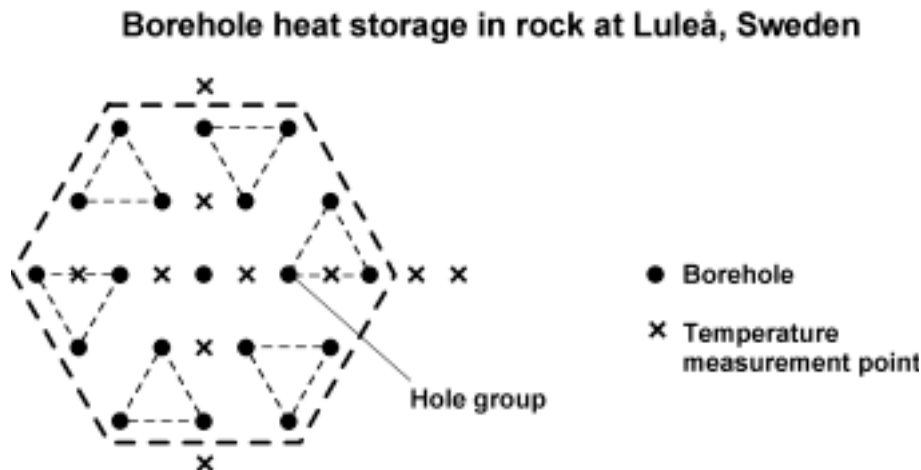


Figure 2–3: Reciprocal localization (1.3 meters) of the 19 boreholes in the small-scale pilot plant for borehole heat storage in rock at Luleå, Sweden (modified after Nordell et al., 1984).

In their conclusions and recommendations Nordell et al. (1984) report that hydraulic fracturing was performed in two stages using a single- and double packer unit, respectively, and fracturing occurred at pressures between 60 to 120 bars. The absence of shut-in pressure and the very uniform breakdown pressure indicate a bedrock with almost zero virgin stresses. This result is consistent with the general assumption of a stress-relieved bedrock for the uppermost 20-50 meters in the glaciated terrains of Northern Sweden. The permeability of the bedrock increased after both types of hydraulic fracturing, but was reduced by a factor of three after explosive fracturing. Similarly, the mean borehole permeability increased after each fracturing. In spite of increased permeability, hydraulic- and explosive fracturing of the test plant have shown that fracturing alone is not enough for conductivity enhancement needed for water circulation. Nordell et al. (1984) recommend the use of propping agents, and in particular quartz sand, to increase the flow capacity of the fractures.

In “Stimulation experiments with water and viscous fluid at the HDR geothermal research site in the Bohus granite, SW Sweden”, Eliasson et al. (1988) summarize some of the stimulation work performed at Fjällbacka HDR-site (hot dry rock). The stimulations were carried out to obtain the high-permeability heat-exchange zone required for HDR-production. For the purpose of finding developing cracks and a suitable position for the next well to be drilled, the displacement of pressurized fluids was controlled by microseismic detection of concurrent stress release pulses.

In order to test the straddle packer equipment under realistic conditions, shallow hydrofracturing tests between 50 and 190 meters depth in Fjb1 were done before the deep stimulation program. Performing hydraulic fracturing at 52-55 and 190-193 meters depth, which represented sections with and without existing fractures indicated by different logging methods, fracturing occurred at 15 and 20 MPa (150 and 200 bars) respectively. Available pumping capacity was 10 litres/second.

The deep stimulation program in Fjb1, where a total of 399 m³ of fluid was consumed, was carried out in the 447-478 section as five injection sequences: (1) Initial water injection, (2-3) first and second mini frac, (4) main water injection, and (5) main

viscous injection with propping agents (Eliasson et al., 1988). The different injection sequences were carried out to compare the effects and find the most effective stimulation procedure. The main objective of injecting 25 m³ viscous propping agent mixture in the fifth injection sequence was to increase the residual fracture width near the borehole and hereby reduce the near-well pressure losses in the circulation phase. The propping agent mixture consisted of 0.2-0.4 millimetres quartz sand, water, viscosifier (hydroxyethyl cellulose) and chemical breaker (celluclast). The propping agent mixture was injected immediately after pumping 200 m³ of viscous gel into the formation (injection sequence four) where the pumping rate and the pressure level were 21 litres/second and 10.7-13.2 MPa (107-132 bars), respectively. The pumping rates and the maximum pressure levels in the whole deep stimulation program, injection sequence one to five, were ranging from 20-30 litres/second and 13-18 MPa (130-180 bars), respectively. Having an overpressure of approximately 3 MPa (30 bars), the well was vented eight days after the main viscous injection. Temperature logs run after the stimulation indicated two hydraulically conductive zones, and hydraulic tests revealed a permeability increase from 10⁻¹⁷ m² (10μD) to 10⁻¹⁴ m² (10 mD) for the most conductive flow paths (Jupe et al., 1993; in Broch, 1994). A total of 35 microseismic events were recorded in connection with injection sequence four and five, and the major seismic activity occurred towards the end of the injection, during the injection of propping agents. This microseismicity formed a horizontal planar structure at a depth of approximately 460 m, and these results were used to target the drilling of the second 500 metres deep borehole, Fjb3.

Four separate stimulations in Fjb3, including the use of viscous fluids, backflushing, acidisation and 0.25-0.60 millimetres quartz sand as propping agents (Sundquist et al., 1988), were performed at a later stage in the project with the objective of reducing the reservoir impedance. Only minor changes in the overall conductivity were observed as a consequence of these stimulations, but the Skin factor was reduced from +5 to -5. Subsequent, an open-loop circulation took place between borehole Fjb3 and Fjb1. Water was injected into the 449-480-section in borehole Fjb3 with a constant flow rate of 1.83 litres/second. The total pumping time was 846 hours and the injection pressure was approximately 4.5 MPa (45 bars). Minor improvement in the production flow rate was observed towards the end of the test period, and the maximum recovery was 51% (Jupe et al., 1993; in Broch, 1994).

2.1.3 Rock stresses influencing the fracture orientation

The tectonic stress situation in the surrounding bedrock is of major importance for the orientation of fractures. In a virgin bedrock, fractures induced by hydraulic fracturing are parallel the maximum principal stress and normal to the minimum principal stress direction. The water pressure required for the initiation of a new fracture is the sum of the minimum principal stress (σ_{\min}) and the tensile strength of the rock (σ_t).

The following paragraph is mainly based on Myrvang (1996). As a starting point, the area around a vertical drilled borehole influenced by the water pressure induced by hydraulic fracturing is considered. The principal stress pattern is supposed to be normal and parallel to the borehole (figure 2-4). The rising water pressure between the collars of rubber on the double packer induces tangential stresses around the

borehole. The fracture initiation pressure P_c , required for the initiation of a tensile fracture is given by equation 2.2.

$$P_c = \sigma_{\theta\min} + \sigma_t \quad [2.2]$$

$$\sigma_{\theta\min} = 3\sigma_{H2} - \sigma_{H1} \quad [2.3]$$

equation 2.3 in 2.2 gives:

$$P_c = 3\sigma_{H2} - \sigma_{H1} + \sigma_t \quad [2.4]$$

where $\sigma_{\theta\min}$ represents the minimum tangential stress in the borehole wall, σ_t is the tensile strength of the bedrock, while σ_{H1} and σ_{H2} are the maximum and minimum principal stress in the horizontal plane, respectively. All the fracture planes are, under the present circumstances, supposed to be vertical and parallel σ_{H1} . Further propagation of the fracture depends on the rock stress situation. The fracture will always tend to follow the way of least resistance, i.e. parallel to the maximum principal stress and normal to the minimum principal stress. In cases where the minimum principal stress is horizontal, σ_{H2} , the tensile fracture will propagate vertically equivalent to the situation described for the area of influence around the borehole. Having the opposite situation, where the minimum principal stress is the vertical component σ_v , the fracture will propagate vertically within the area of influence for the borehole. Outside the area of influence for the borehole, the fracture will turn and gradually create a horizontal fracture plane normal to the vertical minimum principal stress σ_v .

Bedding and existing fractures having a different orientation than the present rock stresses, may influence the orientation of a fracture propagated by hydraulic fracturing.

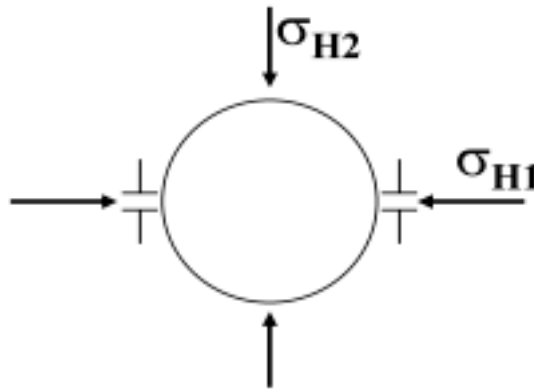


Figure 2–4: A vertical borehole seen from above. The principal stresses determine the fracture orientation within the area of influence for the borehole during hydraulic fracturing. σ_{H1} and σ_{H2} represent the maximum and minimum principal stresses in the horizontal plane, respectively. Outside the area of influence for the borehole, the fracture plane will develop parallel and normal to the maximum and minimum principal stress, respectively.

2.1.4 Rock stress measurements

This paragraph is mainly based on Amadei and Stephansson (1997). Hubbert and Willis (1957; in Amadei and Stephansson, 1997) were the first to claim that the orientation of fractures created with hydraulic fracturing are related to the principal stress situation in the bedrock. The relation between hydraulic fracturing and the rock stress situation was first understood, analysed and documented theoretically and

experimentally by Haimson (1968; in Amadei and Stephansson, 1997). Through further development, hydraulic fracturing has become one of the most commonly employed methods for in-situ rock stress measurements.

Rock stress measurements using hydraulic fracturing are performed by SINTEF's Civil and Environmental Engineering, department of Rock and Soil Mechanics (Jóhannsson, 2001). The measurements are carried out in test sections of 1.3 meters, limited by a double packer unit. The aim of the fracturing tests is to determine the value and direction of the minimum and maximum principal stress.

The test procedure for hydraulic fracturing used is based on the recommendations by ISRM (International Society for Rock Mechanics) (Kim and Franklin, 1987). The closure pressure or the instantaneous shut-in pressure, P_s , represents the stress normal to the fracture plane and is interpreted as the minimum principal stress (σ_{\min}) (Jóhannsson, 2001). P_s is determined from a diagram showing pressure and flow as a function of time (figure 2–5). By drawing a tangent to the pressure-time curve immediately after fracturing, the closure pressure (P_s) is determined as the point where the pressure-time curve diverges from the tangent (figure 2–6). A theoretical measure of the tensile strength (σ_t) of the rock is given by the difference between initial fracture pressure (P_c) and reopening pressure (P_f) in the second and third fracturing cycle, as:

$$\sigma_t = P_c - P_f \quad [2.5]$$

The validity of equation 2.5 assumes a complete closure of the fracture between each cycle with hydraulic fracturing. Further, Bredehoeft et al. (1976; in Amadei and Stephansson 1997) claim that the value of P_f describes the pressure level where the existing fracture starts to open with hydraulic fracturing.

When the initiated fracture orientates approximately parallel to the borehole, an estimate of the maximum principal stress is given by following equation (Jóhannsson, 2001):

$$\sigma_{\max} = 3P_s - P_f - P_0 \quad [2.6]$$

Where

- σ_{\max} ~ maximum principal stress
- P_s ~ closure pressure or instantaneous shut-in pressure
- P_f ~ reopening pressure
- P_0 ~ pore pressure

The pore pressure can often be ignored for most of Norway's crystalline continental rocks.

An impression packer is employed in order to determine the minimum and maximum principal stress directions. The impression packer is lowered down to the test section and the new fractures are oriented right after the stress measurement. Theoretically, the new fracture- or stress directions, could be determined by filming the borehole wall with an optical televiewer.

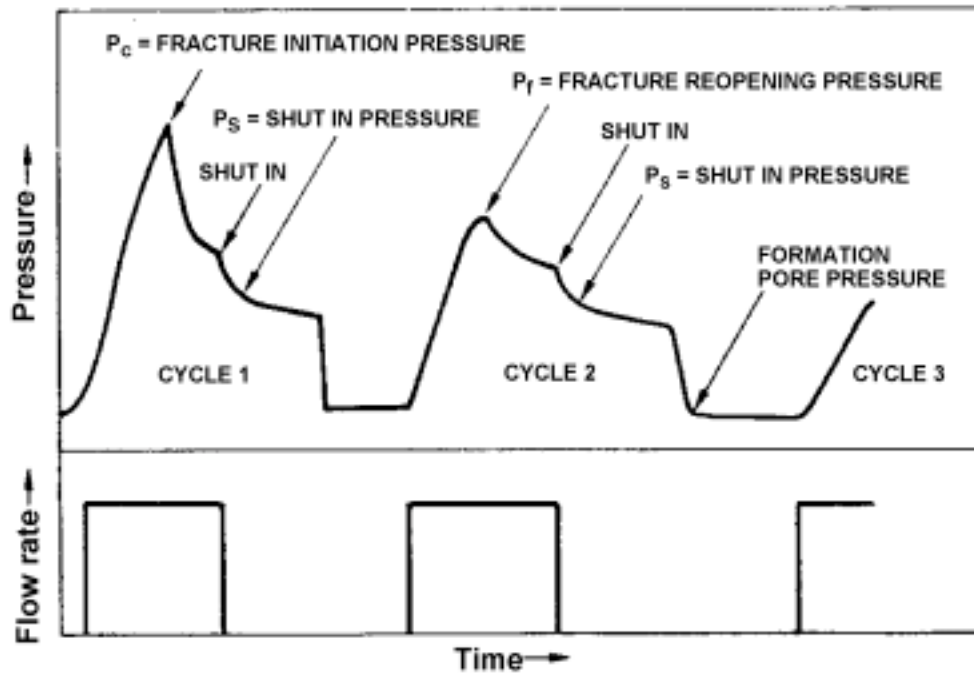


Figure 2-5: Idealized pressure-time diagram for hydraulic fracturing. After ISRM commission on Testing Methods (1987).

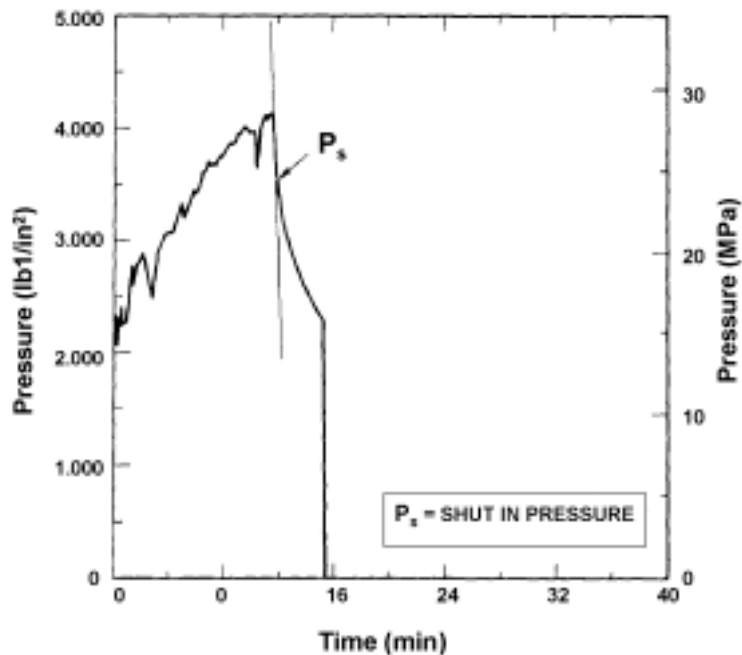


Figure 2-6: A determination of the closure pressure or the shut-in pressure (P_s), as suggested by ISRM, can be done by drawing a line tangential to the pressure-time curve immediately after fracturing (pressure drop). The closure pressure is determined to be the point where the drawn tangent diverges from the pressure-time curve. The illustration is from Aggson and Kim (1987) in Scheldt (2000).

2.1.5 Important rock properties

According to equations 2.4 and 2.5, the tensile strength (σ_t) of the rock has great influence on the magnitude of the fracture initiation pressure P_c when performing hydraulic fracturing. Because of the elaborate and demanding work required to determine the laboratory value of the tensile strength of a rock sample, the tensile strength is expressed by the point load index (I_s). The point load index, which is a result of an induced tension test (Hansen et al., 1998), is approximately equal to the tensile strength (Myrvang, 1996):

$$I_s \sim \sigma_t \quad [2.7]$$

According to Broch et al. (1971) in Myrvang (1996) the point load index I_s is related to the uniaxial compressive strength σ_c as follows:

$$\sigma_c \sim 24 I_s \quad [2.8]$$

Many measurements performed by the Laboratory of Rock Mechanics at SINTEF showed that the relation between the point load index I_s and the uniaxial compressive strength σ_c varies a lot, where the mean value is:

$$\sigma_c \sim 10 I_s \text{ (Myrvang, 1996)} \quad [2.9]$$

Young's modulus and Poissons ratio (ν), or the deformation properties, are two important mechanical properties. At the Laboratory of Rock Mechanics at SINTEF, Young's modulus is found by measuring the compression when the rock sample is exposed to a certain stress level. Young's modulus is determined by the stress and strain ratio at a load of 20 bars, and expresses the stiffness of the rock. A high value of Young's modulus describes a stiff rock (Hansen et al., 1998). Poissons ratio or the "number of lateral expansion" is the ratio between the lateral expansion and the axial compression of the rock sample at a load of 20 MPa (Hansen et al., 1998). A linear relationship between the stress and strain (ϵ) is expressed by Hook's law, where Youngs modulus is the proportionality coefficient (equation 2.10) (Irgens, 1991).

$$\sigma = E\epsilon \quad [2.10]$$

Hook's law implies that two areas with different values for Young's modulus, being exposed to equal compression, gets different stress values. Highest stress values are achieved for the area having the highest Young's modulus (Myrvang, 1996). Figure 2–7 gives an overview of the strength- and deformation properties as compressive strength (σ_c), tensile strength (σ_t), Young's modulus and Poissons ratio (ν) for selected rock types and is based on data from laboratory tests of rock samples performed by SINTEF (Hansen et al., 1998). The selected rock types in figure 2–7 can be associated to the geological conditions at the pilot plants at Bryn (quartzite, quartzitic sandstone and sandstone) and EAB (limestone and clay shale/clay stone) (paragraph 3.2 and 3.3), respectively. In general, the size of the test samples also influences the test results. The laboratory values obtained for the different mechanical rock properties are normally higher than the real in-situ values for the bedrock. This regards both the compressive strength and Young's modulus, and is caused by the fact that the in-situ bedrock contains more fractures and planes of weakness which will reduce the strength and stiffness (Myrvang, 1996).

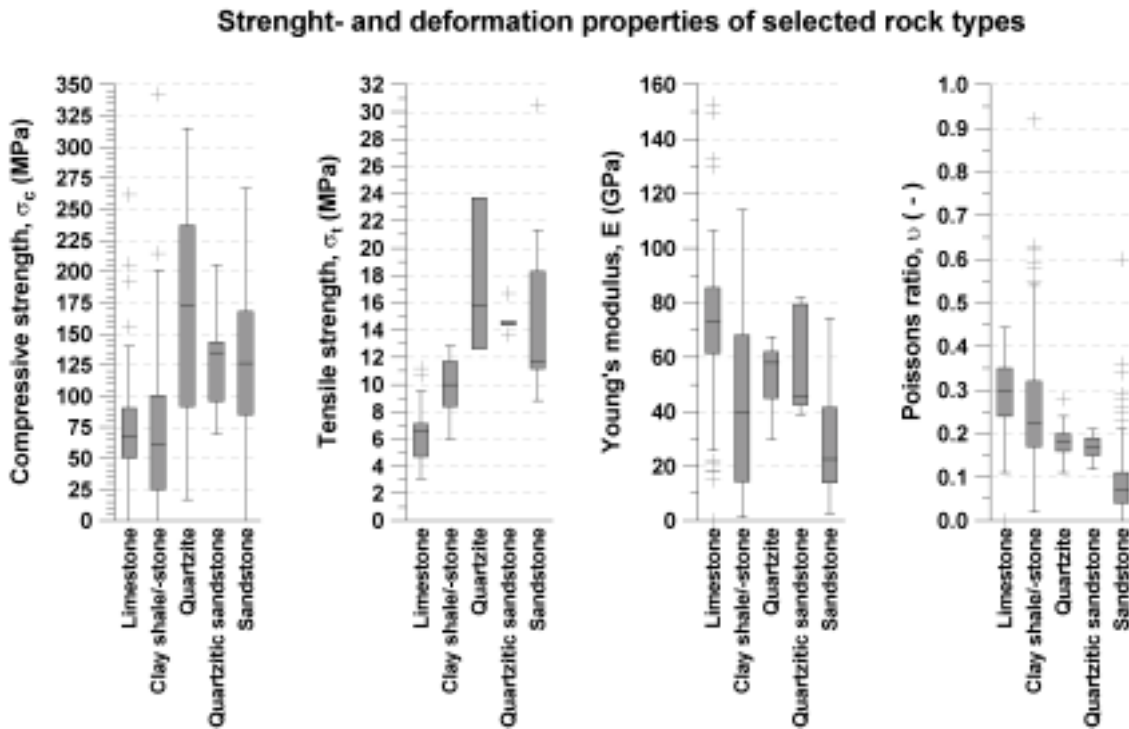


Figure 2-7: Mechanical properties for selected rock types showing the compressive- and tensile strength, Young's modulus and Poissons ratio. The maximum-, minimum-, median-, upper- and lower quartile values are indicated in the boxplots (made with basis in data from Hansen et al., 1998).

2.1.6 Hydraulic fracturing with water - how to do it

Hydraulic fracturing is performed by placing a single- or double packer unit at a certain depth in a borehole. The packers, which consists of hard-wearing rubber, seals against the borehole wall either by using mechanical compression, or by filling a liquid (water or a light oil) or air into the packer units (figure 2-8). Using a double packer unit like the one used in the project, FrakPak - AIP 410-550 pressurized with a light oil, the complete isolation of the borehole section is followed by the actual stimulation by hydraulic fracturing. Water is pumped into the borehole section through a perforated steel tube, and a successive rise in the pressure level is maintained until a fracture is created or until the maximum working pressure of 200-250 bars is reached. The pressure level is maintained until a sudden pressure drop occurs, i.e. fracture initiation, or the stimulation can be ended without anything happening. In the latter case, the strength of the rock and the stresses present are too high to initiate- or reopen a fracture.

The sudden pressure drop, characterizing the initiation- or a reopening of a fracture, is caused by the dissipation of water into the bedrock through the opened fracture (figure 2-10). The initiated fracture is extended by increasing the pumping rate.

The downhole equipment in this project consists of the double packer unit assembled with thin-walled steel tubes extending slightly above the borehole top. The steel tubes come in three meters lengths and have a diameter of 5/4 inches. A high-pressure water hose is assembled at the top of the steel tube by using a T-coupling unit, and an air bleed-

off valve is mounted on the other side of the T-coupling unit (figure 2–9). Sufficient water pressure is provided by using two high-pressure pumps.



Figure 2–8: A small high-pressure oil pump for the pressurization of upper and lower packer on FrakPak - AIP 410-550 using a low viscosity oil. In front: Two ports for the measurement of the packer pressures.



Figure 2–9: A T-coupling unit on top of the downhole equipment for hydraulic fracturing where a high pressure water hose from the tank lorry is connected. The hydraulic hose below the water hose is for the measurement of water pressure.

Hydraulic fracturing using a single packer unit results in the initiation of only one fracture in the whole borehole column below the packer and is referred to as column fracturing. On the other hand, the use of a double packer unit makes it possible to initiate fractures on different levels in the borehole and is referred to as sectional fracturing. A double packer unit furnished with separate pressurization, can also be used for column fracturing by pressurizing the upper packer only. Common procedure for hydraulic fracturing in the groundwater industry is to place the equipment at the bottom of the borehole and then start with performing column fracturing. After the first initiation of a fracture, the remaining part of the borehole is treated with sectional fracturing. This procedure ensures the initiation of a maximum amount of fractures and the risk of getting the downhole equipment stuck in the borehole is reduced. Doing the opposite, starting at the top and performing sectional fracturing downwards, involves greater risk for the equipment to get stuck if loose rock fragments fall down and jam between the double packer and the borehole wall.

2.1.7 Hydraulic fracturing with injection of sand

The injection of propping agents, such as small and hard bullets like rounded quartz sand, peanut shells, ceramic pebbles et cetera, is common procedure together with hydraulic fracturing in the oil industry. In order to avoid settling of the propping agent before injection, the agents are combined with a viscous mixture of water and thickener. The

purpose of using propping agents is to keep the fractures open after pressure release when performing hydraulic fracturing. The small bullets or grains of sand will then work as spacing material and keep the two fracture surfaces apart (figure 2–10). In theory the need for propping agents or injection of sand in the groundwater industry should be similar to the need in the oil industry, but only a few experiments with limited success are reported (paragraph 2.1.1). A possible explanation for the limited amount of reported success and data regarding the use of propping agents in the groundwater industry, may be the lack of suited equipment and a complicated procedure compared to ordinary hydraulic fracturing with water-only.

Before the injection of sand or propping agents can take place, the desired fracture at a preferred level in the borehole has to be initiated or reopened with ordinary hydraulic fracturing. Using maximum pumping rate, the fracture will be expanded, and after a while a sufficient low counter pressure in the formation should be reached. A sufficient low counter pressure, in this study roughly lower than 100 bars when using a pumping rate of 500 litres/minute, ensures that the pressure required to transport the viscous mixture with sand into the fracture does not exceed the maximum working pressure for the equipment. In order to avoid settling of the sand, the viscous mixture is transferred to a 50 litres volume, high-pressure tank just before injection (paragraph 2.2.2, figure 2–13). The viscosity of the mixture can be characterized as sauce. A few droplets of breaker enzyme are added before closing the high-pressure tank. The high-pressure tank is assembled with the water hose from the tank lorry and a by-pass hose parallel to the tank. The water flows through the by-pass hose when performing hydraulic fracturing with water-only, and after switching the valves to the injection mode, the water is led through the high-pressure tank. In this way, the water is pressing the sand mixture downhole and into the already opened fracture (figure 2–10). Using maximum pumping rate, the tank will be emptied quickly, and the injection should be shut down. In theory, the best effect of the stimulation is achieved when some of the sand grains keep the fracture open at the borehole wall, and when the remaining grains are distributed somewhere else within the fracture. This will ensure good hydraulic communication between the water bearing fracture and the borehole, which in turn means a higher yield for the borehole. Pumping too much water into the fracture after the injection of sand will flush the sand away from the critical location at the fracture opening on the borehole wall. On the other hand, shutting down the stimulation too early will increase the risk of getting the downhole equipment stuck since a large amount of sand will remain between the packer elements.

Hydraulic fracturing - principle

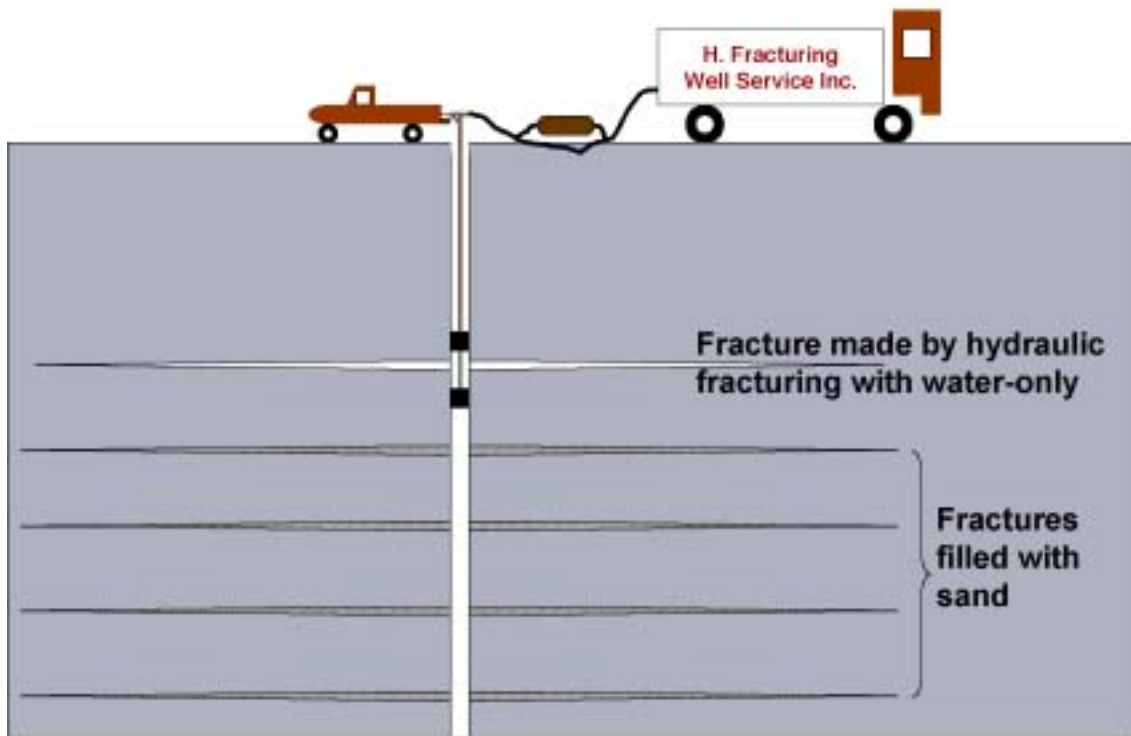


Figure 2–10: Schematic diagram showing the principle of hydraulic fracturing with water-only, and of hydraulic fracturing with injection of sand.

2.1.8 Measurements of water- and packer pressures

Measurement and logging of the packer pressures and the water pressure in the borehole section, or -column, were done during the hydraulic fracturing. Pressure sensors, measuring pressures in the range of 0-500 bars, were connected to: (1) the compressor unit for the pressurization of the packer elements (figure 2–8 and 2–12) and, (2) the steel tube which was in direct contact with the water pressure in the borehole section or -column (figure 2–9 and 2–12). The signals from the pressure sensors were transmitted to, and processed in a measuring bridge, which was connected to a data logger where all the data were recorded. Finally, the stored data were loaded into a laptop.

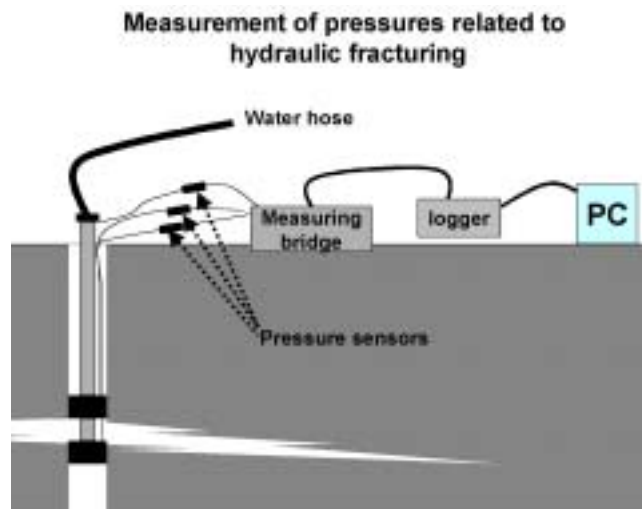


Figure 2–11: Schematic diagram showing the setup used for measurement of the packer pressures and the water pressure in the borehole section or -column during hydraulic fracturing.



Figure 2–12: At left: Pressure sensors connected to a measuring bridge, which is connected to a data logger. The recorded data are loaded into a laptop. At right: A pressure sensor.


2.2 Equipment development

2.2.1 Double packer - FrakPak - AIP 410-550

Equipment for hydraulic fracturing of boreholes in crystalline bedrock has been developed by Brønnteknologiutvikling AS (BTU). The equipment consisted of two fluid-pressure expanding packers assembled to a perforated steel tube, a so-called double packer or straddle packer. The packer elements were made of rubber strengthened with aramid, and the double packer was tested in the laboratory to withstand a pressure of 300 bars. After a field test at Lade (paragraph 3.1 and 4.2.3), the double packer became further

equipped with separate pressurizing of the packer elements. Some technical data for FrakPak - AIP 410-550 are given in table 2–2.

Table 2–2: Technical data for the fluid-pressure expanded double packer, FrakPak - AIP 410-550.

Outer diameter:	4 3/8" / 110 mm	
Inner diameter:	2" / 50 mm	
Maximum expansion diameter:	7" / 180 mm	
Element material:	HNBR and aramid	
Material of mechanical parts:	AISI 316	
Working pressure:	250 bars	
Test pressure:	300 bars	
Blow pressure:	500 bars	
# of expansion up to 250 bars:	> 300 in 5.5" test pipe	
# of stimulations in the field:	40-60	

The advantages of FrakPak - AIP 410-550 compared to the system where the packer elements are mechanically compressed to a larger diameter are:

- Large radial expansion (0.56"/14 mm). At relief, the packers returns completely to its original diameter.
- Many repeated inflations.
- Large mechanical anchor force at axial movement (130 tons at 300 bars inflatable pressure).

2.2.2 High-pressure tank for the injection fluid

A high-pressure tank, for the storage of injection fluid used in the procedure for hydraulic fracturing with injection, has been developed by BTU (figure 2–13). The tank, which withstands a pressure of 250 bars and has a volume of 50 litres, was made of a thick steel tube where spherical ends were welded on to the pipe. Every end consists of two coupling points for the high pressure hose. A by-pass hose parallel to the high-pressure tank makes sure the fracturing of the borehole section can be performed prior to the injection of sand. The actual sand injection takes place as described in paragraph 2.1.7. Before the injection, the tank is filled up via the fill-up point at the top of the tank and closed by screwing on the filler cap.



Figure 2–13: A high-pressure tank for storage of the injection fluid used in the procedure for hydraulic fracturing with injection of sand.

2.2.3 Injection packer for the central borehole

In the planning phase for the pilot plant at Bryn, where the energy extraction is based on circulating groundwater, the water from the heat exchanger was supposed to be returned into the central borehole using an infiltration rate of 20 000 litres/hour. The high infiltration rate would probably have cause a pressure buildup, and a sealing injection packer in the upper part of the borehole was necessary in order to withstand the pressure. A conventional sealing- or injection packer is not designed to deal with pressures of this magnitude, expected to be in the range of 5-10 bars, in a long-run period. Therefore, a new injection packer suited for the central borehole at Bryn was developed and made by BTU (figure 2–14 and table 2–3). The injection packer is set and pulled in one run.

Table 2–3: Some technical data for the injection packer.

Diametres		Strenght parametres	
RIH outer diameter packer	130 mm	Setting force	10 tons
Outer diameter slips	98 mm	Anchor capacity	40 tons
Set outer diameter packer/slips	140 mm	Diff. pressure	100 bars



Figure 2–14: Injection packer for the re-injection of groundwater into the central borehole at Bryn.

2.2.4 Air pressure mixer

The experiences from Bryn (paragraph 5.2.10) showed that the time required to obtain a satisfactory hydration of the thickener (guar gum) and water was a time-consuming parameter in the procedure for hydraulic fracturing with injection of sand. Therefore, as a part of the method development, a CPIM-mixer (**C**ontinuous-**P**articulate-**I**ntensive **M**ixing) was developed by BTU to ensure a rapid hydration of the guar gum powder and water. The CPIM-mixer, a United States Patent 4,191,480, consists of two silos, one for water and one for guar gum powder (figure 2–15). The silos have a volume of approximately 10 litres each. The system is pressurized with air pressure, and by pushing a button, the powder and water are flushed through a conical spreading unit which makes the water wet each grain of guar gum powder. This air pressured wetting of every single grain of powder ensures a complete hydration of guar gum and water in a few seconds.

The mixture is flushed into a collecting unit below the outlet. The CPIM-mixer has a mixing jet diameter of 34 millimetres and a capacity of approximately 7.5 litres/second.



Figure 2–15: Air pressure mixer for the mixing and rapid hydration of thickener and water.

2.3 Geophysical logging equipment

2.3.1 Optical televiewer

Information about geological features like the degree of fracturing, fracture patterns, rock type, mineralized fractures, and strike and dip can be collected from an optical televiewer recording, i.e. a video film of a borehole. The logging equipment for the optical televiewer consists of a probe with the video camera unit and a personal computer recording the film (figures 2–16 and 2–17). The built-in camera unit is at the bottom of the two meter long probe which is equipped with centralizers. The video camera unit consist of a camera, light emitting diodes, hyperbolic mirror, black needle, a brick of rubber, and glass (figure 2–18). In the operation mode, light from the diodes hits the hyperbolic mirror which illuminates the borehole wall. Reflected images of the borehole wall are centred by the mirror and recorded by the camera. The images from an optical televiewer inspection have a resolution of 360 or 720 dots per inch (dpi), and recommended logging speed is approximately one meter of borehole wall per minute.



Figure 2–16: Probe for optical televiewer inspection of boreholes equipped with centralizers. Video camera unit at the right.



Figure 2–17: Computer controller and cable reel for optical televiewer.

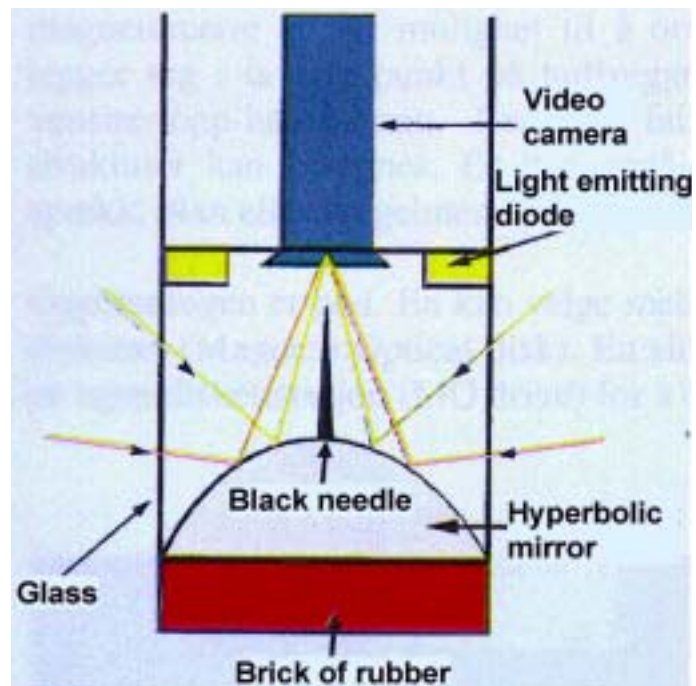


Figure 2–18: Schematic diagram showing the recording of points at the borehole wall, and the components in the video camera unit of the optical televiewer.

2.3.2 Temperature, electric conductivity and natural gamma (TCN-log)

A probe measuring the temperature (T) and the electric conductivity (C) of the water in a borehole, and the natural gamma radiation (N) of the bedrock is used in connection with the optical televiewer. The TCN-sensors are mounted at the end of a two meter long probe equipped with centralizers. Both the cable and the personal computer are used in the measurements in the same way as described for the optical televiewer, and a continuous log showing the values of the three parameters in the whole borehole is achieved.

Recommended logging speed is approximately three meters of borehole wall per minute.

A continuous log of the temperature and electric conductivity of the water in a borehole is a useful tool for identifying possible water-bearing fractures. The properties of the water emanating from a water-bearing fracture can differ, in terms of changed ionic composition and to some extent with the temperature, compared to the remaining water in the borehole. In addition, the temperature profile gives a picture of the local geothermal gradient. Mineralogical changes in the bedrock caused by a changed level of potassium, are registered in the profile showing the total and natural gamma radiation in the borehole. Potassium, which is a radioactive element, is among others present in alkali feldspar (Elvebakk and Rønning, 2001). Together, the information from the drilling report, optical televiewer and the gamma log makes it easier to determine the type of rock present in the borehole.

2.3.3 Impeller flowmeter probe

The flow of water emanating from the surrounding bedrock into a borehole can be measured using an impeller flowmeter probe from the same logging set and with the same configuration as the optical televiewer and the TCN-device (figure 2–19). The flow in both up- and downwards direction in the borehole is recorded by a propeller (figure 2–20). The velocity or the number of revolutions for the propeller is registered in a personal computer, and inflowing water will disturb the velocity pattern in the borehole. Flow measurements in boreholes can be performed in two ways when using the impeller flowmeter, either (1) by continuous measurements where the probe is taken up- and downwards in the borehole at a constant rate, or (2) by stationary measurements where the probe is placed at a certain level in the borehole. Stationary flow measurements should be performed by placing the propeller just above and just below a fracture level. Continuous flow measurements will give the propeller a certain velocity, and the net velocity or the flow is then given by taking the difference between the up- and down velocity (Elvebakk and Rønning, 2003). Because the propeller is already rotating, the most accurate determination of small changes in the flow pattern is obtained by performing continuous flow measurements. The presence of water-bearing fractures in the borehole can be further enhanced by performing simultaneous pumping. The pump should be placed above the probe (figure 2–20), and marked changes in the flow pattern are easier to detect.



Figure 2–19: Impeller flow meter probe (Elvebakk and Rønning, 2003).

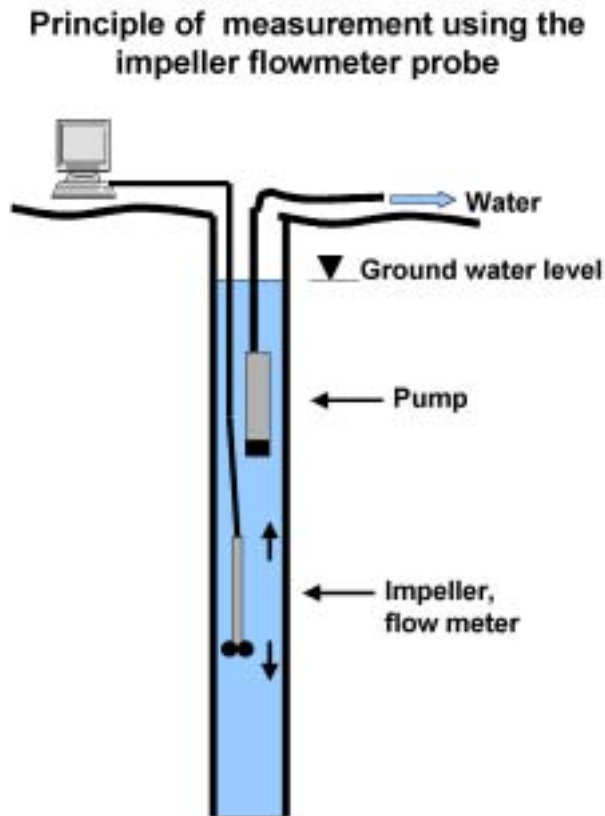


Figure 2–20: The impeller flowmeter probe is a useful tool to identify water-bearing fractures in the borehole (Elvebakk and Rønning, 2003).

2.4 Testing of borehole yield

Test pumping of boreholes in crystalline bedrock is performed in order to quantify the total water yield of a borehole. Occasionally test pumping also aims to identify water-bearing fractures in a borehole.

2.4.1 Equipment for test pumping

Several kinds of submersible pumps have been used at different stages in the study. The pump characteristics for the actual pumps, called pump A, B, C, D and E are shown in figure 2–21. A polyethylene pipe with inner diameter of 32 millimetres has been used as surge pipe in all the test pumping.

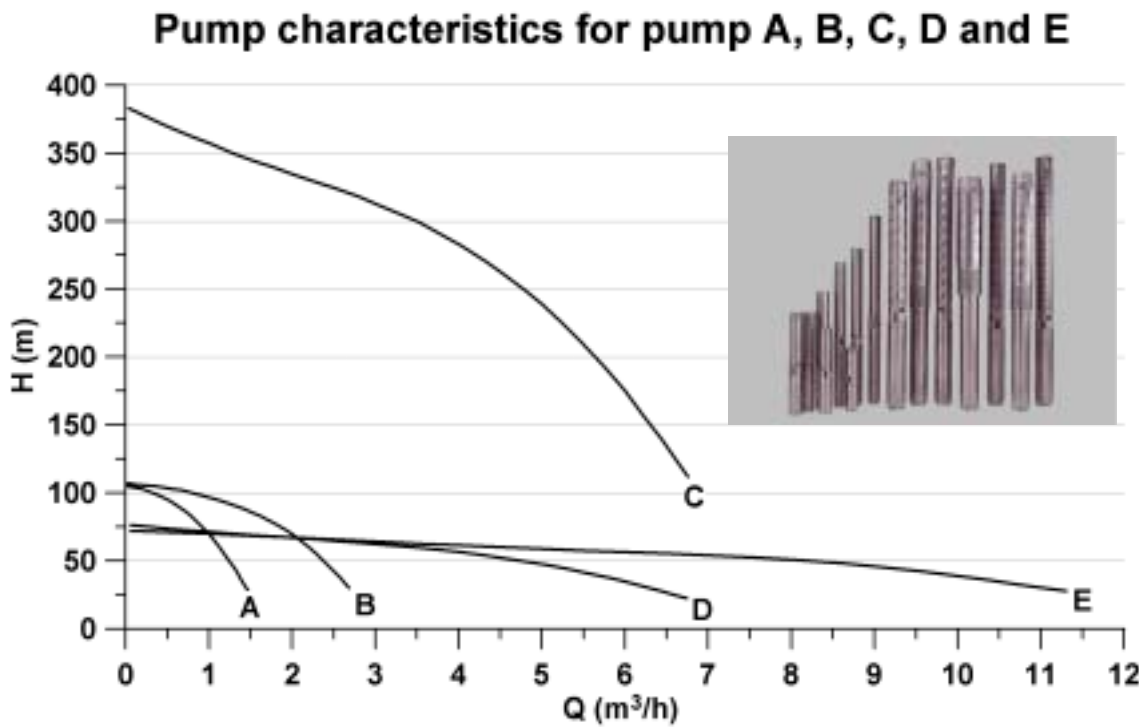


Figure 2–21: Pump characteristics for pump A, B, C, D and E used in the study (after Grundfos, 2004).

Pressure sensors with different measuring ranges have been used to measure any changes in the groundwater level due to the disturbances caused by test pumping and hydraulic fracturing. The variation in the measuring range and the application of the pressure sensors employed in the investigations are listed in table 2–4.

All the flow data from the test pumping were measured by an electromagnetic flow meter. The flow meter was connected to the outlet of the polyethylene pipe (figure 2–22), and the measuring range is from 0.3 to 6.0 m³/hour. All the measured flow and groundwater level data were stored in intervals of eight or twelve seconds in a standard data logger (figure 2–23). The input signal for the data logger is 4-20 mA.

Table 2–4: The variation in the measuring range and application of the pressure sensors.

Area of application for pressure sensors	Measureing range [meters of water column]			
	0-10	0-20	0-100	0-300
Measuring the changes in the groundwater level in the pumping borehole. The pressure sensor is connected to the pumping equipment slightly above the pump, and was used in the test pumping performed at Lade and Bryn (figure 2–22).			X	
Monitoring the response of the groundwater level in the surrounding boreholes for the borehole where test pumping and hydraulic fracturing were performed at Bryn and EAB.	X			
Measuring the changes in the groundwater level in the pumping boreholes at EAB. The setup is similar to Lade and Bryn, described above.				X
Monitoring changes in the groundwater level above the upper packer in the pumping borehole when performing sectional- or columnar test pumping at Bryn.		X		



Figure 2–22: Pressure sensor connected to the test pumping equipment (left), and a flow meter (right).



Figure 2–23: Data logger used in the study (ETM Pacific, 2003).

2.4.2 Different kinds of test pumping: Ordinary, columnar- and sectional

Different kinds of test pumping have been employed in the study. Ordinary test pumping has been performed at Lade and at the pilot plant at EAB. In this context, *ordinary test pumping* means the pumping of groundwater from a borehole in crystalline bedrock without using sealing packers. The pumping equipment consists of a submersible pump, power supply and a surge pipe.

Performing both columnar- and sectional test pumping have been necessary at Bryn. The meaning of *columnar test pumping* in this context describes a test pumping procedure where one sealing packer is located above the pump. Atmospheric pressure equilibration in the water column where the test pumping is performed, is provided by a ventilation tube going through the packer and up to the surface. The sealing packer is pressurized by compressed air. The use of a sealing packer makes it possible to exclude large and highly conductive fracture zones, intersecting the borehole, from the pump test.

The actual pumping equipment consists of a submersible pump, power supply, surge pipe and a sealing packer furnished with a ventilation tube.

In this context, *sectional test pumping* describes a test pumping procedure where the submersible pump is placed between two sealing packers. The active test pumping section, or the distance between the packers, is 15 meters. Similar to the columnar test pumping set up, a ventilation tube through the upper packer provides atmospheric pressure equilibration in the test pumping section. The pumping equipment consists of a submersible pump, power supply, a surge pipe and two sealing packers where the upper packer is furnished with a ventilation tube (figure 2–24).

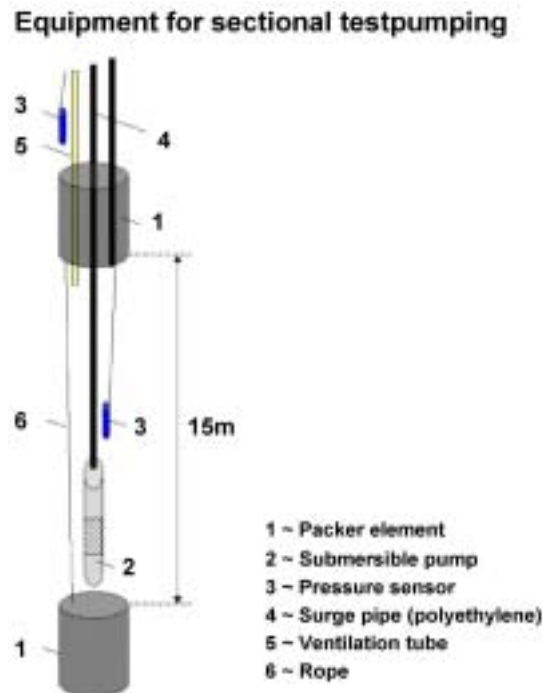


Figure 2–24: Equipment for sectional test pumping.

2.4.3 Sink- and rise tests: Theory

The paragraph is based on Storrø et al. (2002).

Data from test pumping consist of diagrams showing:

- How the pumping rate or the emuent groundwater varies as a function of time.
- How the groundwater level (pressure level) in the borehole decreases over time due to the pumping of water: - Sinking curve.
- How the groundwater level in the borehole increases when the pumping is stopped: - Rising curve.

The course of the sinking- and rising curves can locate water-bearing fractures in the borehole. The crossing of water-bearing fracture zones, intersecting the borehole, will appear as breaks in both the sinking- and rising curve. The breaks in the curves appear because when the water level in the borehole is at the same level as a water-bearing fracture zone, the emptying or filling of the larger fracture volume is more time-

consuming compared to a watertight part of the borehole with smaller volume. Sources of error, like disturbance from uncontrolled variations in the pumping rate and decreasing pump capacity with increasing head, can influence the sinking curve. The rising curve is not exposed to any disturbances and is the most reliable source in order to map breaks on the curve or possible water inlets in the borehole. Breaks in the curves are often difficult to identify if the groundwater level is plotted as a function of time. Instead, a curve which presents the velocity of the groundwater changes, the so-called sinking- or rising velocity should be plotted. Thus, the sinking- or rising velocity curve is the derivative of the groundwater level as a function of time, and could easily be obtained since the groundwater level is measured in intervals on eight or twelve seconds.

The maximum short-time production yield for a borehole in crystalline bedrock can be determined by placing the submersible pump in the bottom of the borehole. By using a higher pumping rate than the assumed production yield for the borehole, the groundwater level is lowered down to the water inlet at the pump. The pumping is continued and since the groundwater level is at the same level as the water inlet on the pump, the pump will slurp a mixture of water and air. -Hence the term “slurping”. The volume and rate of pumped groundwater in the whole period of slurping is measured by a flowmeter, and the maximum short-time production yield is determined from these results (paragraph 2.4.4). A long term operation of the pump in the *slurping* mode could cause damages to the pump and should be avoided.

It will not be possible to empty the borehole if the total production yield of the borehole is larger than the specific capacity of the pump. The groundwater level is lowered as usual, but will gradually stabilize in a level defined as a state of equilibrium between the inflow of water into the borehole and the maximum pumping rate at the given head.

Maximum benefit from this kind of analysis are only achieved on the understanding that the pumps have sufficient capacity to perform complete draining of the borehole. Obtaining equipment suited for high-yielding boreholes in crystalline bedrock can be problematic. The equipment often gets expensive, heavy and unhandy.

2.4.4 Estimation of water yield

The water yield for the different boreholes, borehole sections or -columns where test pumping has been performed, can be estimated in several ways. In this study, the results are interpreted in three different ways, called (1) average, (2) rising curve, and (3) pumping rate. These three methods can be described as follows:

- 1) Average: The calculations assume a fluctuating pumping rate or “slurping mode” where the groundwater level is lowered down to the water inlet at the pump, and a mixture of water and air is slurped. The water yield from a test pumping with fluctuating pumping rate can be found by summing all the values, and by dividing this sum with the time period for the fluctuating pumping rate. The water yield, denoted as Q_{average} can be expressed as:

$$Q_{\text{average}} = \frac{Q_{\text{values}}}{\Delta t} \quad [2.11]$$

where Q_{values} is the pumping rate at a given time, and Δt is the time period for the

fluctuating pumping rate. The Q_{average} value may be somewhat high compared to the real production yield because the fluctuating pumping rate tends to stabilize at a somewhat lower level over time.

- 2) Rising curve: Similarly to Q_{average} , the calculation of the water yield from the rising curve assumes a complete lowering of the groundwater level down to the water inlet at the pump. The rising curve results from the rising groundwater level in the borehole after finishing the test pumping, and is plotted as a function of time (paragraph 2.4.3). In theory, the rising curve is supposed to have a linear course. The water yield is calculated with basis in the equation from a linear trend curve fitting the rising curve. The total rise in the groundwater level, Δh is found from the course of the rising curve. The time period Δt for the groundwater rise is calculated from the Δh -value and the trend curve equation. Δh is also used in order to calculate the volume V for the borehole section or -column. The water yield, denoted as Q_{rise} , can be calculated as follows:

$$Q_{\text{rise}} = \frac{V}{\Delta t} \quad [2.12]$$

Complete rising curves are considered to be conservative estimates of the total production yield of a borehole, Q . Q_{rise} is lower than Q because the water has to seep into the drained fractures and fill them up before the borehole section or -column is filled. In this way, the filling of the borehole section or -column is more time consuming than it would have been if the fractures had already been filled. Thus, the highest $\Delta h/\Delta t$ -relation provides the most accurate value for Q_{rise} as a measure of Q .

- 3) Pumping rate: Estimating the water yield by using the pumping rate method implies an interpretation of the pumping rate course after finished pumping. Similar to the Q_{average} - and the Q_{rise} -methods, the calculation of the water yield based on the pumping rate, assumes that the groundwater level is lowered down to the water inlet at the pump. In those cases where the pumping rate follows a steady course, a good picture of the water yield can be achieved by extrapolating the pumping rate after finishing the test pumping. Since the groundwater level is drawn down to the water inlet at the pump, the water yield will reflect the amount of inflowing water into the borehole, borehole column or -section. The value for the water yield estimated by the pumping rate method is relatively conservative due to the fact that the pumping rate is often decreasing over time. In this study, an extrapolated value for the pumping rate after approximately 200 minutes of pumping is read.

The driller's estimate of the short-time production yield of a borehole is common procedure when finishing up the drilling of a borehole. The estimate is calculated from the recovery rate of the groundwater level after draining the borehole with compressed air.

2.5 Water quality in ground source heat pump systems based on circulating groundwater

The section is mainly based on literature from Lindblad-Påsse (1986) and Andersson (1992) in Kalskin (1998).

The three geochemical conditions of major importance for ground source heat pump systems based on groundwater are:

- The content of precipitable elements in the water,
- the content of elements capable of coating metallic surfaces in the water, and
- the content of corrosive elements in the water.

Problems related to precipitation are especially large in plants where the heat exchanged water is reinjected into the groundwater magazine. Reinjection of groundwater is common procedure and desirable to maintain the capacity of the groundwater magazine.

Water quality investigations should be equally important as hydrogeological investigations in the early construction phase of plants based on circulating groundwater to evaluate the risk for chemical precipitation and corrosion. Strict limit values for iron and other elements or chemical compounds are of minor interest since high-rate pumping of large quantities of water can change the water quality. Microorganisms can also cause problems under very different conditions. Still, a few attempts have been made to generate a general classification for the risk of precipitation and corrosion related to the content of certain elements or chemical compounds in groundwater:

- Gustafson (1983) states that 0.3 mg Fe/l and 100 mg Ca/l are the limit values for iron and calcium, respectively. Experiences from the use of groundwater for domestic water supply purposes shows that a calcium content of more than 35 mg/l causes problems with precipitation in kettles, heat elements et cetera.
- In a general classification of water, concerning the risk of precipitation and corrosion, the concentration of iron and manganese are recommended to be less than 1 mg/l and 0.5 mg/l, respectively (Lindblad-Påsse, 1986).

Problems in heat pump systems caused by chemical precipitation is mainly connected to the precipitation of carbonates, iron and manganese. Precipitation of other compounds like calcium sulphate (CaSO_4), barium sulphate (BaSO_4), silicates and sulphur compounds can occur. Precipitation of lime (calcium carbonate, CaCO_3) can occur around the borehole if the carbonate hardness in the groundwater is high. Iron- and manganese deposits are mainly composed of low-solubility iron- and manganese hydroxides, and is an increasing problem when extracting large amounts of groundwater from an aquifer. The growth of iron- and manganese hydroxides is caused by changed redox conditions or by bacterial activity. Bacterial activity can cause precipitation in the pumping borehole and infiltration facility. Chemical precipitation, caused by changes in the redox potential, mostly occurs in the infiltration facility. The solubility of iron in water is highly dependent on the Eh- and pH-conditions, and small changes will cause discernible effect. Due to the catalysing effect of iron bacterias, the bacterial activity is of great importance for the iron deposits. *Gallionella Ferruginea* is the most common iron bacteria. In general, iron- and other chemical precipitations can be treated with strong acids with stabilizers (citric acid/acetic acid) (Lindblad-Påsse, 1986).

Corrosion of metallic tubes can be electrochemical or bacterial. Chemical breakdown of a protecting oxidation coat can also cause corrosion. Well filters, casing- and pumping parts in the borehole, valves and couplings, heat exchangers and evaporators are most likely to be exposed to corrosion in ground source heat pump systems based on circulating groundwater. In this setting, the pH-value can cause acid- and alkaline corrosion, and interferes chemical balances of importance for corrosion and the growth of anti-corrosive coatings. The corrosivity of the water also depends on the content of dissolved oxygen and carbon dioxide, temperature conditions, flow velocity, dissolved salts and sulphuric acid.

The infiltration borehole in a ground source heat pump system based on circulating groundwater should be designed for backflushing of particulate clogging on a routinely basis. A reduced capacity of the infiltration borehole due to clogging of fine particles in suspension, can be discovered by continuous pressure surveillance of the circulating water in the system.

2.6 Laboratory methods

2.6.1 Water analysis

The paragraph is mainly based on information from the laboratory at the Geological Survey of Norway (NGU-Lab) (2002b). NGU-Lab offers a standard package for groundwater analysis. The most important physical and inorganic parameters for the examination of groundwater for drinking water purposes are included in the analysis. The testing medium consists of (1) a 0.5 litres raw water sample for the pH-, electrical conductivity-, alkalinity-, turbidity- and colour analysis, (2) a filtered (0.45 μm filter-paper) 100 millilitres sample for the anion analysis, and (3) a 100 millilitres filtered and acidified sample (added 0.5 millilitres of ultra pure 65% nitric acid) for the cation analysis (figure 2–25). The water samples are labelled, and stored in a cool place before the analysis is performed. Information about lower detection limit, analysis uncertainty, procedure according to the Norwegian standard (NS), and measuring instruments used in the analysis of all the different parameters is given in tables 2–5 and 2–6.



Figure 2–25: Water sample.

Table 2–5: Lower limit of detection and analysis uncertainty for the analysed cations.

Element	Lower limit of detection (ppb)	Analysis uncertainty (\pm %)	Element	Lower limit of detection (ppb)	Analysis uncertainty (\pm %)
Si	20	10	V	5	5
Al	20	10	Mo	10	10
Fe	10	5	Cd	5	20
Ti	5	5	Cr	10	10
Mg	50	5	Ba	2	5
Ca	20	5	Sr	1	5
Na	50	10	Zr	5	10
K	500	20	Ag	10	10
Mn	1	5	B	20	10
P	100	5	Be	1	5
Cu	5	5	Li	5	20
Zn	2	5	Sc	1	5
Pb	50	20	Ce	50	20
Ni	20	5	La	10	10
Co	10	5	Y	1	5

Table 2–6: Measuring range, lower limit of detection, analysis uncertainty and procedures according to Norwegian standard (NS) for the analysis of anions, electric conductivity, pH, t-alkalinity, colour and turbidity.

Parameter	Measuring range	Lower limit of detection	Analysis uncertainty (\pm % rel)	Procedure (NS#)
F ⁻	-	0.05 mg/l	\pm 10 % rel	-
Cl ⁻	-	0.1 mg/l	\pm 10 % rel	
NO ₂ ⁻	-	0.05 mg/l	\pm 10 % rel	
Br ⁻	-	0.1 mg/l	\pm 10 % rel	
NO ₃ ⁻	-	0.05 mg/l	\pm 10 % rel	
PO ₄ ³⁻	-	0.2 mg/l	\pm 10 % rel	
SO ₄ ²⁻	-	0.1 mg/l	\pm 10 % rel	
el. cond.	0.04-0.2	0.07 mS/m	\pm 3 % rel	NS-ISO 7888
"	>0.2	"	\pm 1 % rel	
pH	-	-	0.05 pH-units	NS 4720
t-alkalinity	0.04-0.2	0.04 mmol/l	\pm 0.04 mol/l	NGU-SD 3.7B (follows the earlier NS 4754)
"	0.2-2.0	"	\pm 4.0%rel	
"	>2.0	"	\pm 1.0 %rel	
colour	-	1,4	\pm 7.5 %rel	Equivalent to NS 4787 (1988)
turbidity	0.05-1.0	0.05 FTU	\pm 0.04 FTU	NS 4723
"	1.0-10	"	\pm 0.4 FTU	
"	10-100	"	\pm 4.0 FTU	
"	100-1000	"	\pm 40 FTU	

2.6.2 XRF-, XRD- and petrographical analysis

This paragraph is mainly based on NGU-Lab (1999a and 1999b). X-ray fluorescence (XRF) spectrometry is a method for the quantification of elements in a sample. XRF-analysis can determine the contents of major (> circa 0.5%) and trace (< circa 0.5%) elements. The XRF-analysis is performed by radiating high-energy X-rays into the sample. The radiating makes the elements return rays of fluorescence, and the given wavelengths are characteristic for the given elements. By using angular dependent reflection through a suitable crystal, the separated wavelengths are then registered by a detector. XRF-analysis suits elements with atomic number greater than nine. The detection properties vary, but are generally at ppm-level. A sample (isoformed/melted sample) of minimum three grams is needed to analyse the major elements like SiO₂, Al₂O₃, Fe₂O₃¹, TiO₂, MgO, CaO, Na₂O, K₂O, MnO og P₂O₅, while a sample of minimum seven grams is needed to analyse the tracer elements (V, Cr, Co, Ni, Cu, Zn, Ga, Sc, As, Mo, W, Ag, Cd, Sn, Sb, Rb, Sr, Y, Zr, Nb, Ba, La, Ce, Nd, Yb, Pb, U, Th, S, Cl og F). The analysis of S, Cl and F can be considered as semi quantitative.

X-ray diffraction (XRD), is an important analysis method for the identification of minerals. The method of analysis is principally based on the fact that the reflection of a monochromatic X-ray, directed to the surface of a crystal, is dependent on the grid structure of the crystal. The XRD-analysis is performed by varying the incoming angles

1. Total Fe is reported as Fe₂O₃.

of the X-rays, and the corresponding exit angles are registered. Both angles are analogous to the lattice spacing related to different sets of planes, and is registered as a diffractogram. Thus, every mineral will have its own unique pattern, like a fingerprint for this mineral. The identification is done by comparing the unidentified patterns to patterns for known minerals. Patterns for the known minerals are brought out from a database. Principally, the area below a peak in a diffractogram is proportional to the concentration of the mineral causing the peak. Some effects are often present dealing with XRD-analysis. For instance, line overlap, matrix effects, unsuited reference materials et cetera, are effects which complicate this kind of quantification. NGU-Lab uses a computer controlled instrument, which has a programmable optic and a software based identification.

Petrographical analysis of rocks is made using thin sections. Thin-sections are made by cementing the rock material in a capsule of resin, and then make 0.30 micrometers slices. The different minerals are identified by using different optical techniques when studying the thin-section under the microscope.

2.7 Measuring the terrain level

It is not known whether hydraulic fracturing with water-only and hydraulic fracturing with injection of sand can cause changes to the terrain surface. Large changes to the terrain surface can in the worst cases cause setting damages on nearby buildings. Therefore, potential changes in the terrain level have been recorded using levelling by telescope, before and after stimulation with hydraulic fracturing. An elevation of the nearby surface is the most likely consequence of the hydraulic fracturing due to the high pressures and the large amount of water used in the stimulation. The possible elevation of the surface is given by the difference in height Δh measured, against a fixed reference point outside the assumed area of influence for hydraulic fracturing (figure 2–26).

Levelling possible changes in the terrain - principle

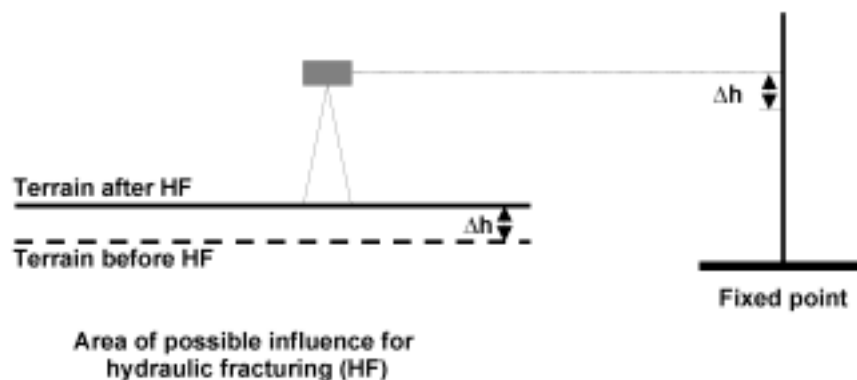


Figure 2–26: Measuring changes in the terrain level by using a levelling telescope.

2.8 Thermal response test

The results from a thermal response test give the effective in-situ value of the rock thermal conductivity and the borehole thermal resistance (Gehlin, 1998). These parameters are important for optimising the design of larger ground source heat pump system with collectors in vertical boreholes. The effective in-situ value of the rock thermal conductivity is mainly the sum of the thermal conductivity of the bedrock (conduction) and the groundwater flow in the borehole (convection).

The thermal response test is performed by heating the collector fluid which circulates in a closed loop collector in the borehole (figure 2–27). The resulting temperature change in the borehole, represented by the mean temperature of the collector fluid, is recorded. The minimum duration of the test should be 60 hours, and the recommended test period is 72 hours (Gehlin, 1998). A high thermal response, or a rapid temperature change in the borehole indicates a low energy absorption in the surrounding bedrock, and the effective in-situ value of the rock thermal conductivity is low. Otherwise, a low thermal response or a slow temperature increase indicates a high energy absorption in the surrounding bedrock, and the effective in-situ value of the rock thermal conductivity is high. The fluid-to-borehole wall thermal resistance, R_b , gives the temperature difference between the fluid temperature in the collector and the temperature at the borehole wall for the specific heat transfer rate (Gehlin, 2002).

The main sources of error related to a thermal response test is (1) leakage of heat, (2) variable electric voltage, (3) correct determination of undisturbed temperature in the ground and (4) groundwater flow and the thermosiphon effect (Gehlin, 2002). In addition, the length of the borehole will influence the thermal properties. Because the temperature increases towards depth and the surface area between the collector fluid and the surrounding bedrock is larger, the effective in-situ value of the rock thermal conductivity is higher for deep boreholes compared to shallow boreholes (Brekke, 2003).

In a study of the thermal conductivity of the rocks in Bærum municipality (figure 2–28 and 2–29), the median value for the Ringerike sandstone at Bryn and the nodular limestone at EAB is measured to be 3.3 and 2.7 W/m,K respectively (Midttømme et al., 2000).

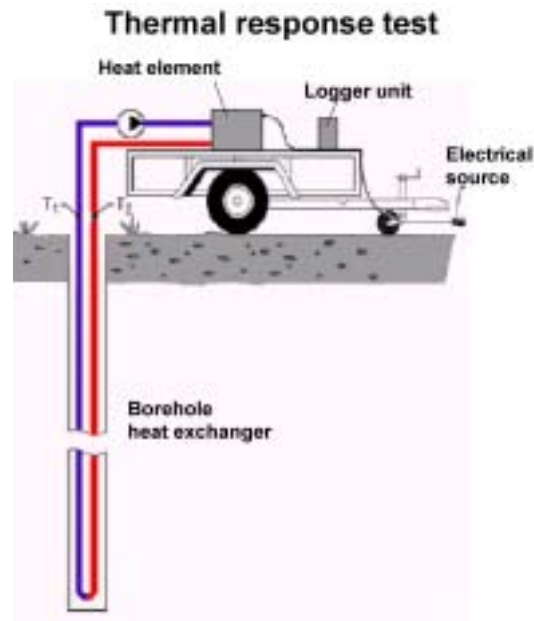


Figure 2–27: Thermal response test equipment (Gehlin, 2002).

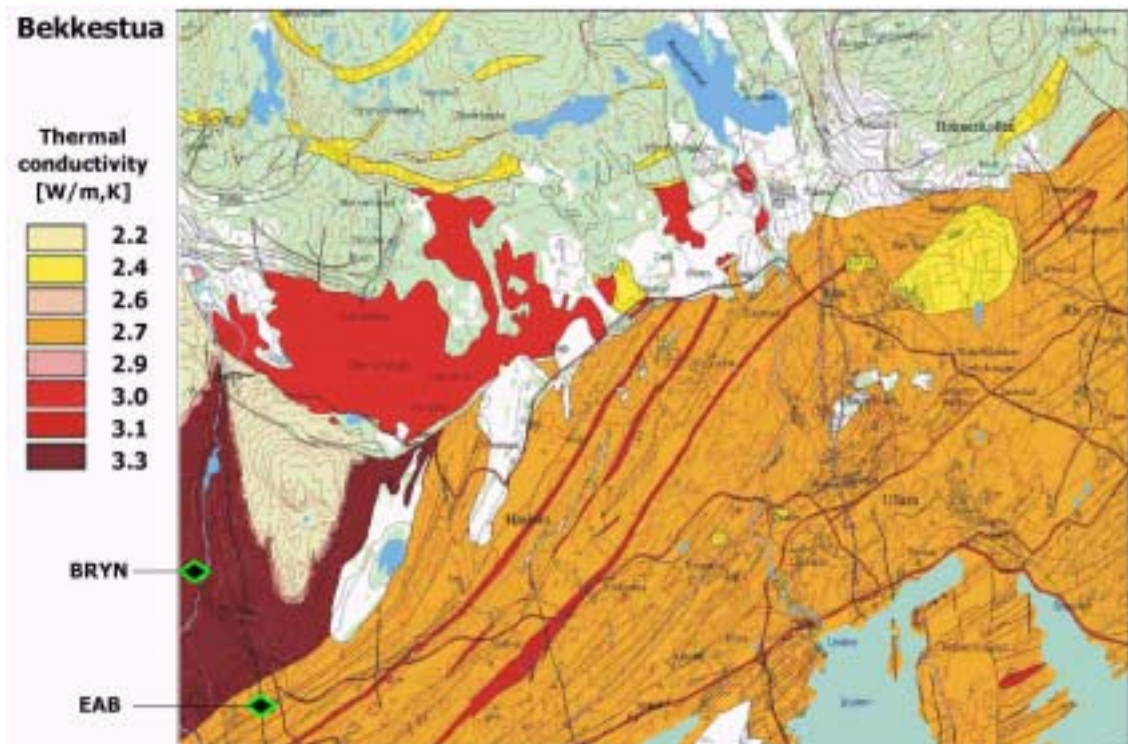


Figure 2–28: The thermal conductivity of the bedrock in the Bærum municipality at Bekkestua map sheet (Midttømme et al., 2000). The location of the pilot plants at Bryn and EAB is indicated.

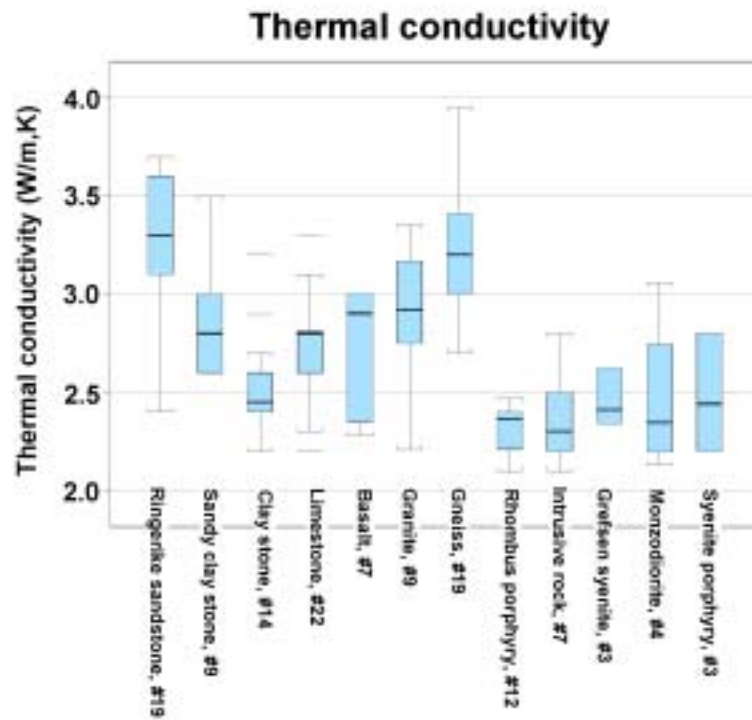


Figure 2–29: Measured thermal conductivity of rock samples mainly from Asker and Bærum municipality presented as boxplots (modified from Midttømme et al., 2004).

Chapter 3 Research areas

The research areas of this project were located at Lade, Bryn and EAB. The pre-testing of equipment and methodology for sectional hydraulic fracturing in boreholes in crystalline bedrock took place at Lade in Trondheim. The two pilot plants are located at Bryn and EAB, about 15 and 13 kilometres west of Oslo, respectively (figure 3–1). The purpose of the pilot plants was to demonstrate the special kind of ground source heat pump system where circulating groundwater gets energy from large and artificially created fracture planes in crystalline bedrock. The pilot plants were sited in Bærum municipality at the request of the company Energiselskapet Asker og Bærum AS, one of the major financial contributors to the project. The exact location was determined in co-operation with the local property department which will take over the plants and all its installations free of charge when the research activities in the project are finished.



Figure 3–1: The research areas of the project were at Lade, Bryn and EAB.

3.1 Lade - investigations, geology and borehole facts

The testing of the newly developed equipment for hydraulic fracturing, FrakPak - AIP 410-550 (paragraph 2.2.1), and the procedure for hydraulic fracturing had to be done in an early phase of the project. The site for this testing included two boreholes in crystalline bedrock just outside NGU's head office building at Lade in Trondheim (figure 3-1). Borehole 1 (inclined) and borehole 2 (vertical) were drilled in 1991 and 2000, respectively. The work performed in these boreholes can be summarized as follows:

- Test pumping before and after hydraulic fracturing.
- Water analysis.
- Borehole inspection with optical televiewer before and after hydraulic fracturing.
- TCN-logging in borehole 2 before hydraulic fracturing with injection of sand.
- Hydraulic fracturing with water-only in borehole 1
- Hydraulic fracturing with injection of sand in borehole 2.
- Levelling of surface points related to hydraulic fracturing operations.

Towards depth, the greenstone layer at Lade is followed by trondhjemite, which explains the increasing amount of quartz appearing in the lower parts of the boreholes. A linear fracture zone close to the boreholes has a strike and dip of 230 and 79 degrees, respectively (Banks, 1991). Borehole 1 is 80 meters deep and has an inclination of 64 degrees towards the fracture zone, while borehole 2 is vertical and 100 meters deep. The distance between the two boreholes is approximately 20 meters. The main water inlet in borehole 1 appears at 39-40 running metres and the groundwater level varies around 23-24 running metres from the top of the borehole (figure 3-2). (In this context the term "running metre" means the depth of the borehole, in meters, measured along the inclined borehole using the top of the borehole as the reference level.) Two minor water-bearing fracture zones appear at 33.5 and 60-61 running metres (Banks, 1991). The results from rock stress measurements carried out for the construction of an underground water treatment plant nearby, showed that the minimal principal stress is 3.2-3.3 MPa (oral communication with Ægir Jóhannsson, SINTEF).

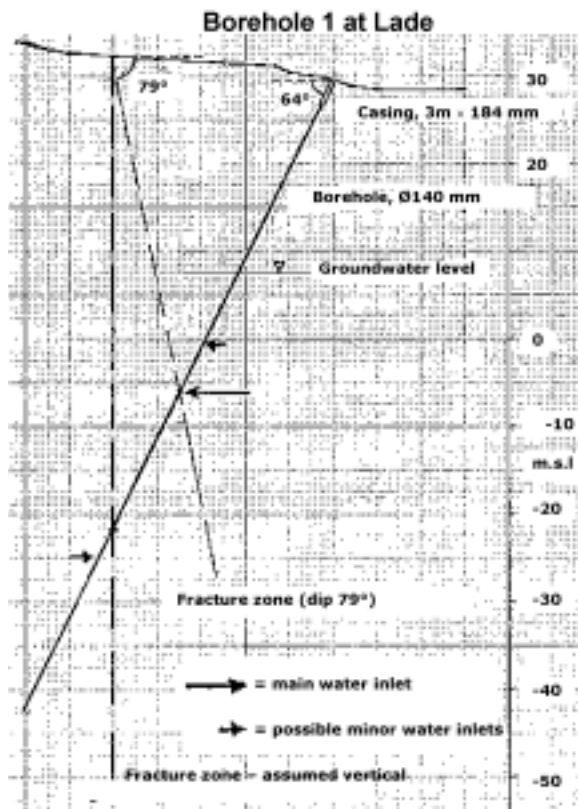


Figure 3–2: Section of borehole 1 at Lade (Banks, 1991).

3.2 Bryn - investigations, geology and borehole facts

Bryn primary school was chosen to be the site for the first pilot plant in the project (figure 3–1). The following investigations have been performed at Bryn:

- Structural geological pre-investigations.
- XRF-, XRD- and thin-section analysis made of drill cuttings.
- Test pumping and groundwater analysis before and after hydraulic fracturing with water-only, and after hydraulic fracturing with injection of sand.
- Rock stress measurements.
- Geophysical logging of the boreholes using the optical televiewer and the TCN-logging device before and after hydraulic fracturing with water-only, and after hydraulic fracturing with injection of sand.
- Hydraulic fracturing with water-only and hydraulic fracturing with injection of sand.
- Levelling of the terrain surface together with hydraulic fracturing with water-only and hydraulic fracturing with injection of sand.
- Thermal response test.
- Test run of the pilot plant.
- Computer modelling of the energy potential of the pilot plant.

The structural geological pre-observations are based on data from Larsen (2001). The bedrock at Bryn consists of a low-metamorphic sandstone of the Ringerike group from the late Silurian time period (figure 3–4). The “Ringerike sandstone” is a generic term for several locations with sandstone-like rock types in Eastern Norway from this geologic time period. The Ringerike sandstone at Bryn is a part of the Kolsås formation (figure 3–5). The pre-investigations revealed that the rock is a massive quartz-rich sandstone, compact and well compressed with a low matrix porosity. The rock is composed of benches with varying thickness of 20-50 centimetres, and the benches are separated by thin layers of shale having a thickness of 1-2 centimetres. The thickness of the Ringerike sandstone in the Kolsås formation, which has an anticlinal shape, is calculated to be about 350 meters at Bryn. The degree of fracturing is very low for the sandstone benches. The few fractures appearing are all very smooth, planar, tight and probably filled with very thin layers of quartz. The fractures are characterized to have a tension origin. The strike and dip of the bedding is 6/13, or strike 6 degrees from north, and dip 13 degrees towards east. Four fracture directions are observed in the nearby area, and the strike and dip relations are as follows: (1) 175/73, (2) 184/35, (3) 100/73 and (4) 303/87. In addition to the low-metamorphic sandstone, eruptive dikes are likely to appear in the boreholes.

The exact location of the boreholes at Bryn was determined by the results from the structural geological pre-observations. Borehole 1, 3 and 5 were placed parallel to the strike direction for the bedding and the fracture direction 184/35, while borehole 2 and 4 were placed normal to the mentioned direction (figure 3–3). The distance from the central borehole to the satellite boreholes is 13 meters, and the distance between the satellites is about 17 meters. The boreholes are 5.5” (140 mm) in diameter and 100 meters deep.

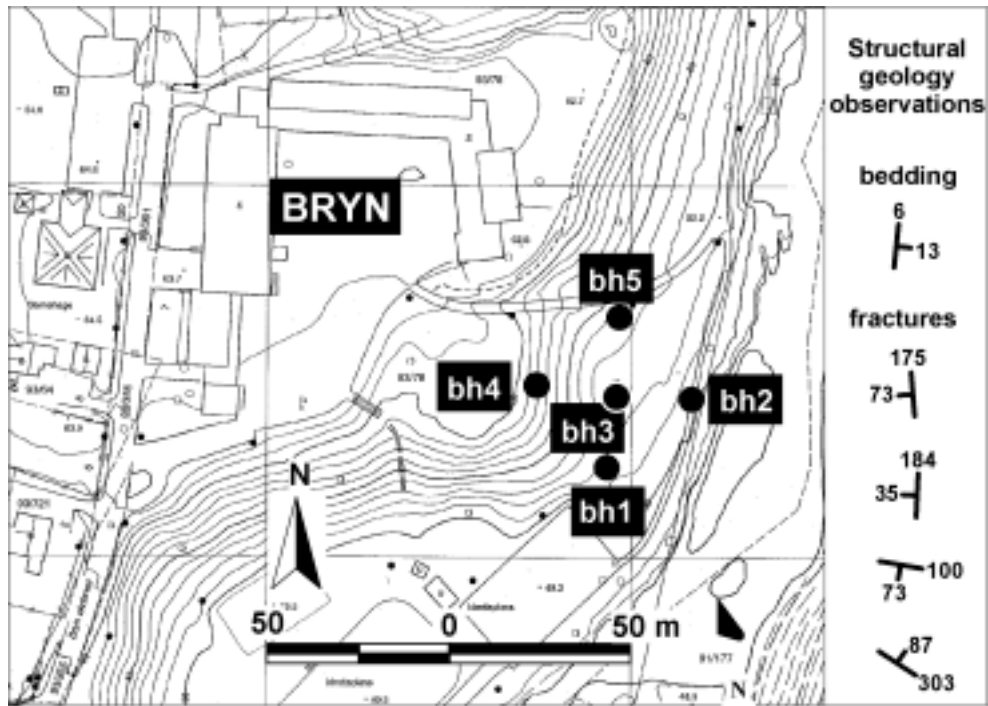


Figure 3–3: The pilot plant at Bryn primary school in Bærum municipality outside Oslo, Norway.

The location of the Bryn- and EAB-boreholes in the stratigraphic sequence

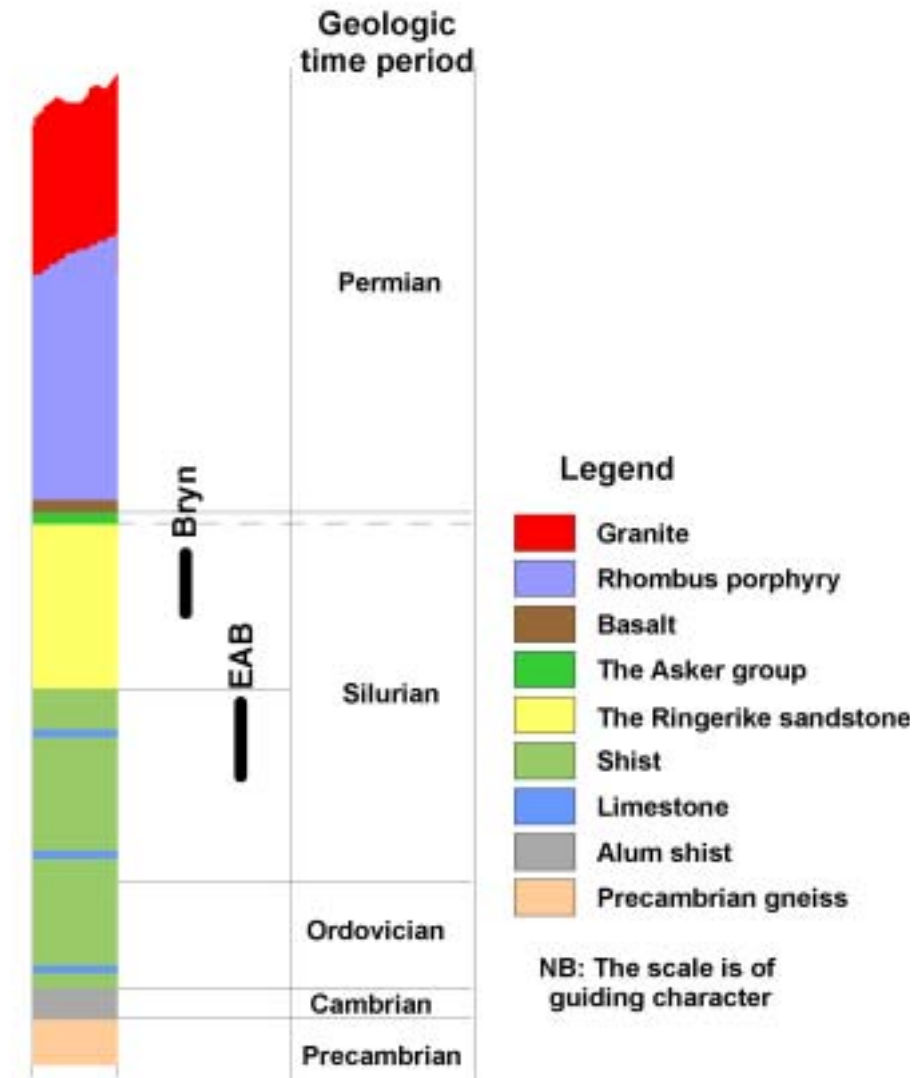


Figure 3–4: Stratigraphical location of the Bryn- and EAB boreholes (after Midttømme et al., 2004). The Ringerike sandstone is calculated to be approximately 350 metres thick at Bryn (Larsen, 2001).

Simplified geological map for Asker and Bærum

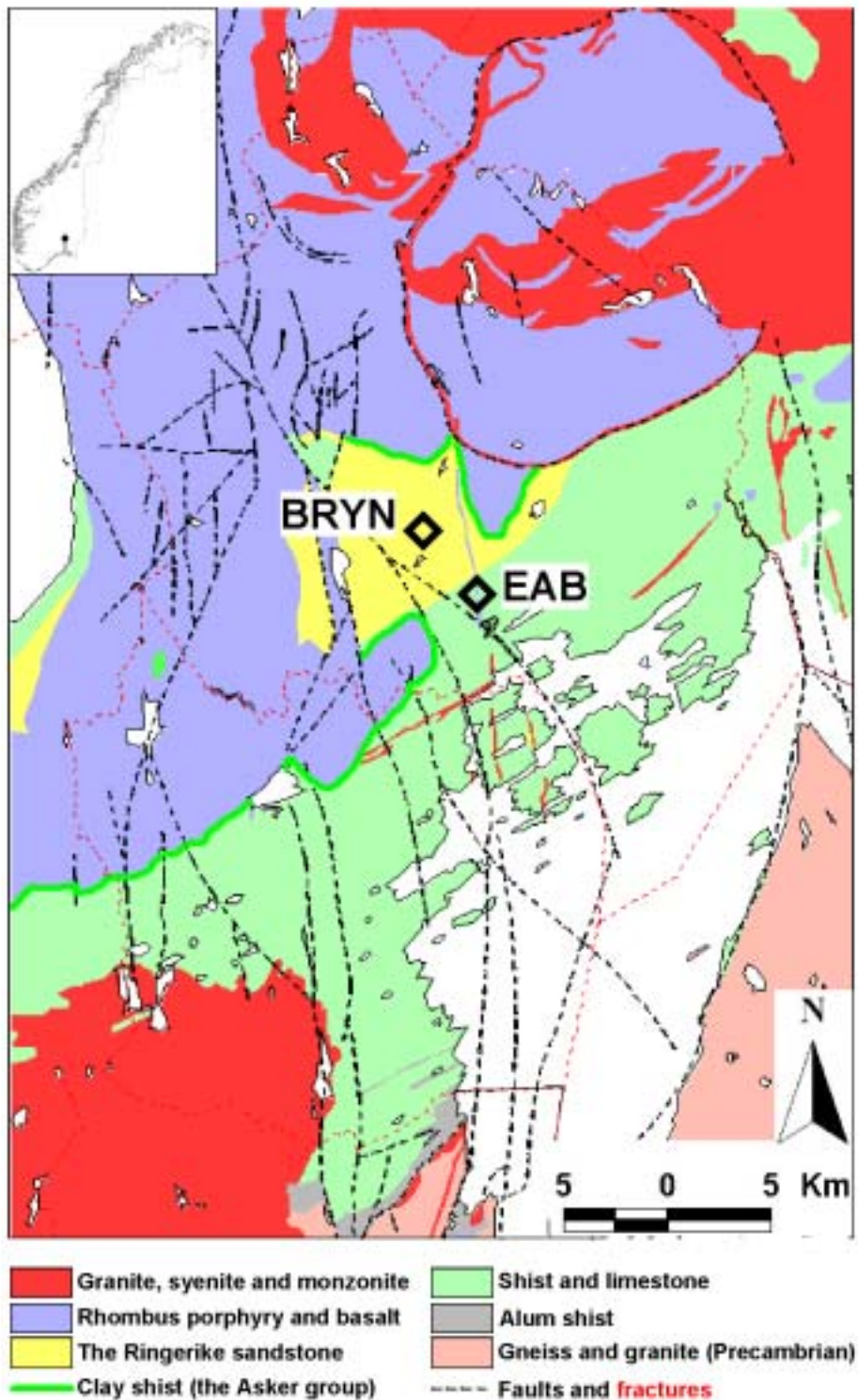


Figure 3–5: Geological location of Bryn and EAB (after Midttømme et al., 2004).

3.3 EAB - investigations, geology and borehole facts

The former property of Energiselskapet Asker og Bærum, referred to as EAB, was chosen as the site for the second pilot plant. Independent of the project, a thermal response test was performed in a 150 meters deep borehole (borehole 1) as early as 1999.

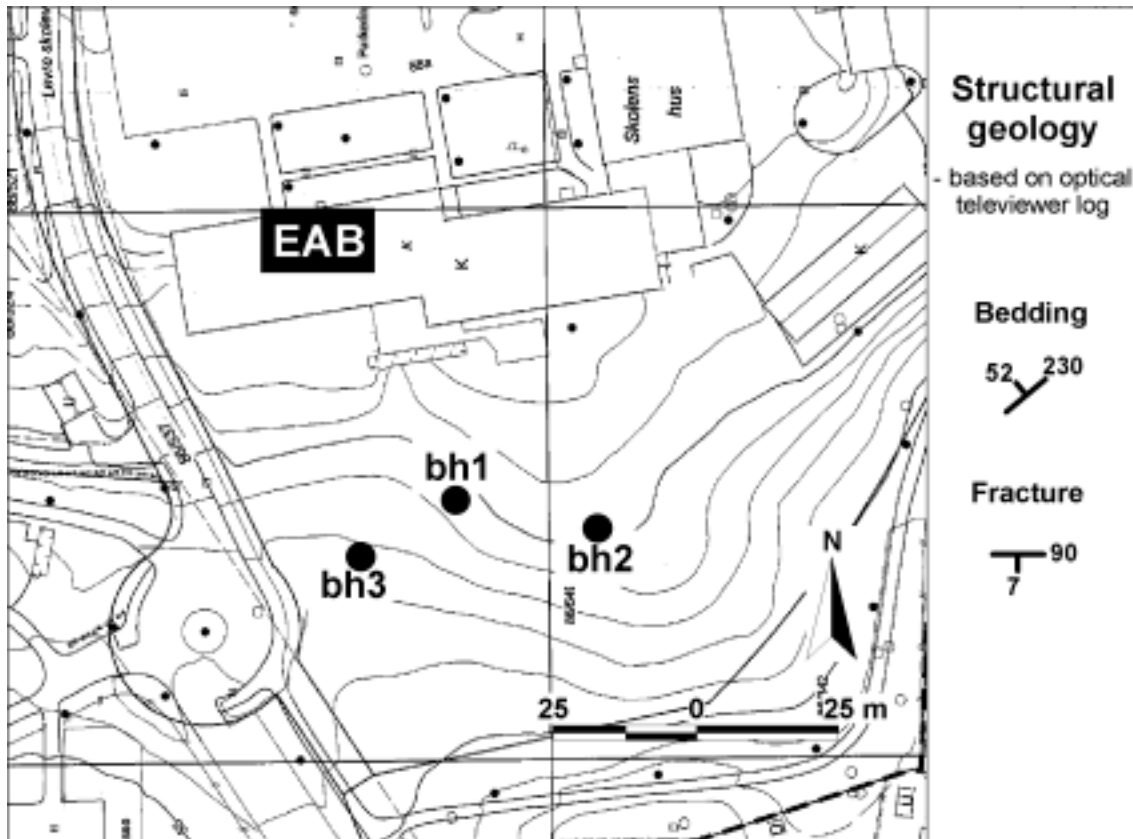


Figure 3–6: The second pilot plant is located at EAB.

The following investigations have been performed at EAB:

- Test pumping and groundwater analysis before hydraulic fracturing with injection of sand.
- Flow measurements before and after hydraulic fracturing with injection of sand.
- Geophysical logging using the optical televiewer and the TCN-logging device before and after hydraulic fracturing with injection of sand.
- Hydraulic fracturing with injection of sand.
- Levelling of the terrain surface related to the hydraulic fracturing with injection of sand.
- Thermal response test.
- Test run of the pilot plant.
- Computer modelling of the energy potential of the pilot plant.

The geological conditions at EAB are mainly based on the interpretation of the optical televiewer log for borehole 1 carried out by Midttømme et al. (2004). The bedrock at EAB mainly consists of nodular limestone, a shale containing lumps or nodules of limestone. The nodular limestone belongs to the lower part of the Steinsfjord formation and the upper part of the Malmøy formation (figure 3–7). The nodular limestone is interrupted by a pure limestone zone at 29 to 37 meters depth. The pure limestone zone belongs to the Malmøy limestone and is a part of the Malmøy formation. Traces of fossils in forms of different kinds of corals can be seen both in the pure limestone and the nodular limestone. At 45 meter depth, the bedrock changes character from nodular limestone to a dark and monotonous shale without any particular bedding. This shale corresponds to the Skinnerbuk formation, and can contain graptolites. Three lime benches, a few decimetres thick and with reduced levels of natural gamma radiation, appears at 59, 70 and 75 meters depth, respectively.

The pilot plant at EAB consist of three boreholes. Two new boreholes (borehole 2 and 3) were added on each side of borehole 1 (figure 3–6). During operation of the pilot plant, boreholes 2 and 3 will be used for pumping, while borehole 1 is the infiltration borehole. The borehole depth is 150, 91 and 88 meters for borehole 1, 2 and 3, respectively. The distance between the central borehole (borehole 1) and the satellites is 20 and 16 meters for borehole 2 and 3, respectively. The distance to borehole 3 was also supposed to be 20 meters, but had to be moved to avoid the crossing of an underground high-voltage cable. To assure no damages to the foundation wall as a consequence of hydraulic fracturing, borehole 2 and 3 were located further away from the nearby office building relative to the existing borehole 1. The regional groundwater flow direction is presumed to be from northwest towards southeast.

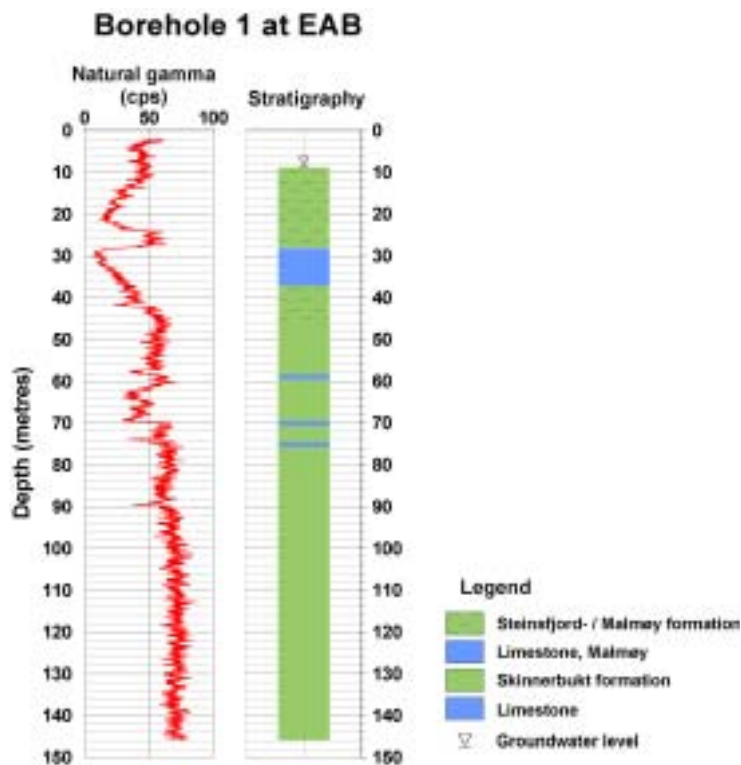


Figure 3–7: The stratigraphical sequence for borehole 1 at EAB, after Midttømme et al. (2004).

Chapter 4 Investigations performed

4.1 Laboratory test - mixing of thickener and water

Laboratory tests have been performed to investigate the hydration rate of the guar gum thickener. The efficiency of the breaker enzyme LEB-H was tested at the same time by adding a few droplets into the viscous mixture of thickener and water. An accurate characteristic of the behaviour of guar gum in water is required for obtaining a rational mixing procedure for water, guar gum, sand and breaker enzyme in the field. Four tests were carried out where the viscosity of the mixture was monitored over time. All the tests involved of one litre of water, and can be summarized as follows:

- 5 kg/m³ guar gum, 100 µl LEB-H added after 120 minutes,
- 7.5 kg/m³ guar gum, 200 µl LEB-H added after 120 minutes,
- 9 kg/m³ guar gum, 300 µl LEB-H added after 120 minutes,
- 10 kg/m³ guar gum, 100 µl LEB-H added after 120 minutes,

According to the supplier, LEB-H is well suited for the disintegration of fluids having a pH-value in the range of 6 to 9 (figure 4–1).

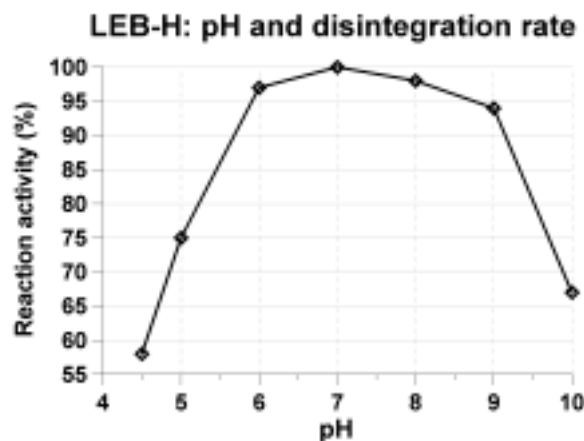


Figure 4–1: The pH dependency of the breaker enzyme LEB-H for effective disintegration of guar gum (Rantec Corporation, 2000).

The viscosity of the different mixtures with the guar gum thickener and water are given in figure 4–2. A doubled amount of guar gum results in a four times higher viscosity. All four mixtures got an immediate reduction in the viscosity after 120 minutes when the breaker enzyme LEB-H was introduced. The degradation ratio was speeded up after adding more LEB-H into the mixture of guar gum and water. The momentarily degradation or viscosity reduction may imply that the amount of added LEB-H can be reduced without losing its degradation ability of the guar gum- and water mixture.

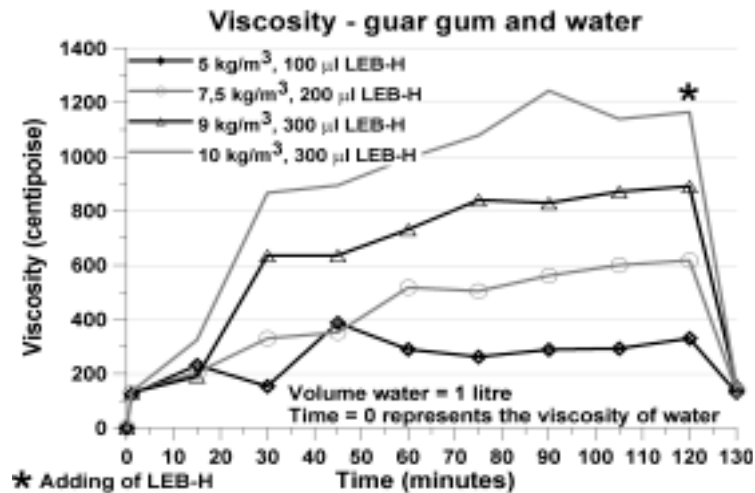


Figure 4-2: Results from the viscosity test of a mixture consisting of the thickener guar gum, water and the breaker enzyme LEB-H.

4.2 Lade

4.2.1 Test pumping, water analysis and geophysical logging

To document the effect of hydraulic fracturing with water-only, test pumping was performed in borehole 1 at Lade before and after the hydraulic fracturing. Test pumping was also performed in borehole 2 before hydraulic fracturing with injection of sand. Pump A was placed at a depth of 73 running metres in the test pumping performed before hydraulic fracturing with water-only, while pump B was placed at 53 running metres in the test pumping after hydraulic fracturing. In borehole 2 pump B was placed at 80 meters depth in the test pumping before hydraulic fracturing with injection of sand. As described in paragraph 5.1.4, no test pumping could be accomplished in borehole 2 after hydraulic fracturing with injection of sand. The flow rate and changes in the groundwater level in the pumping boreholes were monitored and logged for the three pumping tests. Samples for standard groundwater analysis at NGU-Lab were collected during the test pumping performed in borehole 1 before and after hydraulic fracturing.

The optical televiewer and the TCN-logging equipment were used for the borehole inspections in borehole 2 at Lade. Borehole 1 was inspected with an optical televiewer different from the kind used in borehole 2.

4.2.2 Hydraulic fracturing with water-only

The FrakPak - AIP 410-550 double packer was tested in a hydraulic fracturing operation in borehole 1 at Lade. The distance between the packer elements was about four meters. At this time, the double packer was furnished with simultaneous pressurizing of the upper and lower packer element. A Hafo drilling rig was employed for the lowering of the borehole equipment to the desired depth in the borehole (figure 4-3). The complete

equipment setup is described in paragraph 2.1.6. The pumping capacity of the tank lorry was 330 litres/hour. Stimulation with hydraulic fracturing with water-only was performed for every eight meter, in the sections 75-71, 67-63, 59-55, 51-47, 43-39 and 35-31 running meters from the top of the borehole.

4.2.3 Hydraulic fracturing with injection of sand

Hydraulic fracturing with injection of sand was attempted in borehole 2 at Lade. The equipment was rigged up for the stimulation of the section at 84.6-86.6 meters depth. Three containers, each filled with 180 litres of injection fluid consisting of thickener (guar gum), breaker enzyme (LEB-H), quartz sand and water, were planned injected into this borehole section after hydraulic fracturing with water-only (figure 4-4). Specifications concerning the sand type is given in paragraph 4.3.5. The equipment set up was identical to the hydraulic fracturing with water-only operation in borehole 1, except for the necessary injection equipment consisting of a mixer, container, injection pump and mobile power supply (figure 4-5 and 4-6). Maximal working pressure for the injection pump was 170 bars, and the pumping rate was automatically adjusted according to the pressure load.



Figure 4-3: Lowering the double packer into borehole 1 at Lade using a Hafo drilling rig.

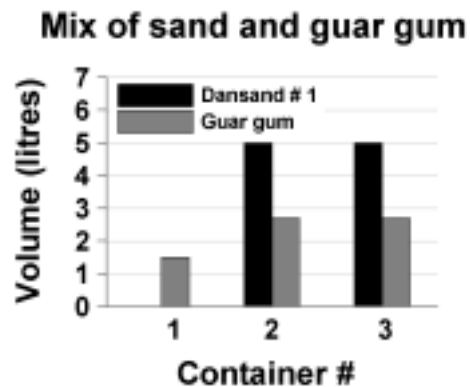


Figure 4-4: The composition of the injection fluid in container 1, 2 and 3 at Lade.



Figure 4-5: A mobile power supply equipment and the mixer-, container- and injection pump unit. The Hafo 2000 drilling rig is in the background.



Figure 4-6: Mixer, container and injection pump.

4.2.4 *Measuring changes in the terrain*

Levelling was done with both an ordinary levelling telescope and a total station to discover possible nearby changes in the terrain surface due to hydraulic fracturing with water-only in borehole 1 at Lade. The best levelling method suited for the purpose will be found by comparing the results from the two methods. In total five measurements with each method were accomplished.

4.3 **Bryn**

4.3.1 *Drilling and XRF-, XRD- and thin-section analysis of drill cuttings*

The drilling of the five boreholes at Bryn were carried out by Brødrene Myhre AS and in co-operation with the Norwegian Well Drillers Association in november 2000 (paragraph 3.2). According to common procedure, a first estimate of the short time production yield of the boreholes was calculated from the recovery rate of the groundwater level after draining the borehole with compressed air. Drill cutting samples were collected for every ninth meter in three of the boreholes, and the samples from borehole three, at 18, 63 and 99 meters depth respectively, were selected for the XRF-, XRD- and thin-section analysis. In addition, a surface rock sample were brought in for thin slice analysis only. The analysis results will reflect the mineralogical compositions, and eventual deviations in the bedrock composition towards depth compared with the surface rock, will be revealed.

4.3.2 *Test pumping, water analysis and geophysical logging*

Ordinary test pumping, using pump B, was attempted in borehole 1 at Bryn before hydraulic fracturing. Almost no drawdown of the groundwater level in the pumping borehole showed that the borehole yield was much higher than the pumping capacity. Consequently, columnar test pumping was performed in the 15-100 column for borehole 1, 2, 3, and 5, while the 20-100 column was tested for borehole 4. Sectional- and columnar test pumping, using pump B, were performed as described in paragraph 2.4.2 in the boreholes at Bryn both after hydraulic fracturing with water-only and after hydraulic fracturing with injection of sand. Additionally, pump C was used for further columnar test pumping after hydraulic fracturing with injection of sand. The water inlet for pump C was at 72, 69 and 62 meters depth for borehole 1-3, 4 and 5, respectively. The extent, pump type, character of the test pumping and the sampling of groundwater for standard water analysis at the NGU-lab are indicated by figure 4-7.

Comprehensive geophysical investigations have been performed in the boreholes at Bryn before and after hydraulic fracturing with water-only, and after hydraulic fracturing with injection of sand. The borehole inspections can be summarized as follows:

- Filming of the borehole walls by using the optical televiewer.
- Measuring the temperature and the electric conductivity of the water, and the total natural gamma radiation from the bedrock.

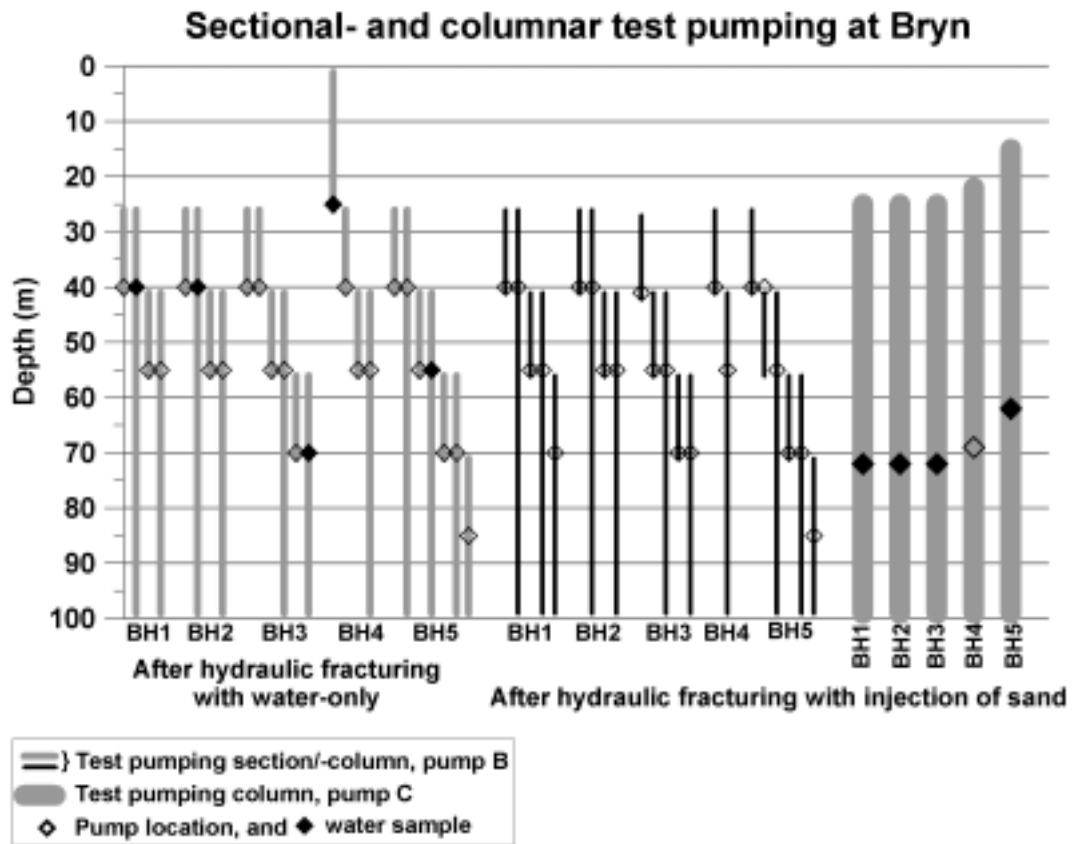


Figure 4–7: The extent of the sectional- and columnar test pumping performed after hydraulic fracturing with water-only and after hydraulic fracturing with injection of sand in the five boreholes at Bryn.

4.3.3 Rock stress measurements

The rock stresses at Bryn were measured by using the hydraulic fracturing technique (paragraph 2.1.4). The aim of the measurements was to determine the direction and value of the maximum and minimum principal stress. The hydraulic fracturing tests in five sections in borehole 4 were performed by SINTEF Civil and Environmental Engineering, Department of Rock and Soil Mechanics, in co-operation with G. Meyer Borebrønnservice AS. The FrakPak - AIP 441-550 double packer equipment was employed in the measurements, and the distance between the packers was adjusted to 1.3 meters. The test sections at 97, 93, 88, 75 and 65 meters depth, without any visible existing fractures before the measurements, were selected on the basis of the results from the optical televiewer. The borehole wall was filmed by an optical televiewer after the measurements in an attempt to orient the new fractures and to determine the stress directions.

4.3.4 Hydraulic fracturing with water-only

Hydraulic fracturing with water-only, in order to increase the number and size of the fracture planes in the bedrock between the boreholes, was performed in 11-13 sections in each borehole at the level between approximately 30 and 95 meters depth at Bryn. In total 63 stimulations were accomplished in co-operation with G. Meyer Borebrønnservice AS. The hydraulic fracturing procedure of a borehole (paragraph 2.1.6) started with columnar hydraulic fracturing in the lower part of the borehole. Columnar hydraulic fracturing was performed until a fracture was created and was then followed by sectional hydraulic fracturing. A detailed summary of the extent, localization and character of the hydraulic fracturing with water-only in the boreholes at Bryn is given by figure 4–8. A strategic location of the double packer around discontinuities like mineral filled fractures and rock boundaries was attempted with basis in the optical televiewer log of the borehole wall.

The FrakPak - AIP 410-550 (paragraph 2.2.1), furnished with separate pressurization of the packers, was employed in the hydraulic fracturing of the boreholes at Bryn. The distance between the packers was three meters. Two water pumps with a capacity of roughly 300 litres/minute each were used, and the maximum pumping rate was approximately 500 litres/minute. The water- and packer pressures were measured for all the boreholes, except borehole 3. The hydraulic fracturing in borehole 3 was done as a pretest, and the pressure logging equipment was not in use. Instead, the water- or the borehole pressures were recorded manually from an analog manometer. Changes in the groundwater level, in some of the surrounding boreholes of the hydraulic fracturing-borehole, were monitored by using the pressure sensors described in paragraph 2.4.1. A simultaneous monitoring of the groundwater levels in all surrounding boreholes were not possible due to the lack of pressure sensors (table 4–1).

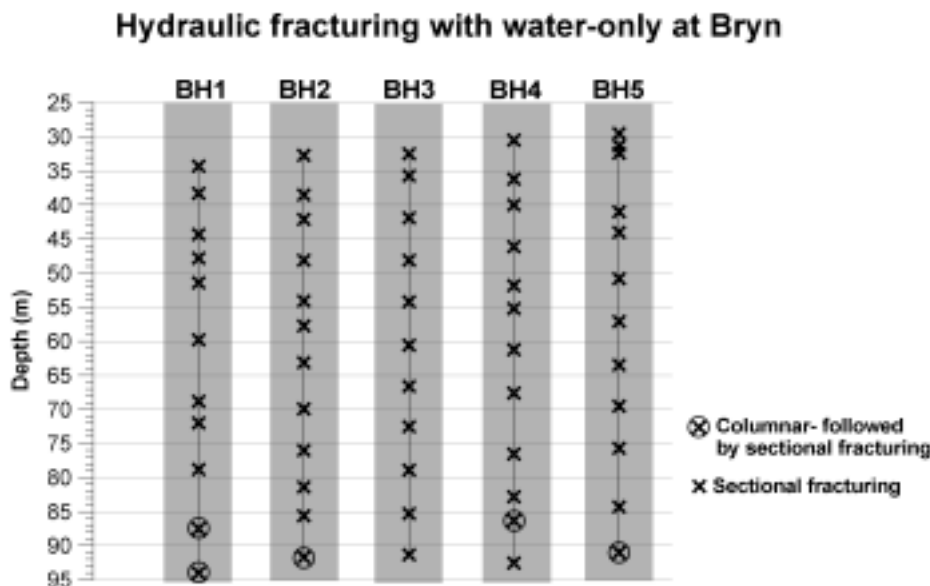


Figure 4–8: A detailed summary of the extent, location and character of the hydraulic fracturing with water-only in the boreholes at Bryn. The centre of each section is marked with a symbol.

Table 4–1: Monitoring of the groundwater level, marked as “x”, in the surrounding boreholes to the borehole stimulated with hydraulic fracturing (HF) with water-only.

	BH1	BH2	BH3	BH4	BH5
BH1	HF	x	x	x	
BH2	x	HF	x	x	
BH3	x	x	HF	x	
BH4	x		x	HF	x
BH5	x		x	x	HF

4.3.5 Hydraulic fracturing with injection of sand

Hydraulic fracturing with injection of quartz sand were performed to achieve a further increase in the borehole yields. In addition to the equipment used in the hydraulic fracturing with water-only at Bryn, a high-pressure tank and a mixer were necessary for the injection procedure (figure 4–9). The mixer was furnished with a pumping unit for the transportation of injection fluid into the high-pressure tank. The assembling of the equipment was according to the description in paragraph 2.1.7. The stimulation was performed in 19 borehole sections of three metres length each divided over the five boreholes at Bryn (figure 4–11). The borehole sections were selected based on the results from hydraulic fracturing with water-only and according to the indicated maximum counter pressures and the belonging maximum flow rate (paragraph 2.1.7). The pressure course during the injection of sand determined whether one or two containers with injection fluid were required for injection into each section. The water-, or the borehole section pressure, and the packer pressures were monitored and logged for all the boreholes except borehole 4, where the data logger was out of order.

Natural quartz sand in two different grain sizes was used as propping agent. The two fractions of sand, called Dansand #1 and Dansand #2, were 0.40-0.90 and 0.63-1.40 millimetres, respectively. The sand is marketed as filter sand, and has been through a production process composed of scrubbing, water grading, drying and sieving. The quartz sand has a value of 7 on Mohs’ scale of hardness, the SiO₂-content is 97-99%, and the specific weight of the sand is 1.4-1.6 g/cm³. The amount and share of the two sand fractions in each container of injection fluid were determined from the recorded counter pressure in the fracture plane during hydraulic fracturing with water-only. Fractures having a low counter pressure got a greater share of coarser sand compared to fractures or borehole sections with a higher counter pressure. The exact mixture of sand and thickener in each borehole section is given in figure 4–12. Each container of injection fluid consisted of 50-60 litres of water and about 10 millilitres of breaker enzyme (LEB-H).

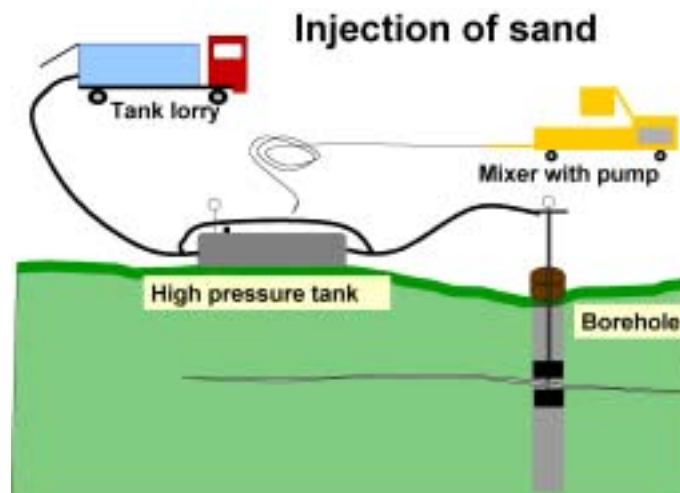


Figure 4–9: Equipment set up for hydraulic fracturing with injection of sand in the boreholes at Bryn.



Figure 4–10: Mixer- and pumping unit.

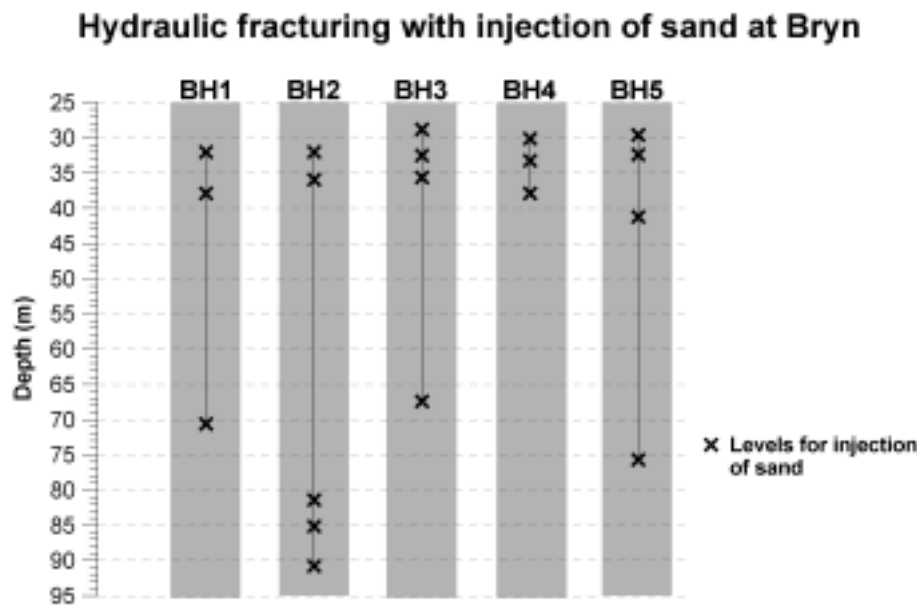


Figure 4–11: Borehole sections for injection of sand into fracture planes at Bryn. The sections were selected with basis in the results from hydraulic fracturing with water-only.

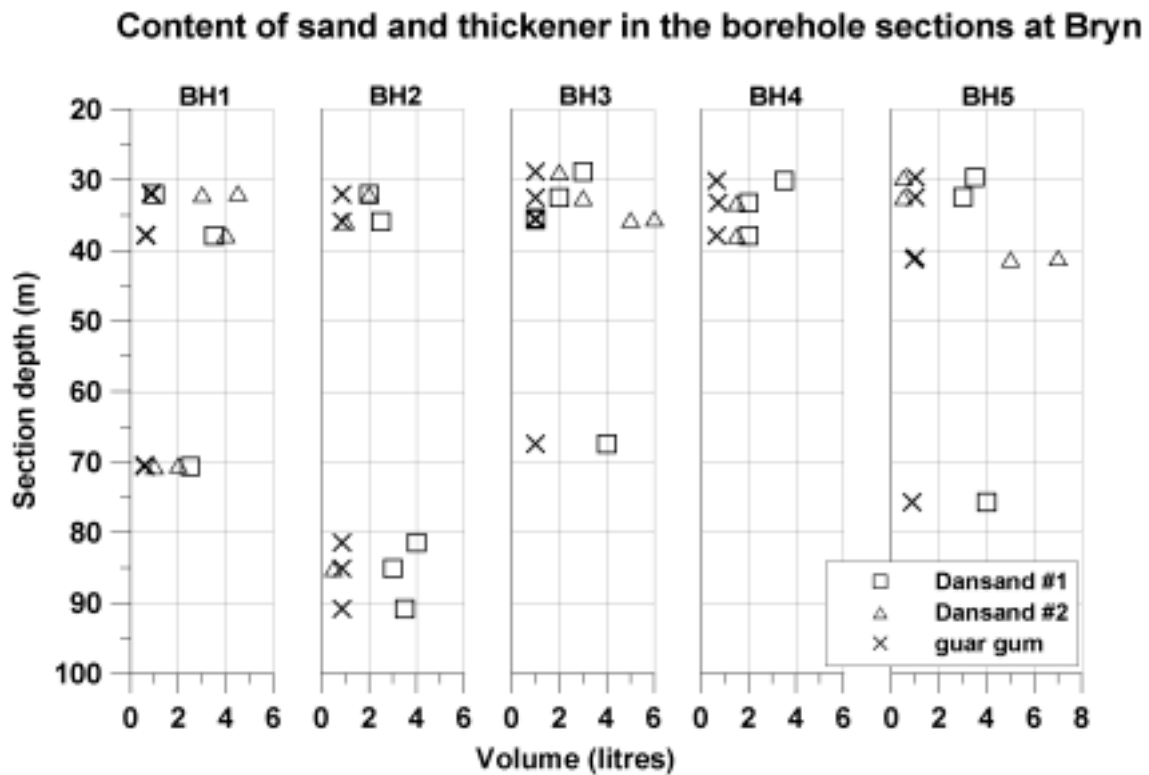


Figure 4–12: The mixture of the two different fractions of sand, Dansand # 1 and 2, and the thickener guar gum injected into each borehole section in the boreholes at Bryn.

4.3.6 Levelling

A levelling telescope was used for the levelling carried out in connection with the two hydraulic fracturing operations at Bryn. The levelling was done towards four points inside the area of influence for the hydraulic fracturing. The four points were either trees or a lamp post, and an inch ruler was fastened to each point for reading. A fixed point was put up outside the area of influence for the hydraulic fracturing. A datum point reference was established before the hydraulic fracturing of each borehole, and a final levelling was performed after finishing the hydraulic fracturing. A general overview of the levelling points within the area of assumed influence for hydraulic fracturing, and the fixed point can be seen in figure 4–13.



Figure 4–13: A general overview of the levelling points within the area of assumed influence for hydraulic fracturing (left), and the fixed point (right). The pictures at Bryn are turned 180° with respect to each other.

4.3.7 Thermal response test

A thermal response test was performed in borehole 3 at Bryn. After measuring the effective in-situ value of the rock thermal conductivity around the borehole, the measurement was continued with simultaneous pumping of groundwater from borehole 2, east of the test borehole. This extended thermal response test will give information about how the thermal conditions in borehole 3 are influenced by an induced groundwater flow. Pump D, with a pumping rate of about 5000 litres/hour, was employed in borehole 2. The value of the undisturbed temperature, used in the calculations of the thermal response, was taken from the temperature log (figure 5–43).

4.3.8 Test run of the pilot plant

The possible short-time energy extraction from the pilot plant at Bryn was tested by heat exchanging cold water from the nearby river towards pumped groundwater from the satellite boreholes. Pump D, having a pumping rate of 5000 litres/hour at a rated head of 47 meters (figure 2–21), was employed in the pumping of groundwater from the satellite boreholes (borehole 1, 2, 4 and 5) and in the pumping of cold water from the river Lomma. Without the use of sealing packers, the pumps extracted water from the complete water column in all the boreholes, including the large fracture zone (paragraph 5.2.1).

Outflowing groundwater was returned into the groundwater magazine through borehole 3. By using the specially designed injection packer (paragraph 2.2.3), placed at 15 meters depth, the injected water was returned below the large fracture zone. The test was performed from the 11th to the 29th of April 2003. The main objectives of the test run were to determine:

- The short-time effect extraction from the pilot plant, and to find out whether or not the river-cooling of the circulating groundwater can be traced as a temperature decrease of the pumped groundwater.
- The infiltration capacity of borehole 3, and to detect possible pressure buildups over time.

The short-time effect extraction from the pilot plant at Bryn can be found by measuring the temperature and rate of the in- and outflowing groundwater from the heat exchanger (figure 4–14 to 4–16). The temperature of the groundwater from the satellite boreholes, the temperature on the inflowing water from the river, and the temperature in the logger unit were also measured. PT1000 thermo elements, and a flowmeter was employed. All the monitored data was recorded in a data logger which is equipped with 12 channels and communicates via a GSM-module (figure 4–16). The pressure level in the closed system of circulating groundwater was monitored by an analog manometer (figure 4–15). All the equipment and the physical arrangements for the test run was organized in a manhole around the top of borehole 3 (figure 4–14 to 4–16).

Testing the effect from the pilot plant at Bryn - Instrumentation

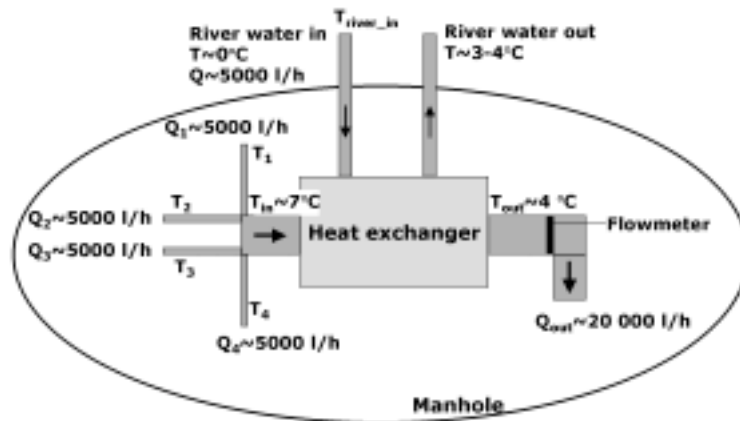


Figure 4–14: Instrumentation of the pilot plant at Bryn. All units are placed together in a manhole around the top of borehole 3. Expected flow rates and temperatures are indicated.



Figure 4–15: Left: The flowmeter and the heat exchanger in the manhole around the top of borehole 3 at Bryn. Right: Manifold collecting the pumped groundwater from the satellite boreholes. The system pressure is monitored by an analog manometer. Temperature sensors were fastened with isolation material and plastic bands.



Figure 4–16: Left: Logging cabinet with a data logger placed in the manhole around the top of borehole 3 at Bryn. A GSM-module makes remote-controlled monitoring possible. Right: The control panel for the pilot plant at Bryn consists of motor protections for the pumps and a flood shelter for the manhole.

4.4 EAB

4.4.1 Test pumping, water analysis, flow measurements and geophysical logging

Ordinary test pumping, using pump C, was attempted in all the boreholes at EAB before hydraulic fracturing with injection of sand. The pumping depths were at 67.3, 66.3 and 71.5 meters for borehole 1, 2 and 3 respectively. Slow and modest drawdown of the groundwater level, caused by pumping in borehole 1 and 2, showed that the borehole yield were higher than the pumping capacity and no value of the borehole yield was obtained. The test pumping in borehole 3 succeeded, and the borehole yield was approximately 5200 litres/hours. Water samples for standard groundwater analysis at the NGU-lab were taken from all the boreholes. The high borehole yields made it difficult to document the effect of hydraulic fracturing with injection of sand by ordinary test pumping (paragraph 2.4.3). As an alternative attempt, and as a part of the method development, the quantification and localization of the groundwater flow into the boreholes were examined by using an impeller flowmeter probe together with simultaneous pumping. Continuous flow measurements were carried out in the borehole intervals 25-145, 25-87 and 25-83 meters for borehole 1-3 respectively, before and after hydraulic fracturing with injection of sand. Pump D was located at 20 meters depth and pumped with a rate of approximately 5000 litres/hour.

Equivalent to Bryn, extensive geophysical investigations in the boreholes at EAB were done before and after hydraulic fracturing with injection of sand. The investigations can be summarized as follows:

- Optical televiewer logs of the borehole walls.
- Continuous measurements of the temperature- and the electric conductivity of the water, and the total natural gamma radiation from the borehole wall (TCN-logs).

4.4.2 Hydraulic fracturing with injection of sand

Different from Bryn, the hydraulic fracturing with water-only and hydraulic fracturing with injection of sand was performed as one operation at EAB. The equipment used at EAB was identical to the equipment used at Bryn except for the mixer- and pump unit. An attempt to use an air pressure mixer unit (paragraph 2.2.4) to mix water and thickener failed, and an industry drill furnished with a mixing device was employed in the mixing of the injection fluid at EAB. At first a concentrate of water and the thickener guar gum was made. The concentrate was diluted to the right consistence after some time of hydration, and a desired amount of sand was added (figure 4–17). Finally, the ready mixture of water, guar gum and sand was transferred manually into the high-pressure storage tank. A few droplets of the breaker enzyme LEB-H, were added into the storage tank immediately before pressurization and injection.

An overview of the three metres long borehole sections stimulated with hydraulic fracturing with injection of sand, randomly selected for approximately every sixth meter, is given in figure 4–18. Hydraulic fracturing with injection of sand was performed in a total of 25 borehole sections divided over the three boreholes at EAB. In addition, hydraulic fracturing with water-only was accomplished in 9 sections, and an attempt of

injecting a mixture of water and thickener was tried in one section. Water- and packer pressures were measured and logged for all stimulations. Similar to Bryn, two different fractions of sand was used. The exact mixture of sand and thickener in each container with injection fluid is shown in figure 4–19. Each container with injection fluid consisted of about 50 litres of water and about 10 millilitres of breaker enzyme (LEB-H).



Figure 4–17: Mixing of water, guar gum (thickener) and sand. Filling of injection fluid into the high-pressure tank is shown in the upper right corner.

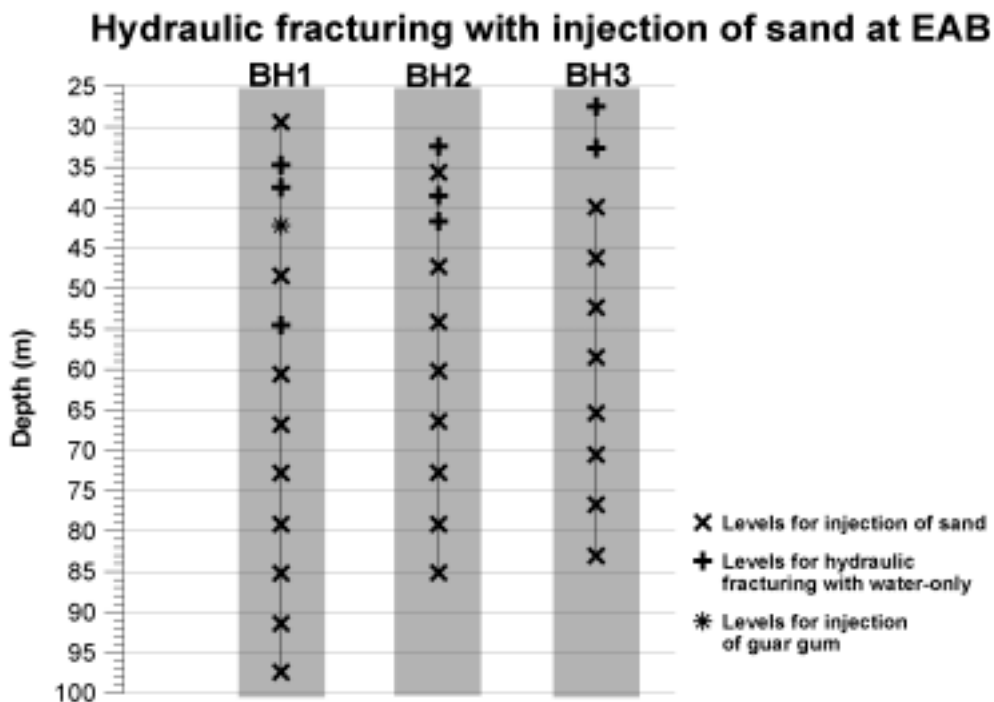


Figure 4–18: Levels for hydraulic fracturing with injection of sand in the boreholes at EAB.

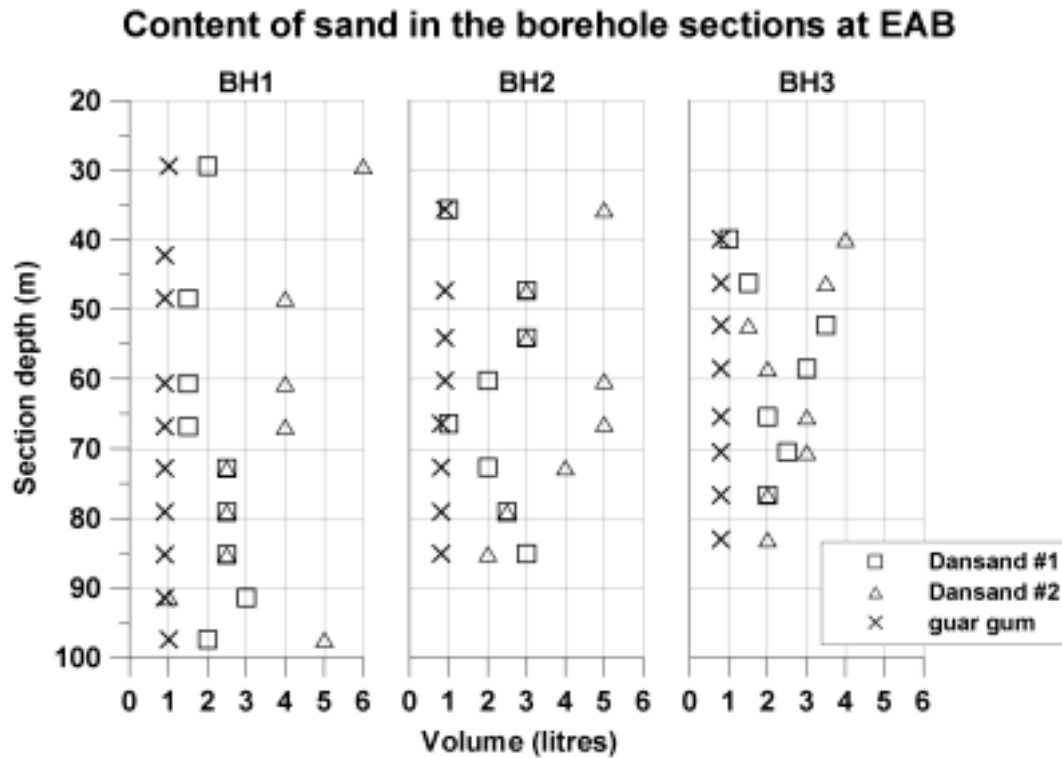


Figure 4–19: The content of the two sand fractions, Dansand number 1 and 2, and the thickener guar gum injected into each of the borehole sections at EAB.

4.4.3 Levelling

Similar to Bryn, a levelling telescope was used for the levelling before, during and after hydraulic fracturing with injection of sand at EAB. The levelling was performed towards four measuring points, at the top of the casing in the boreholes and towards a fixed point outside the area of assumed influence of the hydraulic fracturing, respectively. A levelling staff was used in the measurements (figure 4–20).



Figure 4–20: The levelling set up at EAB. Levelling telescope and levelling staff.

4.4.4 Thermal response test

Similar to Bryn, a thermal response test was performed in borehole 1 at EAB. After measuring the effective in-situ value of the rock thermal conductivity around the borehole, the measurement was continued with simultaneous pumping (pump D) of groundwater from borehole 3, west-southwest of the test borehole. The value of the undisturbed temperature, used in the calculations of the thermal response, were taken from the temperature log (figure 5–72).

4.4.5 Test run of the pilot plant

The possible short-time effect extraction from the pilot plant at EAB was tested by connecting the thermal response test unit to the heat exchanger in the manhole around the top of borehole 1. Warmed water from the heater in the thermal response test unit was heat exchanged with colder groundwater pumped from borehole 2 and 3. Pumps of kind E were installed in each of borehole 2 and 3 at 85 metres depth, and the pumping capacity was 8000 litres/hour at a rated head of 51 metres (figure 2–21). Outflowing groundwater was returned into the groundwater magazine through borehole 1. The special designed injection packer (paragraph 2.2.3), originally made for the borehole 3 at Bryn, was placed at 15 meters depth and ensured a sufficient returning of the water into the groundwater magazine. Similar to the set up and the test run at Bryn (paragraph 4.3.8, figure 4–21) a 17 day long test period was performed in December 2003/January 2004. The clogging risk of the circulating system was tested after shutting down the heat supply from the thermal response test unit by maintaining the pumping in borehole 2 and 3 and the reinjection into borehole 1. The pumping was ended the 24th of March, after 97 days of continuous pumping.

Testing the effect from the pilot plant at EAB - Instrumentation

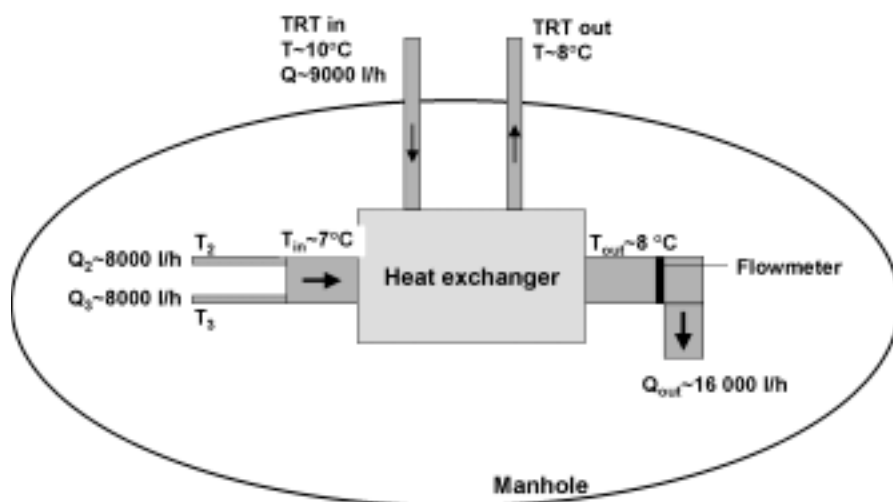


Figure 4–21: Instrumentation of the pilot plant at EAB. All units are gathered together in a manhole around the top of borehole 1. Expected flow rates and temperatures on the groundwater and the collector fluid from the thermal response test equipment (TRT) are indicated.



Figure 4–22: The heat exchanger in the manhole around the top of borehole 1 at EAB. The inflowing groundwater from borehole 2 and 3 are connected through a T-coupling to the heat exchanger. The outflowing water will be reinjected into the groundwater magazine via borehole 1 (on the picture). The in- and out collectors of the TRT-unit will be connected to the two upper exits, with yellow caps, on the heat exchanger. The system pressure is monitored by an analog manometer.

4.5 Modelling of energy potentials

4.5.1 Software presentation - FEFLOW and HFM

The paragraph is mainly based on Spangelo (2002).

FEFLOW (Finite Element subsurface FLOW system) is an advanced finite-element software package for modelling of saturated and unsaturated groundwater flow with contaminant transport, heat transport and saltwater intrusion (Waterloo Hydrogeologic, 2004). FEFLOW was originally designed for modelling problems in porous media, but fracture elements can be included in the latest version v5.0 (figure 4–24). FEFLOW has a well developed graphical user interface (figure 4–23). Background information for the study area, like different kind of maps, point-, line- and planar information, are loaded from data files or could be plotted manually and then interpolated. A mesh is automatically generated in the marked study area. A finer mesh should be manually generated around key points to obtain a high accuracy and to avoid spending time on needless calculations. A three dimensional model can be created by dividing the ground into different layers, and the layers can be formed into desirable shapes. Physical properties, boundary conditions and formulas are manually assigned to the different features in the model. The modelling can be stopped anytime during the running, and the results can be visualized both during and after ended modelling period.

The main drawback with FEFLOW is the complexity which makes the software very time-consuming to learn. As with all of modelling, the input data decides the quality of the results. The input data in a FEFLOW model can be very accurate and detailed. However, these kind of data are very seldom available, and the model designer has to get the best out of the input data at hand.

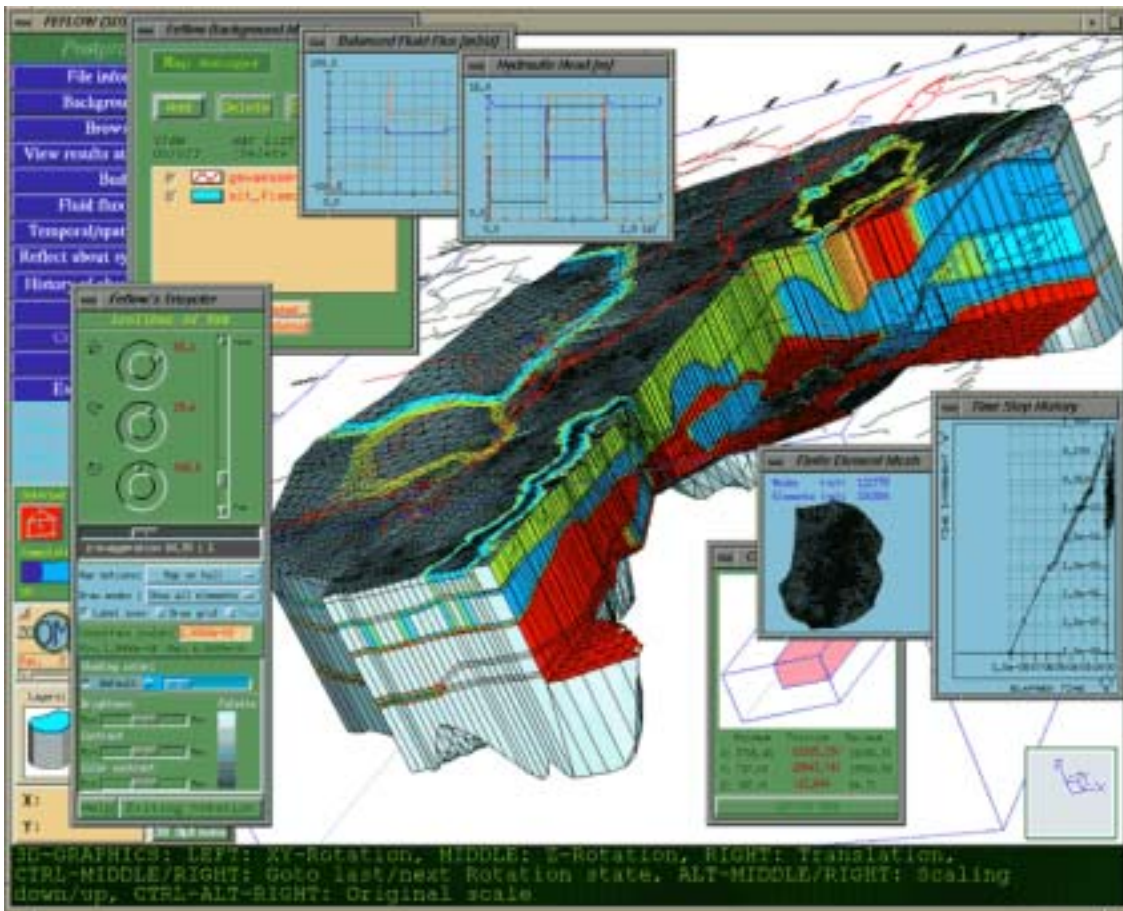


Figure 4–23: The visualisation tools in FEFLOW are numerous (Waterloo Hydrogeologic, 2004).



Figure 4–24: This is how fractures can be designed in FEFLOW. The black lines represents fracture channels, while the black area is a fracture plane (Spangelo, 2002).

The HFM or the Hydraulic Fracture Model is designed for the modelling of seasonal energy storage in a HYDROCK-plant, and is developed by G. Hellström at Lund Institute of Technology, Department of Mathematical Physics. The HYDROCK-concept is previously described in paragraph 2.1.2 (figure 2–2), and results from earlier modellings with the HFM software are presented in Hellström and Larson (2001).

Compared to FEFLOW, HFM is a relatively simple Fortran code where all the input data, only numbers, are listed in a certain way in an input file. The bedrock is divided into horizontal layers where the heat capacity and thermal conductivity have to be specified. The fracture planes in the model are regarded as horizontal and disc shaped, and is defined by the depth and radius inputs. Fracture permeability is a relative number given by the distribution of the circulating water in the system onto every single fracture plane.

The results from a HFM-modelling are given as a numeric list in an output file. Only the results after a certain modelling period, given in the input file, is generated in the output file. Symmetrical modelling of a HYDROCK-plant, consisting of for instance four satellite boreholes, makes it possible to only calculate the results for an one-eighth segment of each fracture plane. The generating of this limited amount of data makes the output file appear well arranged. The physical results from the modelling are the temperature of the outflowing water from the plant, the temperature in the horizontal layers of bedrock and the temperature in the fracture planes. The temperatures in the bedrock are given at certain points along streamlines for the groundwater in the fractures planes (figure 4–25).

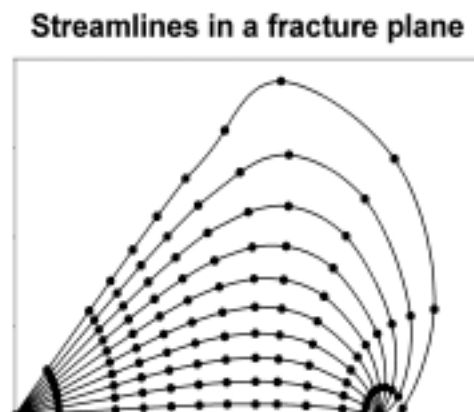


Figure 4–25: Streamlines in an one-eighth segment of a circular fracture plane with a central borehole and four satellite boreholes. Modelled temperatures are given at the points along the streamlines (modified after Spangelo, 2002).

HFM is solely based on the HYDROCK-concept and has not so many sophisticated features as FEFLOW. All plants are considered as symmetrical, and the distance between the central and the satellite boreholes is given as an average distance. The fracture planes are considered to be complete and thus also the hydraulic communication. In the cases where there is no hydraulic communication between the central and the satellite borehole at a certain depth and fracture level, the heat exchange area in the model is larger than it should be. All bedrock layers and fracture planes are considered to be horizontal, and no groundwater flow outside the plant can be added to the model.

4.5.2 Comparison of the FEFLOW- and HFM software at Bryn

The two softwares FEFLOW and Hydraulic Fracture Model (HFM) were compared in a semester project by Spangelo (2002), which the following paragraphs are based upon unless indicated otherwise. The aim of the study was to find the software best suited for the modelling of the energy potential of the pilot plant at Bryn and EAB.

Five comparable modelling cases were set up to reveal inequalities between the two softwares, and were not so much focused on a realistic modelling of the physical pilot plant at Bryn (table 4–4). The ground source heat pump system at Bryn, based on circulating groundwater, was designed with basis in the HYDROCK-concept (figure 2–2). By varying one parameter at the time, the results will determine how sensitive the softwares are for the change of this parameter. Case 1 was the most realistic, and was supposed to be compared with case number 3 and 4. The aim of the unrealistic high temperature gradients in case 2 and 5 were to increase the temperature deviations between the cases with varying- and equal flow distribution between the fracture planes. All the input values were calculated from available data, or based on an estimated value if the data turned out to be incomplete. The “common” and “individual” input parameters for FEFLOW and HFM, used in the five modelling cases, are listed in table 4–2 and 4–3. By neglecting the borehole wall surfaces, the total surface area of the fracture planes can be set equal to the heat exchange area. The heat exchange area is a key parameter for the energy potential of the ground source heat pump system based on groundwater and should be implemented as realistic as possible. According to the results from the hydraulic fracturing with water-only at Bryn and the hydraulic communication between the satellite boreholes and borehole 3 (paragraph 5.2.9), the fracture planes seemed to be asymmetric in all three dimensions. Since symmetrical fracture planes had to be implemented in HFM, this was also done for FEFLOW (figure 4–26). The number of symmetrical and horizontal fracture planes was determined by considering the hydraulic communication between the central borehole and a satellite borehole as a quarter fracture plane. The total number of fracture planes was then found by dividing the sum of the quartiles on four. This calculation gave six fracture planes which was located at 32, 40, 44, 60, 72 and 84 meters depth according to their appearance in the boreholes. The best estimate of the flow distribution in the HFM-model, implemented as relative values, was calculated based on the groundwater level changes in borehole 3 (paragraph 5.2.9) caused by hydraulic fracturing in the satellite boreholes. The relative flow distribution was then found by dividing the change in the groundwater level within a desired interval by the total change in the groundwater level for the whole borehole. FEFLOW used the fracture aperture as an input parameter instead of the flow distribution. The fracture aperture was however, calculated from the flow distribution. The calculation was done with basis in the HFM-modelling where a constant value of two millimetres was put in for the fracture aperture (table 4–3).

Table 4–2: Common input parameters for FEFLOW and HFM used in the modelling cases of the pilot plant at Bryn (Spangelo, 2002).

Common input parameters	Value
The plant: # of satellite boreholes: Distance from the central (borehole 3) to the satellite boreholes: Borehole depth: Radius of fracture planes: Operation period: Flow rate in the satellite boreholes: Temperature of injected water into the central borehole, T_i : Density of circulating water:	4 (borehole 1, 2, 4 and 5) 12.5 meters 100 meters 15 meters 7 months $Q_{\text{central}}/4$ 1°C 1000 kg/m^3
Thermal data: Thermal conductivity of the bedrock: Thermal heat capacity of the bedrock: Surface temperature:	3.3 W/(m,K) (Midttømme et al., 2000) $0.85\text{ kWh/(m}^3\text{K)}$ 6.0°C (Stene, 1997)

Table 4–3: Individual input parameters for FEFLOW and HFM used in the modelling cases of the pilot plant at Bryn (Spangelo, 2002).

Individual input parameters	Value
HFM parameters: Heat conductivity resistance between the bedrock and the fluid: Fracture aperture (constant value): Flow distribution among the fracture planes, fracture depth (meters) - share of flow:	$0.3\text{ (Km}^2\text{/W)}$ 2 mm 32-0.22, 40-0.21, 44-0.13, 60-0.04, 72-0.32 and 84-0.09.
FEFLOW parameters: Flow equations: Thermal flux when the thermal gradient is 13.5 W/(km,K) : Thermal flux when the thermal gradient is 100 W/(km,K) : Fracture apertures, fracture depth (meters) - aperture (mm): Total area of the six fracture planes:	Darcy's law and Hagen Poiseuille 0.0446 W/m^2 0.33 W/m^2 32-1.6, 40-2.5, 44-1.2, 60-1.8, 72-2.2 and 84-2.2. 4776 m^2

Table 4–4: Modelling cases (Spangelo, 2002).

Case #	Description
1	- The flow rate in the central borehole, $Q_{\text{central}} = 20\ 000$ litres/hour. - Vertical temperature gradient = 13.5 K/km - Varying flow distribution between the fracture planes.
2	Similar to case #1, except the vertical temperature gradient = 100 K/km
3	Similar to case #1, except the flow rate in the central borehole = 5000 litres/hour.
4	Similar to case #1, except for having an equal flow distribution among the fracture planes.
5	Similar to case #2, except for having an equal flow distribution among the fracture planes.

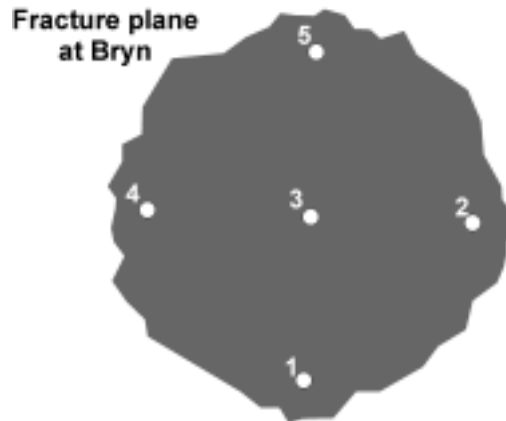


Figure 4–26: The fracture plane extension used in the FEFLOW-modelling of the pilot plant at Bryn.

4.5.3 FEFLOW-modelling of the energy potentials at Bryn and EAB

A more accurate modelling of the energy potential of the pilot plant at Bryn was accomplished as a part of the post-graduate thesis by Spangelo (2003). The part of the paragraph referring to Bryn is based on Spangelo (2003) unless indicated otherwise. FEFLOW was chosen to be the modelling tool based on the results from the comparison of FEFLOW and HFM (paragraph 4.5.2). Five different modelling cases were performed for the pilot plant at Bryn. The most important input parameters, in addition to or different from the “common input parameter”-list regarding the plant- and thermal properties used in the comparison of FEFLOW and HFM (table 4–2 and 4–3, paragraph 4.5.2), are presented in table 4–5. Compared to the FEFLOW-modelling in paragraph 4.5.2, these modellings:

- used the same fracture distribution, depth and apertures,
- had a tighter mesh around the fracture planes, and
- considered the injection borehole and the production boreholes as vertical and columnar fracture elements instead of source and sinks.

The injection of water, $T_1=1^\circ\text{C}$, into the central borehole and the distribution in different ratios into the fracture planes, will cause a drastic decrease of the temperatures in the surrounding bedrock of each fracture plane. The spreading of this cooling in the bedrock was of crucial interest to achieve a better understanding of the most important mechanisms influencing the energy potential of this ground source heat pump system based on circulating groundwater. Accurate values from the cooling process were obtained by increasing the mesh density around each fracture plane. The mesh was tightened around the boreholes in the horizontal plane, and extra horizontal layers close to each of the fracture planes were embedded in the vertical direction. In total, 44 horizontal layers were implemented into the model. The distribution, or the amount of injected or produced water from a certain fracture level can not be calculated when the injection borehole and the production boreholes are regarded as source and sinks on the surface. Instead, a continuous borehole, intersecting all the layers in the model, can be modelled by regarding the boreholes as vertical fracture elements. The injection and production of groundwater was set as boundary conditions at certain points. The boundary condition for the four production or satellite boreholes, where the pumps are placed in the bottom, was set at the deepest fracture plane. The temperatures of the

produced groundwater were read at the boundary condition-points. The boundary condition for the injection borehole, where the sealing packer is located at 15 meters depth, was set at the surface. By setting the boundary conditions as described, the heat transfer between the surrounding bedrock of the injection borehole and the injected groundwater was accounted for. On the other side, the heat transfer between the surrounding bedrock of the satellite boreholes and the groundwater, when the water flows through polyethylene pipes to the surface, was not accounted for. The injection temperature, $T_i=1^\circ\text{C}$, was set as a boundary condition at the injection point.

The amount of circulating water in the ground source heat pump system at Bryn was uncertain, and the modelling cases were run with different flow rates ranging from 3.5 to 20 m³/hour (table 4–5). One modelling case had a varying flow rate, where the flow rate increased with time, in an effort to maintain a relatively stable effect output (figure 4–27).

Table 4–5: The most important input parameters, not listed in table 4–2, used in the FEFLOW modellings of the energy potential of the pilot plant at Bryn (Spangelo, 2003).

Description of input parameters	Value
Borehole depth:	94 meters
Radius of borehole:	7 centimeters
Flow equation:	Hagen-Poiseuille
Thermal gradient:	13.5 W/(kmK)
Heat flux from the depth:	44.55 mW/m ²
Hydraulic conductivity in the bedrock:	10 ⁻⁹ m/s (Driscoll, 1989)
Heat capacity of water:	4.18 kJ/(kgK)
Flow rates in the modelling cases bryn1-5:	3.5, 7, 13, 20 and varying (figure 4–27) m ³ /hour, respectively.

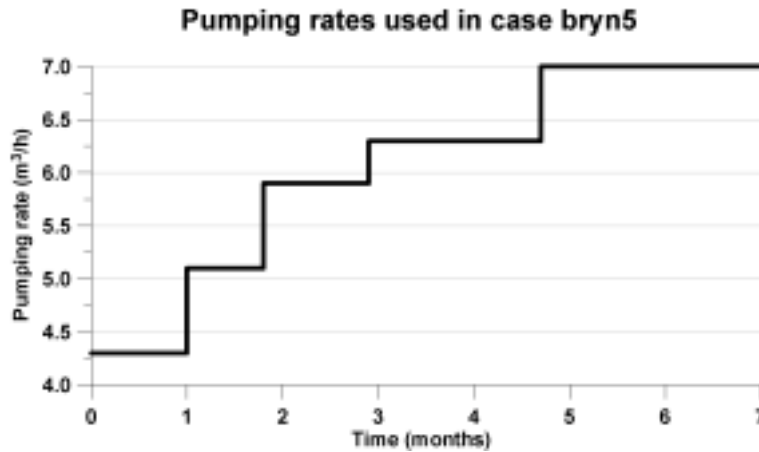


Figure 4–27: The increasing flow rates used in bryn5 (Spangelo, 2003).

The FEFLOW-modelling of the energy potential of the pilot plant at EAB was performed similar to the corresponding Bryn-modelling. The most important input parameters are given in table 4–6. The five fracture planes in the model are calculated based on the observed hydraulic communication, here represented by the groundwater level changes in borehole 1 as a result of the hydraulic fracturing in borehole 2 and 3 (figures 5–79 and 5–80). Analogous to Bryn, the hydraulic communication between a certain level in one of the satellite boreholes and borehole 1 is assumed to constitute of a quarterly fracture

plane. Thus, the 21 observed levels of hydraulic communication are regarded as approximately five horizontal fracture planes (figure 4–28). By dividing all the registered levels with hydraulic communication into five groups, the distribution of the fracture planes are determined based on the mean value of each group (table 4–6). An unsuccessful attempt to determine the flow distribution and the fracture plane apertures from the groundwater level alterations generated by the hydraulic fracturing was tried. The groundwater level data was unreliable since (1) the hydraulic fracturing in most of the upper borehole sections caused an overflow in borehole 1, (2) the volume of water pumped in each stimulation varied, and (3) since the groundwater level had a rising trend during the hydraulic fracturing of a borehole, the initial stimulation resulted in an unrealistically high response compared to the stimulation of the remaining borehole sections. Instead, the high degree of successful fracturing at EAB (paragraph 5.3.5) might indicate a relatively even aperture of the fracture planes. Accordingly, the fracture plane apertures are assumed to be two millimetres (table 4–6). An accurate modelling of the temperature development around the fracture planes was ensured by an increased mesh density, represented by a total of 37 horizontal layers in the vertical direction. The flow rate of the circulating groundwater in the ground source heat pump system at EAB were measured to stabilize around 14 m³/hour (figure 5–84), and the flow rates were set to be 10, 14 and 20 m³/hour for modelling case eab1-3, respectively.

Table 4–6: Input parameters for FEFLOW used in the modelling cases of the pilot plant at EAB.

Input parameters	Value
The plant # of satellite boreholes: Distance from the central- (borehole 1) to the satellite boreholes Borehole 1 - borehole 2: Borehole 1 - borehole 3: Borehole depth: Radius of borehole: Operation period: Flow rate in the satellite boreholes: Temperature of injected water into the central borehole, T _i : Flow rates, modelling case eab1-3:	2 (borehole 2 and 3) 20 metres 16 meters 90 metres 7 centimetres 7 months $Q_{\text{central}}/2$ 1 °C 10, 14 and 20 m ³ /hour, respectively
Thermal data Thermal conductivity of the bedrock: Thermal heat capacity of the bedrock: Thermal gradient: Heat flux from the depth: Surface temperature:	2.7 W/(m,K) (Midttømme et al., 2000) 2.3 MJ/m ³ ,K 1,1 °C/100m (Midttømme, et al., 2004) 44.55 mW/m ² 6.0 °C (Stene, 1997)
FEFLOW data Flow equation: Horizontal fracture planes, each of 2 millimetres; Depth (m): Total area of the five fracture planes: Hydraulic conductivity in the bedrock: Heat capacity of water: Density of circulating water:	Hagen Poiseuille 32, 42, 53, 66 and 79 3475 m ² 10 ⁻⁹ m/s (Driscoll, 1989) 4.18 kJ/(kgK) 1000 kg/m ³



Figure 4–28: A fracture plane extension used in the FEFLOW-modelling of the pilot plant at EAB.

Chapter 5 Results

5.1 Lade

5.1.1 Borehole yields, possible water inlets and groundwater quality

The results from the test pumping in borehole 1 at Lade (figure 5–1) shows that the pumping rates before and after hydraulic fracturing stabilized at 500 and 1400 litres/hour, respectively. Since a complete drawdown to the water intake of the pump was achieved both before and after hydraulic fracturing with water, the results are to some extent comparable, even though two different pumps were used at different depths. If the test pumping had been performed at equal depths, the yield improvement is expected to have been larger according to the location of the pump at shallower depths after hydraulic fracturing than before hydraulic fracturing. The measured borehole yields were significantly lower than the rated flow at the actual head given by the pump characteristics (figure 2–21).

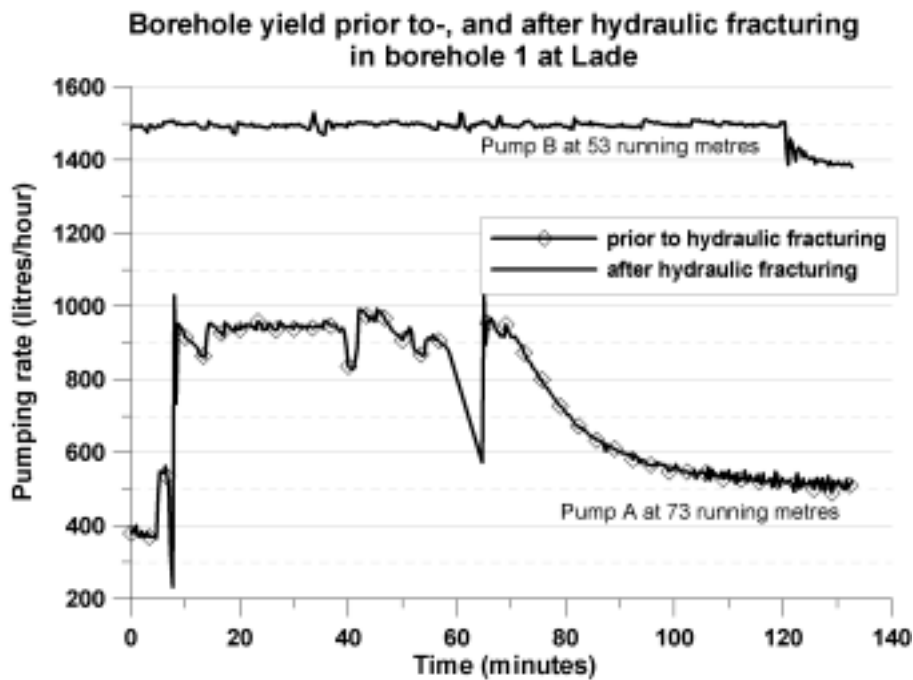


Figure 5–1: Results from the test pumping in borehole 1 at Lade before and after hydraulic fracturing with water-only.

The rising curves from the test pumping (figure 5–2), the only tool for identifying water inlets of the upper 54 running metres of borehole 1 at Lade, indicated to some extent water inlets at approximately 38-40 and possibly at 34-35 running metres (figure 5–2). This is relatively consistent with Banks (1991), reporting a major- and minor water inlet at 39-40 and 33.5 running metres, respectively, and with the results from the

hydraulic fracturing with water-only. The low pressure levels observed during the hydraulic fracturing with water-only in the sections 31-35, 39-43, 63-67 and 71-76 in borehole 1 at Lade implied that these levels contained fracture(s) already opened (figure 5-6). No fracture initiation was obtained for the two remaining borehole sections. The improvement in the borehole yield from 500 to 1400 litres/hour can be explained by the flushing of the already open fracture levels. The eventual water flow in the sections at 63-67 and 71-76 running metres has not been examined.

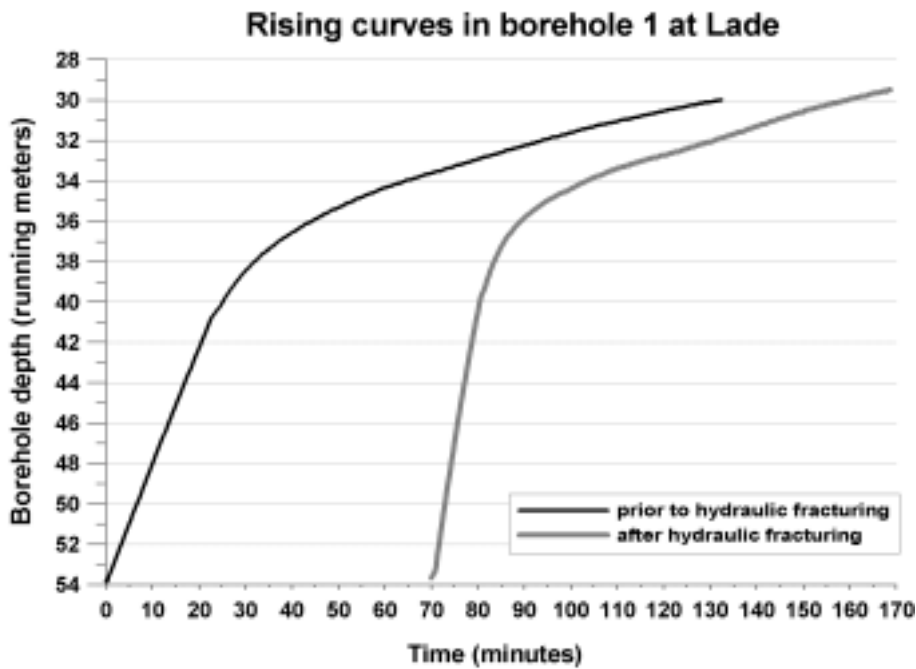


Figure 5-2: Rising curves from the test pumping performed in borehole 1 at Lade before and after hydraulic fracturing with water-only.

The results from the test pumping and groundwater level measurements accomplished in borehole 2 at Lade (figure 5-3) shows that the pumping rate stabilized at 1650 litres/hour. The groundwater level decreased rapidly from the natural level at 25, and stabilized at 48 meters depth. A complete drawdown (slurping) was not achieved.

Only minor changes in the groundwater composition can be related to the hydraulic fracturing with water-only in borehole 1 at Lade (figure 5-4). The pH-values were 7.87 and 7.65 before- and after hydraulic fracturing, respectively. The groundwater is relatively hard and can be characterized as calcium bi-carbonate (Banks, 1991).

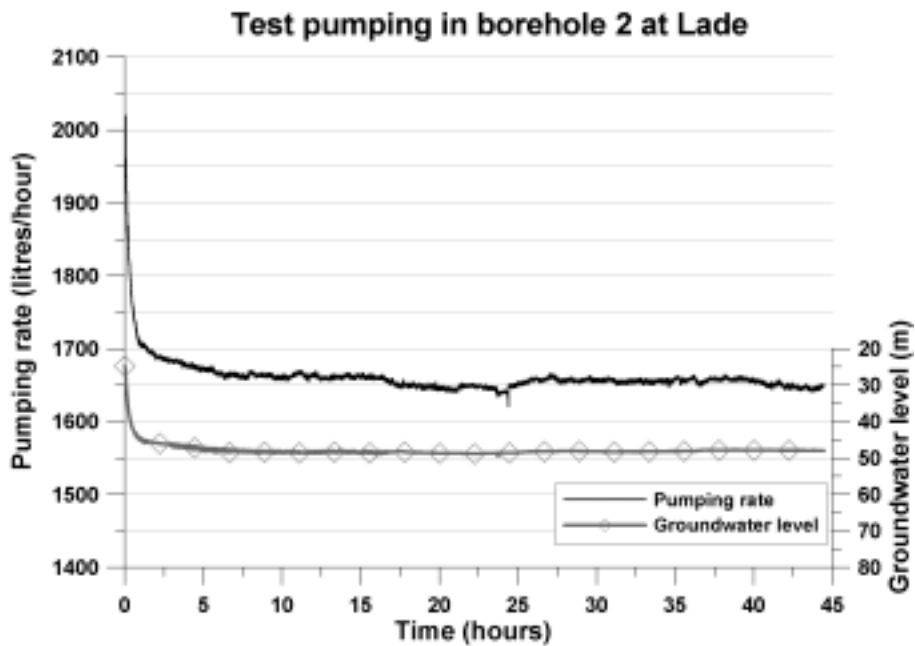


Figure 5–3: The pumping rate and drawdown in borehole 2 at Lade during the test pumping.

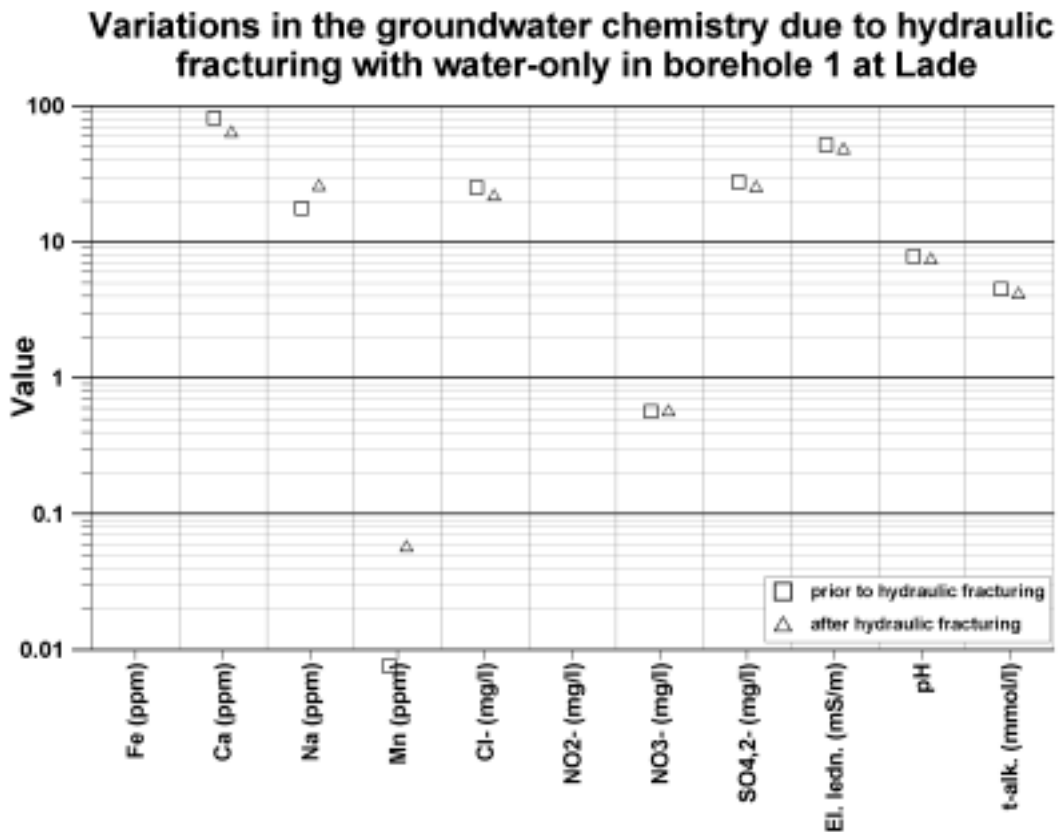


Figure 5–4: Results from a standard water analysis of the groundwater in borehole 1 at Lade before and after hydraulic fracturing with water-only.

5.1.2 Geophysical logging

The borehole inspections with the optical televiewer in borehole 1 before and after hydraulic fracturing were carried out using different logging equipment, and comparing of the two logs to discover any changes in the borehole wall was not possible. The groundwater level in borehole 2 appeared at 24 metres depth on the TCN-log (figure 5–5). A marked change in the electric conductivity and a visible change on the temperature log of the water at 95 metres depth represents a major water inlet discovered as an open hole in the borehole wall with the optical televiewer. The increase in the gamma radiation from 15 to 55 cps (counts per seconds) at 62 metres depth represents a rock boundary where greenstone in the upper part of borehole 2 is followed by a trondhjemite layer.

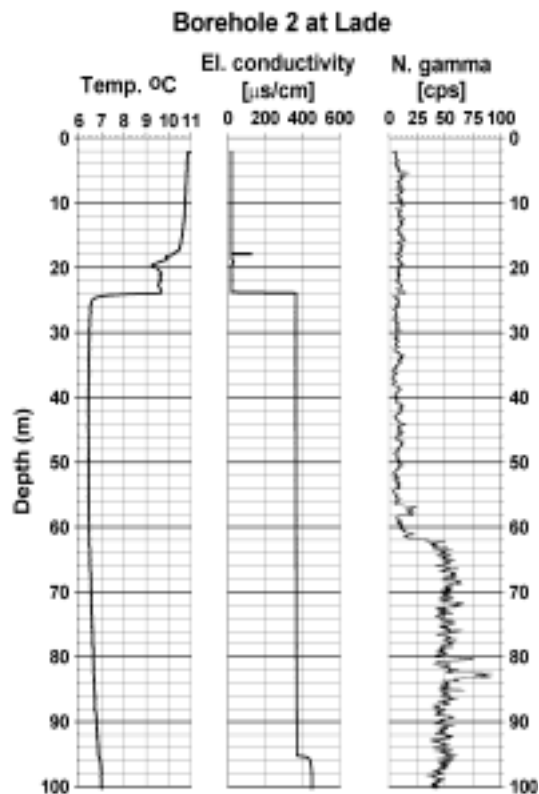


Figure 5–5: The temperature- and electric conductivity of the water, and natural gamma radiation in borehole 2 at Lade.

5.1.3 Hydraulic fracturing with water-only

Results from the hydraulic fracturing with water-only in the six sections in borehole 1 at Lade are shown in figure 5–6. The water pressure of maximum 60 bars in the borehole sections at 75–71, 67–63, 43–39 and 35–31 running metres indicates a reopening/flushing of existing fractures. A relatively high pressure level was required for the hydraulic fracturing in section 59–55, and the water hose was blown reaching 150 bars. Due to the limited working pressures of the equipment, the subsequent hydraulic fracturing in the 59–55- and 51–47-sections were performed at a maximum water pressure of approximately 115 bars. Consequently, the low pressure level and the lack of distinct pressure drops in these sections indicates that no new fractures were initiated.

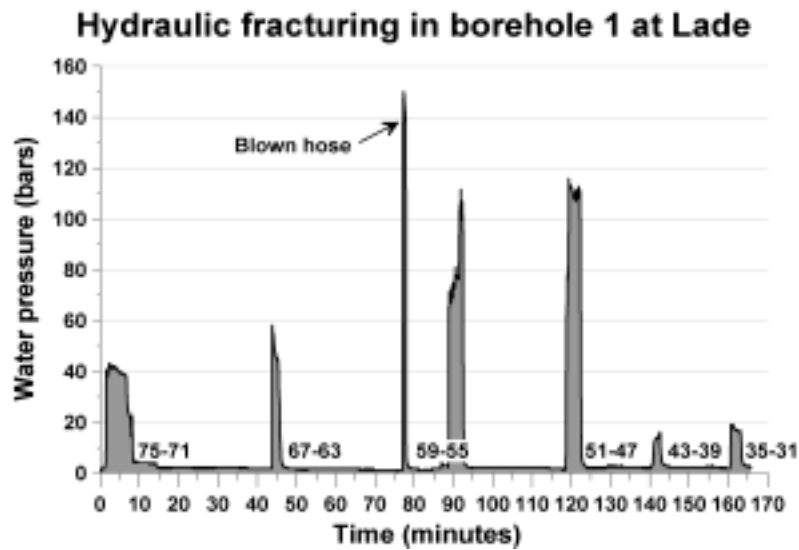


Figure 5-6: Pressure-time curve from hydraulic fracturing with water-only in borehole 1 at Lade.

5.1.4 Hydraulic fracturing with injection of sand

An even pressure rise was observed during the pumping of the injection fluids, stored in containers #1 and 2, into the 84.6-86.6-section in borehole 2 at Lade (figure 5-7). Hydraulic fracturing with water-only, reaching a maximum pressure of 60 bars, were done before the injections. The average pumping rates during the injection of containers #1 and 2 were 26 and 20 litres/minute, respectively. In the subsequent hydraulic fracturing with water-only, performed to flush the injection fluid into the fracture plane, the maximum water pressure increased to approximately 100 bars. The hydraulic fracturing was followed by the injection of fluid from container #3 into the same fracture plane. The pressure course behaved similarly compared with the injections from containers #1 and 2, but the pumping rate was lowered to 7 litres/minute. Analogous to the injections from containers #1 and 2, the injection from container #3 was followed by hydraulic fracturing with water-only (not shown in figure 5-7). A sudden pressure drop in the packer- and water pressure indicated failure of one of the packer elements, couplings or the pressure hose. After a lifting attempt, the downhole equipment got completely stuck in the borehole, and subsequent rescue operations were unsuccessful. The double packer and several meters of water pipes remain in the borehole, and no further investigations could be performed in borehole 2 at Lade.

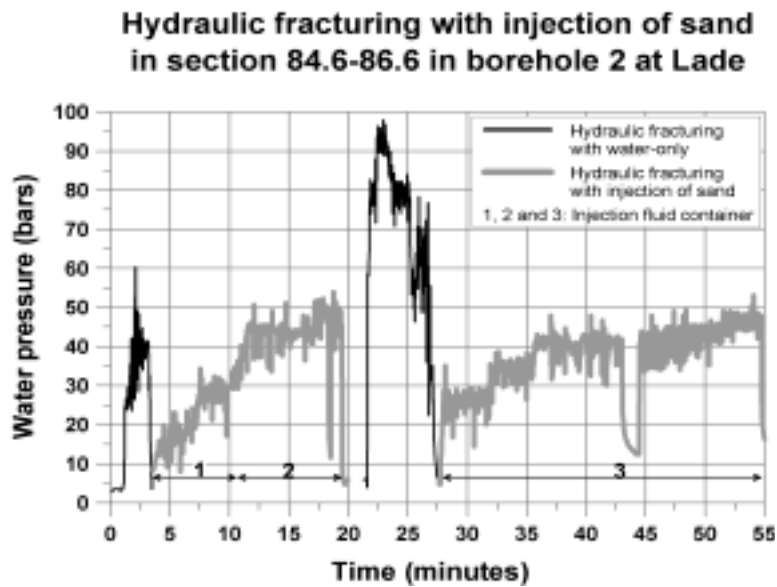


Figure 5–7: Pressure-time diagram from the hydraulic fracturing with water-only and -injection of sand in borehole 2 at Lade. The injection fluid, stored in containers 1-3, were injected at the given time periods.

5.1.5 Changes in the terrain level

Ordinary levelling using a levelling telescope was found to be the best and most accurate way of measuring possible changes of the terrain level caused by hydraulic fracturing with water-only of a nearby borehole. The results from the measurements with the total station were not satisfactory. The levelling results (table 5–1) show that the maximum relative change in relation to a fixed point was 2.0 millimetres, i.e. a lifting of the terrain level of 2.0 millimetres. The remaining measurements indicated a change in the terrain of 1.4, 1.0, 0.8 and 0.5 millimetres.

The validity of the results is unknown. 2.0 millimetres or less are modest values and could be considered as measuring errors. On the other hand, all the measurements verify a minor lifting of the terrain. The modest pressure levels employed during the hydraulic fracturing, only flushing of existing fractures, indicate that the measured terrain changes most likely can be referred to as measuring errors.

Table 5–1: Results from the levelling before and after hydraulic fracturing with water-only (HF) in borehole 1 at Lade.

	Fixed point	Point #1	Point #2	Point #3	Point #4	Point #5
Levelling before HF (m)	3.40950	2.25100	0.71300	2.69020	0.96610	3.65700
Levelling after HF (m)	3.30350	2.14700	0.60800	2.58500	0.86150	3.55150
Deviation (mm)	106.0	104.0	105.0	105.2	104.6	105.5
Relative change (mm) (= Deviation fixed point - deviation point #X)	-	2.00	1.00	0.80	1.40	0.50

5.2 Bryn

5.2.1 Drilling and XRD-, XRF- and thin-section analysis of drill cuttings

A few intrusive diabase dikes were hit during the drilling of the five boreholes in the Ringerike sandstone at Bryn (figure 5–40). The driller's estimates of the short-time production yield of the boreholes at Bryn were 1500, >10000, 5000, >10000 and 8000 litres/hour for borehole 1-5, respectively. These large quantities of water are likely to come from a sub-horizontal exfoliation fracture at 12-13 meters below the terrain surface for borehole 1-3 and 5, and at 17 meters depth for borehole 4.

The XRD- and XRF-results, based on NGU-Lab (2001c), are summarized in tables 5–2 and 5–3, respectively. The interpretation of the analyses was carried out by Nordstrand (2001). Quartz, muscovite, amphibole, chlorite, plagioclase, potassium feldspar and calcite were the major mineral constituents in the drill cuttings from 18, 63 and 99 metres depth of borehole 3 at Bryn. The content of quartz is lowest at 18 metres (table 5–2).

A few inequalities were revealed in the comparison of the borehole-thin-sections with the thin-section made of a surface rock sample (figure 5–8 to 5–11). In addition to the Ringerike sandstone, a sandy clay stone and a basic dyke appears in the thin-sections made of drill cuttings from 18, 63 and 99 metres depth in borehole 3. The basic dyke mainly consists of fine grained epidote, carbonate, serpentine and chlorite. The major constituents in the Ringerike sandstone, interpreted from a thin-section analysis of a surface-rock sample, are quartz (40-50%) and plagioclase (30-50%), while small amounts of amphibole and epidote are identified (Nordstrand, 2001).

Table 5–2: The mineral composition (%) of the bedrock at Bryn obtained by XRD (Nordstrand, 2001).

Mineral	18 metres depth (%)	63 metres depth(%)	99 metres depth (%)
Quartz	18.1	30.0	26.3
Muscovite	23.1	26.0	28.4
Amphibole	21.6	15.5	13.6
Chlorite	17.8	2.0	5.5
Plagioclase	11.3	12.5	13.9
Potassium feldspar	6.7	14.0	12.3
Calcite	1.4	-	-
SUM	100.0	100.0	100.0

Table 5–3: Elemental composition (wt%) of the bedrock at Bryn obtained by XRF (Nordstrand, 2001).

Mineral component	18 metres depth (%)	63 metres depth (%)	99 metres depth (%)
SiO ₂	51.66	55.75	55.94
Al ₂ O ₂	13.55	15.38	14.95
Fe ₂ O ₃	8.65	7.08	7.13
TiO ₃	1.95	0.72	1.07
MgO	8.11	5.93	5.95
CaO	8.53	8.23	8.34
Na ₂ O	1.36	1.32	4.45
K ₂ O	2.21	3.59	3.02
MnO	0.12	0.10	0.10
P ₂ O ₅	0.35	0.19	0.24
Ignition loss	2.34	0.84	0.96
SUM	98.83	99.12	99.15

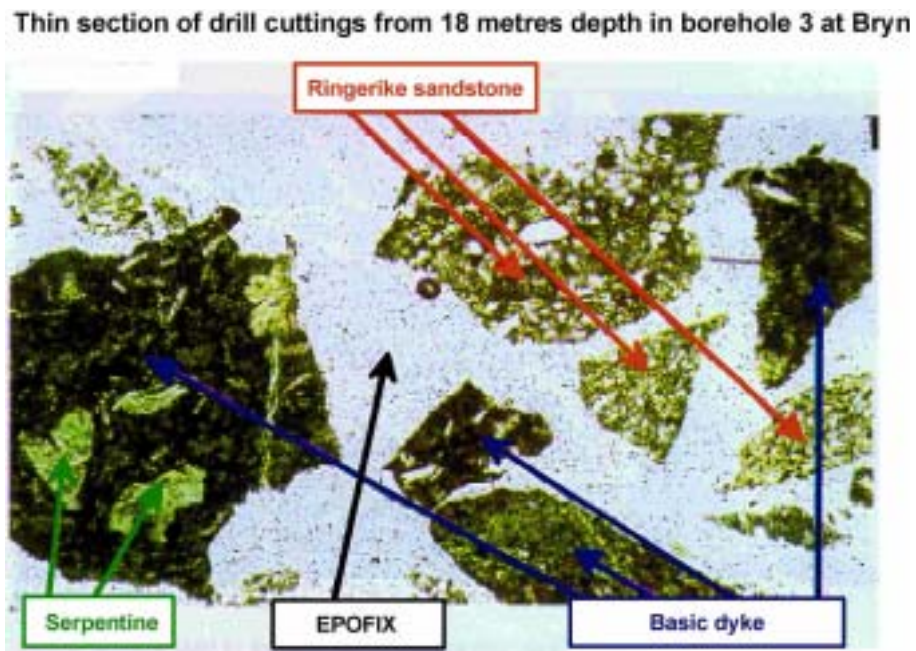


Figure 5–8: Thin-section from 18 metres depth in borehole 3 at Bryn (Nordstrand, 2001).

Thin section of drill cuttings from 63 metres depth in borehole 3 at Bryn

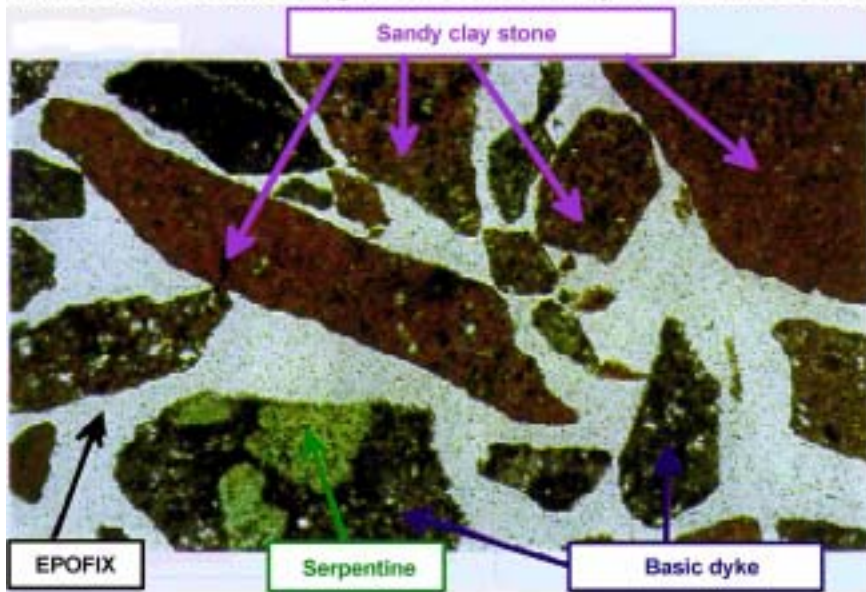


Figure 5–9: Thin-section from 63 metres depth in borehole 3 at Bryn (Nordstrand, 2001).

Thin section of drill cuttings from 99 metres depth in borehole 3 at Bryn

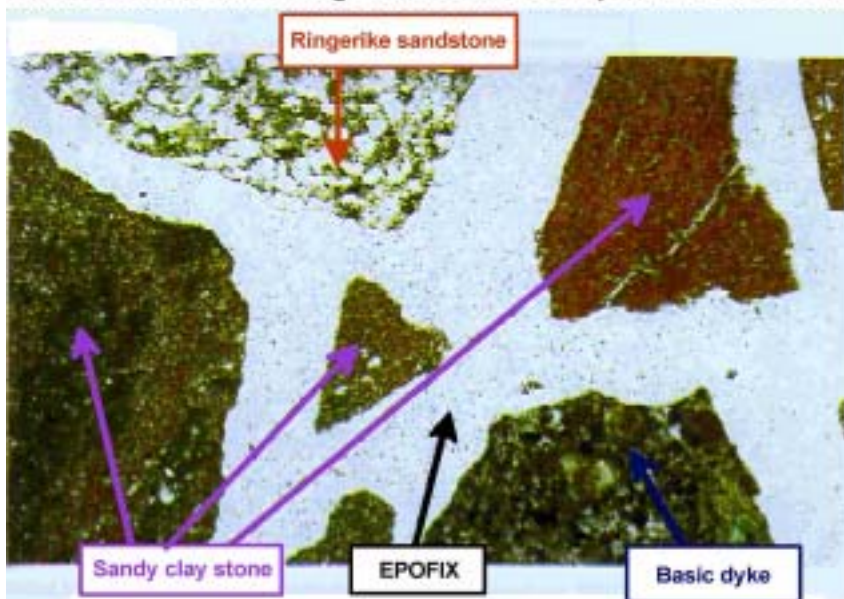


Figure 5–10: Thin-section from 99 metres depth in borehole 3 at Bryn (Nordstrand, 2001).

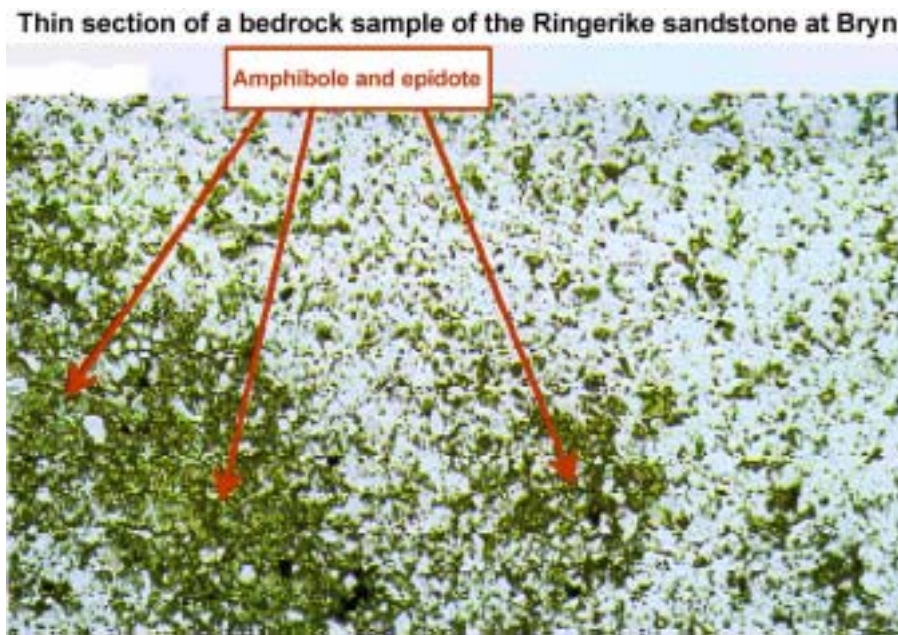


Figure 5–11: A thin-section of the Ringerike sandstone (Nordstrand, 2001).

5.2.2 Borehole yields and groundwater level disturbances

The results from the different kind of test pumping (ordinary-, columnar- and sectional-) performed in the boreholes at Bryn before and after hydraulic fracturing with water-only, and hydraulic fracturing with injection of sand, are presented in figures 5–12 to 5–23. The diagrams show the pumping rates and the groundwater level alterations measured in the nearby boreholes. The borehole yield varies a lot. Figure 5–12 presents the pumping courses from the columnar test pumping in borehole 1 to 5 before hydraulic fracturing with water-only. Borehole 1 and 4 achieved a stable pumping rate, while borehole 2, 3 and 5 had a fluctuating pumping rate.

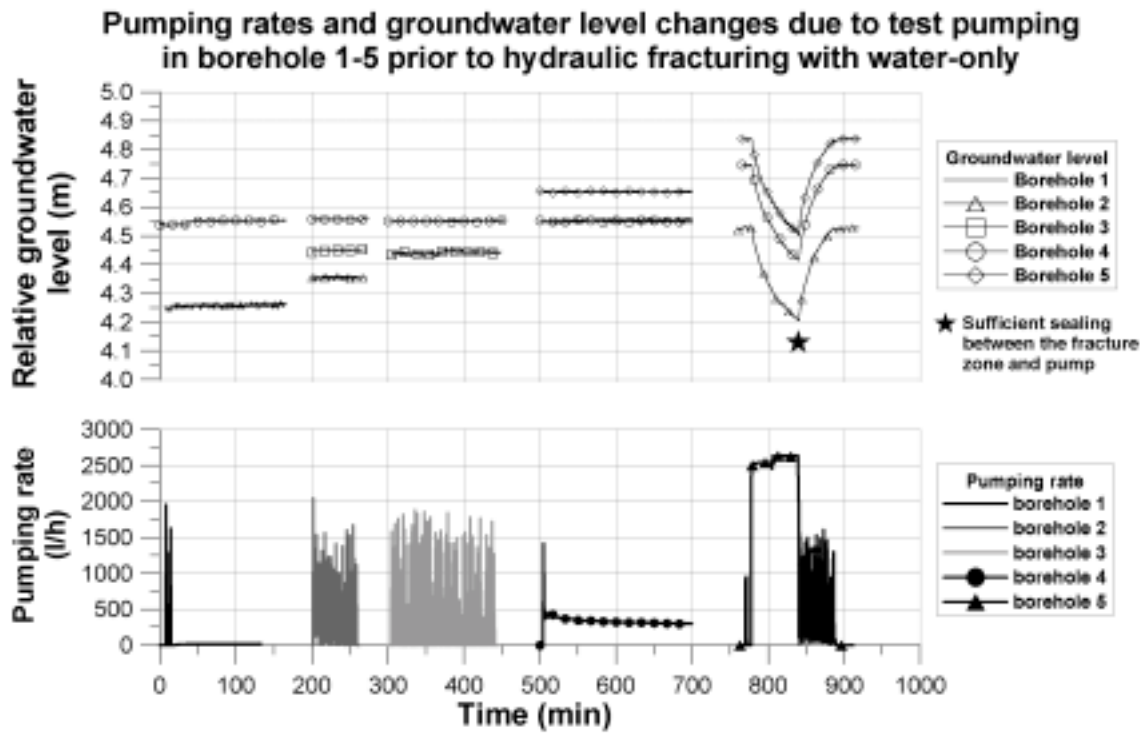


Figure 5-12: Pumping rates and groundwater level changes due to the columnar test pumping in borehole 1 to 5 at Bryn before hydraulic fracturing with water-only.

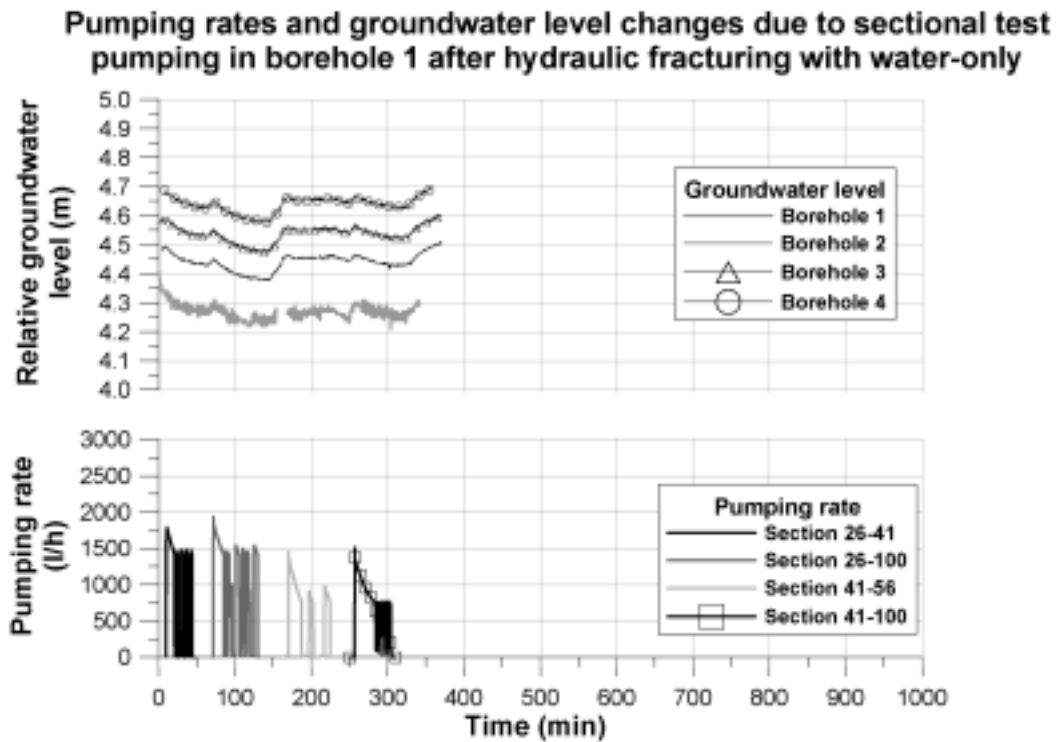


Figure 5-13: Pumping rates and groundwater level changes due to the sectional test pumping in borehole 1 at Bryn after hydraulic fracturing with water-only.

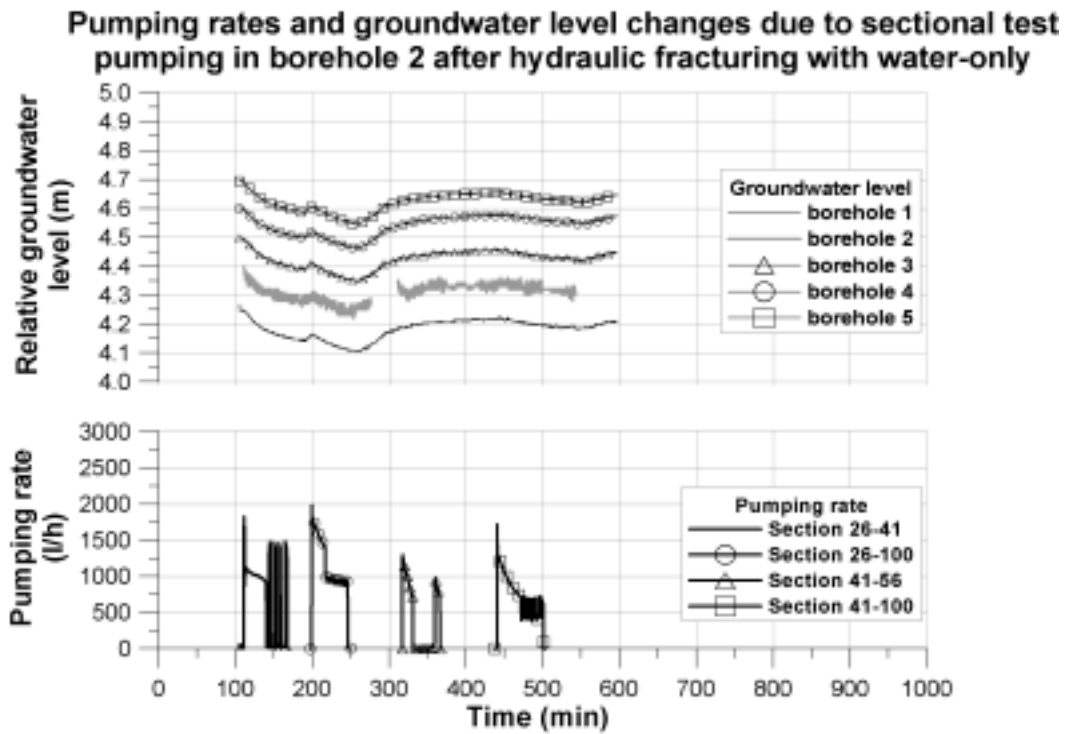


Figure 5–14: Pumping rates and groundwater level changes due to the sectional test pumping in borehole 2 at Bryn after hydraulic fracturing with water-only.

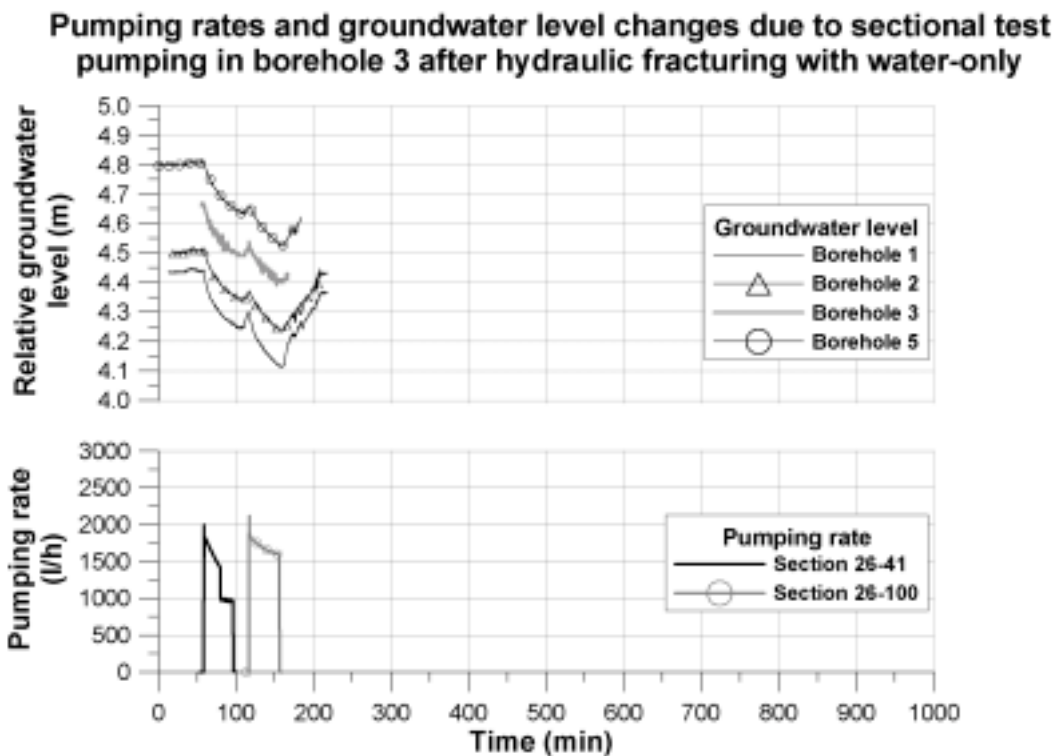


Figure 5–15: Pumping rates and groundwater level changes due to the sectional test pumping in borehole 3 at Bryn after hydraulic fracturing with water-only.

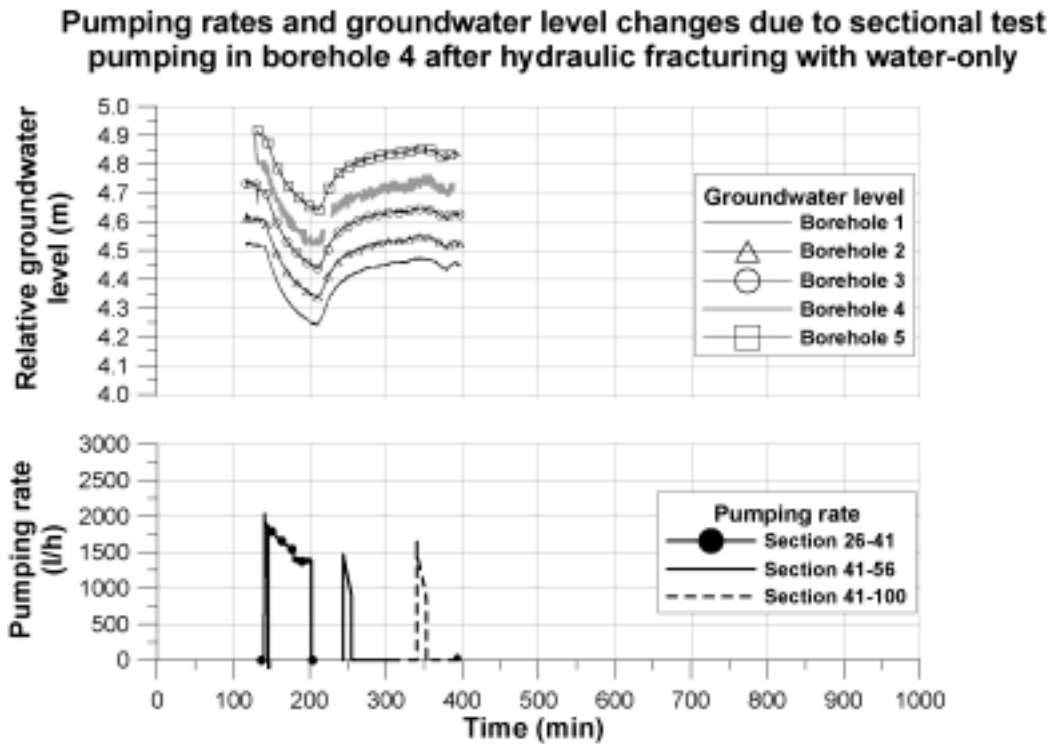


Figure 5–16: Pumping rates and groundwater level changes due to the sectional test pumping in borehole 4 at Bryn after hydraulic fracturing with water-only.

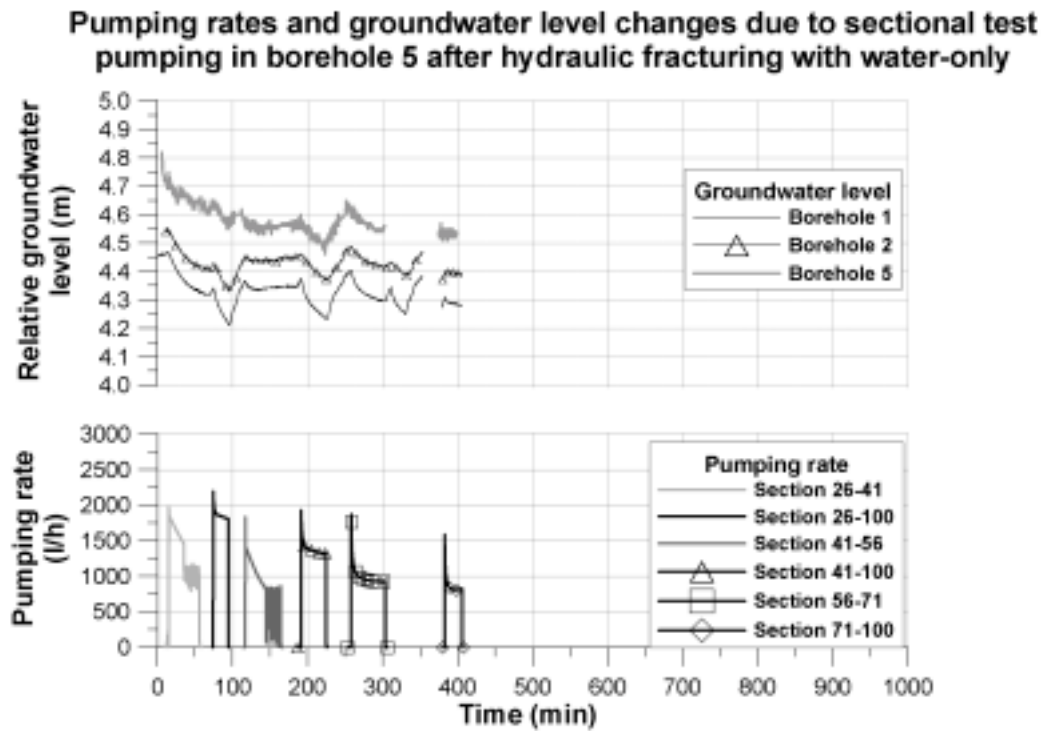


Figure 5–17: Pumping rates and groundwater level changes due to the sectional test pumping in borehole 5 at Bryn after hydraulic fracturing with water-only.

Pumping rates and groundwater level changes due to sectional test pumping in borehole 1 after hydraulic fracturing with injection of sand

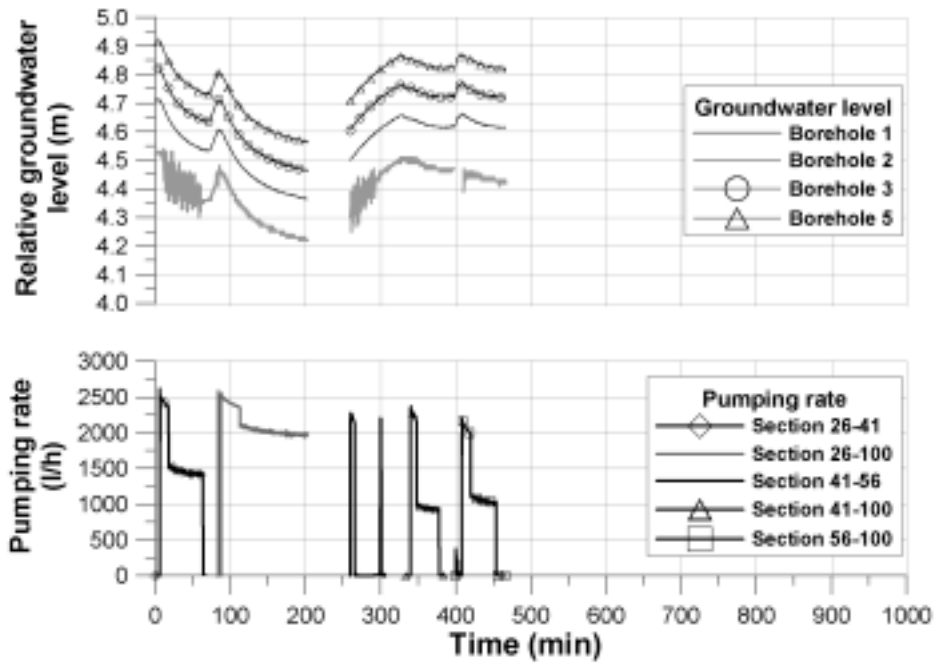


Figure 5–18: Pumping rates and groundwater level changes due to the sectional test pumping in borehole 1 at Bryn after hydraulic fracturing with injection of sand.

Pumping rates and groundwater level changes due to sectional test pumping in borehole 2 after hydraulic fracturing with injection of sand

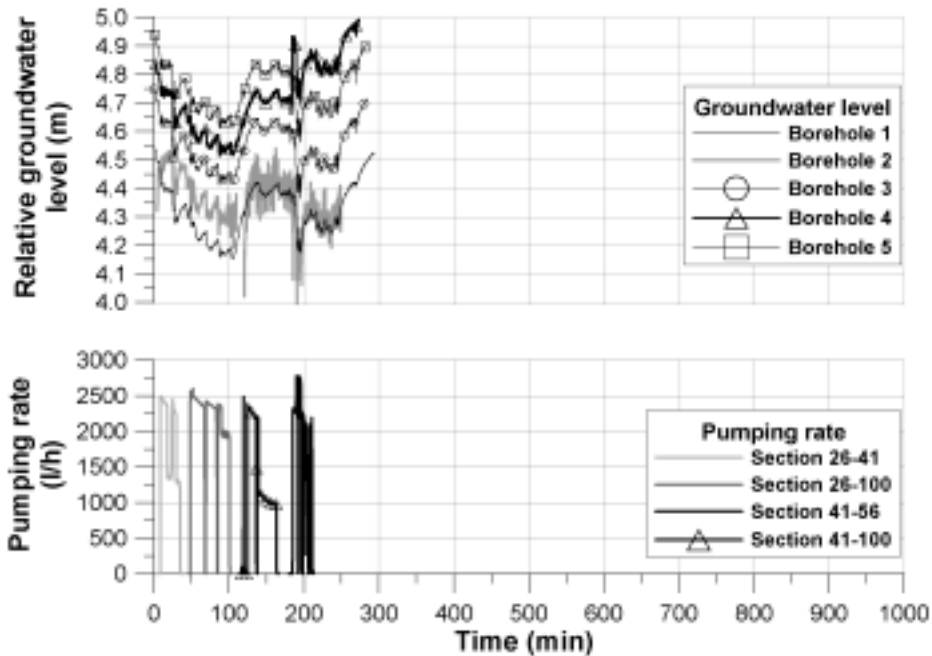


Figure 5–19: Pumping rates and groundwater level changes due to the sectional test pumping in borehole 2 at Bryn after hydraulic fracturing with injection of sand.

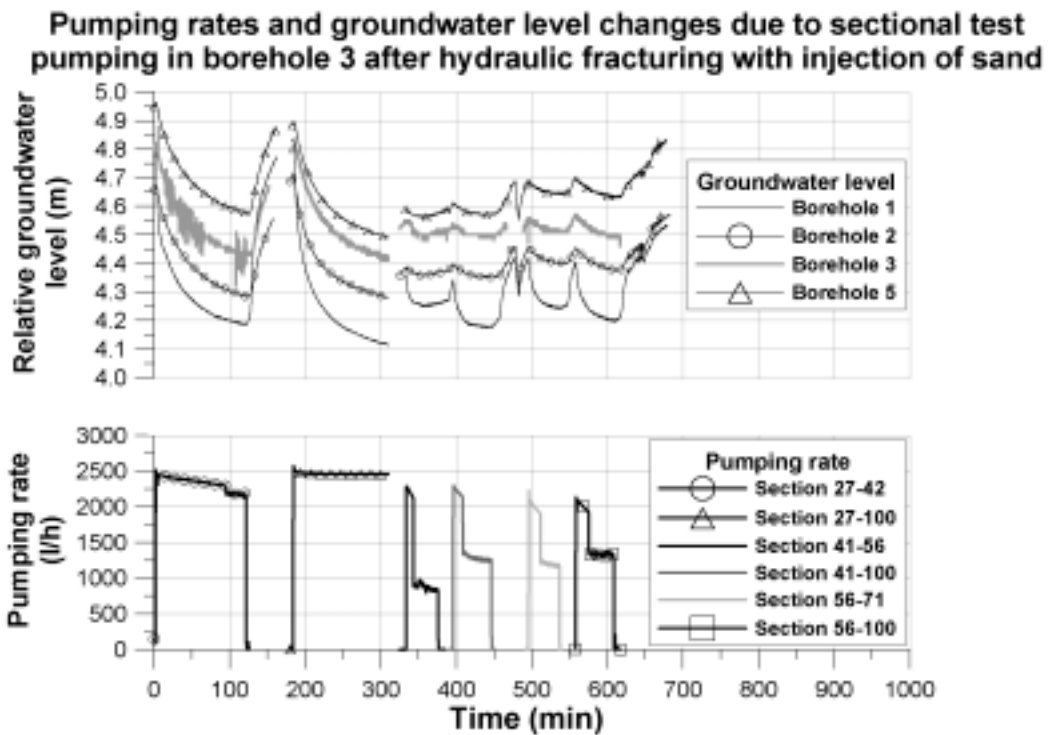


Figure 5–20: Pumping rates and groundwater level changes due to the sectional test pumping in borehole 3 at Bryn after hydraulic fracturing with injection of sand.

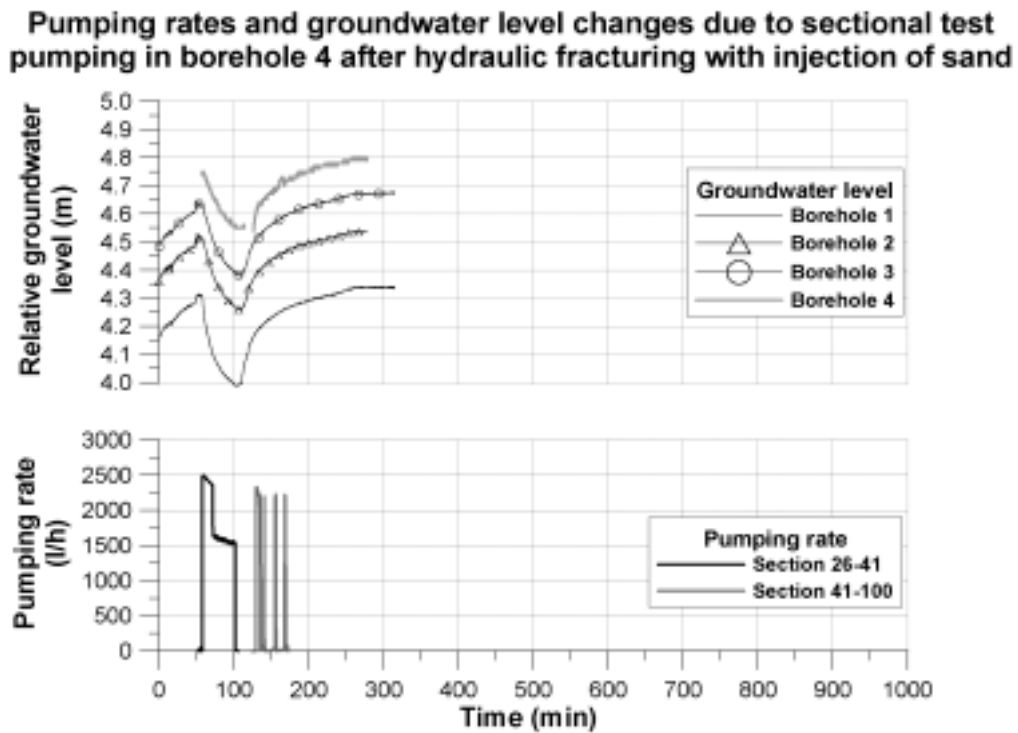


Figure 5–21: Pumping rates and groundwater level changes due to the sectional test pumping in borehole 4 at Bryn after hydraulic fracturing with injection of sand.

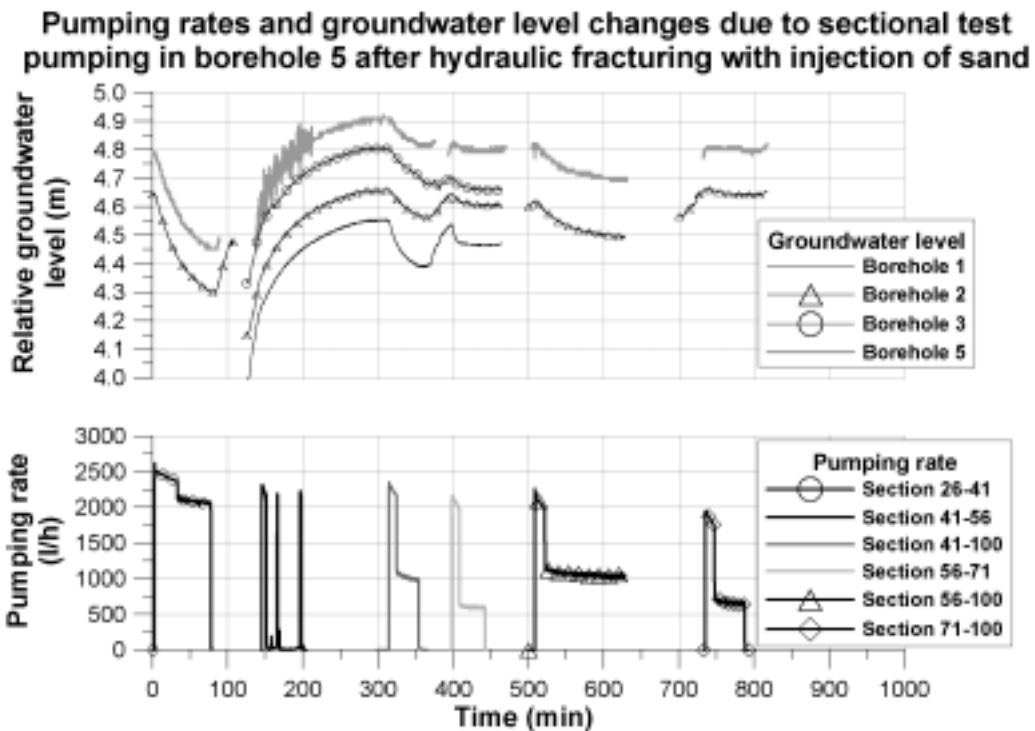


Figure 5–22: Pumping rates and groundwater level changes due to the sectional test pumping in borehole 5 at Bryn after hydraulic fracturing with injection of sand.

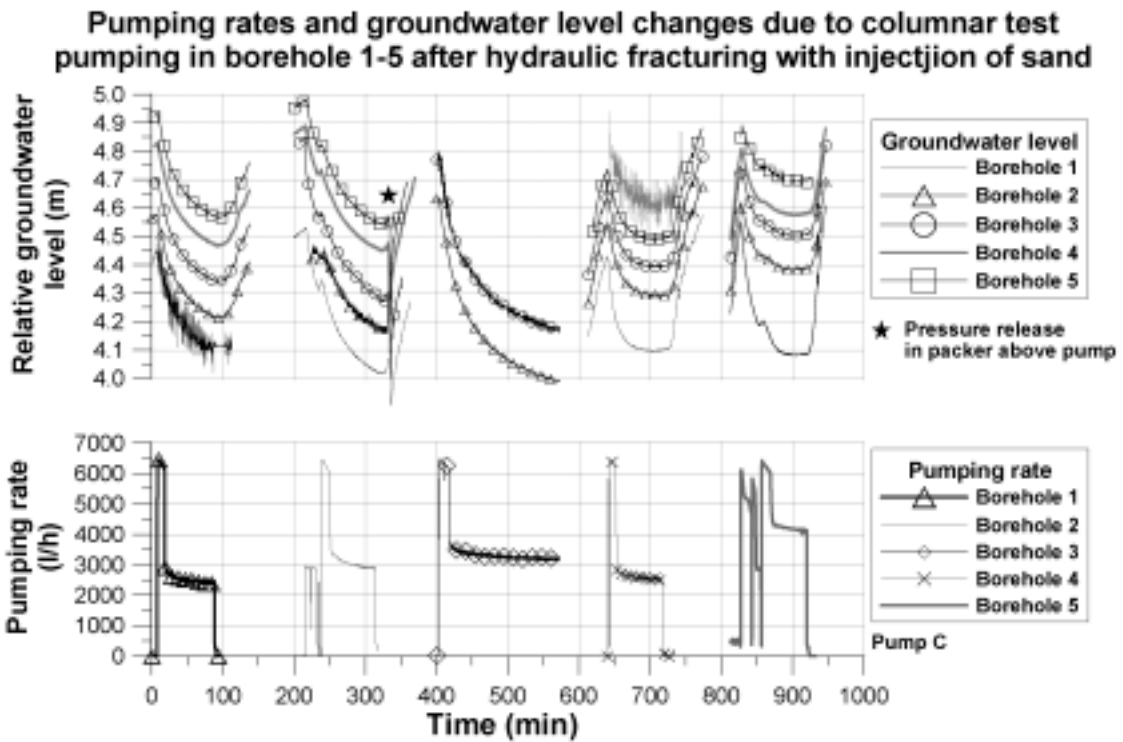


Figure 5–23: Pumping rates and groundwater level changes due to the columnar test pumping in borehole 1-5 at Bryn after hydraulic fracturing with injection of sand.

The groundwater level changes measured in the nearby boreholes for the test pumping-borehole usually have a parallel and almost identical course (figure 5–12 to 5–23). The exception is borehole 1 where the groundwater changes seem to be somewhat larger during the (a) sectional test pumping in borehole 3 and 5 after hydraulic fracturing with water-only, (b) during the sectional test pumping in borehole 3, 4 and partly borehole 5 (section 26-41, 41-100 and 56-71) after hydraulic fracturing with injection of sand, and (c) during the test pumping of borehole 2, 4 and 5 using pump C after hydraulic fracturing with injection of sand.

The yield for the different test pumping sections or -columns, calculated in three different ways (paragraph 2.4.4), are shown in figure 5–24. The abbreviations “pHF”, “aHF” and “aHFS” in the diagrams stand for “prior to hydraulic fracturing with water-only”, “after hydraulic fracturing with water-only” and “after hydraulic fracturing with injection of sand”, respectively. Similar results for the columnar borehole yields at Bryn, calculated in three different ways and determined with pump C after hydraulic fracturing with injection of sand, are presented in figure 5–25. The success of the different kinds of hydraulic fracturing, in terms of increased water yield, is illustrated with selected and comparable results from the test pumping (figure 5–26). These results, based on *pumping rates* or *average*, are from the sectional- or columnar test pumping in:

- The 15-100-column for borehole 1-5 before hydraulic fracturing with water-only.
- Column 26-100 for borehole 1-3, and section 26-41 for borehole 4 and 5 after hydraulic fracturing with water-only.
- Column 26-100 for borehole 1-3, and section 26-41 for borehole 4 and 5 after hydraulic fracturing with injection of sand.

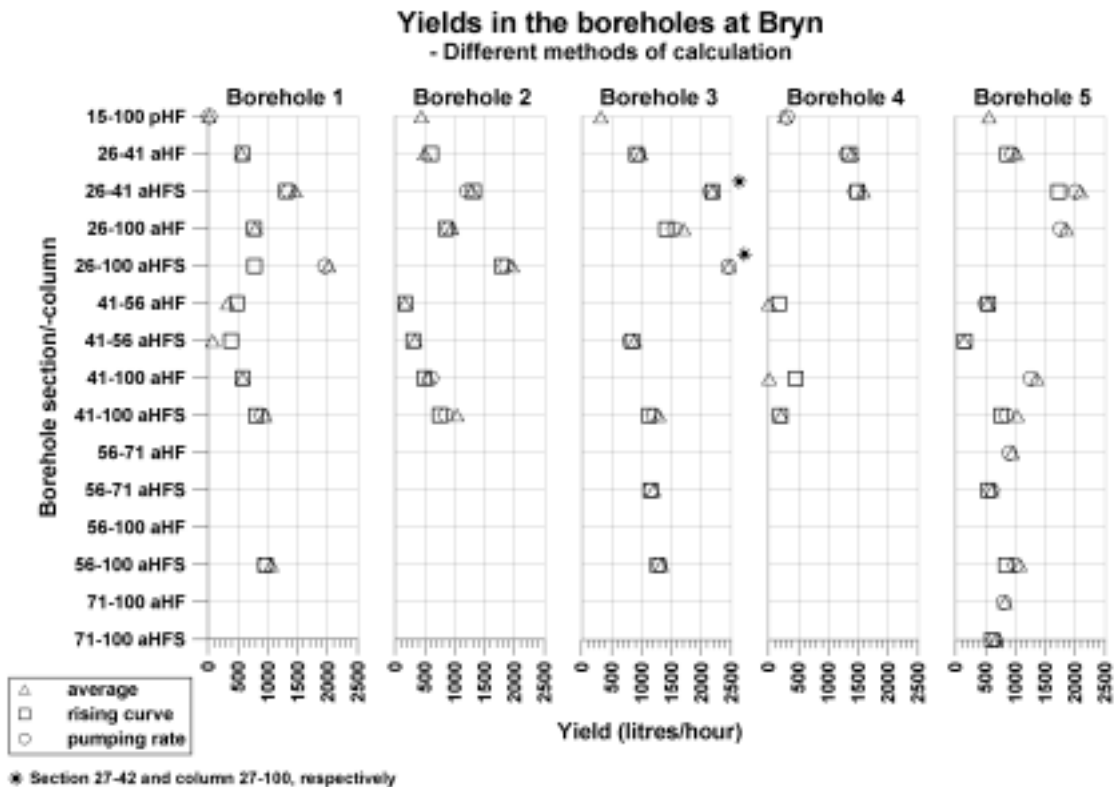


Figure 5–24: Sectional- and columnar yields in the boreholes at Bryn, calculated in three different ways.

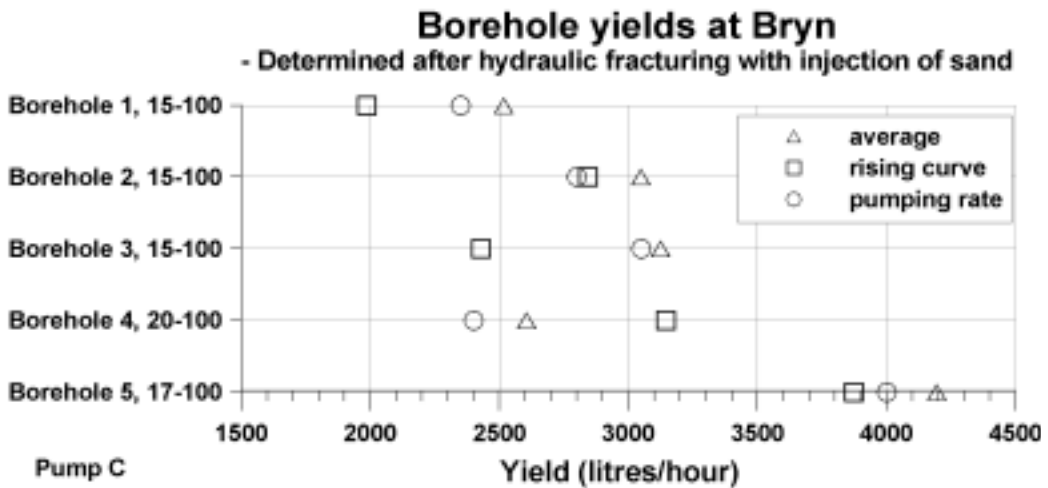


Figure 5-25: Borehole yields at Bryn, calculated in three different ways. Determined with pump C after hydraulic fracturing with injection of sand.

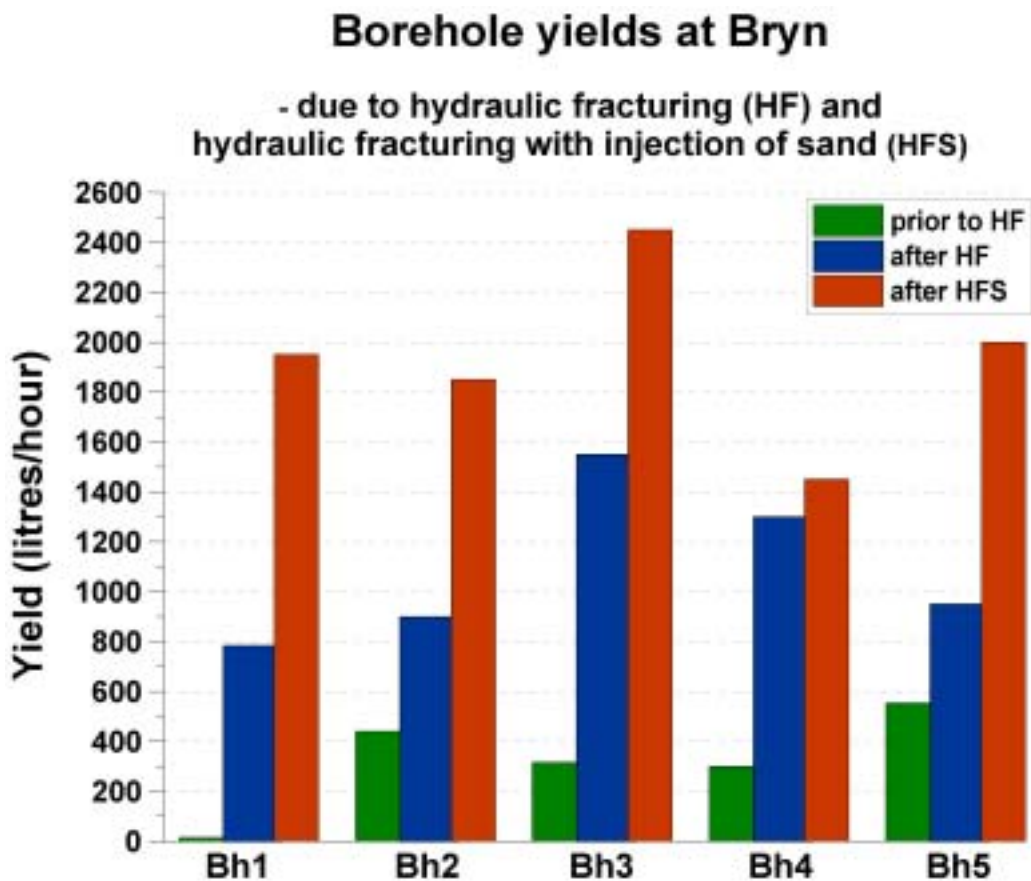


Figure 5-26: Selected and comparable results from the sectional- and columnar test pumping accomplished at Bryn.

5.2.3 Changes in the borehole yield caused by hydraulic fracturing

Figure 5–24 shows an improvement in the borehole yields for most of the boreholes and borehole sections as a consequence of hydraulic fracturing with water-only and hydraulic fracturing with injection of sand. A significant increase in the borehole yield occurred for all boreholes in section 26-41 and partly column 26-100. Since a complete pair of results from the test pumping in column 26-100 was unavailable for boreholes 4 and 5, the results from borehole section 26-41 were used in the comparison of borehole yield-changes in figure 5–26. To match the results from boreholes 1, 2 and 3 (figure 5–24), the borehole yields for boreholes 4 and 5 would probably have been higher in the comparison (figure 5–26) if column 26-100 had been tested both before and after hydraulic fracturing with injection of sand.

The borehole levels having best effect of the injection of sand deeper than 41 metres were partly revealed by the sectional test pumping carried out before and after the hydraulic fracturing with injection of sand (figure 5–24). The main findings in each borehole can be summarized as follows:

Borehole 1

Consistent with the results from the hydraulic fracturing with injection of sand, the yield for section 41-56 in borehole 1, calculated from the *average* pumping rate and the rising curve, was approximately unchanged, while the yield for column 41-100 had increased. The hydraulic fracturing with injection of sand was performed in borehole sections 32.0, 37.9 and 70.6, and only the 70.6-section could possibly have influenced the yield for column 41-100.

Borehole 2

No hydraulic fracturing with injection of sand was performed within section 41-56 in borehole 2, but a minor improvement in the yield for this section can be seen. The minor improvement could be related to the influence of hydraulic fracturing in the surrounding boreholes, or to measuring uncertainties. According to the hydraulic fracturing with injection of sand in borehole sections 81.4, 85.1 and 90.8, a greater improvement in the yield is observed for column 41-100.

Borehole 3

No comparable test pumping data were available in the deeper part of borehole 3.

Borehole 4

The low yield in column 41-100 after hydraulic fracturing with water-only seemed to be further reduced after hydraulic fracturing with injection of sand. The yield-estimates from the *average* pumping rate and rising curve, having such low pumping rates (figure 5–16 and 5–21), should be considered as guiding values only. The hydrogeological conditions in column 41-100 in borehole 4 should be unaffected by the hydraulic fracturing with injection of sand, taking into account that the stimulation of the deepest section took place at 37.9 metres depth.

Borehole 5

Sections 41-56, 56-71, columns 41-100 and 71-100 in borehole 5 have lower pumping rates after hydraulic fracturing with injection of sand compared with before fracturing. Sections treated with injection of sand at greater depths than 41 metres were located at 41.2 metres and 75.7. The water pressure before injection of sand in the 75.7-section stabilized at approximately 70 bars and was about 100 bars after the injection (figure 5–60), while the pressure level was 30-40 bars during the injection of sand in the section at 41.2 metres depth. The low pressure level during the injection of sand in the 41.2-section indicates a relatively open fracture. The measured reduction in the yield of column 41-100, and the improvement of section 26-41 after hydraulic fracturing with injection of sand, makes it reasonable to assume that the open fracture level mentioned above has been included in the test pumping of section 26-41. The open fracture level might also be located at shallower depths than 41 metres. In addition, some inaccuracies related to the depth specifications may be associated with the lowering of the test pumping equipment and the lowering of equipment for hydraulic fracturing (paragraph 5.6.3). A minor change in the temperature- and electric conductivity of the water was observed at approximately 39 metres depth (figure 5–45) after hydraulic fracturing with water-only and after hydraulic fracturing with injection of sand. This event is likely to represent the reopening of the fracture caused by the hydraulic fracturing of section 41.2. An observed reduction in the yield deeper than 41 metres in borehole 5, implies an ineffective injection of sand in the 75.7-section.

Table 5–4: Different operations related to hydraulic fracturing and test pumping at Bryn.

Date	Operation
17.12.2000	Hydraulic fracturing with water-only in borehole 3.
Total of four days within the period of 15.-28.05.2001	Hydraulic fracturing with water-only in borehole 1, 2, 4 and 5.
26.-29.06.2001	Sectional- and columnar test pumping of all the boreholes.
22.-25.10.2001	Hydraulic fracturing with injection of sand in all the boreholes.
30.11.-07.12.2001	Sectional- and columnar test pumping of all the boreholes.

The sectional- and columnar test pumping was performed approximately one month after its respective stimulation with hydraulic fracturing (table 5–4). Except for borehole 3, hydraulic fracturing with water-only and the test pumping after hydraulic fracturing with injection of sand were performed within a time frame of seven months. Assuming that the injection of sand in the section at 75.7 metres depth was inefficient (see argumentation above), the part of borehole 5 at deeper levels than 41 metres, has only been affected by hydraulic fracturing using water-only. Then, the observed reduction in yield for the lower part of borehole 5 may be explained as a long-term effect of hydraulic fracturing with water-only. The initiated- or reopened fractures may, to some extent, have closed up due to the rock stresses in the area. This is a well known effect described in the literature (Smith, 1989, and Gale and MacLeod, 1995). The relatively successful hydraulic fracturing with water-only in borehole 5, compared to the other boreholes at Bryn, may have enhanced the observed yield-reduction, interpreted as a possible long-term effect of hydraulic fracturing with water-only. Five out of eight pressure-time curves, from the hydraulic fracturing with water-only, were interpreted as an initiation-

or reopening of fractures below 41 metres depth in borehole 5 (figures 5–46 and 5–50). Among these, four major- and one median-sized fracture.

A graphical presentation of the yield improvement due to hydraulic fracturing with water-only in the boreholes at Bryn together with the corresponding median values for stable pressure level after fracture initiation for fractures interpreted as large (figure 5–46) is presented in figure 5–27. The quantitative yield improvement in terms of litres/hour shows that the hydraulic fracturing with water-only was most effective for borehole 3, while borehole 1 had the highest percentual yield improvement of 5127%. The large percentual improvement in borehole 1 is caused by the low initial yield. In general, the percentual and quantitative yield improvement show the same trend since borehole 1, 3 and 4 have the largest yield improvement, while borehole 2 and 5 have the lowest. Borehole 1 and 4 have the lowest median values for the stable pressure level for fractures interpreted as large, while the corresponding values for borehole 2 and 5 are highest. Based on a limited data set from hydraulic fracturing with water-only in Newfoundland, Canada, Gale and MacLeod (1995) reports that it would appear that the higher the injection pressure required to maintain maximum flow rate, the lower the absolute increase in well yield. In this context, the injection pressure required to maintain maximum flow rate corresponds to the stable pressure level. Despite of a limited data set from the hydraulic fracturing with water-only at Bryn as well, Gale and MacLeods (1995) observations agree with the behaviour of the boreholes at Bryn, except for borehole 3. In spite of the high yield improvement, the stable pressure level for borehole 3 is relatively high. Looking behind the pressure data set from the hydraulic fracturing with water-only at Bryn, the pressure levels from borehole 3 was recorded manually (table 5–11) while digital measurements of the water pressures were carried out in the remaining boreholes. The manually read water pressures in the field were observed to be approximately 20 bars higher than the results from the digital pressure measurements (paragraph 5.2.9), and this will to some extent explain the deviating relation between the high yield improvement and the high stable pressure level for borehole 3.

Gale and MacLeod (1995) reports that large increases in well yield appear to be correlated with strong backflows of cloudy and sediment laden water when the injection cavities were opened to the atmosphere after stimulation. A similar trend is only seen for borehole 1 and 4 at Bryn, having a high yield improvement, where four observations of coloured backflow in each of the boreholes were connected to the reopening or initiation of a fracture. Three of the fractures in borehole 1 and 4 with coloured backflow were interpreted as large (figures 5–46 and 5–51). The most deviating results according to Gale and MacLeod (1995), almost tending to the opposite, is found in borehole 3 and 5. Borehole 3 has the highest yield improvement, while borehole 5 has the lowest. Borehole 3 has only two observations of coloured backflow connected to the reopening or initiation of fractures interpreted as large, while four registrations of coloured backflow related to large fractures were observed in borehole 5. Coloured backflow from one large- and two middle sized fractures were observed after the hydraulic fracturing with water-only in borehole 2 where, a relatively modest yield improvement was achieved.

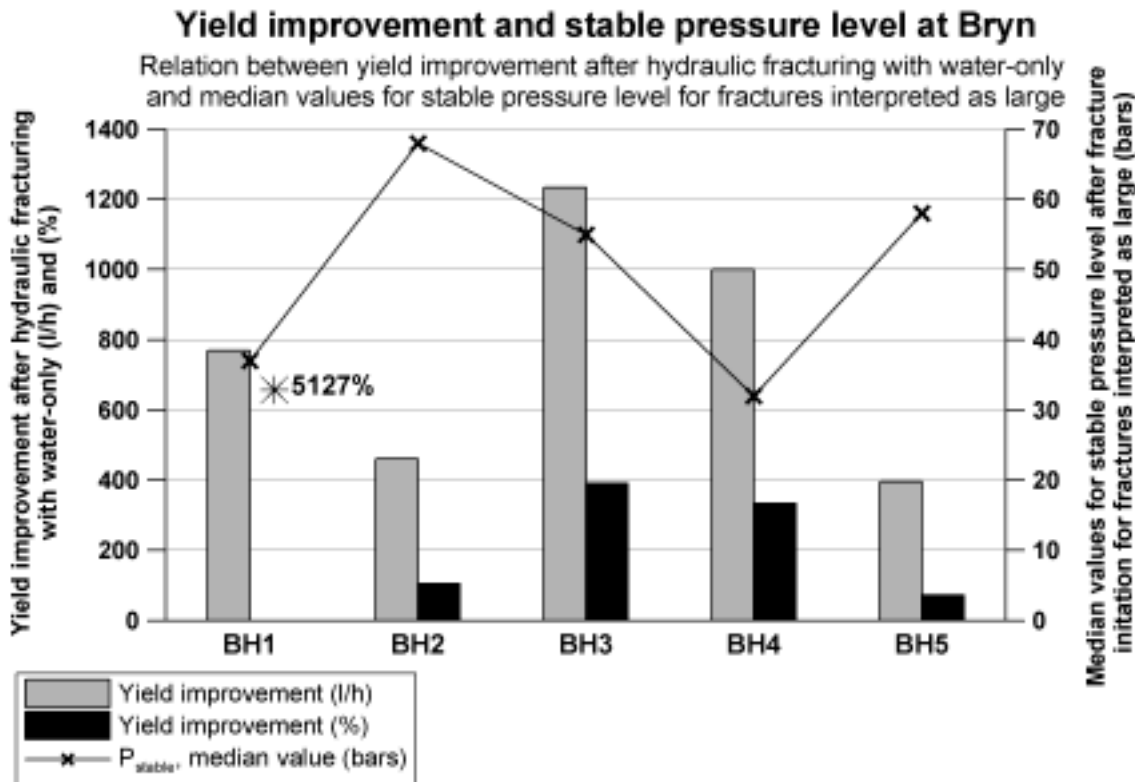


Figure 5–27: Yield improvement after hydraulic fracturing with water-only and median values for stable pressure level for fractures interpreted as large.

The weaknesses of the method, using sectional- and columnar test pumping as a measure on comparable borehole yields after hydraulic fracturing with water-only and hydraulic fracturing with injection of sand, are associated to several factors. Only test pumping where the same kind of pump has been placed at the same depths are considered as completely comparable. A different location of the pump will result in different yields due to changed head and friction losses in thin water bearing fractures. Small leakages between the sealing packer and borehole wall, resulting in a higher yield, may have occurred during the sectional and columnar test pumping. Minor inaccuracies could also be connected to the depth specifications of the downhole equipment for all kinds of investigations performed as separate working operations (paragraph 5.2.8).

5.2.4 Rising curves

Rising curves, showing a continuous course of the rising groundwater level after ended pumping were made of the test pumping data from Bryn. The rising velocity of the groundwater were also plotted in these diagrams. Major water inlets into the borehole, marked with arrows, can be recognised as a flattening of the rising curve, and as minimum values for the rising velocity of the groundwater. Figures 5–28 to 5–32 shows the rising curves from the columnar test pumping of boreholes 1-5 performed after hydraulic fracturing with injection of sand. Possible water inlets are indicated with arrows. The rising curves from the sectional test pumping performed after hydraulic fracturing with

water-only and hydraulic fracturing with injection of sand are presented in Appendix 1 and Appendix 2, respectively.

Corresponding sinking curves from the test pumping at Bryn is not included due to inconsistent results with the rising curves. The reduced quality of the sinking curves was probably caused by: 1) Disturbance from uncontrolled variations in the pumping rate, and 2) decreasing pump capacity with increasing head (paragraph 2.4.3).

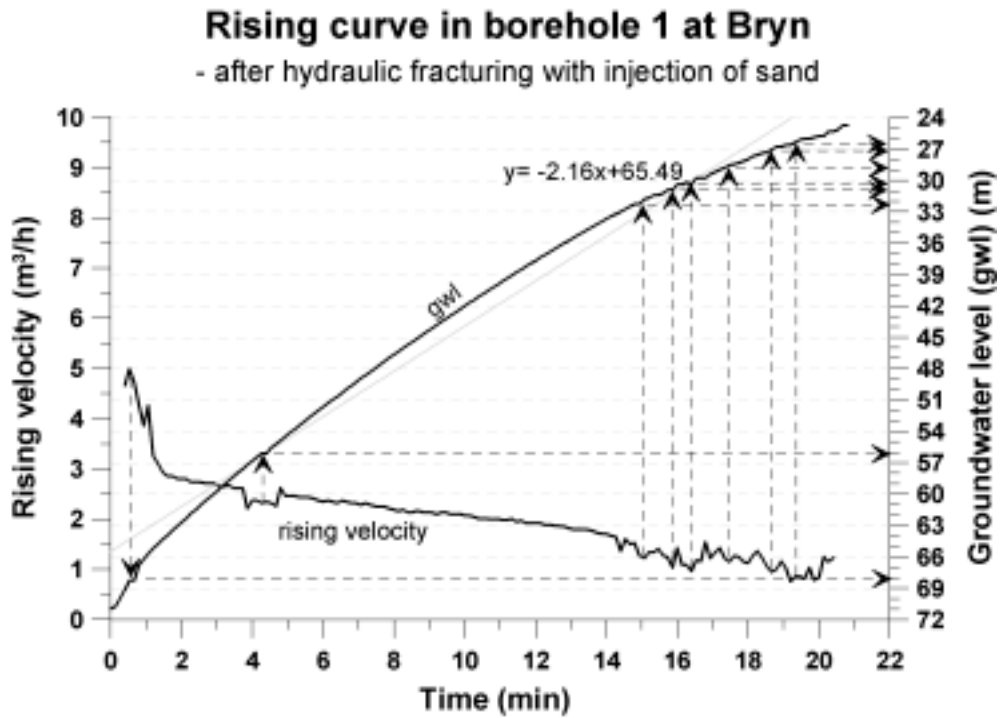


Figure 5–28: The rising curve in borehole 1 at Bryn. Possible water inlets are indicated.

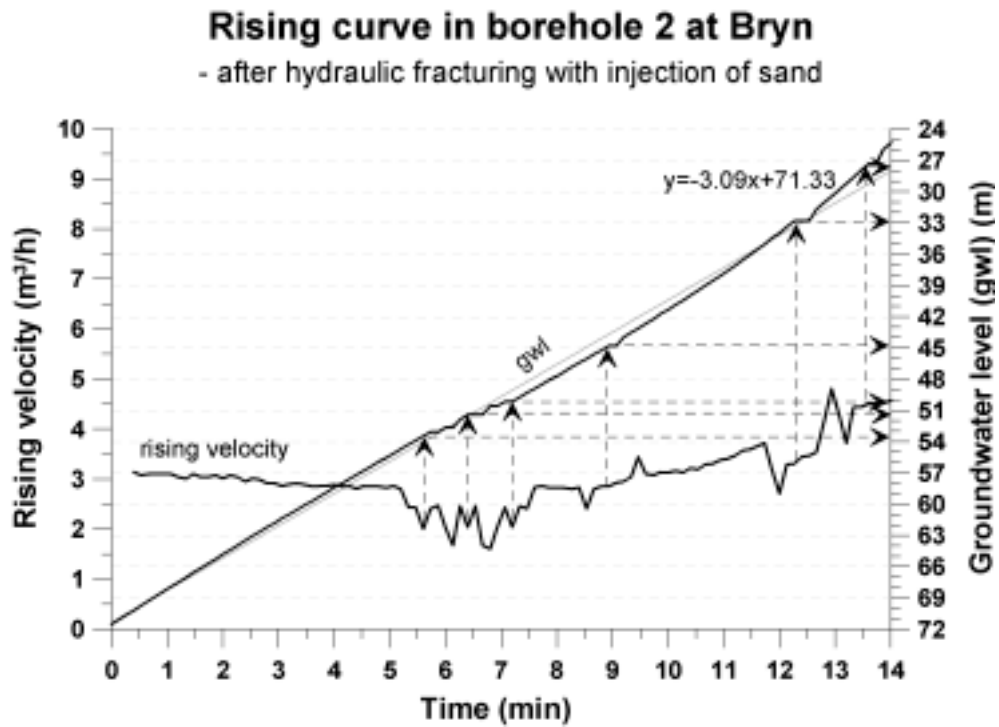


Figure 5–29: The rising curve in borehole 2 at Bryn. Possible water inlets are indicated.

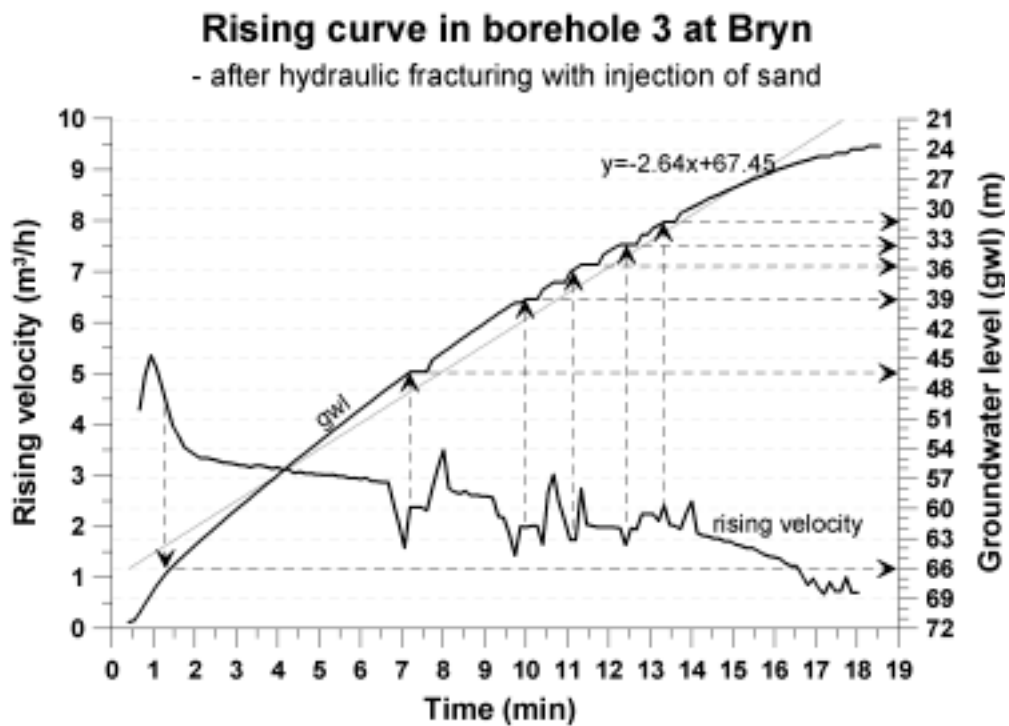


Figure 5–30: The rising curve in borehole 3 at Bryn. Possible water inlets are indicated.

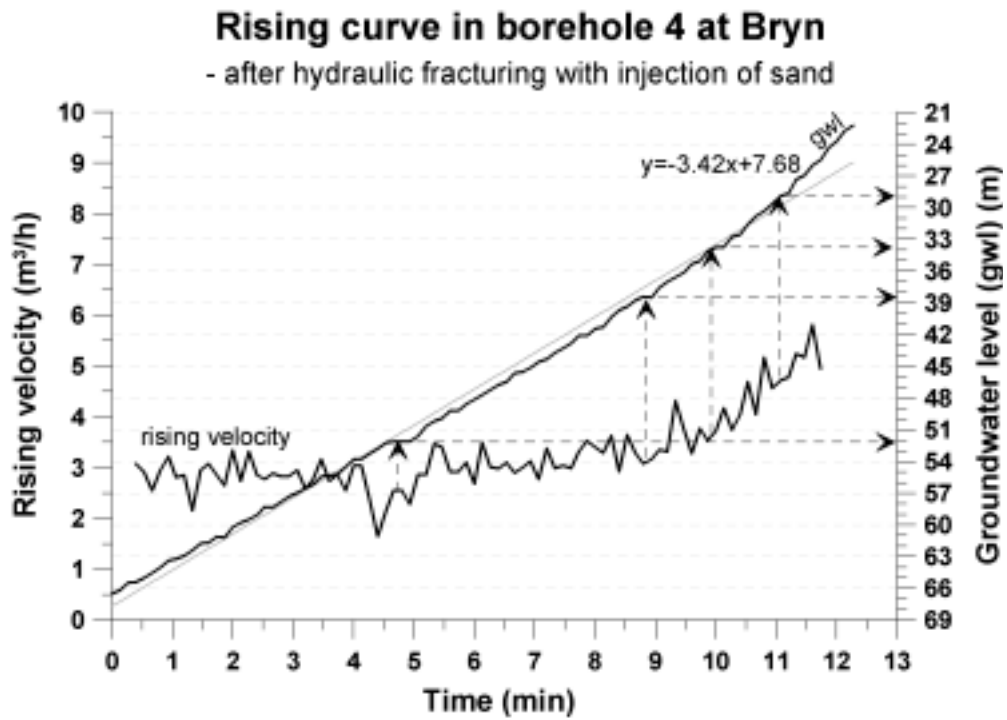


Figure 5–31: The rising curve in borehole 4 at Bryn. Possible water inlets are indicated.

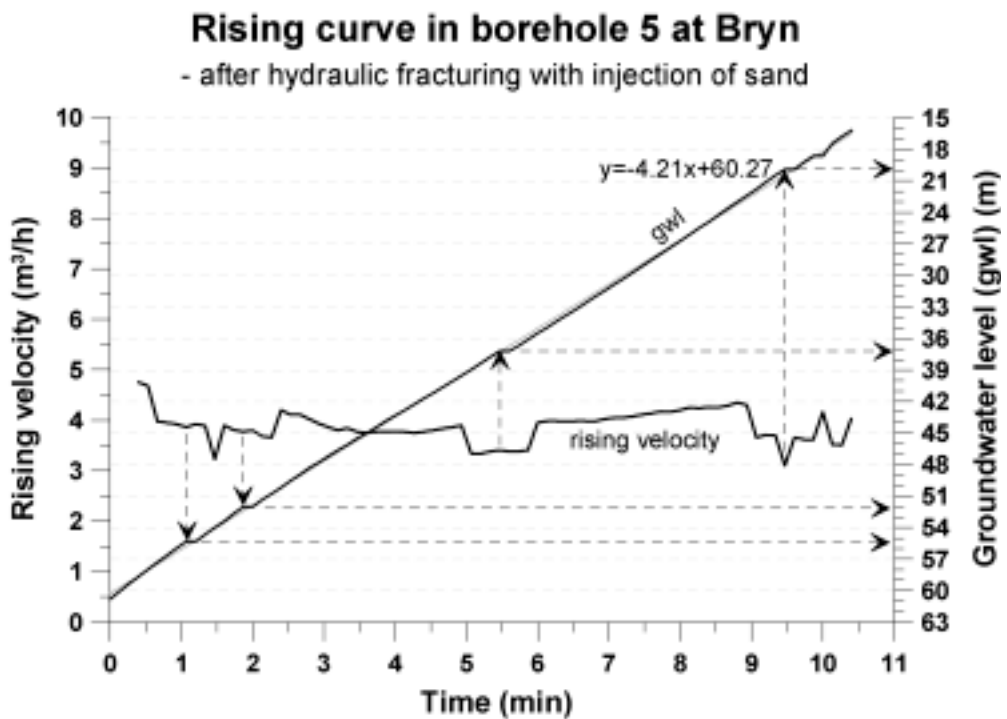


Figure 5–32: The rising curve in borehole 5 at Bryn. Possible water inlets are indicated.

5.2.5 Groundwater chemistry

Figure 5–33 gives a box plot presentation of selected results from the water analysis performed on the groundwater samples collected during the test pumping at Bryn (figure 4–7). The results are based on data from NGU-Lab (2001a, 2001b and 2002a). The groundwater in the boreholes at Bryn can be characterized as calcium rich with relatively high values of dissolved sodium and chloride. The largest change for some of the parameters is observed after hydraulic fracturing with water-only where the values for chloride and NO_3^- were significantly reduced. Minor reductions were observed for calcium and the total alkalinity, while the sodium, and sulphate value were a little increased. Iron was also introduced in the water. A closer look at the pH-value (figure 5–34) reveals that the pH-values are considerably higher after hydraulic fracturing with water-only compared with the remaining measurements, except for borehole 4. Since the water sample in borehole 4 was collected in the upper 26 metres of borehole, the water was likely to consist of water from the open fracture zone at 17 metres. The corresponding water samples for the remaining boreholes were collected during test pumping using pump B in the deeper column of the boreholes (figure 4–7), where the water, compared with the flowing water in the open fracture zone at 17 metres, is relatively stagnant. Frengstad (2002) showed that there is a significant correlation between increasing groundwater pH median values and increasing borehole depth. The same pattern is generally displayed for sodium, while median NO_3^- concentrations seem to decrease with increasing borehole depth. Also, water drawn from one high-yielding fracture is expected to have lower ionic strength than compared with water drawn from many small fractures with a larger water-rock interface. The high pH-value after hydraulic fracturing with water-only together with the lowered calcium concentration and the total alkalinity may indicate a water-rock interaction where bi-carbonate is saturated. The decreasing concentration of chloride might be a result of dilution caused by the injection of water, or caused by the pumping of old water which is unaffected by quaternary deposits. The latter explanation also supports the increasing sulphate-value. The introduction of iron may be a result of more anoxic groundwater conditions.

The increase of NO_2^- and NO_3^- after hydraulic fracturing with injection of sand might be a result of the introduction of the guar gum thickener together with the sand. The pH-value, total alkalinity and sulphate returns to its original level, the chloride, calcium, iron and manganese concentrations remains stable, while a small increase in the content of sodium can be seen. These observations indicate water with shorter retention time and lower electric conductivity which may correspond to the pumping of water from the largest water bearing fractures in the upper part of the borehole columns (figure 5–24). Even though pump C was located between 62 and 72 metres depth, this pump is stronger than pump B (figure 2–21) and would to a larger extent be capable of drawing water from the major water inlets in the upper part of the borehole column, but below the sealing packer for the natural fracture zone.

The groundwater quality in the boreholes at Bryn is considered to be satisfactory for ground source heat pumps system and the direct use of circulating groundwater. The limit values referred to in paragraph 2.5 are not exceeded. But the maximum concentrations of iron and manganese of 0.3 and 0.2 mg/l, respectively (figure 5–33) could increase in an operation mode, and cause operational problems by clogging of the heat exchanger, fracture planes and pump installations. In addition, the calcium concentration is

somewhat high, and an adequate water-quality monitorings program is highly recommended.

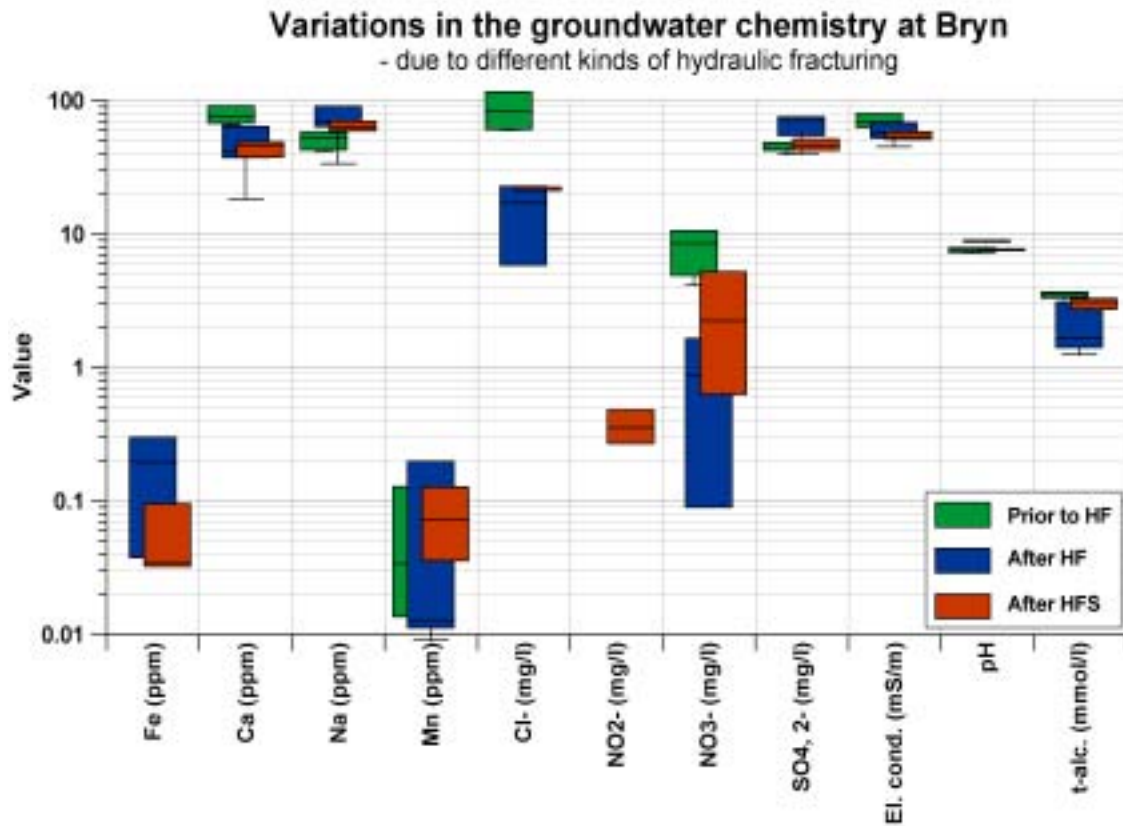


Figure 5–33: Selected results from the groundwater analysis collected during the test pumping at Bryn (based on data from NGU-Lab, 2001a, 2001b and 2002a).

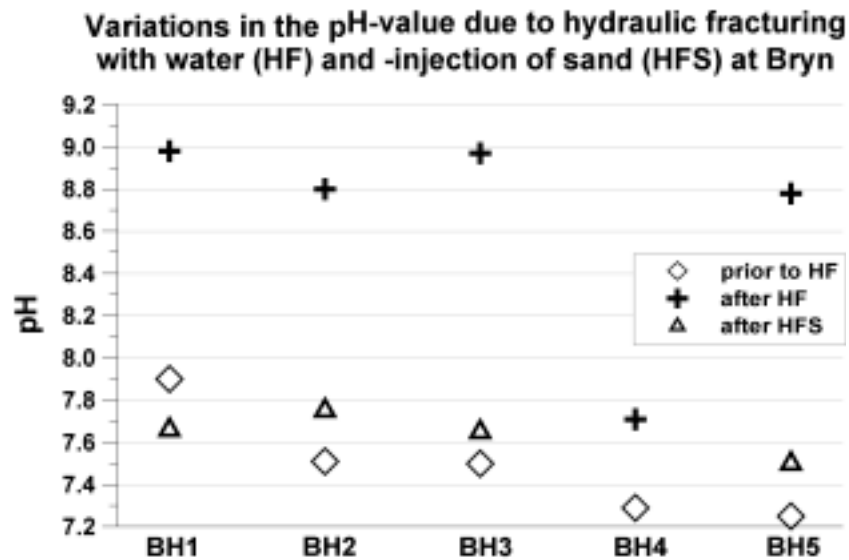


Figure 5–34: pH-values before and after hydraulic fracturing with water-only, and after hydraulic fracturing with injection of sand (HFS).

5.2.6 Rock stresses

This paragraph is based on Jóhannsson (2001).

The rock stress measurements, performed as five hydraulic fracturing tests in borehole 4, were successful. A distinct fracturing was observed for all test sections in the first hydraulic fracturing cycle, and an equally distinct jacking of the initiated fracture(s) were present in the following cycles (figure 5–35). The fracture initiation pressure in the first test cycle varies from 140-228 bars, while the reopening pressure varies from 33-129 bars. The value of the shut-in pressure is considered to be equal to the minimum principal stress, and varies from 46-167 bars or 4.6-16.7 MPa. The theoretical value of the tensile strength of the rock, calculated as the difference between the fracture initiation pressure and the reopening pressure in the second and third test cycle, is in the order of 7-11 MPa. All results from the rock stress measurements are presented in table 5–5.

The use of the optical televiewer for the orientation of the initiated fractures was unsuccessful. Comparing the two optical televiewer logs, recorded before and after the hydraulic fracturing tests, revealed that it was impossible to discover any changes on the borehole wall within the test sections. Based on earlier experiences, the maximum principal stress direction may be oriented parallel to the dominating vertical fracture system in the area (Jóhannsson, 2001).

Tabell 5–5: Rock stresses from the hydraulic fracturing tests at Bryn (Jóhannsson, 2001).

Borehole depth (m)	Fracture initiation pressure P_c (bars)	Reopening pressure P_f (bars)		Instantaneous shut-in pressure P_s (bars)			Estimated maximum principal stress (MPa)
		2 nd cycle	3 rd cycle	1 st cycle	2 nd cycle	3 rd cycle	
97	188	82	76	92	67	65	15
93	228	129	125	167	144	136	32
88	180	108	110	127	123	107	25
75	140	33	35	49	47	46	11
65	168	55	54	60	72	53	13

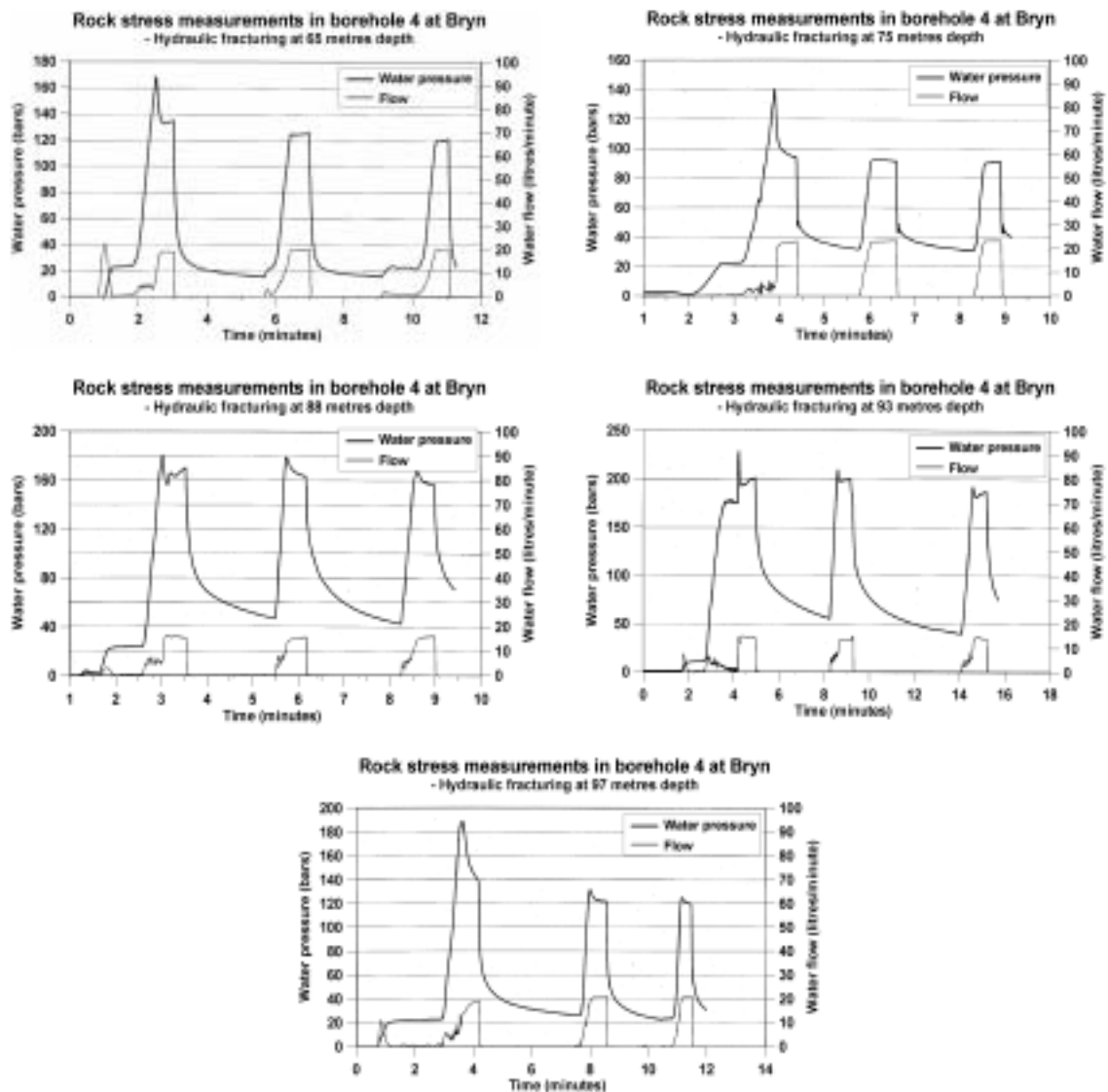


Figure 5-35: Time-pressure- and time-flow curves from the hydraulic fracturing tests carried out in five sections in borehole 4 at Bryn. A marked fracturing of the rock mass takes place in the first cycle, while the initiated fracture(s) is jacked in the second and third cycle (Jóhannsson, 2001).

5.2.7 Borehole conditions - degree of fracturing, temperature, conductivity and radioactivity

A strategic location of the double packer during hydraulic fracturing was possible after a thorough inspection and fracture mapping carried out with the optical televiewer. Physical changes in the borehole wall due to hydraulic fracturing with water-only and hydraulic fracturing with injection of sand were observed in a few cases at Bryn. For instance at 82.2 meters depth in borehole 2 (figure 5-36), where a fracture existing before hydraulic fracturing with water-only is clearly more open both after hydraulic fracturing with water-only and after hydraulic fracturing with injection of sand.

Fracture mapping was done using the optical televiewer. The joint rosettes from borehole 1-5 at Bryn (figure 5-37) show that the main fracture direction in the Bryn area

is approximately north-south. The dip of the main fracture direction varies within 40-60° towards west. An example of a fracture analysis stereogram and a belonging frequency analysis log, made from the optical televiewer fracture mapping of borehole 1, is presented in figures 5–38 and 5–39, respectively. Similar frequency histograms and stereograms for the remaining boreholes at Bryn are presented in appendix 3. The upper table at the left for the stereogram (figure 5–38) summarizes the mean strike direction and dip angle, the number of fracture observations and the mean fracture density in the borehole for each fracture system. The lower table presents the mean strike and dip direction for the intersecting line between two fracture planes. The different colours in the belonging frequency analysis log for borehole 1 (figure 5–39) corresponds to the identified fracture systems in the stereogram. Each fracture observation is plotted as arrows at the actual dip angle in the left part of the diagram, and the tail represents the dip direction. North is defined up. The frequency histograms in the middle of the diagram presents the fracture density as numbers of fractures per borehole meter for the actual fracture system within the actual zone. The borehole is divided into several zones indicated with black horizontal lines. The numbers above the frequency histograms represents the mean strike direction and dip angle, while the subsequent line is the mean fracture density for the whole borehole. The column at right displays the borehole deviation from the vertical direction where the tail indicate the dip direction of the deviation.

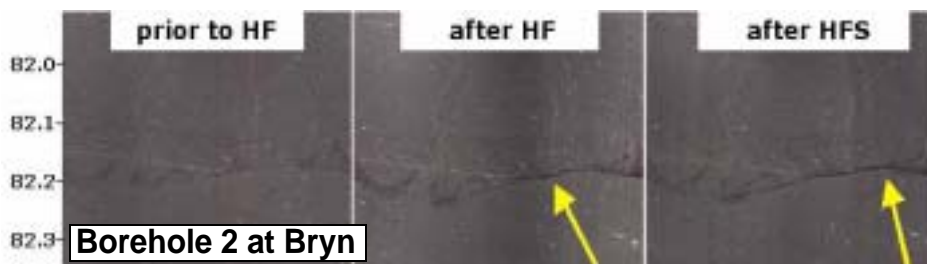


Figure 5–36: The images from the optical televiewer shows a few decimetres of borehole 2 at Bryn before (at left) and after hydraulic fracturing with water-only (centre), and after hydraulic fracturing with injection of sand (at right). The fracture at 82.2 metres is clearly more open both after hydraulic fracturing with water-only and hydraulic fracturing with injection of sand.

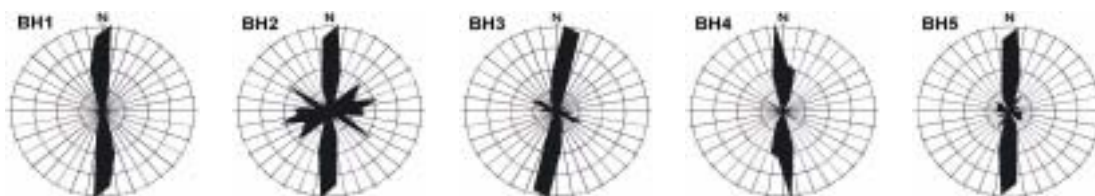


Figure 5–37: Joint rosettes from borehole 1 to 5 at Bryn before hydraulic fracturing with water-only. The dip of the main fracture direction varies between 40 to 60° towards west.

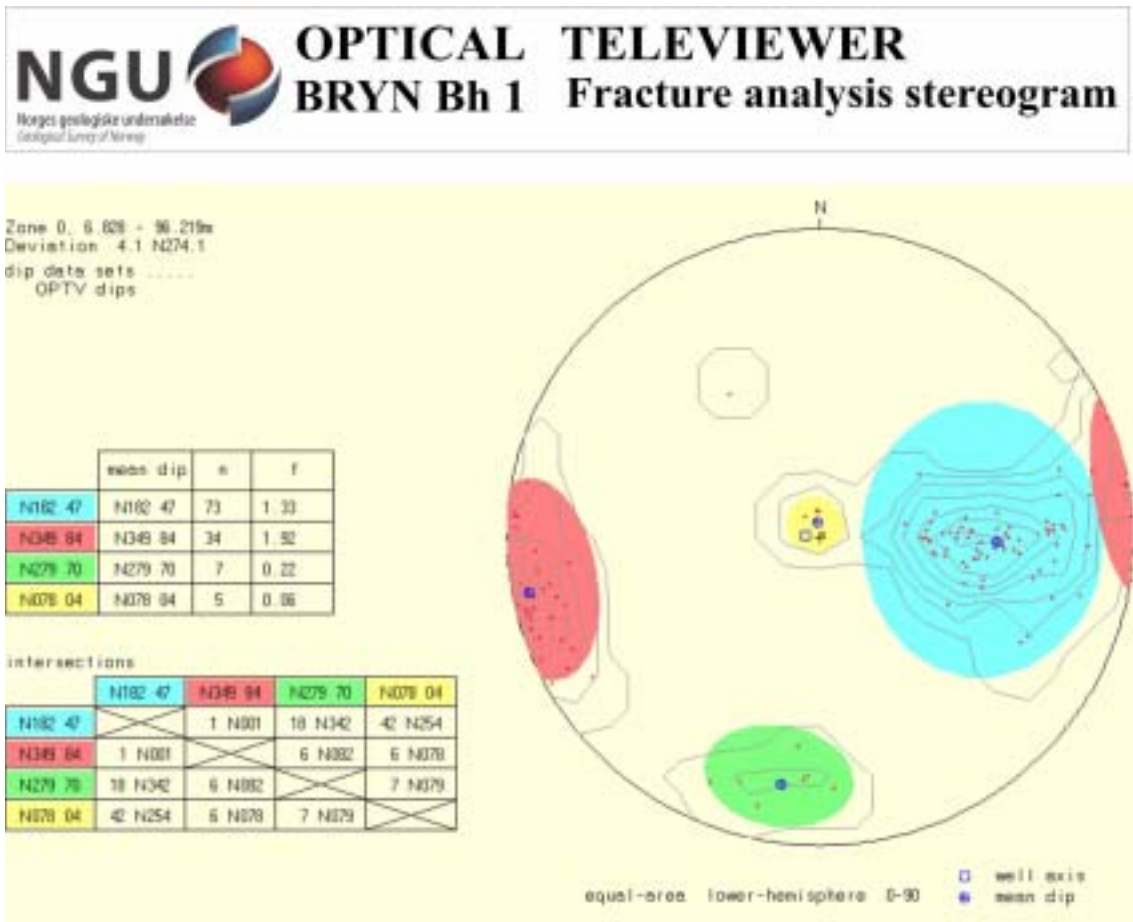


Figure 5–38: A fracture analysis stereogram for borehole 1 at Bryn. The different colours represent a fracture system and correspond to the colours used in the frequency analysis log (figure 5–39).

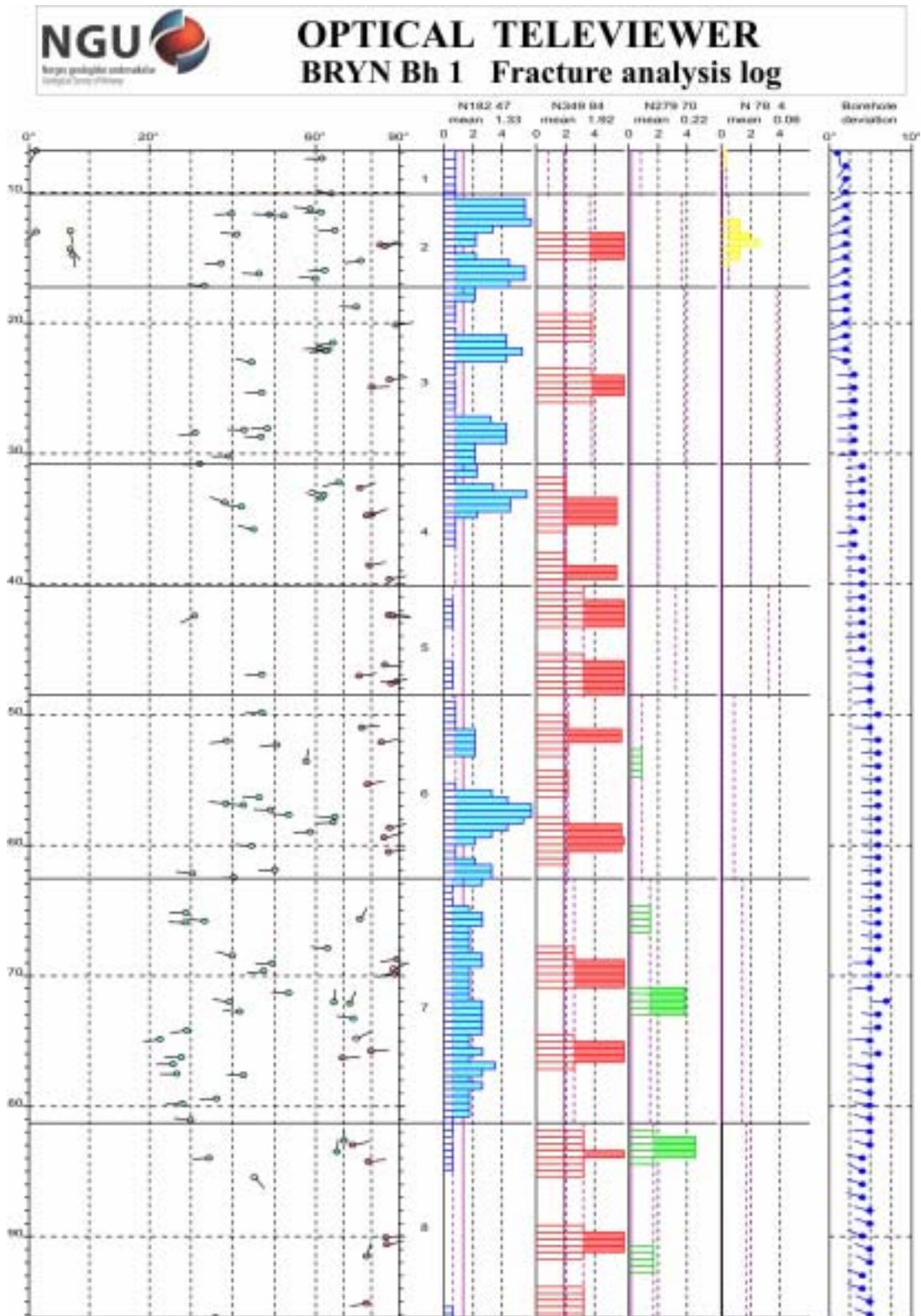


Figure 5–39: Frequency analysis log for borehole 1 at Bryn. The different colours represent a fracture system also displayed in the corresponding fracture analysis stereogram (figure 5–38).

A simplified stratigraphy for boreholes 1-5 at Bryn is presented in figure 5–40, based on the optical televiewer recordings and the natural gamma radiation logs. Three stratigraphic units are recognised as (1) a sandstone with alternating bright and dark bedding (Ringerike sandstone), (2) a homogenous unit dominated by a white mineral (probably quartz) with lower radioactivity than the sandstone, and (3) a diabase intrusion. The diabase has lower radioactivity than the surrounding units, and appears as a dark grey and homogenous rock. Diabase intrusions are very common in the nearby area of Bryn.

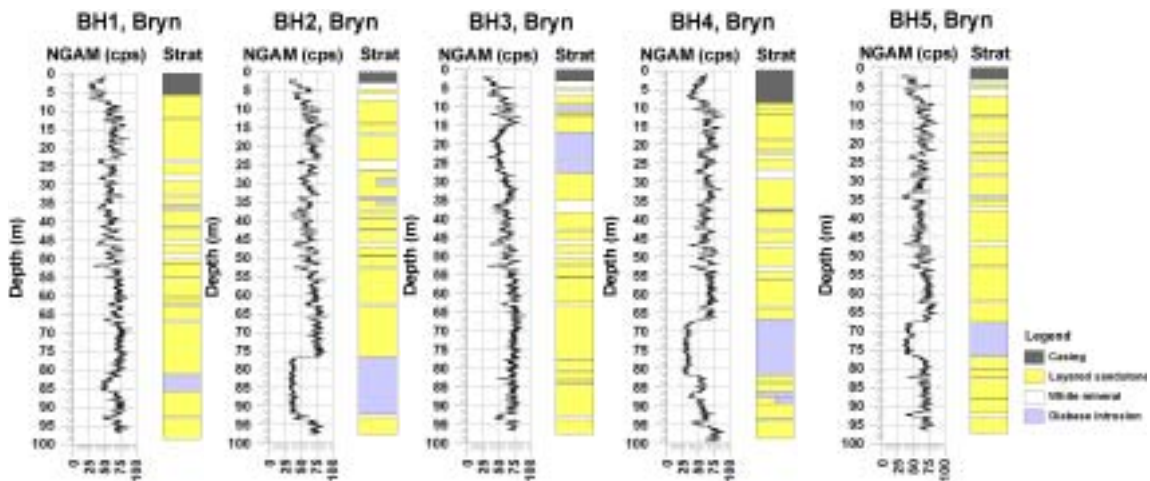


Figure 5–40: A simplified stratigraphy for boreholes 1-5 at Bryn.

The logs of the temperature- and electric conductivity of the water in boreholes 1-5 at Bryn, recorded before and after hydraulic fracturing with water-only and after hydraulic fracturing with injection of sand, are presented together with the natural gamma log and the levels- and results for the different kinds of hydraulic fracturing in figures 5–41 to 5–45. The undisturbed groundwater level was at 0-1 metre for boreholes 1, 2, 3 and 5, and at approximately 5 metres in borehole 4. The naturally occurring and horizontal fracture zone at 12-13 metres depth in boreholes 1, 2, 3 and 5, and at 17 metres depth in borehole 4, is recognised as a dramatic change in both the temperature and electric conductivity. The logging was performed at different times of the year and the temperatures in the upper 15-20 metres of the boreholes is clearly influenced by seasonal variations in the air temperature. Changes in the temperature- and/or the electric conductivity of the water, due to hydraulic fracturing with water-only or hydraulic fracturing with injection of sand, indicate that new or existing fractures are initiated or reopened within some of the stimulated sections.

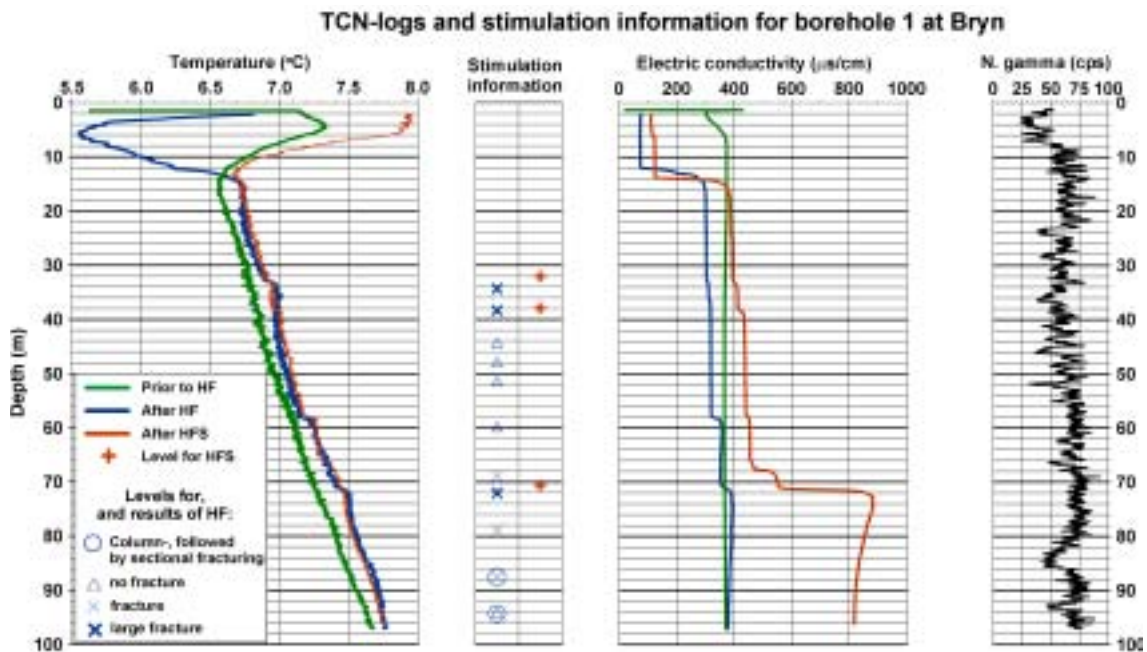


Figure 5–41: Temperature- and electric conductivity logs compared with levels- and results from hydraulic fracturing with water only (HF) and hydraulic fracturing with injection of sand (HFS) in borehole 1 at Bryn.

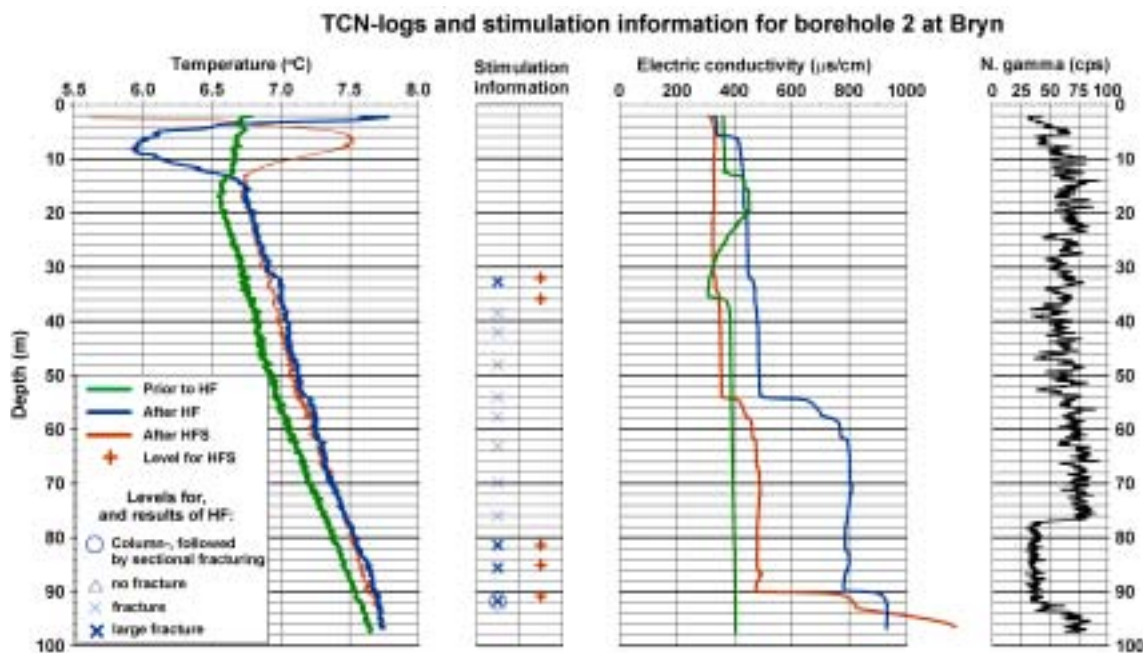


Figure 5–42: Temperature- and electric conductivity logs compared with levels- and results from hydraulic fracturing with water only (HF) and hydraulic fracturing with injection of sand (HFS) in borehole 2 at Bryn.

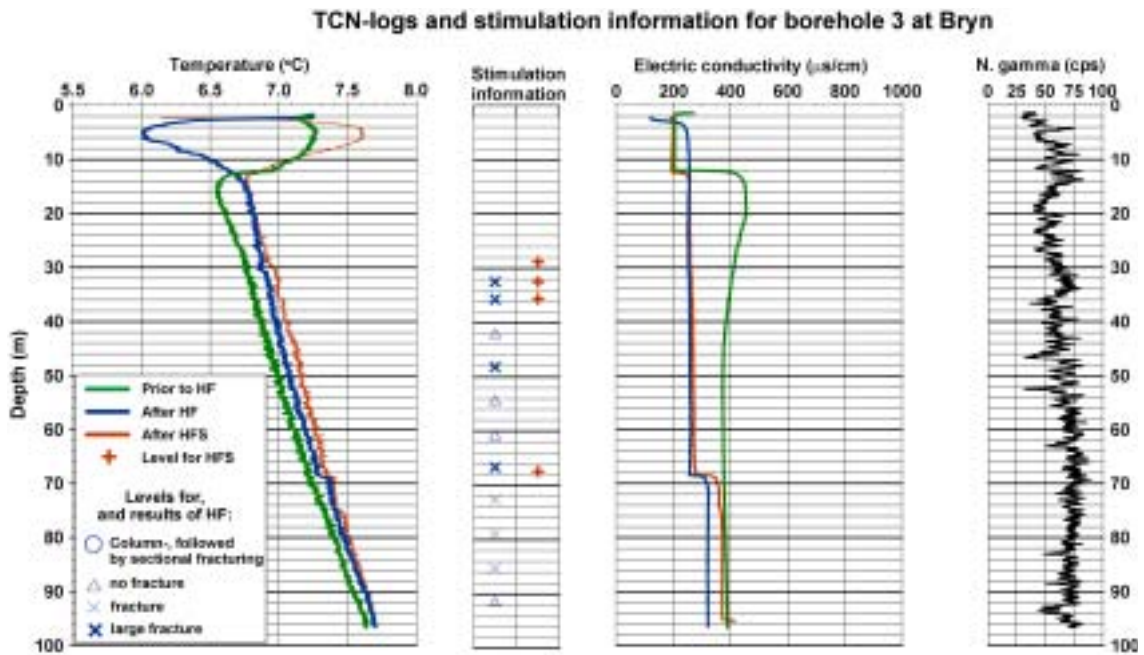


Figure 5–43: Temperature- and electric conductivity logs compared with levels- and results from hydraulic fracturing with water only (HF) and hydraulic fracturing with injection of sand (HFS) in borehole 3 at Bryn.

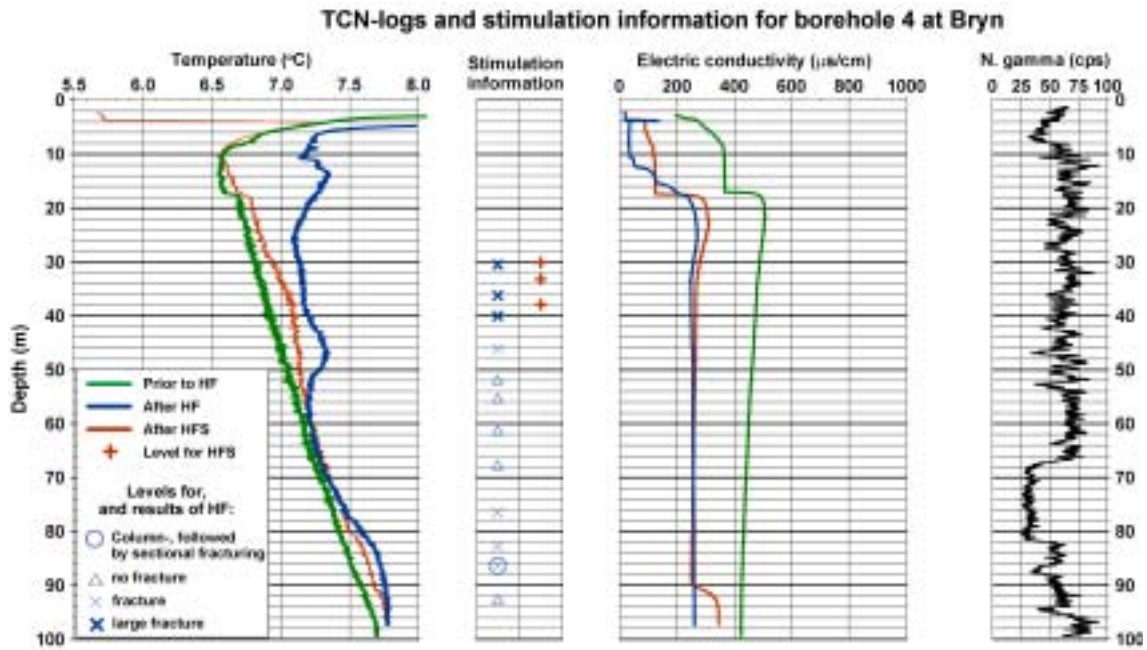


Figure 5–44: Temperature- and electric conductivity logs compared with levels- and results from hydraulic fracturing with water only (HF) and hydraulic fracturing with injection of sand (HFS) in borehole 4 at Bryn.

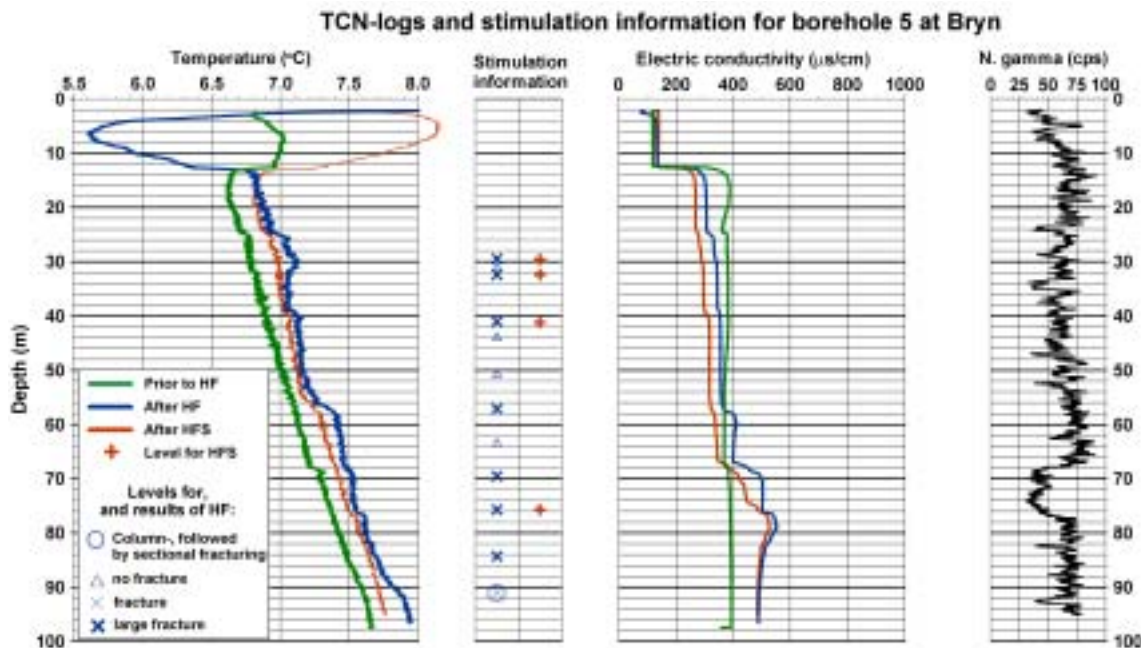


Figure 5–45: Temperature- and electric conductivity logs compared with levels- and results from hydraulic fracturing with water only (HF) and hydraulic fracturing with injection of sand (HFS) in borehole 5 at Bryn.

5.2.8 Identification of possible new water inlets in the boreholes

An attempt to identify new water inlets in the boreholes at Bryn has been done to verify the efficiency of the hydraulic fracturing. In this context, a new water bearing fracture is considered to be a confirmation of a successful stimulation with hydraulic fracturing in the particular borehole section. The identification of possible new water inlets in the boreholes at Bryn is done using figures 5–41 to 5–45 which display the temperature- and conductivity logs together with the levels and results for the different kinds of hydraulic fracturing. The largest breaks in the curves, representing changes in the properties of the water, can be seen for the electric conductivity and also repeatedly on the temperature logs. Except for the irregularities at 36 and 68 metres depth in borehole 2 and 5, respectively, the chemical conditions in the boreholes before the hydraulic fracturing, here represented by the electric conductivity curves, are constant at depths greater than 25 metres. Corresponding to the electric conductivity logs and except for a minor irregularity at 68 metres depth in borehole 5, the temperature data display an even gradient towards depth. The temperature gradient is 13.5 K/km. All irregularities on the temperature- and electric conductivity logs, recorded after hydraulic fracturing with water-only or after hydraulic fracturing with injection of sand, represent an increase in the measured value.

In general, inflowing water often has the same physical and chemical properties as the surrounding water in the borehole. These water inlets would not be visible on the logs showing the temperature- and electric conductivity of the borehole water. Rise data (figure 5–28 to 5–32) from the test pumping after hydraulic fracturing with injection of sand, using pump C, is compared with the results from the geophysical logging and the sections treated with hydraulic fracturing (figures 5–41 to 5–45). An unrealistically high number of water inlets is indicated at some rising curves, and the results from the rise

data are therefore considered as uncertain. Small variations and uncertainties related to the depth specifications have to be accounted for in the comparison of data, collected at six different times, when carrying out the following borehole investigations: (1) hydraulic fracturing with water-only, and (2) hydraulic fracturing with injection of sand, (3-5) measurements of the temperature- and the electric conductivity of the water, accomplished before and after the hydraulic fracturing with water-only and hydraulic fracturing with injection of sand, and (6) test pumping with the collecting of rise data. In addition, inaccuracies in the depth specification of the lowering- and lifting equipment used in the hydraulic fracturing operations (points 1 and 2) were discovered (paragraph 5.6.3). Using all the available data, possible new water inlets related to the hydraulic fracturing in borehole 1 to 5 are identified and presented in tables 5–6 to 5–10, respectively. The abbreviations *HF* and *HFS* mean *hydraulic fracturing with water-only* and *hydraulic fracturing with injection of sand*, respectively.

Table 5–6: Possible new water inlets related to the hydraulic fracturing in borehole 1 at Bryn.

Time	Data	Observation	Discussion
after HF	el. cond. & temp.	Two breaks identified on the electric conductivity log at 58 and 71 metres, and a minor deviation in the temperature gradient at 34 metres.	The events at 71 and 34 metres can be related to the fracturing, interpreted as large fractures, of sections 72.0 and 34.3 (figure 5–41), respectively. The large pressure level (160-200 bars, figure 5–47) during the stimulation of section 59.8 was considered to be too high for fracture initiation, and the incident at 58 metres can hardly be related to the stimulation.
after HFS	el. cond. & temp.	An incident at 58 metres.	The incident was also present on the logs after hydraulic fracturing with water-only.
after HFS	el. cond.	Four breaks on the curve were observed at 33, 38, 68 and 71 metres depth	Three of the events can be related to the injection of sand in the borehole sections at 32.0, 37,9 and 70.6 metres. A major increase in the conductivity value at 71 metres, from approximately 550 to 900 $\mu\text{s}/\text{cm}$, indicated a larger inflow of ionic water. The incident at 68 metres could not be related to the injection of sand, but to the hydraulic fracturing with water in section 68.8. However, no indication were present on the logs after hydraulic fracturing with water-only.
after HFS	rise	Rising curve: 56 and 32-27 metres.	From these observations, the possible water inlets at 32-27 are partly verified by the logs for the temperature- and the electric conductivity of the water. The possible water inlets at 55 and 56 metres might be connected to the previous observations at 58 metres.

Chapter 5 Results

Table 5–7: Possible new water inlets related to the hydraulic fracturing in borehole 2 at Bryn.

Time	Data	Observation	Discussion
prior to HF		The normal value for the electric conductivity of the water in borehole 2 shows an irregularity at 36 metres.	
after HF	el. cond.	Two large incidents at 54 and 90 metres, and five minor at 32, 58, 62, 63, 71 and 83-86 metres.	The changes in the conductivity value corresponds with the results from the hydraulic fracturing with water where an average- or large-sized fracture was reopened or initiated in sections 32.7, 54.1, 57.7, 63.1, 69.9, 81.4 and 85.6 (figure 5–42). The 81.4-section fracture is also recognized on the optical televiewer both after hydraulic fracturing with water-only and hydraulic fracturing with injection of sand (figure 5–36). Columnar hydraulic fracturing with water-only, followed by sectional hydraulic fracturing, was performed at 91.7 metres resulting in a reopening or initiation of a large fracture (figure 5–42). The distance between this borehole section and the discovered increase of the conductivity value (approximately 750-950 $\mu\text{s/cm}$) at 90 metres is theoretically too long to be associated with each other. However, small uncertainties in the depth specification may have occurred, and it is not unrealistic that the new water bearing fracture is revealed by the hydraulic fracturing with water.
after HF	temp	Irregularities at 32 and 54 metres.	The irregularities at 32 and 54 metres are also observed on the temperature log.
after HFS	el. cond.	Irregularities on the conductivity log were recognized at 35, 54, 58, 62, 67, 86, 90 and 93 metres. The events at 54, 58, 62 and 90 metres were already present on the corresponding log after hydraulic fracturing with water-only.	The hardly visible changes in the electric conductivity log at 35 and 86 metres, and the increase from approximately 500 to 800 $\mu\text{s/cm}$ at 90 metres, can be related to the hydraulic fracturing with injection of sand in borehole section 35.9, 85.1 and 90.8, respectively. The conductivity change at 35 metres could also be associated with the water inlet observed in natural condition. A major increase for the electric conductivity value can be seen at 93 metres, which is not connected to the injection of sand. A higher concentration of fine particles towards the end of the borehole (100 metres) can cause high values for the electric conductivity. The same phenomenon was observed during the borehole inspections at EAB, performed before hydraulic fracturing with injection of sand (figure 5–72 to 5–74). The irregularity at 67 metres is not related to hydraulic fracturing with injection of sand.
after HFS	rise	Rising curve: 54, 50-52, 45, 33 and 28 metres	The observation at 54, and partly 33 metres were verified by the temperature- and the conductivity log. The indicated water inlets at 50-52, 45 and 28 metres were not related to any kind of hydraulic fracturing.

Table 5–8: Possible new water inlets related to the hydraulic fracturing in borehole 3 at Bryn.

Time	Data	Observation	Discussion
after HF & HFS	el. cond. & temp.	A single irregularity were discovered at 68 metres.	The irregularity was probably connected to hydraulic fracturing with water in section 66.6, causing a reopening- or initiation of a large-sized fracture, (figure 5–43), and the injection of sand in section 67.4.
after HFS	rise	Rising curve: 66, 46, 39, 36, 34 and 31 metres.	From these observations, the possible water inlet at 66 metres was partly verified by the temperature- and conductivity log. The suggested water inlets at (46,) 36, 34 and 31 might be associated with the hydraulic fracturing with water-only and hydraulic fracturing with injection of sand in the corresponding borehole sections at (48.1,) 35.7, 35.6 and 32.5, respectively. The indicated water inlet at 39 metres was not related to any kind of hydraulic fracturing.

Table 5–9: Possible new water inlets related to the hydraulic fracturing in borehole 4 at Bryn.

Time	Data	Observation	Discussion
after HF	Temp.	The temperature log shows an irregularly course, and deviations from the natural gradient can be seen at 38, 51, 77 and 83 metres.	The temperature deviation at approximately 38 metres, supposing an inaccurate specification of depth, could be related to the hydraulic fracturing with water-only in section 36.2 or 40.0. The fracturing (figure 5–44) caused by hydraulic fracturing with water-only in sections 76.5 and 82.8 metres corresponds to the observed temperature deviations at 77 and 83 metres, respectively. Even though the pressure level (180 bars, figure 5–49) during the hydraulic fracturing with water-only in the 51.8-section was interpreted as too high to represent a fracture, the deviating temperature gradient at 51 metres may indicate the opposite, that a minor water bearing fracture was created in this level.
after HFS	el. cond & temp.	Appearing events at 90 and 36 metres on the conductivity- and temperature log, respectively.	The recorded incident at 90 metres can hardly be connected to any kind of hydraulic fracturing. The minor temperature deviation at 36 metres can be associated to hydraulic fracturing with water-only and/or hydraulic fracturing with injection of sand in the section at 36.2 and 37.9 metres, respectively.
after HFS	rise	Rising curve: 52, 39, 34 and 29 metres.	From these observations, the suggested water inlets at 52 and 39 metres are verified by the temperature log of the borehole water. The suggested water inlets at 34 and 29 metres might be connected to the hydraulic fracturing with water-only and hydraulic fracturing with injection of sand in the sections at 33.2 and 30.5 and/or 30.1, respectively.

Table 5–10: Possible new water inlets related to the hydraulic fracturing in borehole 5 at Bryn.

Time	Data	Observation	Discussion
prior to HF	el. cond. & temp.	The normal value for the temperature- and the electric conductivity of the water in borehole 5 shows an irregularity at 68 metres.	
after HF	el. cond. & temp.	Appearing changes on the conductivity log were at 39, 57, 67, 69 and 76 metres, while deviations on the temperature log were observed at 29, 32, 39 and 92 metres depth.	The changes at 29, 32, 57, 69, 76 and 92 metres correspond to the results from the hydraulic fracturing with water-only where fracture reopening or -initiation were interpreted to take place in the borehole sections at 29.5, 32.4, 57.1, 69.5, 75.7 and 91.0, respectively (figure 5–45). Assuming an inaccurate specification of depth, the conductivity- and temperature deviation at 39 metres may be connected to the hydraulic fracturing with water-only of section 41.0. The break on the curve at 68 metres, reflecting the natural condition of the borehole, might be recognized at 67 metres after hydraulic fracturing with water-only.
after HFS	el. cond.	Irregularities on the conductivity log registered at 39, 57, 67 and 74-76 metres.	All the irregularities have already been identified on logs measured after hydraulic fracturing with water-only. Besides an eventually previous relation to hydraulic fracturing with water-only, the irregularities at 39 and 74-76 were associated to the hydraulic fracturing with injection of sand in the sections at 41.2 and 75.7, respectively. An inaccuracy of minimum 0,7 metres in the depth specification is required for the relation between the 39 event to the 41.2-section.
after HFS	rise	Rising curve: 55, 52, 37 and 20 metres.	No suggested water inlets on the rising curve was directly verified by corresponding changes on the temperature- and conductivity log. Despite an unsuccessful fracturing (figures 5–45 and 5–50), the suggested water inlets at 52 metres could possibly be related to hydraulic fracturing with water-only in the 50.8-section. The water inlet at 55 metres may be connected to the hydraulic fracturing with water-only in the 57,1-section. Whether or not the suggested water inlet at 37 metres could be connected to some kind of hydraulic fracturing is uncertain. The suggested water inlet at 20 metres was not associated to any kind of hydraulic fracturing.

5.2.9 Hydraulic fracturing with water-only

From a total of 63 stimulations with hydraulic fracturing with water-only, 44 (70%) pressure-time curves were interpreted as an initiation of new fractures or a reopening of existing fractures (figure 5–46). A higher degree of fracturing was expected. Pressure-

time diagrams from almost all the sections and columns stimulated with hydraulic fracturing with water-only in boreholes 1, 2, 4 and 5 are shown in figures 5–47 to 5–50. Significant pressure drops represent a fracturing of the bedrock. Manually read water pressures from the hydraulic fracturing of borehole 3 and column 91.0 in borehole 5 are listed in table 5–11. According to observations in the field, the analog manometer showed approximately 20 bars higher than the digital pressure measurements. This is not corrected for, and should be taken into consideration in the data analysis.

A rough estimate of the volume of water used in the hydraulic fracturing with water-only in each borehole section or -column is made from the field notes, pumping rates, length of the stimulation periods and the pressure levels. The volume estimates are presented in figure 5–51 together with a summary of the amount and colour of the backflow from each borehole section or -column. Backflow expresses the return flow of water from the borehole sections or -columns at pressure release after ended hydraulic fracturing with water-only. Some details concerning the backflow are observed and noted in most cases.

A total of 19 observations of backflow colour are registered in figure 5–51, and three of these observations were clear water without sediments. The quantity of the backflow were characterized as large for 15 of the remaining 16 observations. The colour on the backflow, representing the chemistry of the water and/or coloured by sediments loosened from the fracture surfaces, varied from grey in most of the cases to greyish brown, brown and bluish grey. Comparing the backflow results with the the location of the 22 borehole sections where hydraulic fracturing with water-only was interpreted to reopen or initiate a large fracture in the boreholes at Bryn (figure 5–46), reveals that 12 of these large fractures were observed to have a coloured backflow. The remaining four observations of coloured backflow are interpreted to represent the reopening or initiation of middle sized fractures. Two of the three observations of backflows of clear water are related to borehole sections where no fracture was initiated. The third observation of large amount of clear water in return from a fracture cavity was after hydraulic fracturing with water-only in the diabase part of borehole 2, at 91.7 meters depth (figures 5–40 and 5–42).

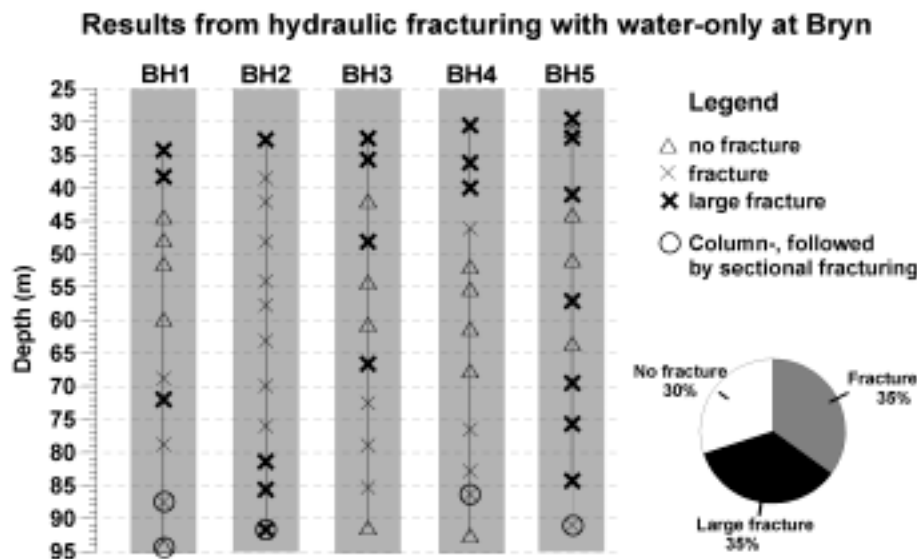


Figure 5–46: Results from the hydraulic fracturing with water-only of the 63 borehole sections or -columns in borehole 1-5 at Bryn.

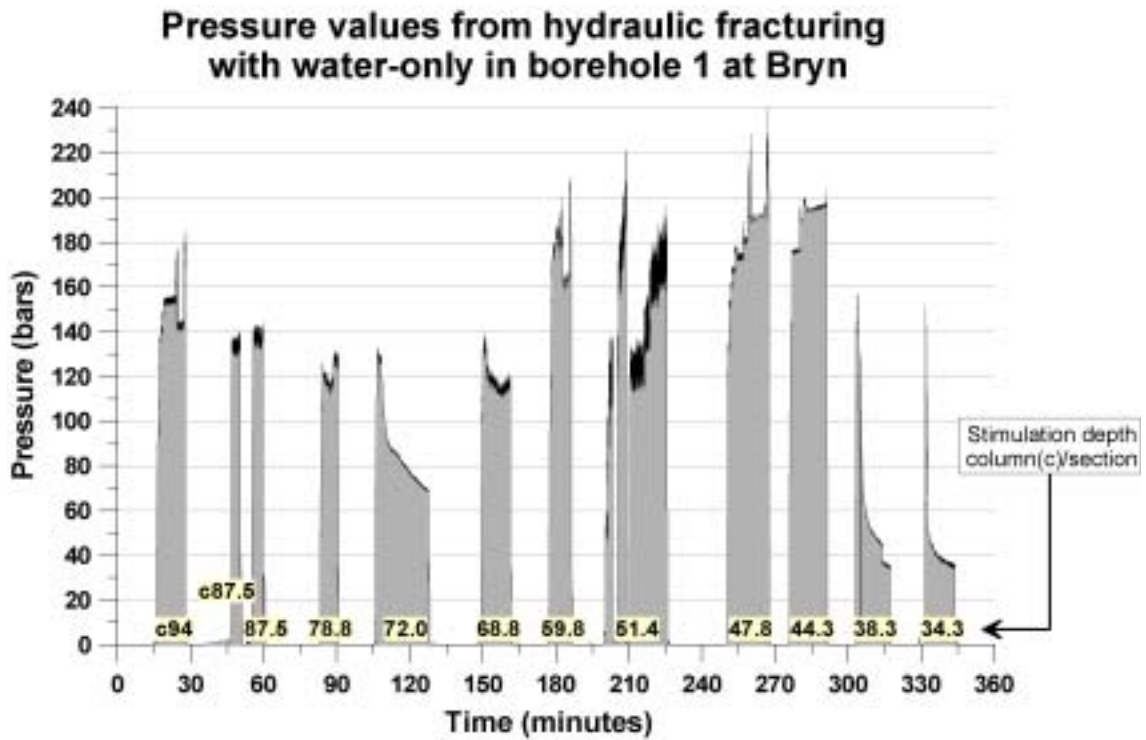


Figure 5–47: Pressure-time curves from hydraulic fracturing with water-only in borehole 1.

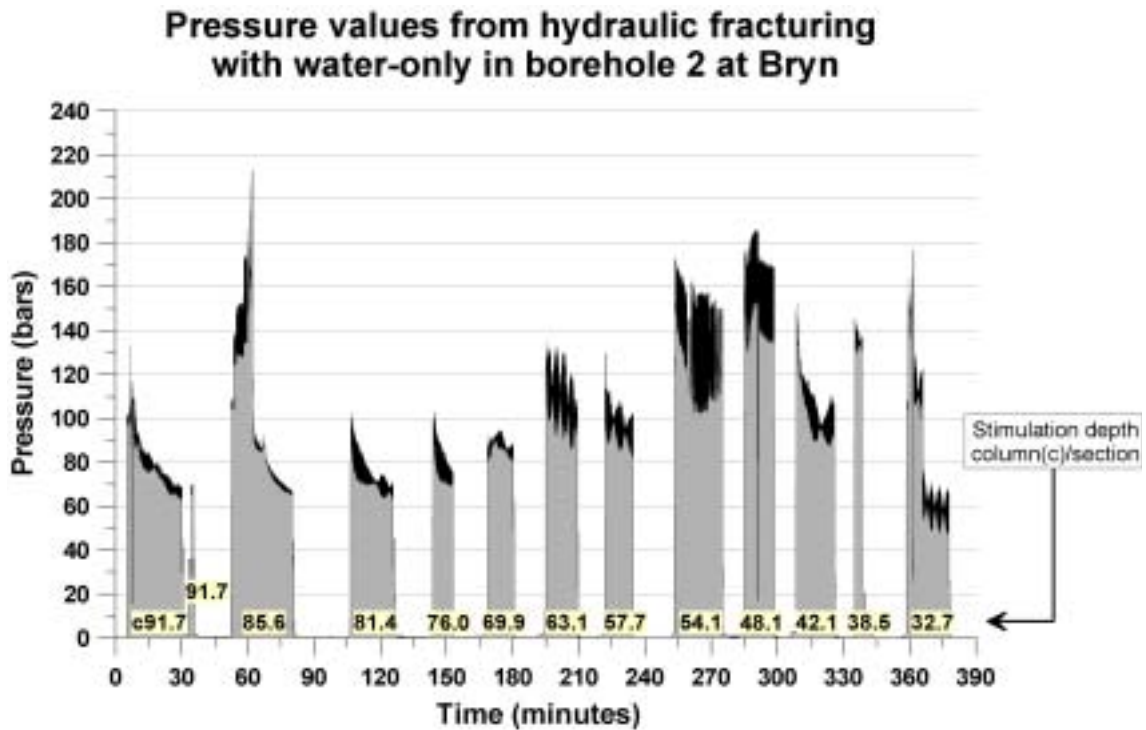


Figure 5–48: Pressure-time curves from hydraulic fracturing with water-only in borehole 2.

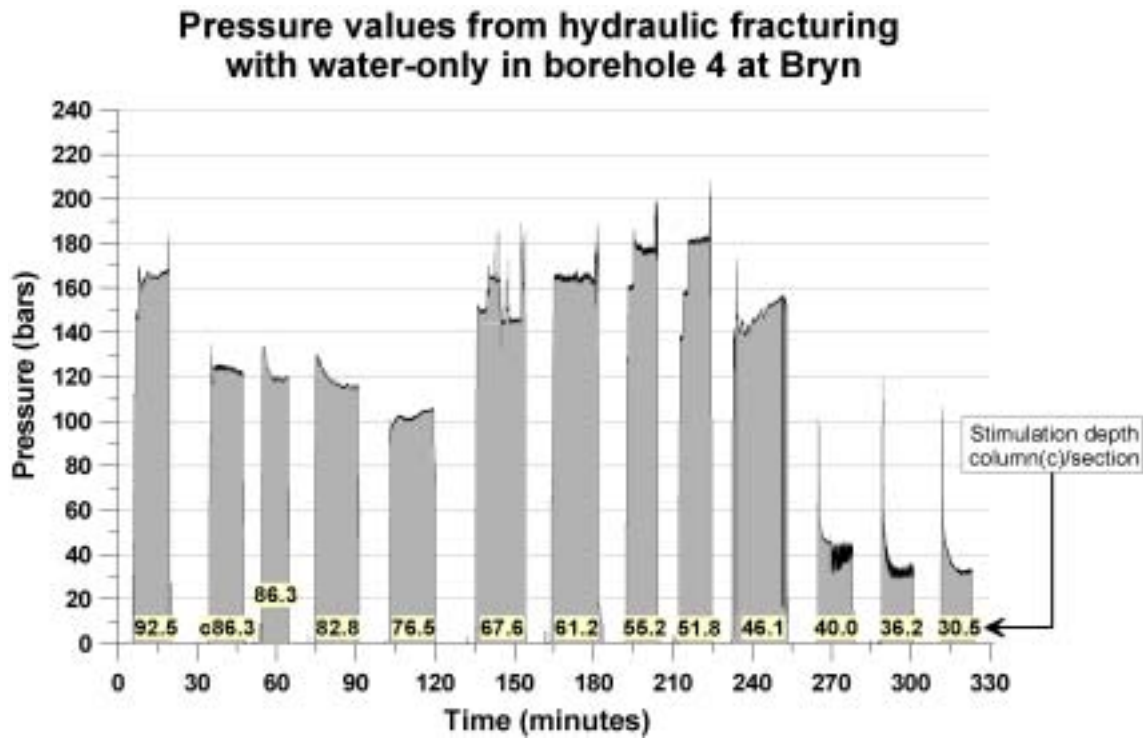


Figure 5–49: Pressure-time curves from hydraulic fracturing with water-only in borehole 4.

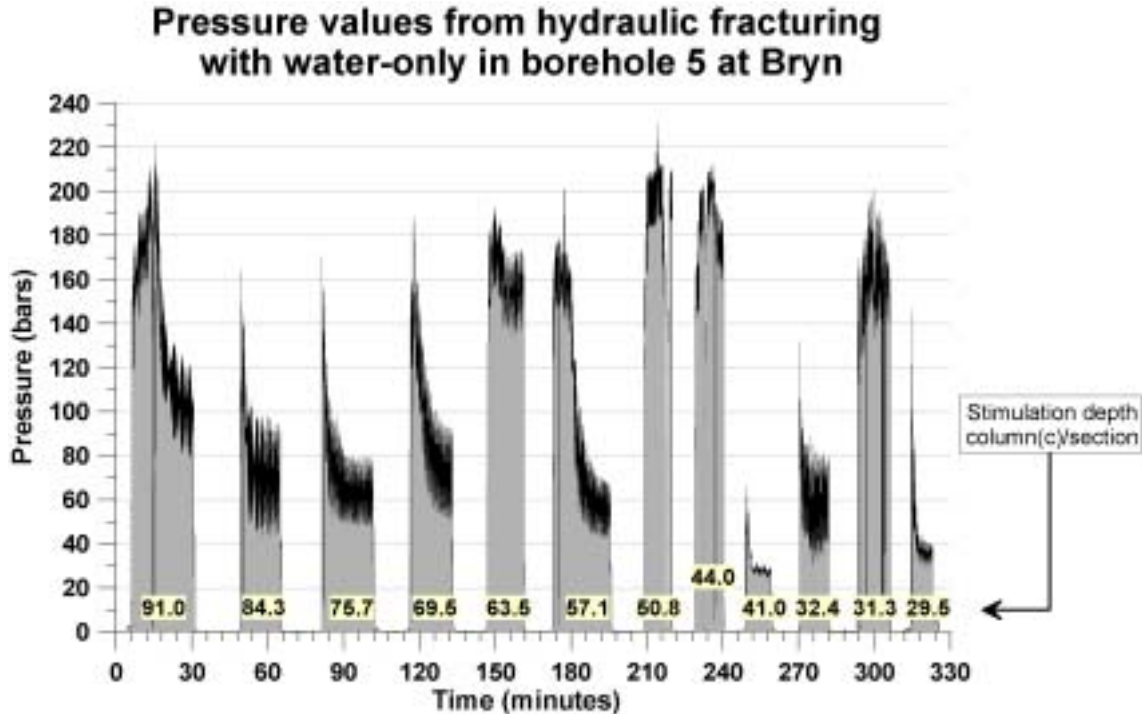


Figure 5–50: Pressure-time curves from hydraulic fracturing with water-only in borehole 5.

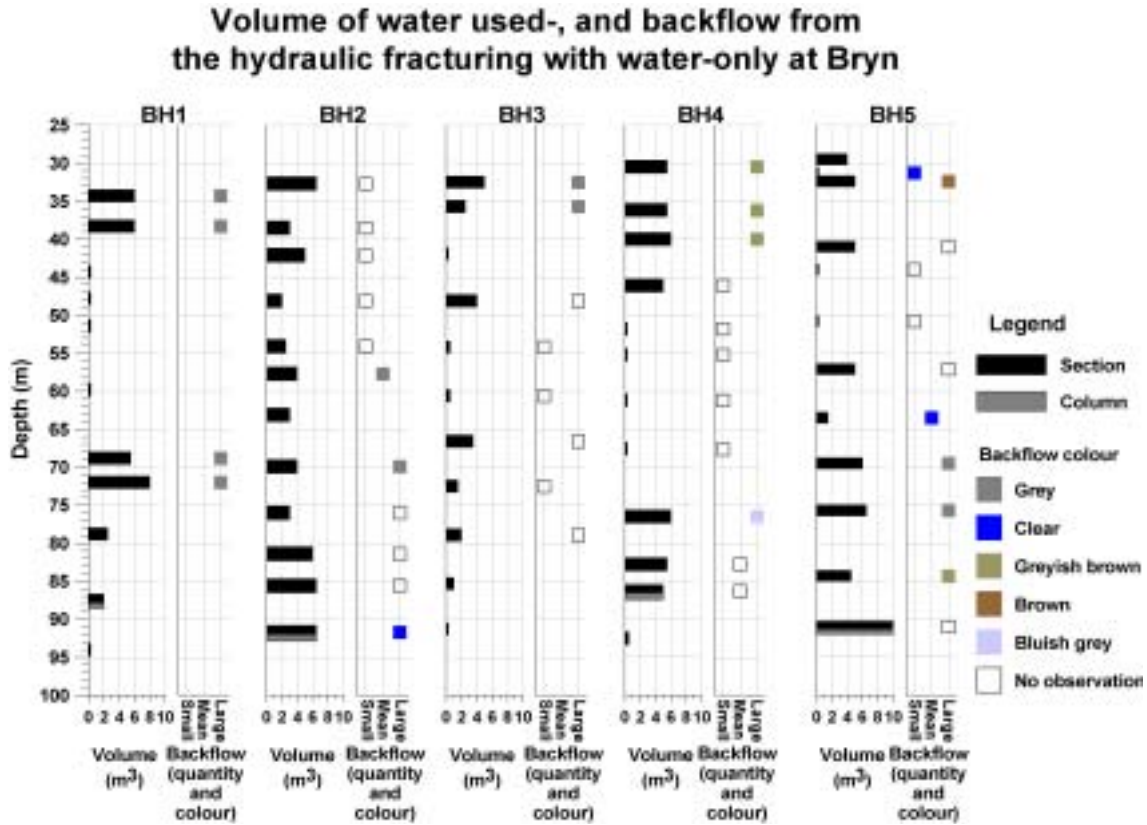


Figure 5–51: Rough estimates of the volume of water used in the hydraulic fracturing of each borehole section or -column. The backflow volume and its colour are indicated in most cases.

Table 5–11: Manual recordings of the maximum and minimum water pressure from hydraulic fracturing with water-only in borehole 3 and the deepest level in borehole 5 at Bryn. According to field observations, the manually read pressure values on the analog manometer were approximately 20 bars higher than the digitally logged pressure values.

Borehole #	Level (m)	P _{maks} (bars)	P _{min} (bars)
3	91.3	205	-
3	85.3	210	160
3	78.9	180	150
3	72.5	190	-
3	66.6	175	95
3	60.6	210	-
3	54.2	220	-
3	48.1	205	70
3	41.9	200 (250)	-
3	35.7	160	40
3	32.5	140	40
5	91.0 (column)	200	110

Changes in the groundwater level in the surrounding boreholes as a consequence of hydraulic fracturing accomplished in one of the other boreholes are shown in figures 5–52 to 5–56. Corresponding pressure-time curves from the hydraulic fracturing with

water-only are plotted as well. The groundwater alterations are approximately parallel for all the boreholes. Borehole 1 and partly borehole 3, seemed to respond somewhat more to the hydraulic fracturing with water-only than the remaining boreholes, especially to the hydraulic fracturing in boreholes 3, 4 and 5. A brief summary of the main observations in figures 5–52 to 5–56 are listed in 5–12

Table 5–12: Summary of the groundwater level changes in the surrounding boreholes as a consequence of hydraulic fracturing accomplished in one of the other boreholes.

Hydraulic fracturing in:	Observations of changing groundwater level in surrounding boreholes
Borehole 1	Almost identical groundwater changes in boreholes 2, 3 and 4.
Borehole 2	Borehole 1 shows a higher response compared with boreholes 3 and 4.
Borehole 3	Major groundwater fluctuations in borehole 1, minor fluctuations in borehole 4 and almost no fluctuations in borehole 2.
Borehole 4	More or less parallel groundwater level changes, but the change in borehole 1 is somewhat larger compared with boreholes 3 and 5.
Borehole 5	A parallel alteration for the groundwater level in boreholes 1 and 3. Borehole 4 has minor alterations, particularly to the hydraulic fracturing in the deeper part of borehole 5.

The extra response of the groundwater level in borehole 1 was also registered during the test pumping (paragraph 5.2.2). The degree of parallelism is probably related to the presence of the highly dominating large fracture zone, intersecting all the boreholes at Bryn (paragraph 5.2.1). When communication was established between the hydraulic fracturing- or test pumping borehole and one of the surrounding boreholes, the hydraulic response was propagated via the fracture zone towards the remaining boreholes. Due to the relatively low flow rates, compared with the flow rates during the hydraulic fracturing with water-only, the highest degree of parallelism can best be seen on the groundwater alterations observed during the test pumping.

The main fracture direction in the Bryn area is approximately north-south, while two minor fracture directions were reported in the northeast-southwest and southeast-northwest directions (figure 5–37). Boreholes 1, 3 and 5 are located on a line approximately 6° from north (figure 3–3). The significant groundwater alterations monitored in boreholes 1 and 3 during the hydraulic fracturing of the deeper part of borehole 5 (figure 5–56) confirmed a probable fracture reopening or -initiation parallel to the main fracture direction. The same trend appeared for borehole 1 responding to the hydraulic fracturing in borehole 3 (figure 5–54), but no extraordinary response was registered for borehole 3 during the hydraulic fracturing in borehole 1 (figure 5–52). Unfortunately, the groundwater level in borehole 5 was not monitored during the hydraulic fracturing in boreholes 1 and 3. Two large fractures in the upper part of borehole 5, the 29.5- and 32.4-section, were opened during the hydraulic fracturing without causing the corresponding hydraulic response as the fracturing in the deeper parts of borehole 5 (figure 5–56). The changed hydraulic response in boreholes 1, 3 and 4 might be associated with the opening of horizontal fracture planes instead of vertical fracture planes. At this levels, horizontal fracture planes could be initiated- or reopened due to the reduced overburden pressure and/or to the reopening of an existing horizontal fracture. Assuming the fracturing of the deeper sections in borehole 5 has resulted in an opening of vertical fractures directly intersecting boreholes 1 and 3, a horizontal and

disc-shaped fracture propagation is expected to cause a more uniform and distributed hydraulic response in the surrounding boreholes.

The hydraulic response in borehole 1 to the hydraulic fracturing in boreholes 2 and 4 might be related to the minor fracture directions in the northeast-southwest and the southeast-northwest direction, respectively (figure 5–37). Even though a high degree of fracturing was achieved in the hydraulic fracturing of borehole 2, an unexpectedly low hydraulic response in the surrounding boreholes was registered indicating a fracture propagation outside the other boreholes. The fracture propagation of the three lower sections in borehole 2 may have followed the orientation of the appearing diabase intrusion (figure 5–40).

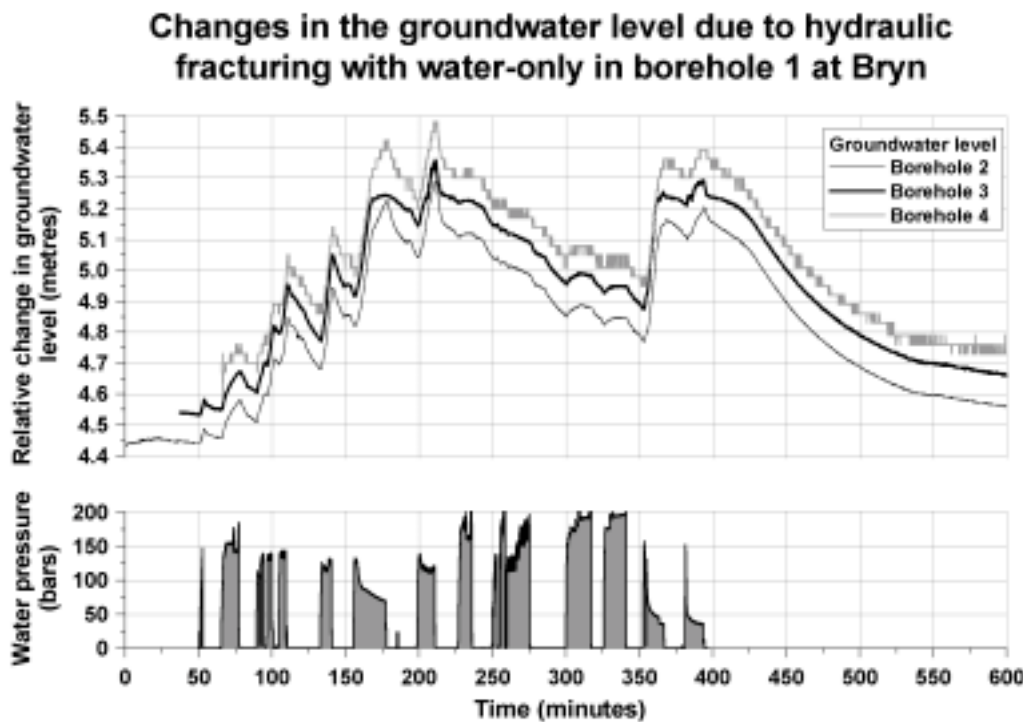


Figure 5–52: Groundwater level changes in boreholes 2, 3 and 4 measured during the hydraulic fracturing with water-only in borehole 1 at Bryn.

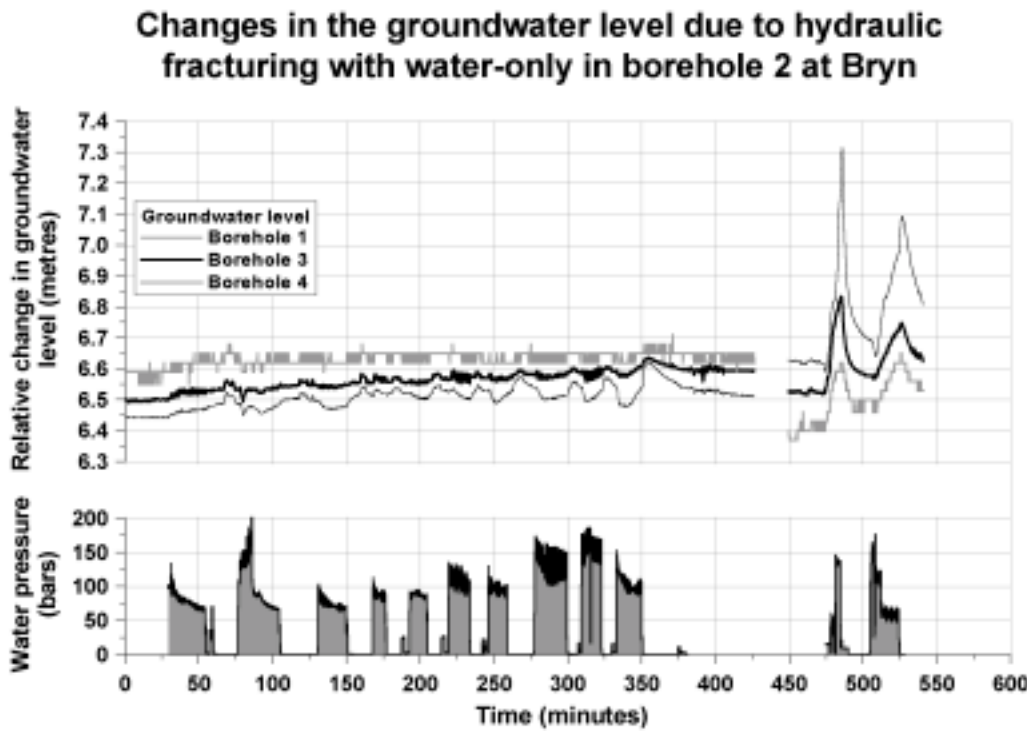


Figure 5–53: Groundwater level changes in boreholes 1, 3 and 4 measured during the hydraulic fracturing with water-only in borehole 2 at Bryn.

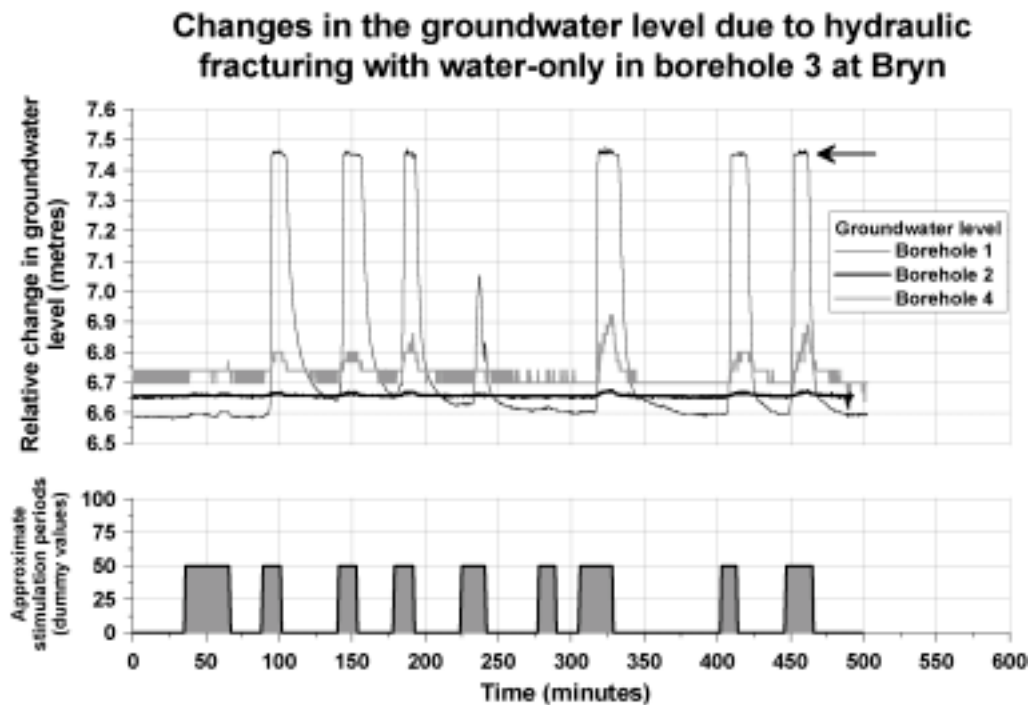


Figure 5–54: Groundwater level changes in boreholes 1, 2 and 4 measured during the hydraulic fracturing with water-only in borehole 3 at Bryn.

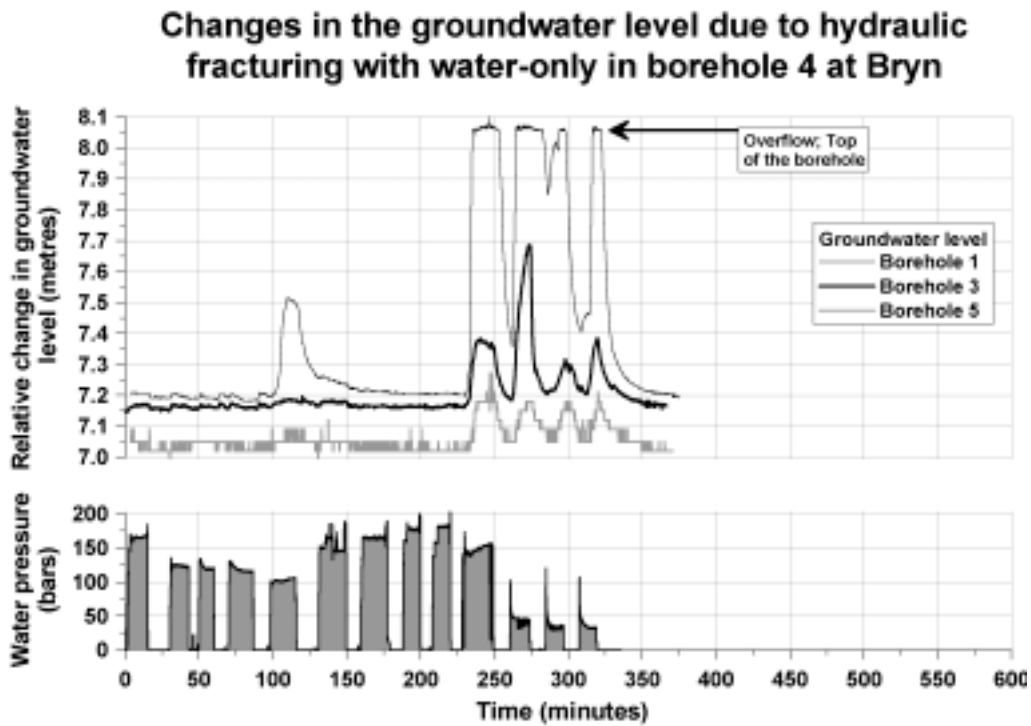


Figure 5–55: Groundwater level changes in boreholes 1, 3 and 5 measured during the hydraulic fracturing with water-only in borehole 4 at Bryn.

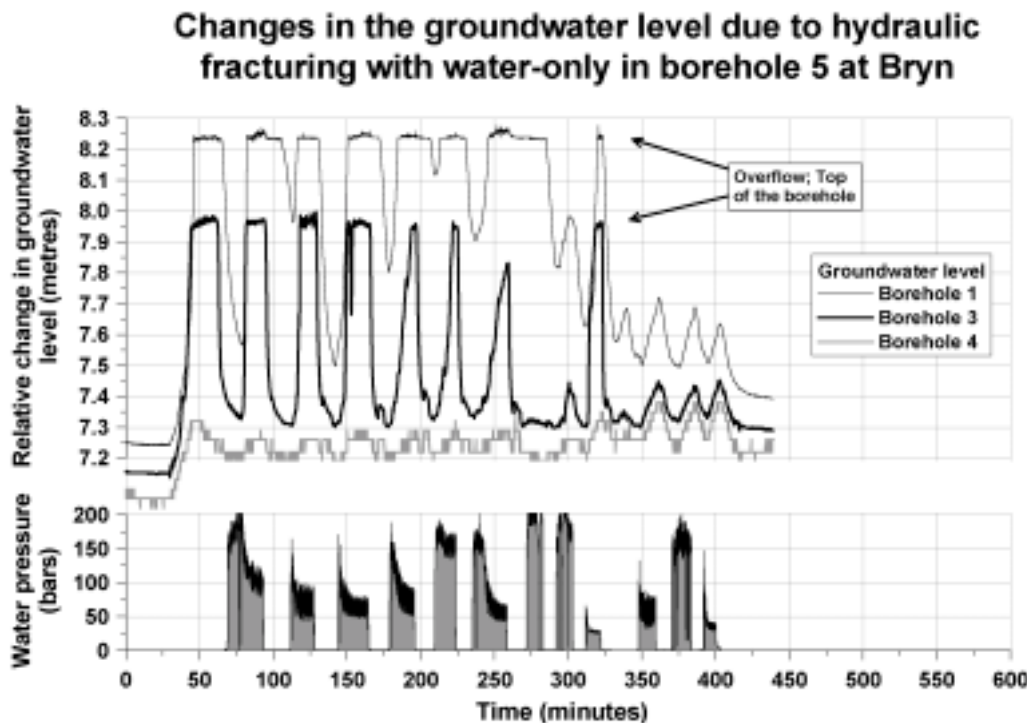


Figure 5–56: Groundwater level changes in boreholes 1, 3 and 4 measured during the hydraulic fracturing with water-only in borehole 5 at Bryn.

5.2.10 Hydraulic fracturing with injection of sand

Pressure-time curves from the hydraulic fracturing with injection of sand in boreholes 1, 2, 3 and 5 are given in figures 5–57 to 5–60. The pressure levels from borehole 4, which had to be recorded manually from the digital measurements because the data logger was out of order, are presented in table 5–13. The injection of sand at the end of each hydraulic fracturing cycle, marked with the number of the injection fluid container, generates a pressure buildup for most of the sections. The counter pressure levels, or the water pressure in the borehole section immediately before the injection of sand, are shown in figure 5–61. The counter pressures in borehole 4 vary from 20-35 bars (table 5–13).

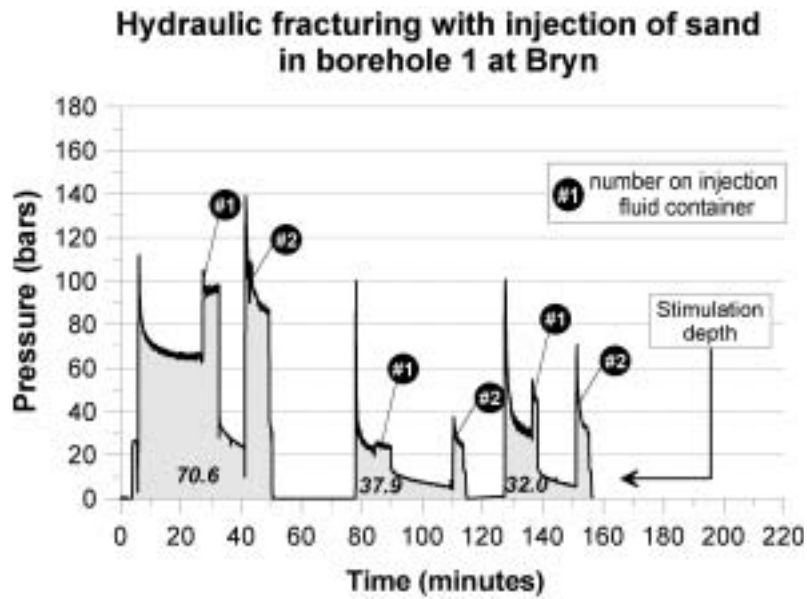


Figure 5–57: Pressure-time curves from hydraulic fracturing with injection of sand in borehole 1 at Bryn.

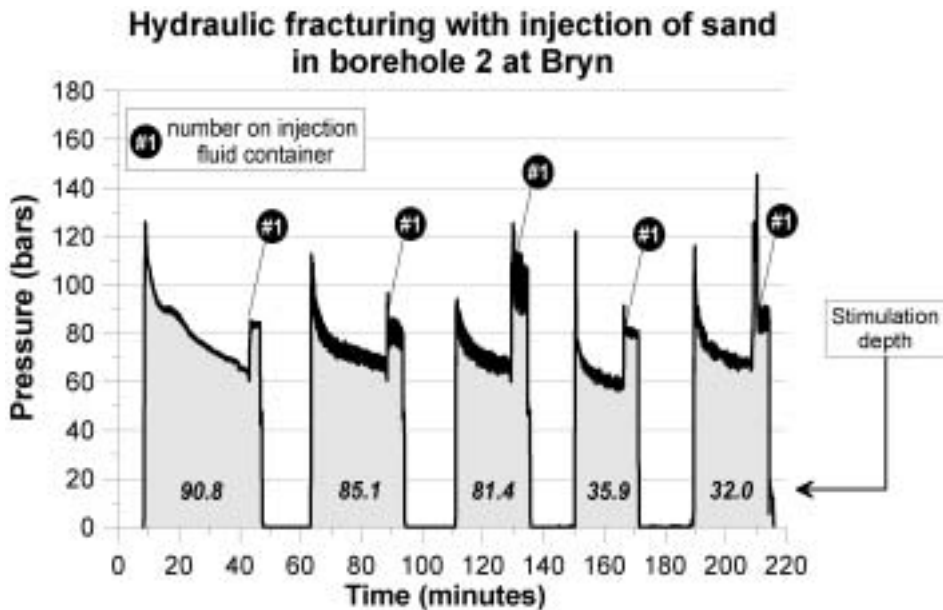


Figure 5–58: Pressure-time curves from hydraulic fracturing with injection of sand in borehole 2 at Bryn.

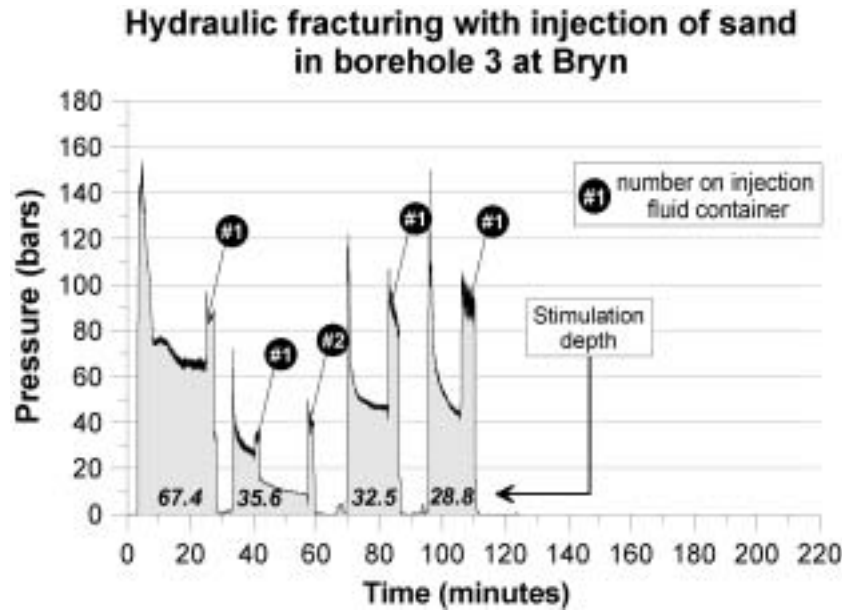


Figure 5–59: Pressure-time curves from hydraulic fracturing with injection of sand in borehole 3 at Bryn.

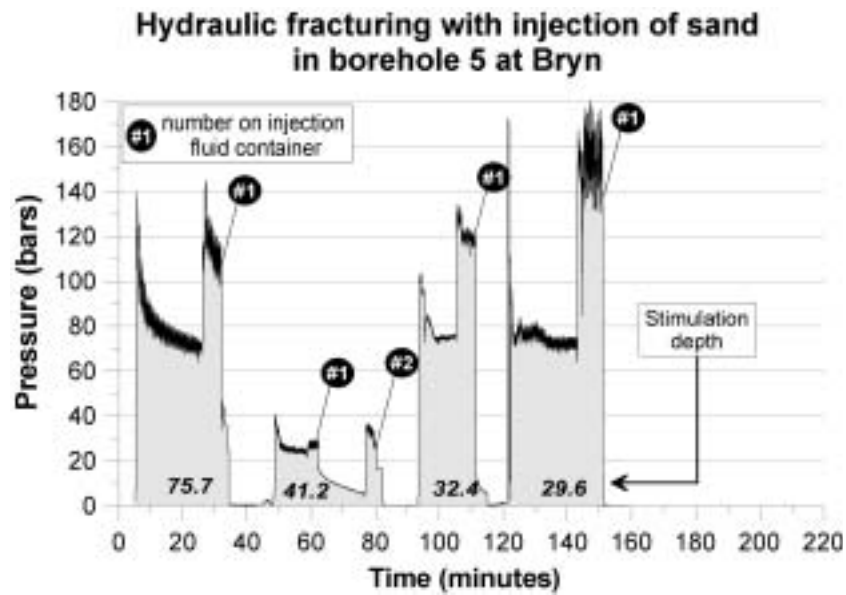


Figure 5–60: Pressure-time curves from hydraulic fracturing with injection of sand in borehole 5 at Bryn.

Table 5–13: Corresponding water pressures from the hydraulic fracturing with injection of sand in borehole 4 at Bryn, manually recorded from the digital measurements.

Section	$P_{reopening}$ (bars)	P_{min} prior to injection (bars)	P_{max} after injection (bars)
37.9	-	35	70
33.2	-	20	65
30.1	80	30	85

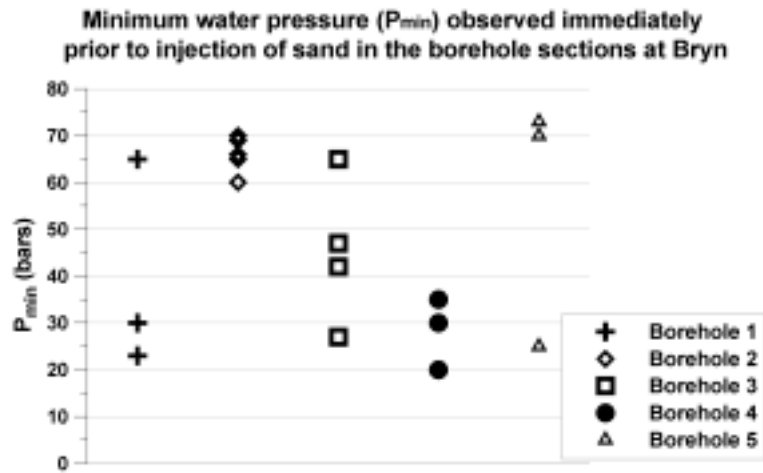


Figure 5–61: The counter pressure in the borehole sections at Bryn immediately before injection of sand.

5.2.11 Terrain level changes

The levelling, performed before and after the hydraulic fracturing with water-only and after hydraulic fracturing with injection of sand at Bryn, resulted in a maximum change of the terrain level of 1.0 millimetres measured in relation to a fixed point (tables 5–14 and 5–15). The largest measuring deviation for the points located within the area of influence for hydraulic fracturing with water-only and hydraulic fracturing with injection of sand was ± 1.0 millimetres. These modest alterations of the terrain level of ± 1.0 millimetres should probably be characterized as measuring errors since the majority of the measurements confirms a stable terrain, and no trend can be read from the deviating measurements.

Table 5–14: Results from the levelling before and after hydraulic fracturing with water-only (HF) in borehole 2-5 at Bryn.

	Fixed point	point #1	point #2	point #3
BH2, levelling before HF (m)	0.319	2.640	0.129	-
BH2, levelling after HF (m)	0.320	2.641	0.129	-
BH2, relative change (mm)	1.0	1.0	0.0	-
BH3, levelling before HF (m)	0.215	0.595	0.871	0.8535
BH3, levelling after HF (m)	0.215	0.595	0.871	0.853
BH3, relative change (mm)	0.0	0.0	0.0	-0.5
BH4, levelling before HF (m)	0.335	0.146	1.875	-
BH4, levelling after HF (m)	0.335	0.146	1.875	-
BH4, relative change (mm)	0.0	0.0	0.0	
BH5, levelling before HF (m)	0.388	0.199	1.450	-
BH5, levelling after HF (m)	0.388	0.199	1.450	-
BH5, relative change (mm)	0.0	0.0	0.0	

Table 5–15: Results from the levelling before and after hydraulic fracturing with injection of sand (HFS) in borehole 1, 2, 3 and 5 at Bryn.

	Fixed point	point #1	point #2	point #3
BH1, levelling before HFS (m)	0.590	0.560	0.968	1.810
BH1, levelling after HFS (m)	0.590	0.560	0.968	1.810
BH1, relative change (mm)	0.0	0.0	0.0	0.0
BH2, levelling before HFS (m)	0.590	0.560	0.968	0.449
BH2, levelling after HFS (m)	0.590	0.559	0.967	0.448
BH2, relative change (mm)	0.0	-1.0	-1.0	-1.0
BH3, levelling before HFS (m)	0.590	0.560	0.967	0.448
BH3, levelling after HFS (m)	0.590	0.560	0.967	0.448
BH3, relative change (mm)	0.0	0.0	0.0	0.0
BH5, levelling before HFS (m)	0.590	0.559	0.967	0.448
BH5, levelling after HFS (m)	0.590	0.559	0.967	0.448
BH5, relative change (mm)	0.0	0.0	0.0	0.0

5.2.12 Thermal response

The effective in-situ value of the rock thermal conductivity and the borehole thermal resistance (R_b) in borehole 3, measured in an undisturbed mode, is calculated to be 3.2 W/m,K and 0.06 K/(W/m) (figures 5–62 and 5–63), respectively. The median value of the thermal conductivity for the Ringerike sandstone was measured to be 3.3 W/m,K (Midttømme et al., 2000) in a laboratory study of the thermal conductivity of the bedrock in Bærum (Bekkestua map sheet) (figures 2–28 and 2–29). Variations within the upper and lower quartile of the measured thermal conductivity values in the referred study, reflecting deviations in the rock properties of the bedrock samples collected at different locations, were in the range of 3.1 to 3.6 W/m,K (figure 2–29). According to these results, the effective in-situ value of the rock thermal conductivity is measured to be 0.1 W/m,K lower than the median value for the thermal conductivity of the bedrock.

The high yield in borehole 3 at Bryn, including the natural fracture zone at 12-13 metres depth (paragraph 5.2.1) together with the yield improvement after stimulation with hydraulic fracturing (figure 5–26), makes it reasonable to assume a significant groundwater flow through the borehole. On this background the natural groundwater flow in the area was expected to influence the thermal response in the borehole, and to be quantified by the effective in-situ value of the rock thermal conductivity. According to the negative differential observed between the effective in-situ value of the rock thermal conductivity and the median laboratory value for the thermal conductivity of the Ringerike sandstone, both the contribution of flowing groundwater and the real value for thermal conductivity of the bedrock is lesser than expected. Supposing a contribution of 0.2 W/m,K from the groundwater flow, the thermal conductivity of the Ringerike sandstone-bedrock around Bryn must be 2.9 W/m,K which is in the lower range of the measured laboratory value. The value of the borehole thermal resistance was as expected, R_b is 0.06 K/(W/m).

The mean temperature, T_{mean} is clearly affected by the groundwater flow, artificially induced after 95 hours by the pumping in borehole 2 (figure 5–63). The lower thermal response, expressed by a reduction of T_{mean} , implies a higher energy absorption which will increase the value of the effective in-situ value of the rock thermal conductivity. A quantification of the improvement in the effective in-situ value of the rock thermal conductivity, caused by the induced groundwater flow, can be done by performing a new thermal response test in borehole 3. As prerequisites, the test borehole must have returned to its thermal state of equilibrium, and the pumping should be started before or simultaneous with the test. The increased effect value at 95 hours is due to the power supply of the pump in borehole 2 (figure 5–62).

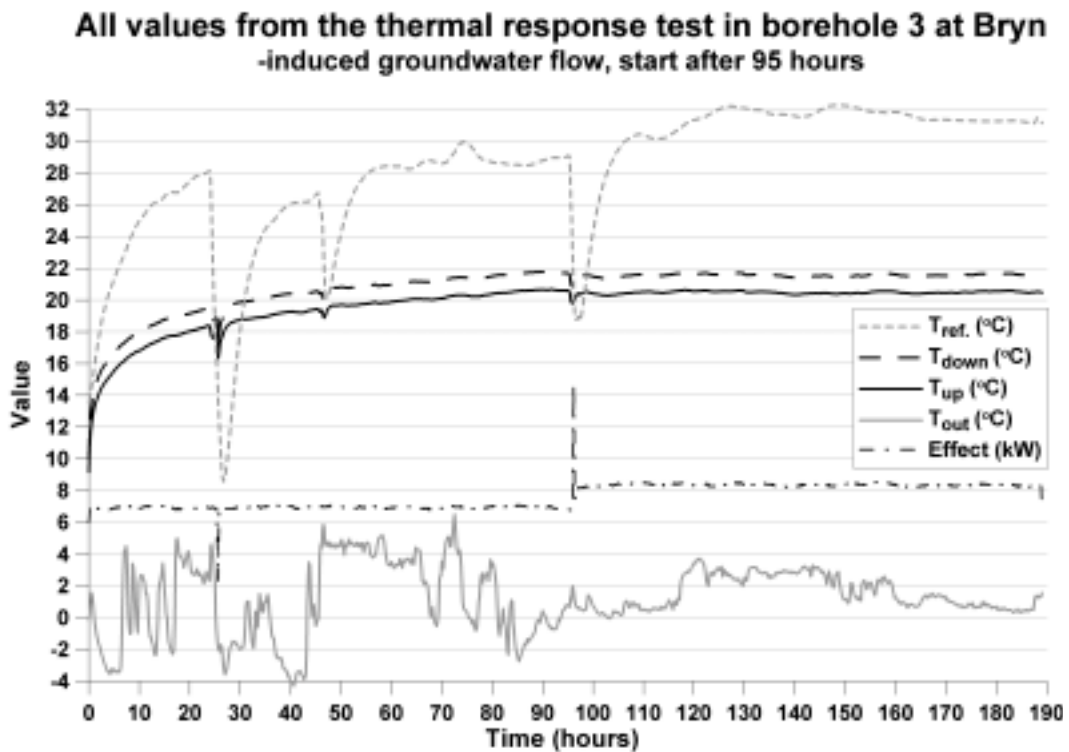


Figure 5–62: All the values from the thermal response test in borehole 3 at Bryn.

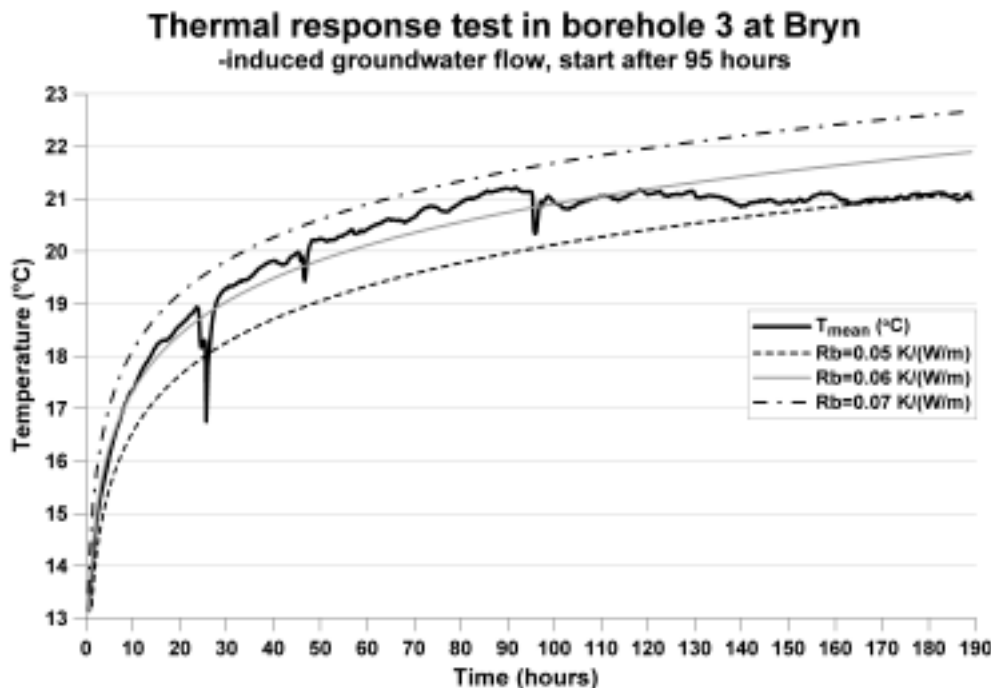


Figure 5–63: The experimental mean fluid temperature (T_{mean}) matching the thermal resistance curves.

5.2.13 Effect extraction from the pilot plant

The most important results from the test run of the pilot plant at Bryn are shown in figure 5–64. A significant pressure buildup of 6.8 bars in the circulation system resulted in a corresponding flow rate of only 3.5 m³/hour, based on two pumps. Still, a temperature differential of 4.5–5°C and an effect of approximately 19 kW were extracted from the pilot plant at Bryn the first 2.5 days of the test. These results were used as input data for the modelling of the energy extraction at Bryn (table 4–5) (Spangelo, 2003). The remaining part of the test run is considered as unsuccessful since important parameters as temperature and flow rate of the cooling-medium (river) were disturbed:

- A weather change on the 13th of April 2003 to sunny and warm weather increased the temperature of the inflowing river water. Consequently, the temperature differential between the river water ($T_{\text{river_in}}$) and the groundwater ($T_{\text{in_HEX}}$) was reduced and so also the effect extraction. Due to sunny weather during the daytime and relatively cold nights, daily variations of up to 2.5°C can be seen for the inflowing river water ($T_{\text{river_in}}$).
- The marked and increasing temperature differential between the inflowing river water ($T_{\text{river_in}}$) and the outflowing groundwater from the heat exchanger ($T_{\text{out_HEX}}$), observed from the 17th of April, can be explained by a reduced pumping rate of river water, caused by debris in the spring flood, causing a partly clogging the water intake at the pump.

The temperature of pumped groundwater from boreholes 1 and 5 ($T_{\text{in_HEX}}$) remained stable at approximately 7.5°C during the test.

The project requires a circulation rate of 20 m³/hour, where the satellite boreholes 1, 2, 4 and 5, are used as pumping boreholes, while borehole 3 is used for infiltration. Since no sectioning of the satellite boreholes were present, large volumes of water could theoretically have been pumped from the boreholes, and the suggested value of 20 m³/hours in the project could easily have been achieved. The main problem at Bryn, limiting the infiltration rate, is the pressure buildup in borehole 3. Trapped air in the circulation system could have been a possible explanation of the pressure buildup in borehole 3 in an early phase of the test. If so, the pressure would have decreased after a while. Instead, the pressure buildup continued and at the end of the test, the circulation rate was lowered to approximately 2.5 m³/hour. An alternative use of the boreholes at Bryn for ground source heat pump-purposes should thus be considered (paragraph 5.2.14).

Possible reasons explaining the low infiltration rate:

- A yield of approximately 3 m³/hour was achieved in the test pumping of borehole 3, employing pump C. Pump C is stronger than pump D used in the test run (figure 2–21). A corresponding test pumping of borehole 3 using pump D would have been more time-consuming, but the same value for the borehole yield would have been achieved at the end. Assuming similar pressure conditions, infiltration and pumping of water should be almost equally difficult. Consequently, the infiltration rate of 2.5 m³/hour and a system pressure of 7.5 bars after 17 days of circulation, initially 3.5 m³/hour, corresponds satisfactory with the results from the test pumping using pump C.
- Minor clogging in the fractures, probably by suspended particles in the circulating groundwater may have occurred.
- Even though the system was designed to avoid introduction of oxygen, pumping of oxygen-rich water from the natural fracture zone at 12-13 metres depth might have occurred. Mixed with deeper and more anoxic groundwater, these small amounts of oxygen might have been enough to cause precipitation of iron- and possibly manganese compounds. The groundwater quality seemed to be satisfying (paragraph 5.2.5), but the content of iron- and manganese in the water could possibly be enough to cause problems under the actual conditions. The increasing system-pressure and the corresponding decreasing infiltration rate during the test run, supports the theory of a continuous process of precipitation and clogging taking place.

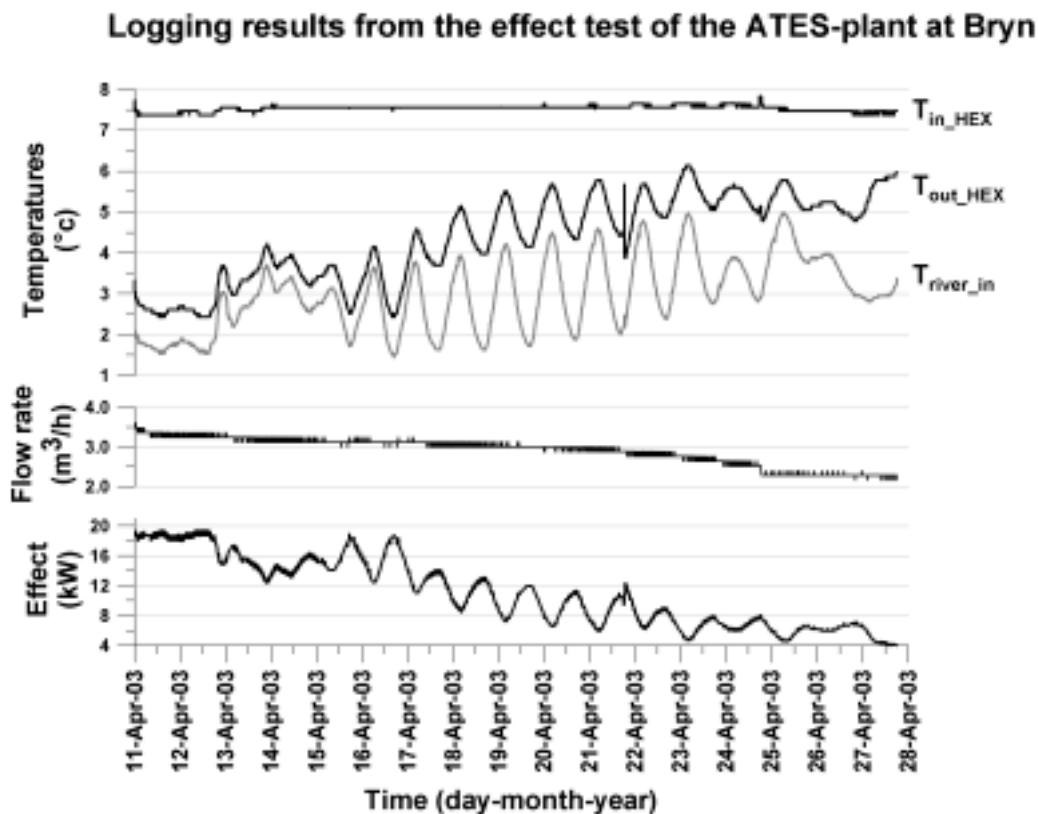


Figure 5–64: A selection of the logged data from the test run of the pilot plant at Bryn.

5.2.14 Recommended alternative use of the boreholes at Bryn

The test run of the pilot plant at Bryn (paragraph 5.2.13) showed that the infiltration capacity of borehole 3, only 2.5 to 3.5 m^3 /hour, was the limiting factor for a satisfactory operation of the plant. A flow rate of 20 m^3 /hour was suggested in the project plan, and the major prerequisite for the use of the concept with circulation of groundwater is lost. Different alternatives for the use of the boreholes at Bryn for ground source heat purposes are discussed:

- The high borehole yields at Bryn, when the fracture zone is included, could be taken advantage of by pumping water from all the boreholes to the heat exchanger or heat pump. The heat exchanged water should be returned either into the storm water run-off pipe in the municipal sewer system or into the river Lomma. Groundwater withdrawals higher than 5 m^3 /hour have to be approved by the Norwegian Water Resources and Energy Directorate (NVE). By using all the boreholes as pumping wells, installing pump D in borehole 3 similar to the other boreholes, the total yield for the plant would be 25 m^3 /hour. A temperature differential of 4°C ($\Delta T = 4^\circ C$) through the operation period will give an effect extraction of 116 kW. However, the withdrawal of such large quantities of water, is not allowed to cause a significant lowering of the groundwater level.
- The boreholes at Bryn could be used as a conventional ground source heat pump system by replacing the pumps with single-U collectors in the vertical boreholes. More boreholes could be added to the plant if desirable.

As a general remark, the best profitability and energy extraction from the plant are obtained by using the boreholes for both heating- and cooling purposes.

5.3 EAB

5.3.1 Borehole yields and groundwater chemistry

The pumping rates and groundwater level measurements from the test pumping of boreholes 1 to 3 at EAB before hydraulic fracturing with injection of sand are presented in figures 5–65 to 5–67. Sudden drops in the pumping rate in the diagrams represent short stop/start breaks. Despite a duration of 18 hours, a full drawdown to the water intakes at 68.3 and 66.3 metres depth for boreholes 1 and 2, respectively, was not achieved in the test pumping. The yield for borehole 1 and 2 are larger than the pump capacity, more than 6300 litres/hour. The sinking curves from the test pumping in boreholes 1 and 2 have no distinctive irregularities, while the water level in borehole 1 rises instantly from 25 to 22 metres and thereafter shows an even rising course. The incident at 22 metres depth in borehole 1 is likely to represent a major water inlet. A complete drawdown to 70 metres depth was achieved in the test pumping of borehole 3, and the pumping rate stabilized at 5200 litres/hour. The sinking curve appears irregular, probably due to an unstable pumping rate, but a significant speed up in the sinking velocity at 28 metres depth is likely to be relevant. The water level rises directly from 70 to 25 metres depth after ended test pumping. These marked incidents on the sinking- and rising curves at 28 and 25 metres depth respectively, may describe two significant water inlets in borehole 3. A complete recovery of the natural groundwater level was not obtained after ended test pumping in the boreholes at EAB. Thus the test pumping order, borehole 3, 2 and 1, might influence the relative change in the groundwater level. The groundwater level in boreholes 1 and 2 was lowered at the same rate due to the pumping in borehole 1 (figure 5–65). The pumping in borehole 2 caused a relatively parallel drawdown in boreholes 1 and 2, but the groundwater level in the pumping borehole was lowered at a faster rate (figure 5–66). Finally, the test pumping in borehole 3 caused an almost identical change in the groundwater level in borehole 1, similar to the changes caused by the test pumping in boreholes 1 and 2 (figure 5–67).

The values of the groundwater quality parameters are almost identical in all the boreholes (figure 5–68). The pH-values are 7.71, 7.78 and 7.77 for boreholes 1-3 respectively (NGU-Lab, 2002b). The groundwater quality in the boreholes at EAB is evaluated to be satisfying for ground source heat pump systems based on circulating groundwater. The limit values referred to in paragraph 2.5 are not exceeded. The groundwater quality may change in the operation mode, and an adequate water-quality monitorings program should be carried out. Similar to the corresponding results from Lade, the groundwater is relatively hard and can be characterized as calcium bi-carbonate.

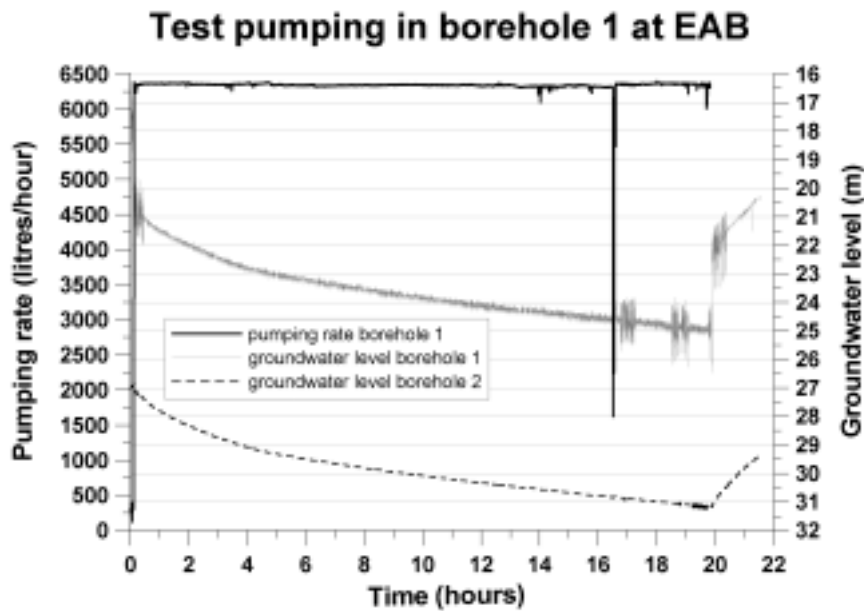


Figure 5–65: Pumping rate and groundwater level changes due to test pumping in borehole 1 at EAB before hydraulic fracturing with injection of sand.

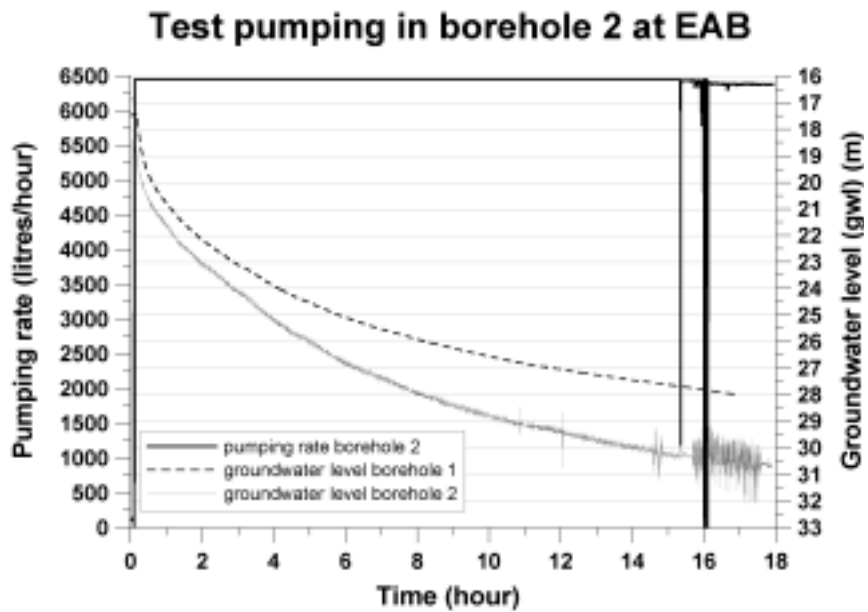


Figure 5–66: Pumping rate and groundwater level changes due to test pumping in borehole 2 at EAB before hydraulic fracturing with injection of sand.

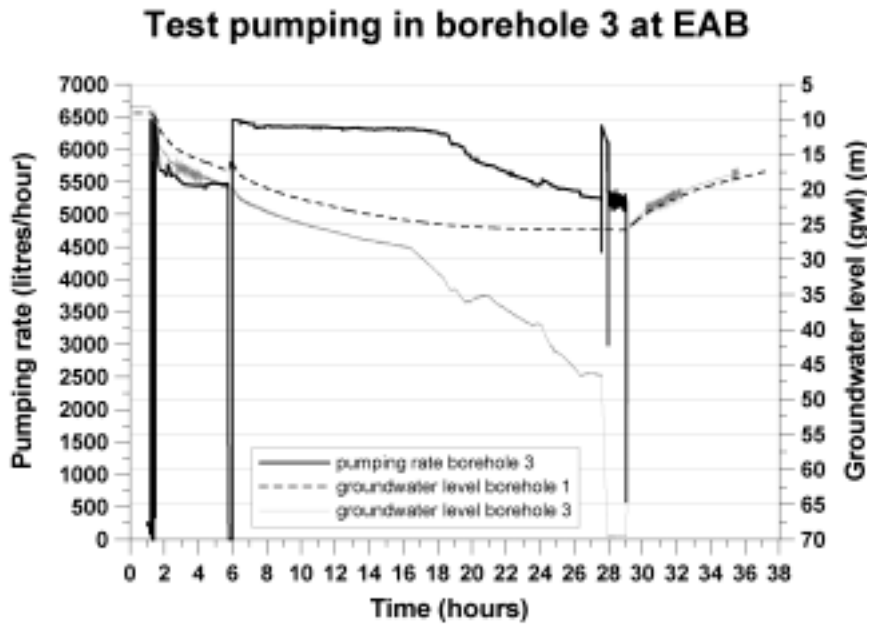


Figure 5–67: Pumping rate and groundwater level changes due to test pumping in borehole 3 at EAB before hydraulic fracturing with injection of sand.

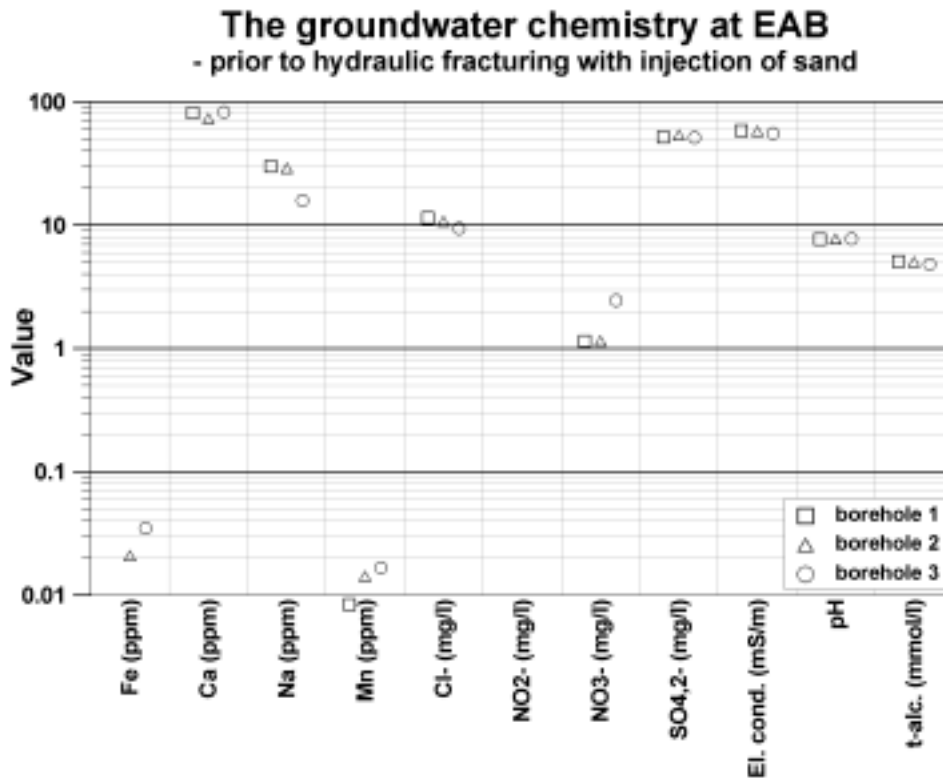


Figure 5–68: Selected groundwater quality parameters in boreholes 1, 2 and 3 at EAB before hydraulic fracturing with injection of sand, based on NGU-Lab (2002b).

5.3.2 Flow patterns

Continuous flow-measurement logs for boreholes 1 to 3 at EAB, before and after hydraulic fracturing with injection of sand, are presented in figure 5–69. Marked changes in the rotational speed of the flow meter, interpreted as major water inlets, are discovered at 109, 37 and 34 metres depth in borehole 1. The greatest inflows are present at 37 and 34 metres. No changes in the flow pattern are observed in borehole 1. The flow pattern in borehole 2 is changed. Three more or less new water inlets are present at 68, 43 and 39 metres. The main water inlet at 33 metres depth, and several significant water inlets in the 25-33 metres interval are barely influenced by the hydraulic fracturing with injection of sand. The main water inlets in borehole 3 appear at 32 and 28 metres depth. The water inlet at 32 metres seems to be unaffected by hydraulic fracturing with injection of sand, while the volume of inflowing water in the 28 metres level has increased. No flow pattern changes are shown in the remaining part of borehole 3.

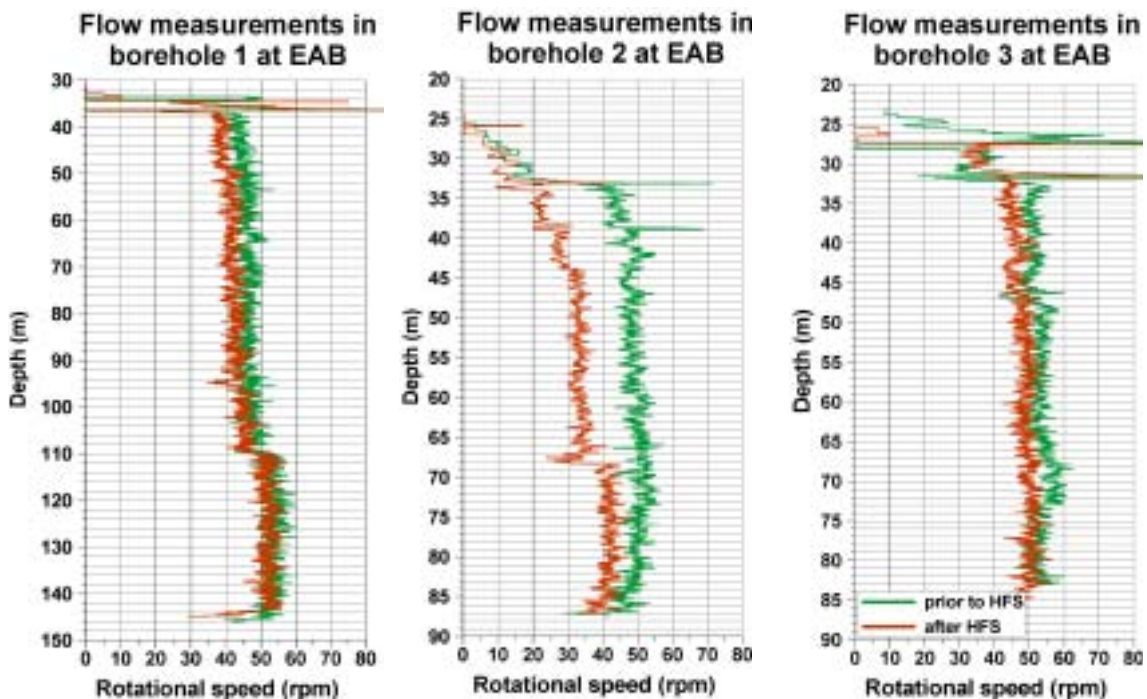


Figure 5–69: Continuous flow-measurement logs from boreholes 1-3 at EAB before and after hydraulic fracturing with injection of sand (HFS).

5.3.3 Borehole conditions - degree of fracturing, temperature, conductivity and radioactivity

The bedrock geology in borehole 1 at EAB, based on an interpretation of the optical televiewer recordings, is previously discussed and presented as a stratigraphic sequence in paragraph 3.3 and figure 3–7, respectively. Physical changes in the borehole wall caused by the hydraulic fracturing with injection of sand can be discovered on a few occasions in the optical televiewer logs. An existing fracture at 60.7 metres depth in borehole 2 at EAB is clearly more open after hydraulic fracturing with injection of sand (figure 5–70). The optical televiewer was used to map fractures in the boreholes. The joint

rossette from borehole 1 (figure 5–71) shows that the main fracture direction is approximately towards northeast-southwest and parallel to the bedding. The mean dip is 52° towards northwest. The frequency histogram for borehole 1 at EAB and the corresponding stereogram are presented in Appendix 3. The temperature- and electric conductivity logs for boreholes 1 to 3 at EAB (figures 5–72 to 5–74) have a different course before and after hydraulic fracturing with injection of sand. The levels- and results of hydraulic fracturing with injection of sand are included in the figures, as well. The borehole logging before and after hydraulic fracturing was done in early September and in the middle of November, two days after completion of the thermal response test in borehole 1. Seasonal variations in the air temperature influence the groundwater temperature in the uppermost 20 metres in all the boreholes. In addition, the groundwater temperature in borehole 1 is affected by heat remaining from the thermal response test. The undisturbed groundwater level was found between 8 to 12 metres depth for boreholes 1, 2 and 3 at EAB. New or enlarged events in the temperature- and/or electric conductivity logs from borehole 1 are observed at 34.5, 51, 94, 110 and 114 metres depth, at 35, 39 and 44 metres depth in borehole 2, and at 28, 39, 64 and 78 metres depth in borehole 3. Apart from the temperature logs in borehole 1 and in the upper 20 metres of the boreholes, the temperature- and electric conductivity logs show almost the same course before and after hydraulic fracturing with injection of sand. A minimum temperature of 7.5°C is measured at 110-120 metres depth in borehole 1, and the temperature follows a natural gradient of 1.1°C towards depth from this point. The temperature courses in boreholes 2 and 3 are similar to borehole 1, but the minimum temperature is approximately 7.2°C .



Figure 5–70: A segment of borehole 2, recorded with an optical televiewer before and after hydraulic fracturing with injection of sand. The existing fracture at 60.7 metres is clearly more open after the hydraulic fracturing with injection of sand.

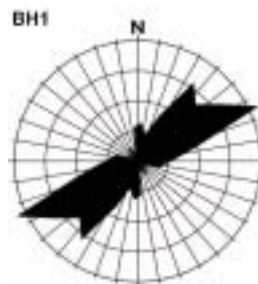


Figure 5–71: Joint rosette from borehole 1 at EAB before hydraulic fracturing with injection of sand. Mean dip is 52° towards northwest.

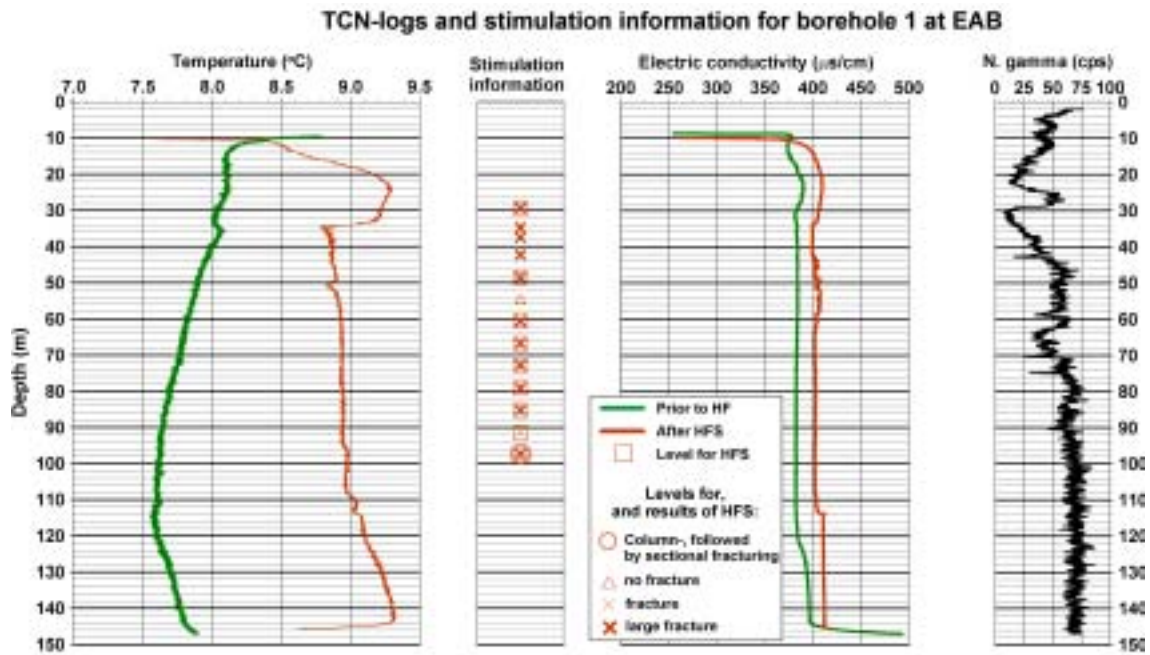


Figure 5–72: Temperature- and electric conductivity logs compared with levels- and results from hydraulic fracturing with injection of sand (HFS) in borehole 1 at EAB.

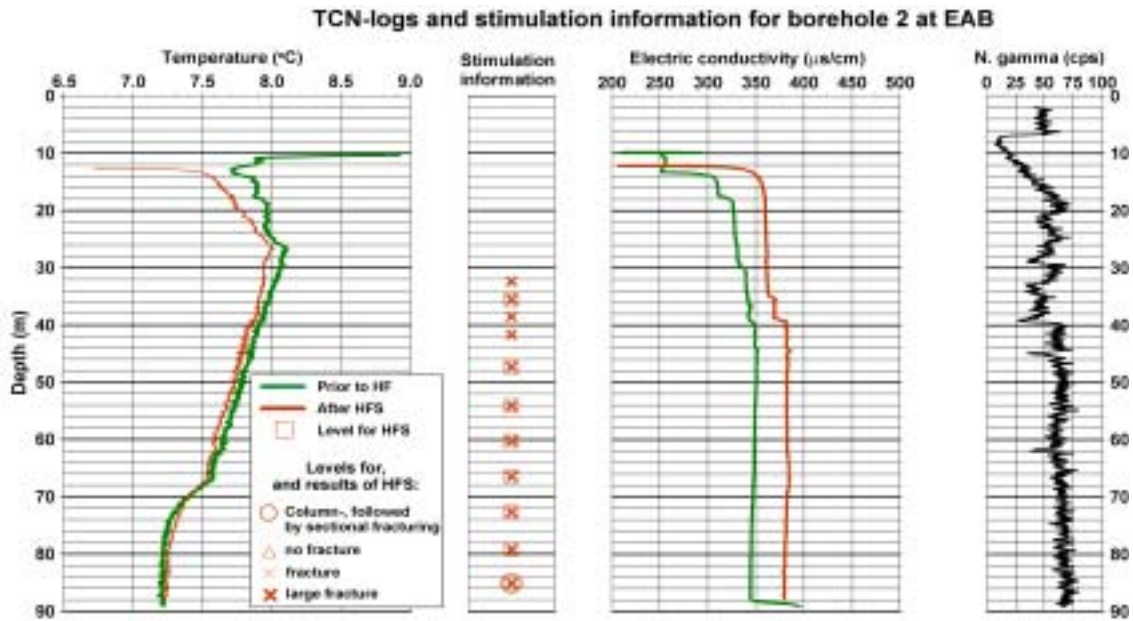


Figure 5–73: Temperature- and electric conductivity logs compared with levels- and results from hydraulic fracturing with injection of sand (HFS) in borehole 2 at EAB.

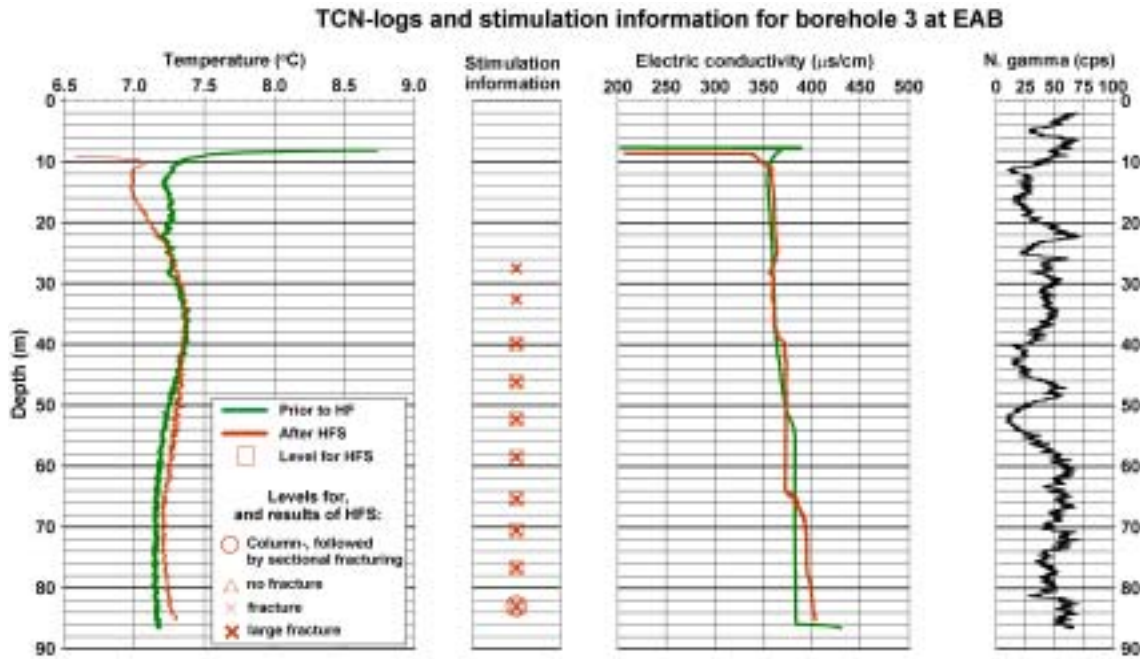


Figure 5–74: Temperature- and electric conductivity logs compared with levels- and results from hydraulic fracturing with injection of sand (HFS) in borehole 3 at EAB.

5.3.4 Identification of possible new water inlets in the boreholes

Similar to Bryn, an attempt to identify new water inlets in the boreholes has been done using the flow measurements (figure 5–69) and the TCN-logs (figures 5–72 to 5–74) to verify the efficiency of the hydraulic fracturing with injection of sand. Naturally occurring irregularities present on the temperature- and electric conductivity curves before hydraulic fracturing with injection of sand, and at greater depths than 25 metres, are found at 35 (borehole 1, figure 5–72), at 30, 39, 67, 88 (borehole 2, figure 5–73), and at 28 and 55 (borehole 3, figure 5–74) metres depth. Small variations and uncertainties related to the specification of depth have to be accounted for in the comparison of all the phases of work included in the borehole investigation, performed at five different times: (1) hydraulic fracturing with water and injection of sand, (2-5) flow measurement logs, temperature- and electric conductivity of the water, measured before and after the hydraulic fracturing with injection of sand. Using all the available data, possible new water inlets related to the hydraulic fracturing with injection of sand are identified and presented in tables 5–16 to 5–18, in a similar fashion as presented for Bryn.

Table 5–16: Possible new water inlets related to the hydraulic fracturing in borehole 1 at EAB.

Data	Observation	Discussion
flow, el. cond. & temp.	No changes in the flow pattern were observed as a consequence of the hydraulic fracturing with injection of sand. The largest inflows were registered at 34, 37 and 109 metres. New or enlarged changes in the temperature and conductivity can be seen at 34.5, 51, 94, 110 and 114 metres.	<p>The low pressure level observed during the hydraulic fracturing with water-only in the borehole sections at 34.7 and 37.5 metres, 10 and 25-35 bars (figure 5–75) respectively, implied that two already open fracture systems were hit and the effect of the hydraulic fracturing was probably minimal. According to the flow measurements, the fractures within the 34.7- and 37.5-sections are the main water inlets in the borehole. The irregularity at 34 metres on the temperature log had increased compared to the original condition. Images from the optical televiewer confirmed the presence of a rock boundary at 37 meters, where the rock changes from pure limestone to nodular limestone (figure 3–7).</p> <p>It is unknown whether the observed changes in the temperature log at 51 and 94 metres are related to hydraulic fracturing with injection of sand. Assuming an inaccurate determination of the depth, the changes could be connected to the hydraulic fracturing at 48.4 and 91.4 metres, respectively. New incidents observed on the temperature- and conductivity log at 110 and 114 metres could possibly be associated with the columnar hydraulic fracturing accomplished at the 97.4-level. The flow measurements revealed a water bearing fracture at 109 metres both before and after hydraulic fracturing with injection of sand.</p>

Table 5–17: Possible new water inlets related to the hydraulic fracturing in borehole 2 at EAB.

Data	Observation	Discussion
flow, el. cond. & temp.	The flow pattern was changed by the introduction of three water inlets at 39, 43 and 68 metres. The main water inlet at 33 metres, and several significant water inlets in the interval 25-33 metres, seemed to be less influenced by the hydraulic fracturing with injection of sand. New or enlarged irregularities on the temperature- and conductivity log were registered at 35, 39 and 44 metres.	<p>The new water inlets at approximately 39, 43 and 68 metres, appearing on the flow velocity curve, are associated with hydraulic fracturing with water and - injection of sand in the borehole sections at 38.5, 41.7 and 66.4, respectively.</p> <p>Minor irregularities are observed on the conductivity- and temperature log, at 39 and 67 metres respectively, both before and after hydraulic fracturing. Assuming small inaccuracies in the depth determinations, the irregularities are likely to correspond to the water inlets at approximately 39 and 68 metres, and thus the corresponding hydraulic fracturing. Still, the presence of these irregularities describing the natural condition, indicates that the two minor, but probably existing, water inlets have been improved by the hydraulic fracturing. The relative low pressure level during the stimulation of section 66.4 and 38.5 (figure 5–76), having an (re)opening pressure of approximately 100 and 65 bars, respectively, may also indicate existing and open fractures present in these levels.</p> <p>The irregularity at 35 metres on the conductivity log can be related to the hydraulic fracturing with injection of sand in the section at 35.6 metres, while the new incident observed on the conductivity log at 44 metres can hardly be related to any kind of hydraulic fracturing.</p>

Table 5–18: Possible new water inlets related to the hydraulic fracturing in borehole 3 at EAB.

Data	Observation	Discussion
flow, el. cond. & temp.	The main water inlets appeared at 32 and 28 metres. The water inlet at 32 metres seemed to be unaffected by the hydraulic fracturing with water-only, while the quantity of inflowing water at 28 metres had increased. New irregularities on the conductivity log were spotted at 28, 39, 64 and 78 metres.	Hydraulic fracturing with water-only was performed in the borehole sections at 27.5 and 32.6 metres. The low pressure level registered during the hydraulic fracturing of section 27.5, approximately 10 bars (figure 5–77), indicated an open and existing fracture. Results from the flow-, and partly the temperature measurements done before hydraulic fracturing, confirm large water inlets present in the 27.5-level. The opening pressure for section 32.6 was slightly above 100 bars, but decreased instantly to 40 bars (figure 5–77). The original flow pattern indicated a partly open- and water bearing fracture present within the 32.6-section (figure 5–69). Even though no new changes can be seen in the flow pattern of the borehole, nor the temperature- and conductivity log, the relatively high (re)opening pressure was probably required to flush away the materials partly clogging the fracture. All observed irregularities on the conductivity log can be related to hydraulic fracturing in borehole sections 27.5, 39.9, 65.4 and 76.7 respectively. Injection of sand was performed in all sections except for the 27.5-level.

5.3.5 Hydraulic fracturing with injection of sand

Hydraulic fracturing with injection of sand was performed in a total of 25 borehole sections at EAB. The injection of the sand mixture at the end of each hydraulic fracturing cycle, marked with an “i” in the pressure-time diagrams (figures 5–75 to 5–77), causes a pressure buildup for most of the borehole sections. Based on the experiences from Bryn, the injection of sand was considered unnecessary if the stable counter pressure during the hydraulic fracturing with water-only was below approximately 40 bars at maximum flow rate. From a total of 37 hydraulic fracturing stimulations, 36 (97%) pressure-time curves, were interpreted as an opening or a reopening of fractures.

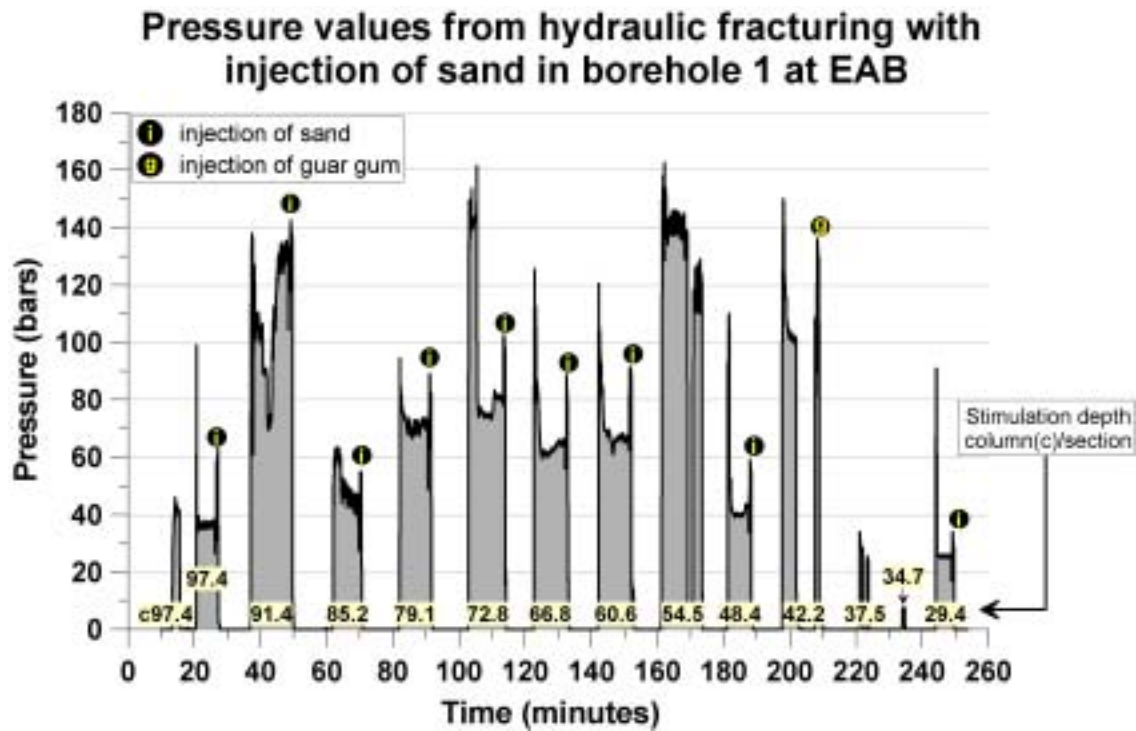


Figure 5–75: Pressure-time curves from the hydraulic fracturing with injection of sand in borehole 1 at EAB.

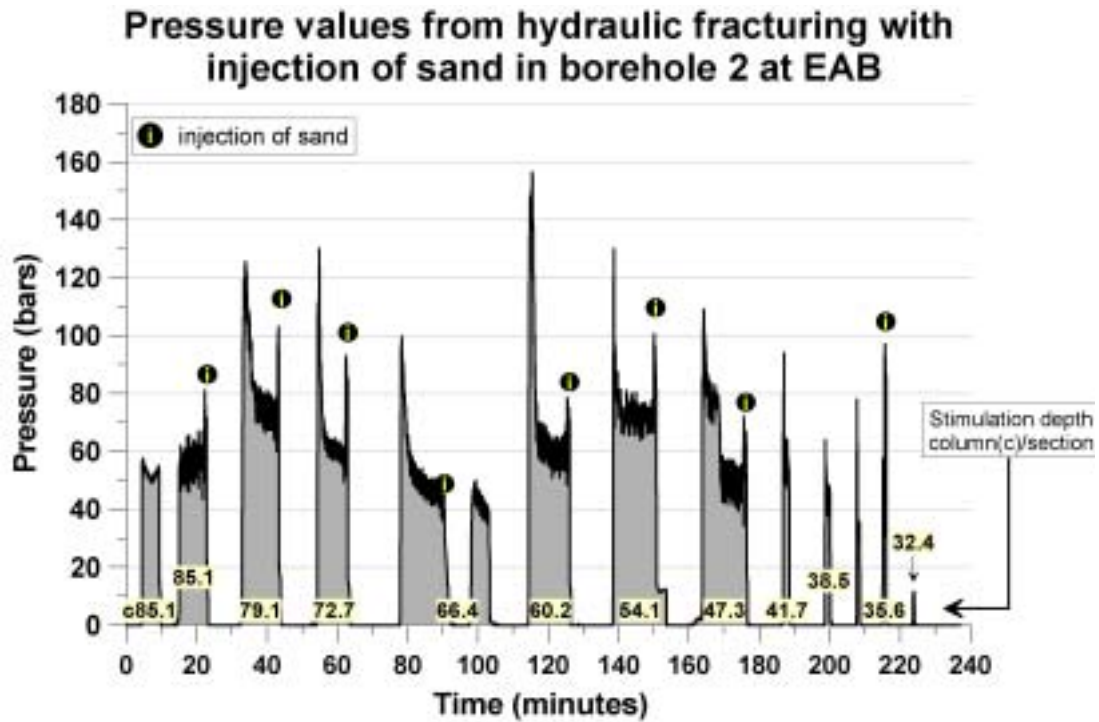


Figure 5-76: Pressure-time curves from the hydraulic fracturing with injection of sand in borehole 2 at EAB.

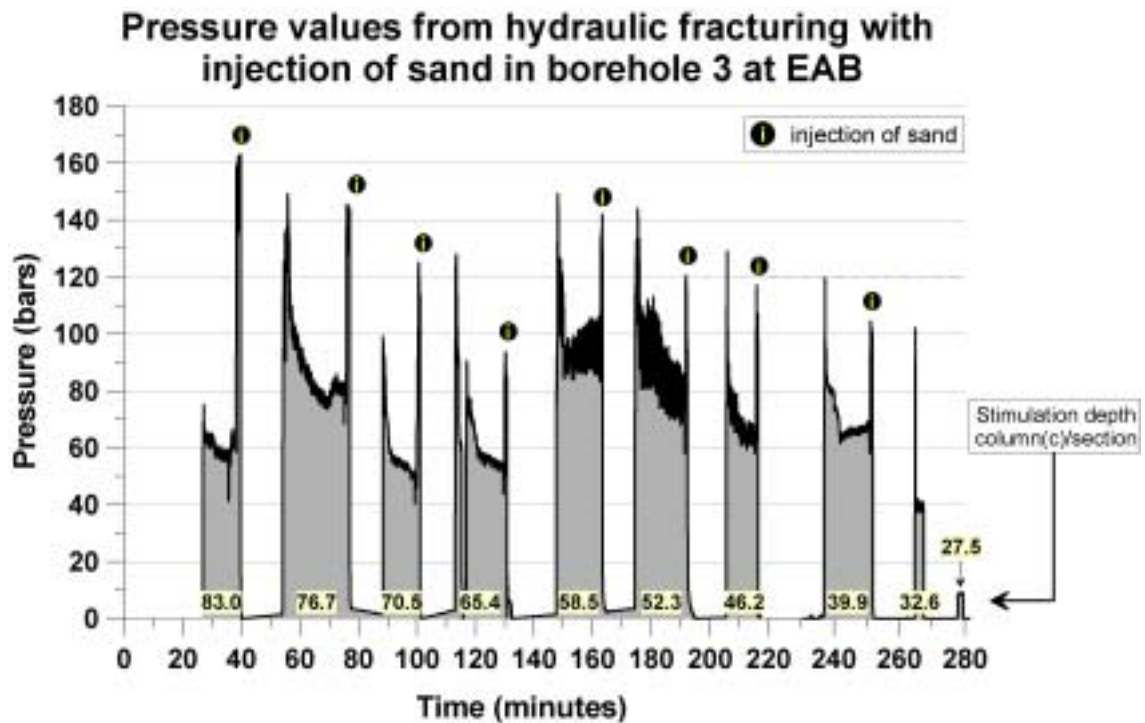


Figure 5-77: Pressure-time curves from the hydraulic fracturing with injection of sand in borehole 3 at EAB.

Changes in the groundwater level measured in the nearby boreholes, resulting from hydraulic fracturing with injection of sand, are presented in figures 5–78 to 5–80. Corresponding pressure-time curves from the hydraulic fracturing with injection of sand are plotted as well. The groundwater alterations are almost parallel in all the boreholes, and similar to Bryn, the degree of parallelism can be related to the main water bearing fractures present between 25-35 metres in boreholes 1, 2 and 3 at EAB (figure 5–69). A somewhat higher hydraulic response were recorded for borehole 1, while boreholes 2 and 3 showed an almost identical behaviour. Located in the middle (figure 3–6), the higher hydraulic response in borehole 1 can probably be explained by the lesser distance to the hydraulic fracturing in either boreholes 2 or 3. The hydraulic fracturing with injection of sand in borehole 1 causes almost identical fluctuations in the groundwater level in boreholes 2 and 3, but a higher response in borehole 3 can be seen after approximately 100 minutes. The groundwater level measurements are disturbed by a partial overflow in boreholes 1 and 3. The hydraulic fracturing with injection of sand in borehole 3 is completed after two days, and thus the groundwater monitorings in boreholes 1 and 2 as well.

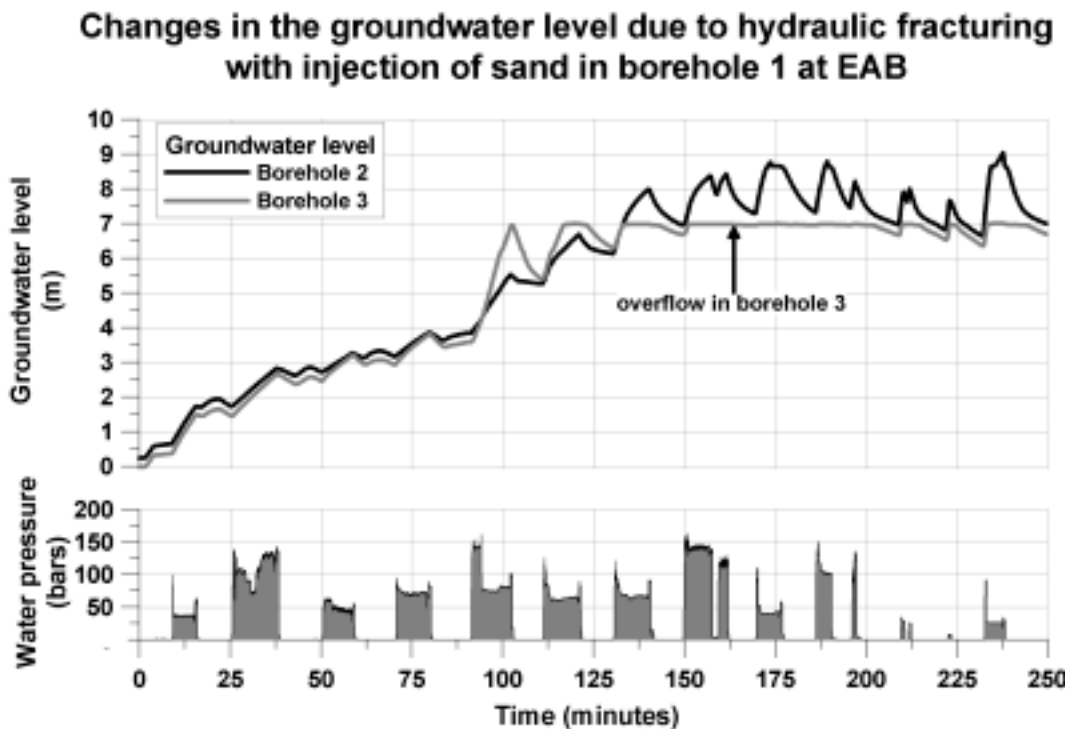


Figure 5–78: Groundwater level changes in boreholes 2 and 3 caused by the hydraulic fracturing with injection of sand in borehole 1 at EAB.

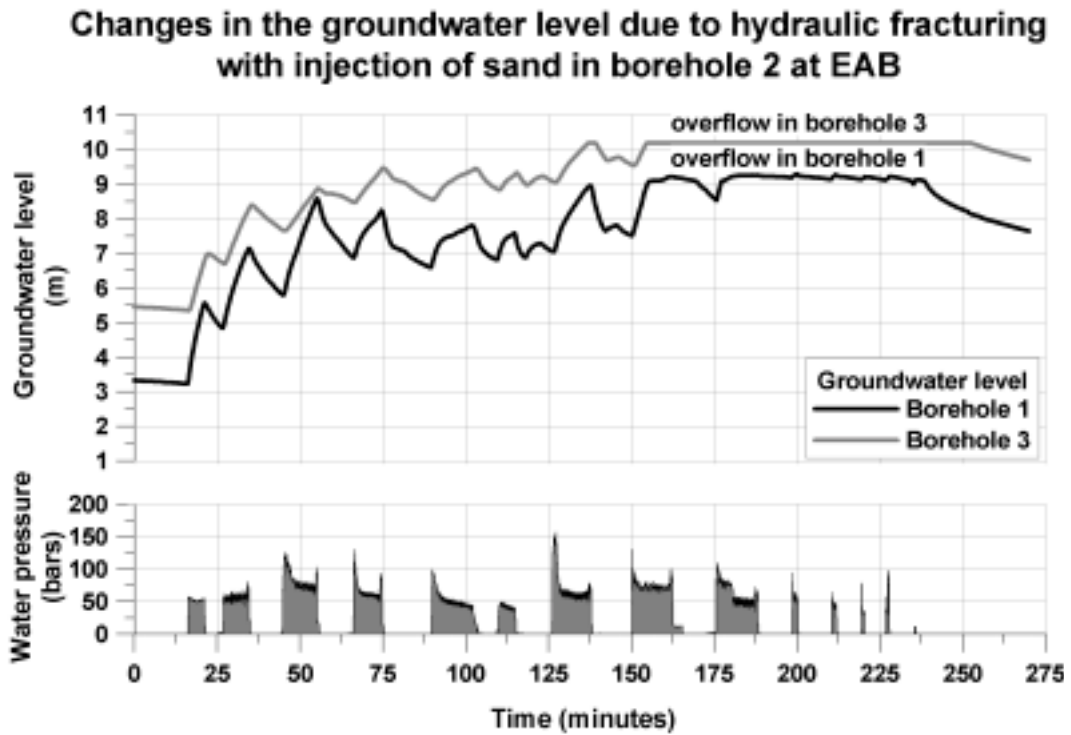


Figure 5-79: Groundwater level changes in boreholes 1 and 3 caused by the hydraulic fracturing with injection of sand in borehole 2 at EAB.

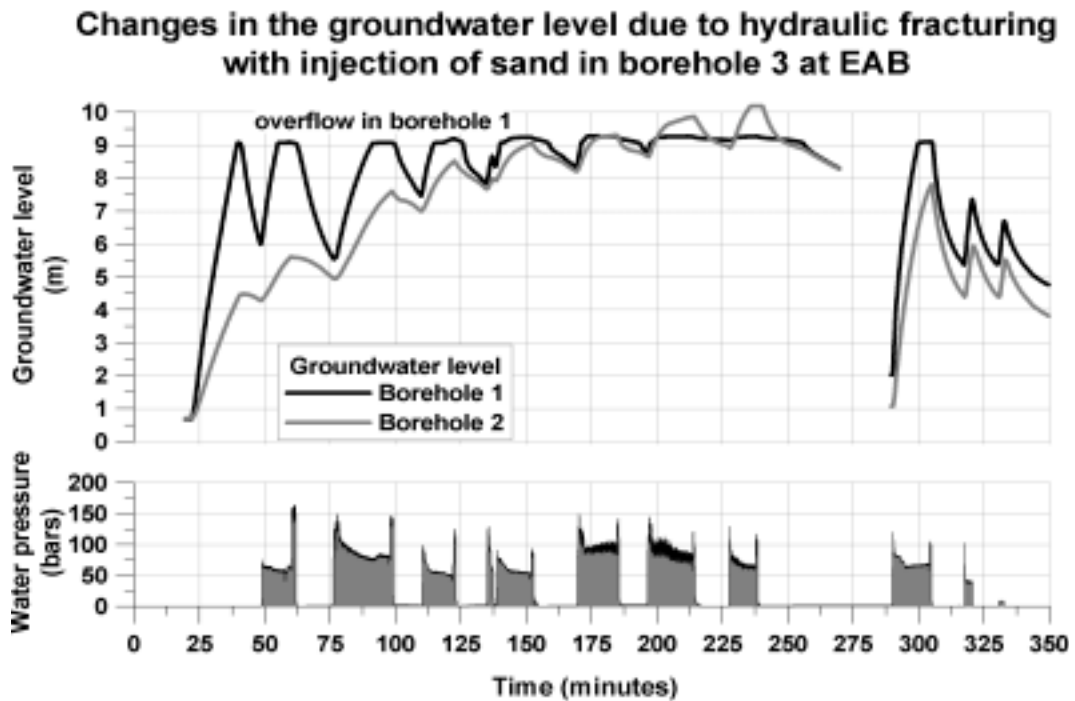


Figure 5-80: Groundwater level changes in boreholes 1 and 2 caused by the hydraulic fracturing with injection of sand in borehole 3 at EAB.

5.3.6 Terrain level changes

The maximum change in the terrain level at EAB, measured in relation to a fixed point before and after hydraulic fracturing with injection of sand in boreholes 1 to 3, was +2.0 millimetres (table 5–19). Which means a 2.0 millimetres elevation of the terrain within the area of influence for hydraulic fracturing with injection of sand. Several internal level changes of +1.0 millimetre in the area of influence were observed. These internal changes may be explained by the occurrence of a partly lifting of some parts of the terrain caused by the influencing hydraulic fracturing. Although, the small changes makes it difficult to determine whether the results reflects real changes or could be regarded as measuring errors.

Table 5–19: Levelling results in boreholes 1 and 3 at EAB.

	Fixed point	point #1	point #2	point #3
BH1, levelling before HFS (m)	3.956	2.404	0.371	2.4695
BH1, levelling after HFS (m)	3.958	2.405	0.371	2.4705
BH1, relative change (mm)	2.0	1.0	0.0	1.0
BH3, levelling before HFS (m)	3.753	2.199	-	-
BH3, levelling after HFS (m)	3.753	2.200	-	-
BH3, relative change (mm)	0.0	1.0	-	-

5.3.7 Thermal response

The effective in-situ value of the rock thermal conductivity and the thermal resistance (R_b) of borehole 1 at EAB, measured in an undisturbed mode, were calculated to be 3.8 W/m,K and 0.07 K/(W/m) (figure 5–81 and 5–82), respectively. In a laboratory study of the thermal conductivity of bedrock samples from the Bekkestua-area in Bærum, the mean value of the thermal conductivity of the bedrock in the EAB-area were measured to be 2.7 W/m,K (figures 2–28 and 2–29) (Midttømme et al., 2000). Consequently, the effective in-situ value of the rock thermal conductivity was measured to be 1.1 W/m,K higher than the thermal conductivity value of the limestone/shale rock at EAB. According to internal variations in the rock properties, the real value for the thermal conductivity of the bedrock around borehole 1 at EAB may deviate from the laboratory value. The slightly sloping terrain, the high borehole yields and the high degree of fracturing as a result of the hydraulic fracturing with injection of sand at EAB, make probable a significant natural groundwater flow in the area. In addition to the thermal conductivity of the rock, the extra 1.1 W/m,K of the effective in-situ value of the rock thermal conductivity value should be associated with the flowing groundwater through the test borehole. The value for the thermal resistance of the borehole, $R_b=0.07$ K/(W/m), is considered normal for a single U-collector.

The pumping in borehole 3, starting after 47.5 hours, disturbed the groundwater flow within the well field and caused an unexpected increase of the T_{mean} -value (figure 5–82). A higher thermal response represented by an increase of T_{mean} , indicated that less energy was absorbed in the bedrock and the effective in-situ value of the rock thermal conductivity was reduced. A possible explanation of the increased thermal response in borehole 1 may be that the pumping in borehole 3 reduced the natural groundwater flow

in borehole 1. Since borehole 1 is located 16 metres east-northeast of borehole 3 (figure 3–6), this approach assumes a groundwater flow in the west-southwest - east-northeast direction. An alternative explanation might be that the pumping in borehole 3 draws on water from the large water bearing fractures at 25-35 metres depth, and the consequence of the loss of water in this part of the borehole might be that warmer water from the deeper part of borehole 1 flows upwards along the collector. The presence of warmer water in larger parts of borehole 1 will increase T_{mean} . The reduction in the effective in-situ value of the rock thermal conductivity caused by the pumping of borehole 3, and the following disturbance of the groundwater flow within the well field, can be quantified by performing a new thermal response test. Similar to the Bryn-case (paragraph 5.2.12), borehole 1 must have recovered to its natural condition and the pumping should be started before or simultaneous with the start-up of the test.

Under ideal conditions, the thermal response test should have lasted a minimum of 65 hours instead of 47.5 before the pump start-up (Gehlin, 2002).

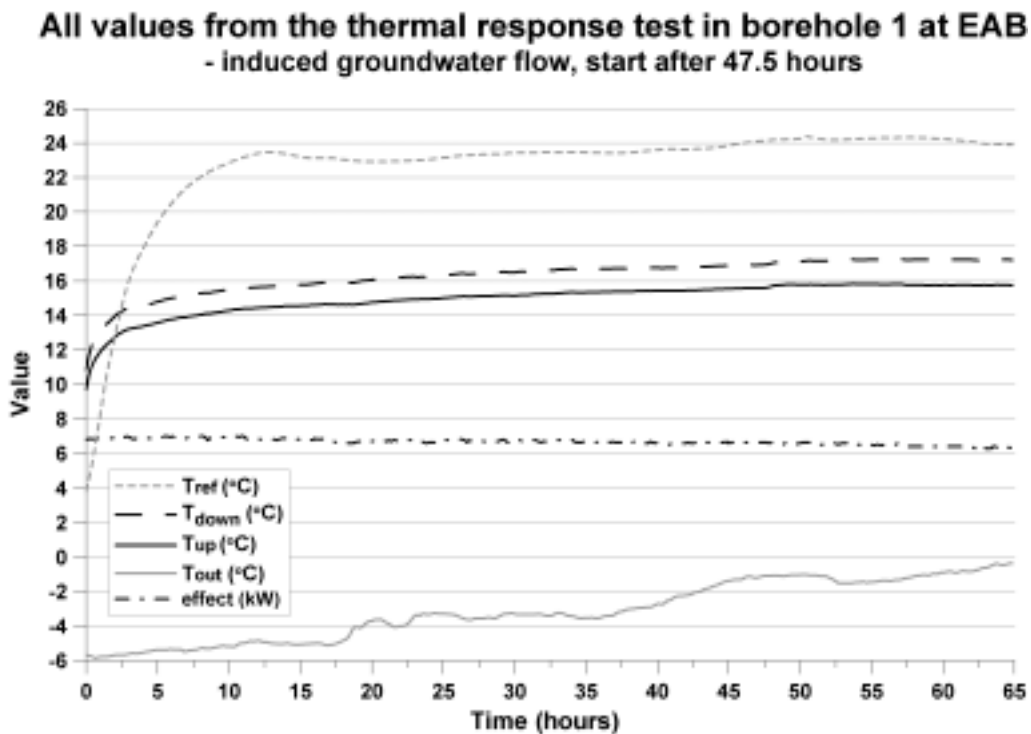


Figure 5–81: Results from the thermal response test in borehole 1 at EAB.

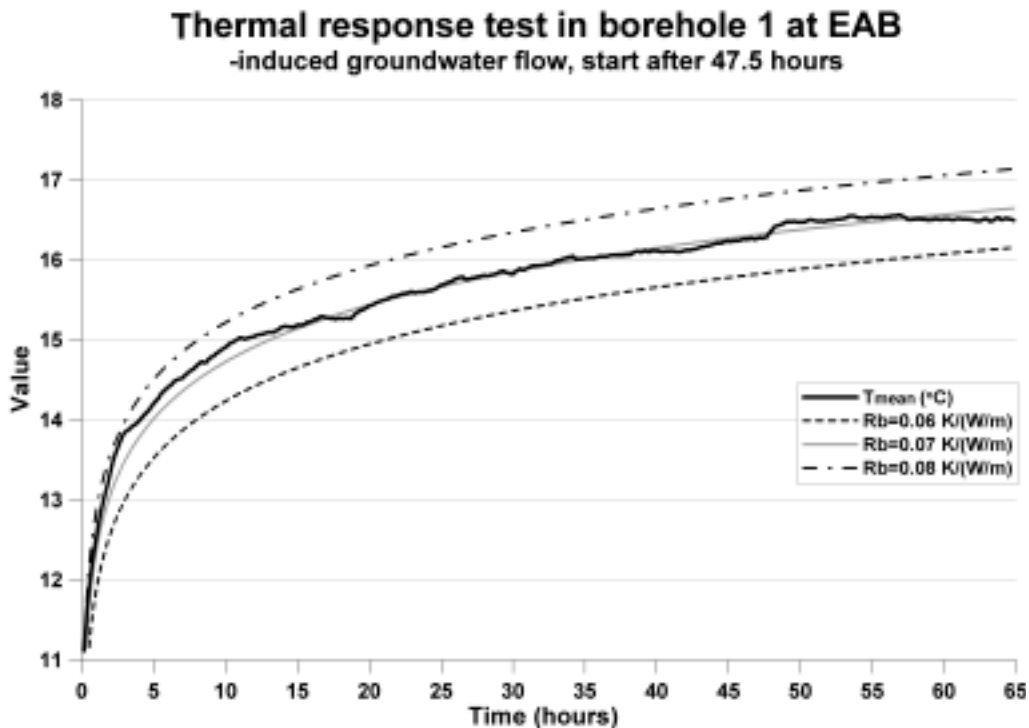


Figure 5–82: Matching the plot of the experimental mean fluid temperature (T_{mean}) with curves for different thermal resistances.

5.3.8 Effect extraction from the pilot plant

Results from the 17-day-long test run of the pilot plant at EAB are shown in figure 5–83. Some temperature- and flow results from three days of circulation of water in the plant ahead of the start-up of the thermal response test equipment are included in the diagram. The circulation rate (pumping- and infiltration rate), from now on referred to as flow rate, was about $15.4 \text{ m}^3/\text{hour}$ in the beginning of the test run, but was slightly reduced to $15 \text{ m}^3/\text{hour}$ due to the power demand of the thermal response test-equipment which received its supply from the same electrical system as the pumps in boreholes 2 and 3 (figure 5–83). The flow rate had a slightly decreasing course, but stabilized at approximately $14.4 \text{ m}^3/\text{hours}$ by the end of the test run (figure 5–84).

Even though the temperature differential between the in- and outflowing water from the heat exchanger (T_{HEX_in} and T_{HEX_out}) remained relatively constant through the test, variations were recognized in the curve for the effect extraction from the water (Effect). Based on equation 6.3, the effect extraction from water was calculated based on the flow rate and the temperature differentials. The measured effect extraction from water did not reach the constant power supply of 10 kW from the thermal response test unit. Possible reasons why 1.5-3 kW were lost in the system are:

- Temperature losses in the heat transfers, i.e. the heat transfer from the collector fluid in the thermal response equipment system to the heat exchanger, within the heat exchanger, and from the outflowing water.
- Accuracy of the temperature measurements of the in- and outflowing groundwater in the heat exchanger. Sources of error might be the accuracy of the temperature

sensor itself, and the influence of the ambient temperature. Since a thick layer of isolating snow covered the manhole through the test period, the influence of the outdoor-air temperature on the ambient temperature in the manhole were considered as minimal. On the other hand, the small temperature differentials measured in the test were sensitive to any sources of error.

In the circulation- test of the pilot plant at EAB, the pump in borehole 2 stopped functioning and, consequently, a drop in the flow rate occurred around the 12th of January (figure 5–84). It is not known why the pump stopped.

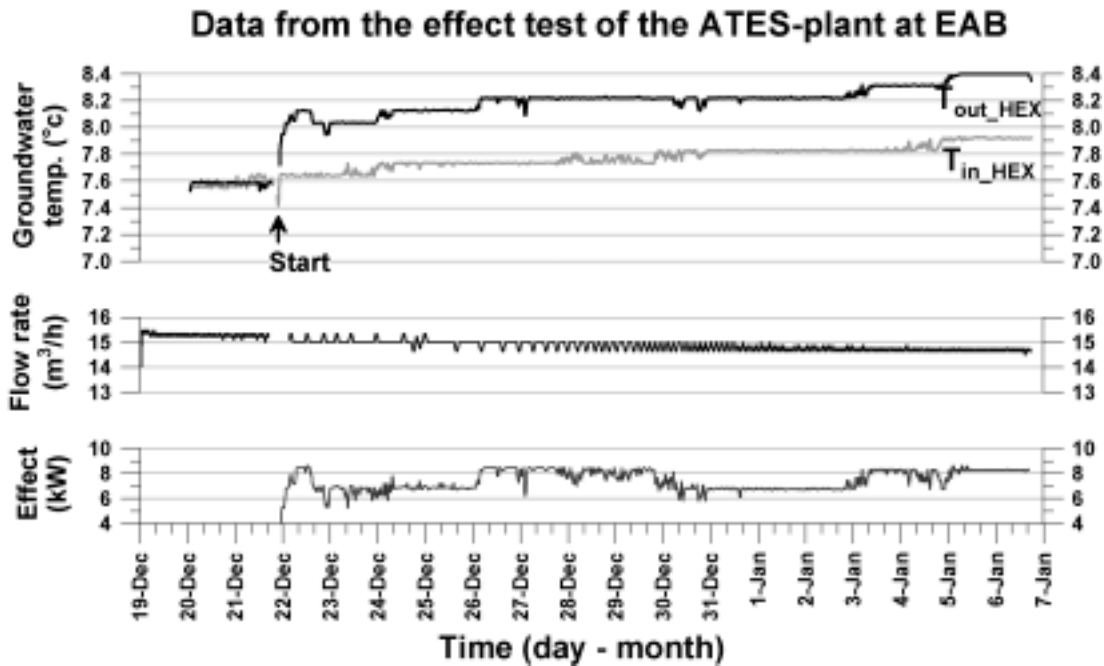


Figure 5–83: Data from the first part of the test run at EAB.

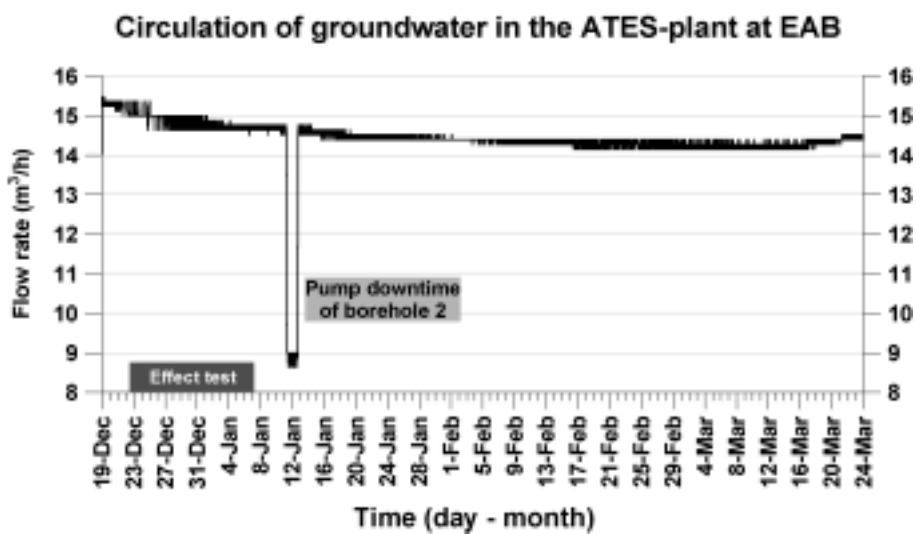


Figure 5–84: The flow rate stabilized around 14 m³/hour during the three months test run of the pilot plant at EAB.

5.3.9 Changes in the borehole yield caused by hydraulic fracturing with injection of sand

Test pumping similar to that performed at Bryn, to document the effect of hydraulic fracturing with injection of sand, was not carried out at EAB due to the initially high-yielding boreholes (paragraph 4.4.1). Even though the direct documentation is missing, the hydraulic fracturing with injection of sand in several sections in each of the boreholes at EAB is likely to have caused an overall increase in the borehole yields. Arguments to support this conclusion include:

- A significant increase in the borehole yields was achieved at Bryn as a consequence of hydraulic fracturing with water-only and hydraulic fracturing with injection of sand (figure 5–26). The boreholes at Bryn were initially low-yielding (<560 litres/hour), unlike those at EAB.
- Compared with Bryn, the degree of fracturing achieved by hydraulic fracturing was higher at EAB. At Bryn 70% of the pressure-time curves from the hydraulic fracturing with water were interpreted as reopening- or initiation of fractures (paragraph 5.2.9). The corresponding number for EAB was 97% (paragraph 5.3.5). Due to the lower pressure level present at EAB (figure 5–97), 94.6% of the reopened- or initiated fractures were interpreted as large, while the corresponding number for Bryn was 35% (figure 5–46).
- After 97 days of continuous pumping from boreholes 2 and 3, and infiltration in borehole 1, the circulation (pumping and infiltration) rate stabilized somewhat higher than 14 m³/hours after having initial values around 15 m³/hours (figure 5–84). A short downtime of the pump in borehole 2 reduced the circulation rate to approximately 9 m³/hour which would be around the maximum rate for the pump in borehole 3 under the actual conditions (figure 2–21). The initial yield for borehole 3 was 5200 litres/hour.

Due to the initially high-yielding boreholes at EAB, the hydraulic fracturing with injection of sand was unlikely to have caused such a relatively large improvement as achieved at Bryn. However, compared with Bryn, the successful stimulation with hydraulic fracturing with injection of sand, in terms of a higher degree of fracturing and stimulation of more sections, should result in an overall improvement of the borehole yields at EAB, maybe even larger than Bryn in terms of quantity.

5.3.10 Recommended use of the boreholes at EAB

The satisfying results of the three months long test run of the pilot plant at EAB, where the circulation rate stabilized around 14 m³/hour, confirmed that the plant can be put into operation according to the original plans (paragraph 3.3). Depending on the average temperature differential through the operation period, the FEFLOW modelled values for energy extraction for heating purposes-only were 92, 102 and 110 MWh (figure 5–95) per year. In general, the use of the boreholes for both heating- and cooling purposes will increase the total energy extraction and the profitability of the plant. The actual user of the energy at EAB is an office building with heating- and cooling demands. The further design of the plant will be determined by the respective authorities in Bærum municipality.

5.4 Modelled energy potential

5.4.1 Comparison of FEFLOW and HFM at Bryn

The following results are mainly based on Spangelo (2002).

Figure 5–85 to 5–87 summarizes the HFM-modelling results of the ground source heat pump system based on groundwater at Bryn. After seven months of operation, the bedrock temperature in the central borehole and the satellite boreholes are affected by the plant in the interval from 20-100 metres depth, i.e. 12 and 16 metres away from the shallowest and deepest fracture plane, respectively (figure 5–85). The cooling is largest around the fracture planes at 32, 40, 60, 72 and 84 metres depth. The HFM-modelled bedrock temperatures after seven months of operation, beyond reach for the fracture planes at levels with major cooling at 38 and 70 metres depth respectively, show that the effect extraction in the ground source heat pump system based on circulating groundwater influences the bedrock temperature up to 30 metres away from the central borehole (figure 5–86). The temperature differentials between the two curves, at 38 and 70 metres, remain even due to the thermal gradient in the vertical direction. The temperature of water produced from the ground source heat pump system during seven months of operation (figure 5–87), shows that the modelling cases with equal flow distribution (case #4 and 5, table 4–4) had higher temperature than the corresponding modelling cases with an unequal flow distribution (cases #1 and 2). The temperature differentials are reduced with time. Case #3 had lower flow rate than the other cases, and the temperature of the produced water got higher than the rest. A comparison of the temperatures of water produced from the ground source heat pump system after seven months of operation, modelled in FEFLOW and HFM, is presented in figure 5–88. The temperatures are quite similar for the five modelling cases. Except for case #3, the temperatures calculated in HFM are a little higher than the corresponding values from FEFLOW. The two softwares show different results in the modelling of unequal- and equal flow distributions, cases #1 and 4, 2 and 5, respectively (table 4–4). In FEFLOW the highest temperature was achieved for the modelling cases with equal flow distribution, while the opposite occurred for the HFM-modellings. Case 3 had a pumping rate of 5000 litres/hour, while the remaining cases operated with a pumping rate of 20000 litres/hour (table 4–4). In FEFLOW, the flow rate within a fracture is calculated based on the fracture aperture and the given pump rate. A reduced pumping rate and equal fracture apertures should lead to a reduced flow and a higher retention time for the water within a fracture. Further, the higher retention time should cause a larger heat exchange between the water and the bedrock and thus a higher temperature of the outflowing water. The opposite behaviour in case 3 indicates that there is probably no correlation between the flow- and pumping rate in HFM.

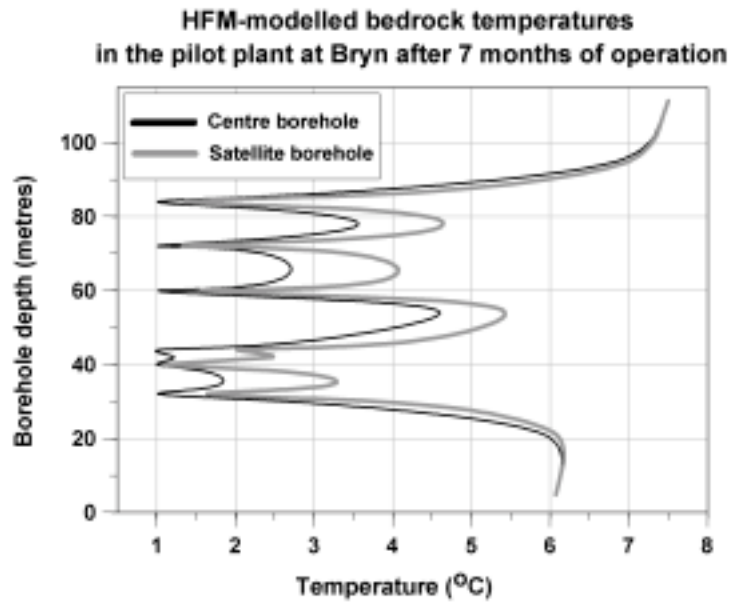


Figure 5–85: HFM-modelled bedrock temperatures in the central borehole and the satellite boreholes in the pilot plant at Bryn after 7 months of operation (modified after Spangelo, 2002).

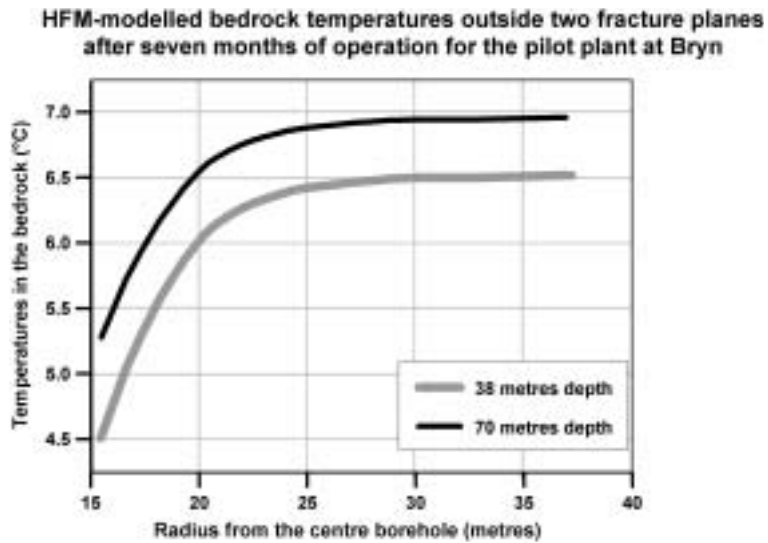


Figure 5–86: HFM-modelled bedrock temperatures outside two fracture planes at 38 and 70 metres depth respectively, after seven months of operation for the pilot plant at Bryn (modified after Spangelo, 2002).

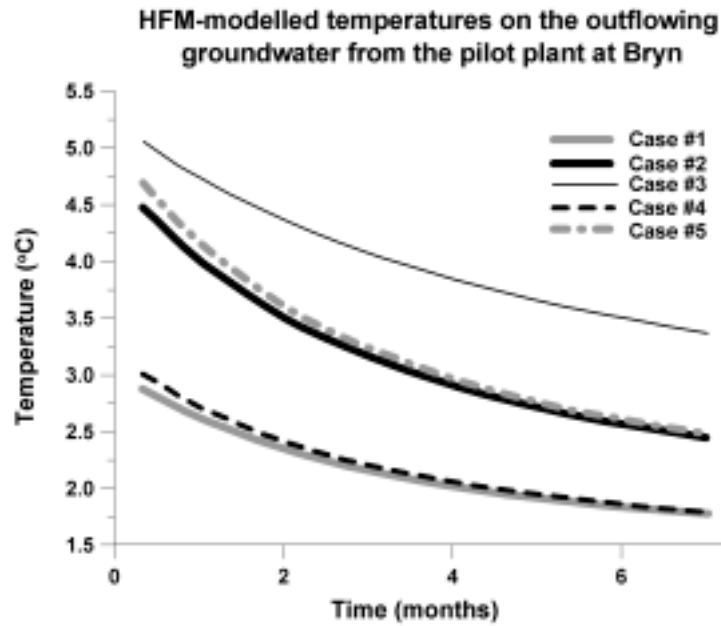


Figure 5–87: The temperature of water produced from the pilot plant at Bryn during seven months of operation. Modelled by HFM (modified after Spangelo, 2002).

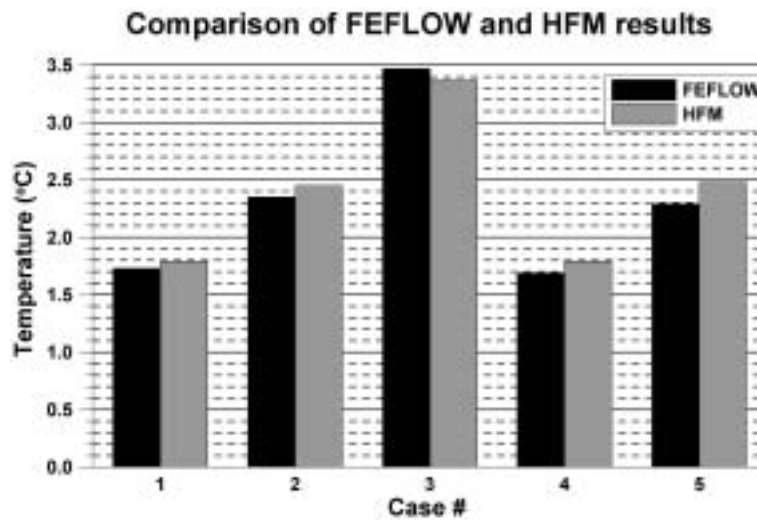


Figure 5–88: A comparison of the temperatures of water produced from the pilot plant at Bryn after seven months of operation, modelled in FEFLOW and HFM (modified after Spangelo, 2002).

5.4.2 Modelled energy potentials at Bryn and EAB

The results from the Bryn-modelling, using FEFLOW, are based on Spangelo (2003). Pumped groundwater from the production boreholes at Bryn (boreholes 1, 2, 4 and 5) had an initial temperature of approximately 7°C for all the five modelling cases having different flow rates (bryn1-5, table 4–5) (figure 5–89). A rapid temperature decrease is observed in the beginning of the operation period, and the temperature decrease is greatest for the modelling cases with highest flow rate. After two months of operation, the temperature curves hold a linear course for all the modelling cases, except the one with

varying flow rate (figure 4–27). After seven months of operation the temperatures of produced groundwater are 4.7, 3.4, 2.4, 1.9 and 3.5°C for bryn1 to 5, respectively. The modelled effect from the pilot plant at Bryn varies for the different modelling cases with different flow rates (figure 5–90). The highest effects, but also the steepest effect decreases in the beginning of the operation period, are present for the modelling cases with highest flow rate. The modelling cases with a flow rate of 3.5 and 4.3-7 m³/hour obtain the most constant effect level of 30-15 kW through the operation period. All modelling cases, except bryn1 with a flow rate of 3.5 m³/hour, seem to stabilize at approximately 20 kW after seven months of operation. The energy extractions from the pilot plant after ended operation period are 94, 135, 169, 188 and 126 MWh for the modelling cases bryn1-5, respectively (figure 5–91).

The FEFLOW-modelled effect extraction of the ground source heat pump system at Bryn increased with increasing flow rate because larger volumes of cold water were heat exchanged with the bedrock. This generates a larger temperature differential between the circulating water and the bedrock, which causes an increased heat transfer and larger effects. After seven months of operation, the temperature on the infiltrated water in borehole 3 at Bryn is less in the modelling cases that have a high flow rate compared with the cases with a lower flow rate. The high flow rate generated a faster cooling of the bedrock and the effect value was reduced at a corresponding rate.

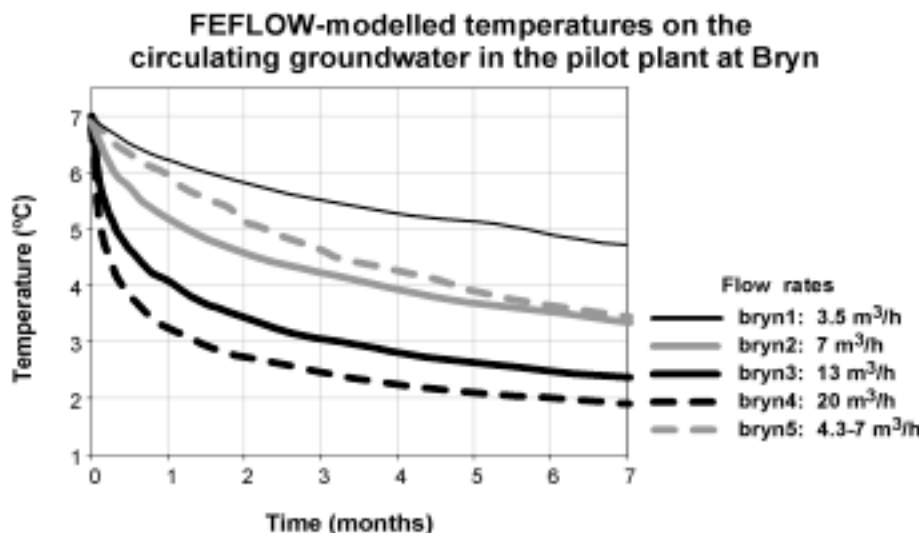


Figure 5–89: Modelled temperatures for produced water with different flow rates during an operation period of seven months in the pilot plant at Bryn (modified from Spangelo, 2003).

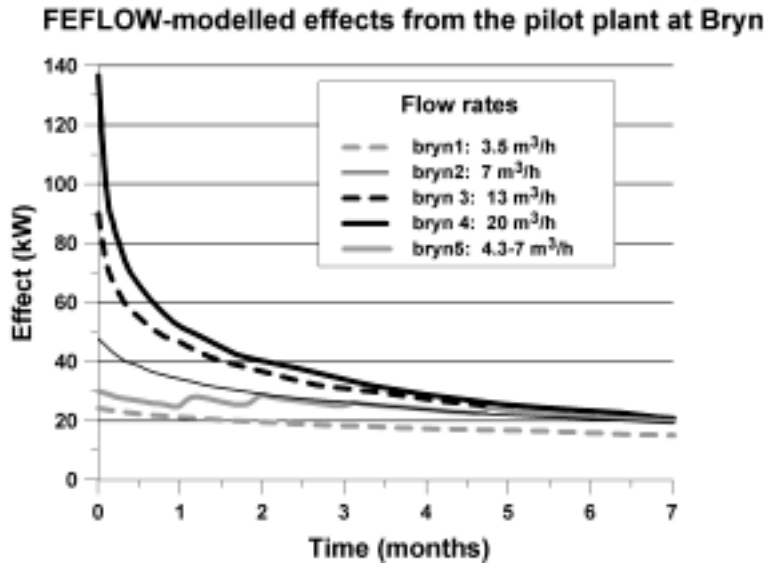


Figure 5–90: Effects available from the pilot plant at Bryn as a function of time and different flow rates (modified after Spangelo, 2003).

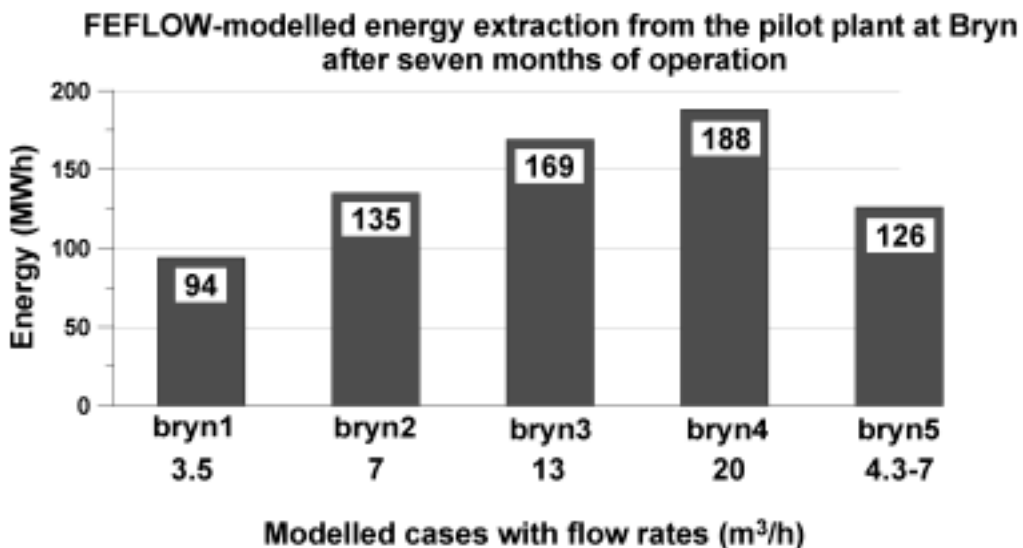


Figure 5–91: A summary of the energy extraction from the pilot plant at Bryn after seven months of operation with five different flow rates (modified after Spangelo, 2003).

Pumped groundwater from the production boreholes at EAB (boreholes 2 and 3) had an initial temperature of almost 7°C for all the three modelling cases having different flow rates (eab1 to 3, table 4–6). Similar to the Bryn-modelling, a rapid temperature decrease is observed in the beginning of the operation period, and the temperature decrease is greatest for the modelling cases with highest flow rate. After two months of operation, the temperature curves slowly decrease towards the minimum temperature at the end of the operation period (figure 5–93). After seven months of operation the temperatures of produced groundwater are 2.1, 1.8 and 1.6°C for eab1 to 3, respectively. The temperature decrease is concentrated within the fracture planes (figure 5–92). Modelled effect from the ground source heat pump system at EAB varies for the different modelling cases with

different flow rates (figure 5–94). The highest effects, but also the steepest effect decreases in the beginning of the operation period, are present for the modelling cases with highest flow rate. All modelling cases seem to stabilize at approximately 14 kW at the end of the operation period. The energy contributions from the pilot plant after ended operation period are 92, 102 and 110 MWh for the modelling cases eab1 to 3, respectively (figure 5–95).

Individually, the results from the FEFLOW-modelling of the pilot plant at EAB showed the same trends as the corresponding results from Bryn. In addition, by comparing the results from Bryn and EAB, the modelling of the Bryn-cases appear to result in higher energy values compared with the EAB-cases. A closer look at cases bryn4 and eab3, both having a flow rate of 20 m³/h, reveals that the energy extraction from the ground source heat pump system at Bryn and EAB were 188 and 110 MWh, respectively. This means that the energy extraction in eab3 is 59% of the energy extraction in bryn4. Tables 4–3 and 4–6 show that the total area of fracture planes at Bryn and EAB were approximately 4776 and 3475 m², respectively, thus the total area of fracture planes at EAB is 73% of the total area of fracture planes at Bryn. The lesser share of extracted energy in eab3 is probably related to: 1) The lesser area of fracture planes at EAB, and 2) the lower thermal conductivity of the bedrock. From figure 5–92 it can be seen that the temperature decrease in the bedrock is concentrated within the fracture plane and not much around. These results indicate that the two major factors for ground source heat pump system based on circulating groundwater in crystalline bedrock, include the total heat exchanger area and the ability of the bedrock to conduct energy onto the fracture surface, i.e. the thermal conductivity of the bedrock.

Some uncertainties are associated with the long term extrapolation of the FEFLOW-results for the pilot plants at Bryn and EAB, modelled only for a seven months period.

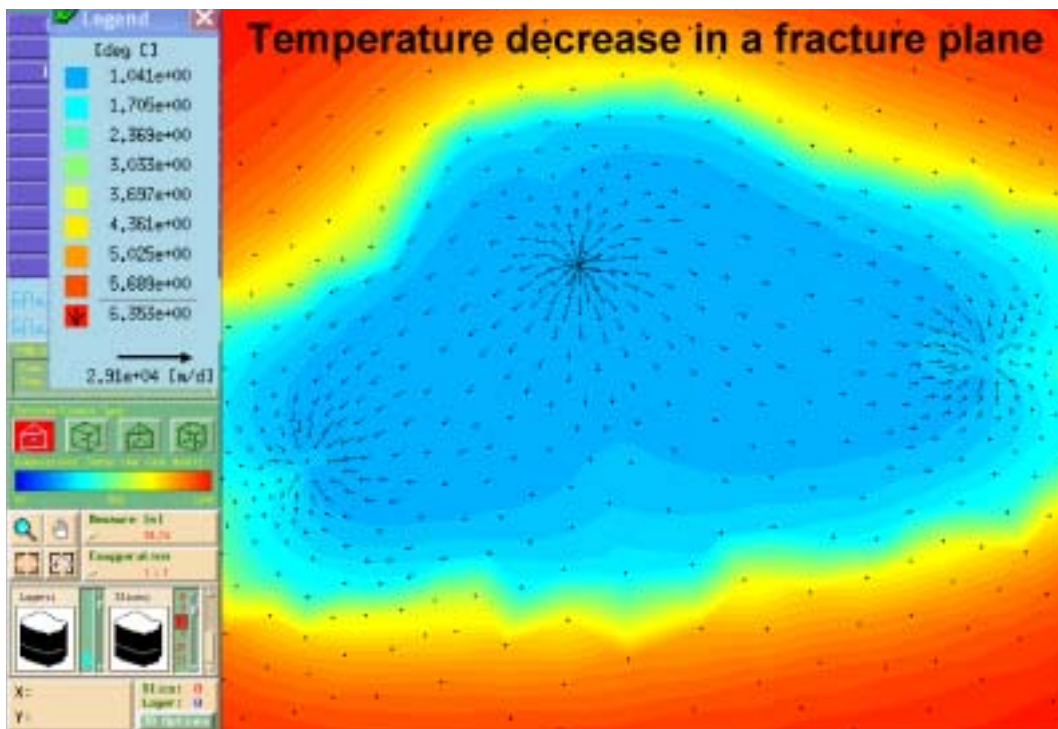


Figure 5–92: The temperature decrease is concentrated within the fracture plane at EAB.

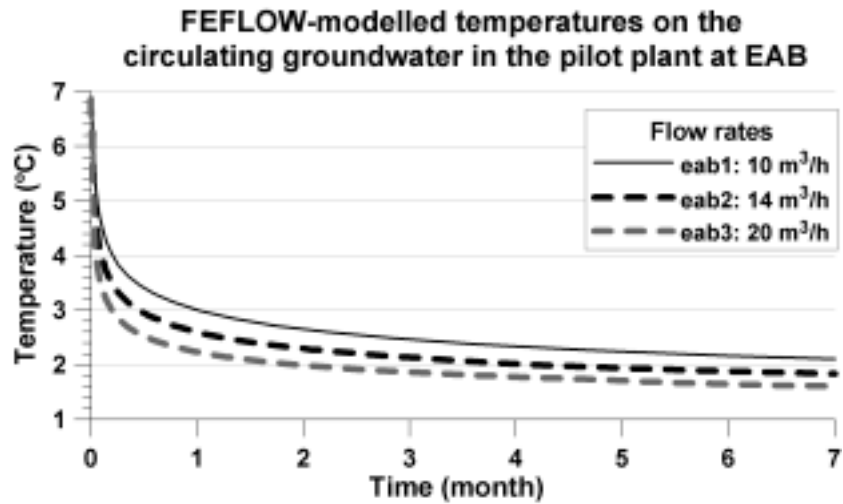


Figure 5–93: Modelled temperatures for produced water with different flow rates during an operation period of seven months for the pilot plant at EAB.

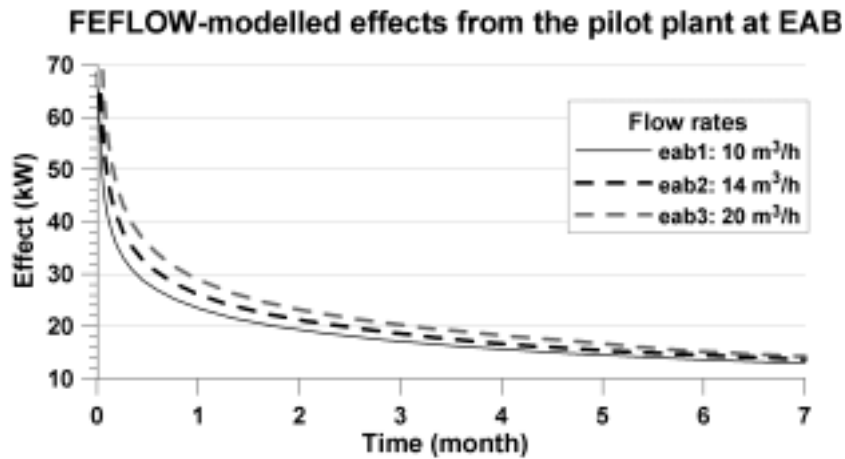


Figure 5–94: Effects available from the pilot plant at EAB as a function of time and different flow rates.

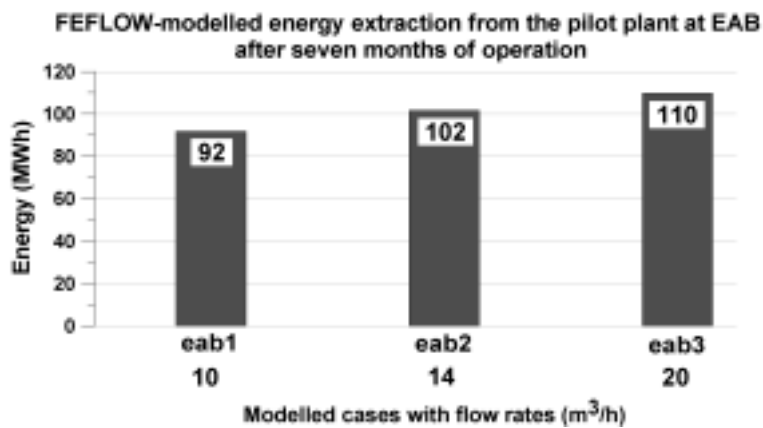


Figure 5–95: A summary of the energy contribution from the pilot plant at EAB after seven months of operation with three different flow rates.

5.5 Comparison of the pressure levels from hydraulic fracturing

70% (44 out of 63) of the pressure-time curves from the hydraulic fracturing with water-only performed at Bryn was interpreted as an initiation- or reopening of fractures. The corresponding number for EAB was 97% (36 out of 37).

The maximum pressure before fracturing, and the stable pressure levels after fracturing with hydraulic fracturing with water-only at Bryn and EAB are presented in a box plot in figure 5–97. The maximum-, minimum-, median-, upper- and lower quartile value of the given pressure levels are illustrated in the plots. In this context, the maximum pressure level is defined as the highest pressure level immediately before fracturing (figure 5–96). The term stable pressure level represents the relatively stable pressure appearing after fracturing, measured just before ending the hydraulic fracturing with water-only in the respective borehole section or -column. The stable pressure level is often identical to the minimum pressure, except for those cases where a pressure buildup in the fracture system occurs. The median values for the maximum pressure before fracturing were 144 and 107 bars at Bryn and EAB respectively, while the corresponding values for the stable pressure level after fracturing were 73 and 53.5 bars. The maximum pressure before fracturing could also be considered as the fracture initiation pressure. According to Macaulay (1987), Baski (1987) and Waltz (1988) in Smith (1989), where the water pressure required to clean, open or initiate fractures is reported to be between 500 to 2000 psi (34.5 to 138 bars) in most applications while 3000 psi (207 bars) is required for very hard rock and deeper wells, the fracture initiation pressure at Bryn could be considered as above average level representing a hard bedrock. The corresponding fracture initiation pressure levels at EAB is within the average range. The corresponding pressure levels reported by Gale and MacLeod (1995) were in the range of 2-10 MPa (20-100 bars) and significantly lower than the values from Bryn. However, the Swedish studies in paragraph 2.1.2, Sundquist and Wallroth (1990), Nordell et al. (1984) and Eliason et al. (1988), reported of pressure levels at 10.5 and 22 MPa (105 and 220 bars), 60 to 120 bars, and 15 and 20 MPa (150 and 200 bars), respectively. These values correspond better to the pressure levels experienced at Bryn and EAB and may be due to approximately equal stress- and geological conditions. Herrick (2000) referred the borehole pressure, experienced among the water well contractors in the US, to range from 500 to 5000 psi (34.5 to 345 bars) depending on formation and equipment.

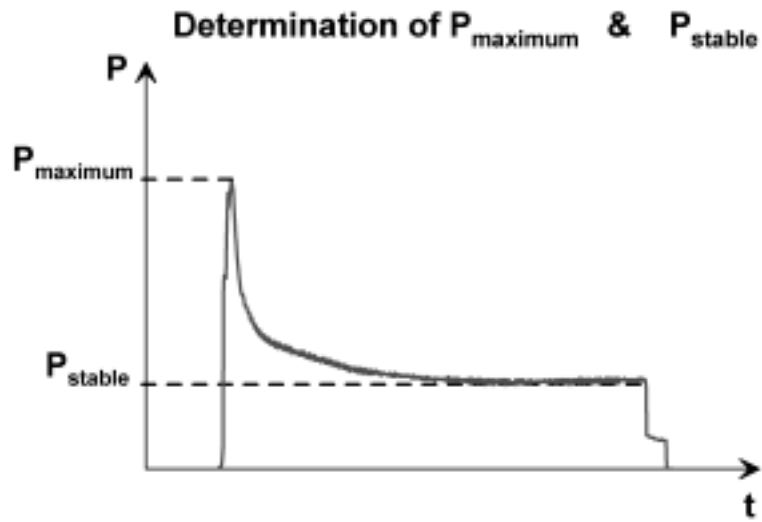


Figure 5–96: Determination of P_{maximum} and P_{stable} from a pressure-time curve from hydraulic fracturing with water-only.

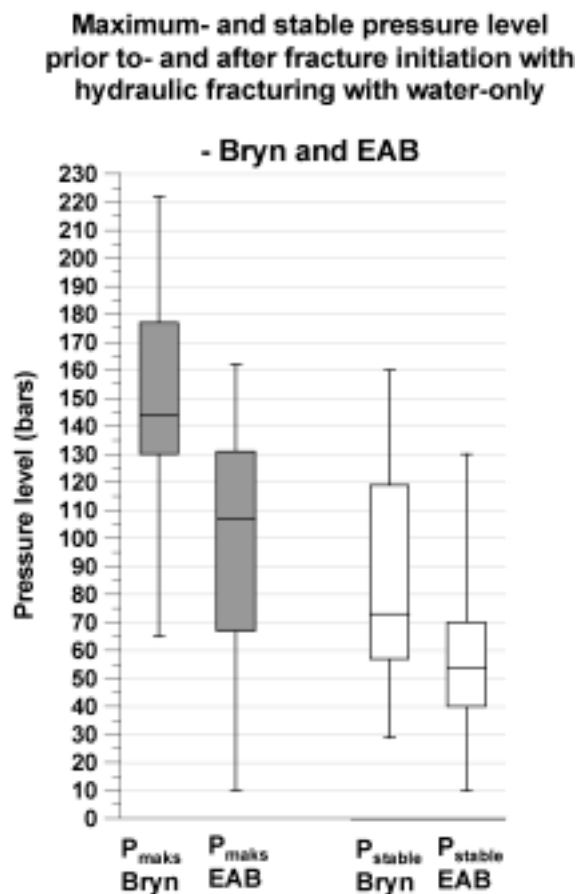


Figure 5–97: A box plot presentation of the maximum pressure before fracturing and the stable pressure level after fracturing with hydraulic fracturing with water-only.

5.6 Method development

The following paragraph summarizes the experiences, and gives an evaluation of the equipment and methods employed in this study.

5.6.1 *Double packer - FrakPak - AIP 410-550*

The equipment for hydraulic fracturing has worked well through the whole study except for two or possibly three occasions where the packer element failed. The first problem with the equipment, occurred during the first testing of the methodology for hydraulic fracturing with injection of sand in a test borehole at Lade (paragraph 5.1.4). Since the equipment got stuck in the borehole, it is not known which part of the equipment that failed. A sudden and complete drop in the packer pressure indicated that either one of the packer elements, couplings or the pressure hose failed. If one of the packer elements was blown, a study of the destroyed packer element would have been useful for further improvement of the FrakPak - AIP 410-550. The injection of the highly viscous sand mixture, also having a relatively high concentration of sand, may have increased the wearing of the equipment. At this point, the packer elements on the double packer were pressurized simultaneously through the same supply hose. The equipment had been pressurized approximately ten times before the failure. New and improved equipment for hydraulic fracturing was made for the field experiments at Bryn. The improvement implied a separate pressurizing of the packer elements. Separate pressurizing render possible columnar hydraulic fracturing, and the opportunity to flush loose fragments away from the borehole section if the equipment is suspected to be stuck. The lower packer element on the double packer was blown when performing hydraulic fracturing in borehole 2 at Bryn. The rupture (figure 5–98) appeared on the upper part of the packer, in the transition between the rubber coated fabric and the edge of steel. The packer element had been pressurized 41 times before the failure. A blown packer element can easily be replaced with a new one within two hours. The destroyed packer element is loosened and removed. The threads are greased and the new packer element is assembled. The damaged packer element should be returned to BTU which will replace the destroyed rubber coated fabric. Since the steel is reused, the expenses related to the “new” packer element is limited to the rubber itself and the working hours required to replace it. A small rip at the upper edge in the transition between steel and rubber on the lower packer, similar to the case with the destroyed packer element at Bryn, was discovered after the hydraulic fracturing of borehole 2 at EAB (figure 5–98). The packer element had been pressurized 56 times before the rip detection.

At the end of the study, the upper packer element has been pressurized approximately 124 times without observing technical problems.



Figur 5–98: Blown lower packer element from the hydraulic fracturing with water-only in borehole 2 at Bryn (left), and a rip on the packer element from the hydraulic fracturing with injection of sand in borehole 2 at EAB (right).

5.6.2 Hydraulic fracturing with water-only

The first practical experience with hydraulic fracturing in this study was during the testing of the newly developed double packer at Lade. The remaining equipment employed in the testing, was suited for other applications but could be used after minor adjustments (paragraph 4.2.2). Hydraulic fracturing of six sections in borehole 1 at Lade, included a repair of the blown pressure hose, was carried out during an extended working day. The desired values for the maximum water pressures were not reached due to the lack of appropriate high-pressure equipment.

The downhole equipment for hydraulic fracturing gets easily stuck in the borehole during a hydraulic fracturing operation, and it is very important to take necessary precautions to avoid needless mistakes and expensive losses. The loss of equipment in borehole 2 at Lade after the experiment with hydraulic fracturing with injection of sand (paragraph 5.1.4) demonstrated the importance of having experienced personnel and appropriate equipment to avoid getting stuck in the borehole. At Lade, the downhole equipment probably got stuck because the pressure supply hoses for the packer elements was improperly tied against the water tubes. The improper fastening of the pressure supply hoses, made it difficult to provide a sufficient removal of the loose hoses when the equipment was moved upwards in the borehole. After a few metres lifting, the loose ends of the pressure supply hoses probably fell down between the packer elements and the borehole wall, bundled up and the equipment got completely stuck.

G. Meyer Borebrønnservice, a company with expertise on hydraulic fracturing, was hired as a contractor to do the hydraulic fracturing with water-only and the hydraulic fracturing with injection of sand at Bryn and EAB. Except for the double packer (paragraph 2.2.1) and the high-pressure tank (paragraph 2.2.2), the contractor provided necessary accessories such as a tank lorry with high-pressure equipment, water tubes and a winch. Compared to testing with hydraulic fracturing at Lade, the equipment of the contractor and its arrangement appeared to be more streamlined, robust and better adjusted for the purpose.

5.6.3 Hydraulic fracturing with injection of sand

An injection pump was employed for the injection of sand in borehole 2 at Lade in addition to the ordinary equipment for hydraulic fracturing (paragraph 4.2.3). The injection pump is driven by a diesel aggregate and is commonly used for the sealing of rock cavities. The pumping rate of the injection pump was too low under the given circumstances, and the pump seemed not to be suitable for the injection of the thick mixture of sand, thickener, water and enzyme. The low pumping rate made the injection of sand become a time-consuming process with increasing risk for settling of sand between the packer elements in the borehole section.

The high-pressure tank (paragraph 2.2.2), for temporarily storage of injection fluid (sand, thickener, water and enzyme), was developed before the hydraulic fracturing with injection of sand at Bryn. The new procedure for injection of sand (paragraph 2.1.7) implies flushing of water at a high rate through the high-pressure tank. The experiences from Bryn and EAB demonstrated that the new injection procedure was simple, effective and reliable.

Different methods for mixing- and filling of injection fluid into the high-pressure tank were used at Bryn and EAB. A combined mixing- and pumping unit was employed at Bryn, while manually mixing of the injection fluid, using a rod mixer assembled to a drill, followed by a manually filling of injection fluid into the high-pressure tank, took place at EAB. Neither of the mixing- and filling procedures for injection fluid satisfies the effectiveness required for commercial utilization. Based on the experiences from Bryn and EAB, advantages and disadvantages related to the procedures for the mixing and filling of injection fluid can be summarized as follows:

- The mixing- and pump unit employed at Bryn allow for pumping of injection fluid from the storage unit into the high-pressure tank. The high viscosity of the injection fluid made the pumping slow, and some sand settled and remained in the storage unit. Lumps were easily formed during the mixing of water and thickener in the mixing device of the equipment employed at Bryn. Splashing was also a problem, especially before the hydration of the thickener (guar gum). Access to only one mixing unit slowed down, and sometimes delayed the progression of the work.
- The initial mixing of thickener and water to a thick mass, usually in several tubs at the same time, followed by dilution and adding of sand to the desired viscosity and concentration of sand, respectively, worked well at EAB. Needless and time-consuming breaks were avoided by having large volumes of ready injection fluid available at all time. Compared with Bryn, manually filling of the high-pressure tank with injection fluid turned out to be more efficient than pumping. Mixing of the injection fluid immediately before the filling into the high-pressure tank made the sand remain in suspension.

The following factors should be addressed in the further development of streamlined and automatic equipment for hydraulic fracturing with injection of sand:

- Based on the experiences from Bryn and EAB, the injection of sand seems to be most effective when using powerful pumps and high-pressure equipment. The high-pressure water-front presses the injection fluid ahead. In advance, the

borehole section is fractured by hydraulic fracturing with water-only, leading the water in a by-pass hose parallel to the high-pressure tank. The injection of sand takes place immediately after the fracturing, while the fracture is still open.

- A good mixture, without any lumps, of the thickener guar gum and water can be achieved by initial mixing of a relatively large amount of thickener and a small volume of water. Since the hydration time for the thickener is approximately 15 minutes, the mixture has to be diluted with water after some time. Several raw-mixtures of water and thickener should be ready at any time to ensure a continuous production of injection fluid.
- The desired amount and grain sizes of sand should be added to the injection fluid during the mixing and immediately before the filling of the ready injection fluid into the high-pressure tank.
- The high-pressure tank should be constructed for quick filling of injection fluid, and the closing mechanism ought to be simple and fast. A small volume of breaker enzyme has to be added before the closing of the tank.

At Bryn the hydraulic fracturing with water-only and the hydraulic fracturing with injection of sand were performed as two separate operations in order to document the effect of each of them. The hydraulic fracturing with injection of sand took place in the borehole sections apparently having the largest fractures previously opened by hydraulic fracturing with water-only. An inaccurate determination of the depth, using the lowering equipment belonging to the contractor, was probably the reason why it turned out to be a problem to recover the desired fracture levels in the boreholes. On a few occasions the desired fracture level was not found, while several attempts were necessary in other cases. However, the majority of the desired fracture levels were found without any problems. Performing hydraulic fracturing with water-only and hydraulic fracturing with injection of sand as one operation, similar to the EAB-case, will solve this problem.

At EAB, an attempt of using an air pressure mixer for the mixing of water and thickener (paragraph 2.2.4 and 4.4.2) failed due to inexperienced personnel and lack of time. The air pressure mixer worked well in the laboratory, but a few adjustments are probably necessary to avoid splashing and a slippery ground. Generated with air pressure, the hydrated mixture leaves the mixer at a high rate which caused considerable splashing. A splash protection could be arranged by assembling a hose to the outlet of the mixer, and by leading the hose into a sealed tub. Having several tubs to work as temporarily storage for the hydrated mixture of water and thickener, several raw-mixtures could be made ready for further use.

5.6.4 Experiences with the optical televiewer

The strategic location of the double packer at Bryn, around discontinuities like mineral filled fractures or rock boundaries identified by the optical televiewer (paragraph 4.3.4), was assumed to cause a higher degree of fracturing than the corresponding random selection of borehole sections at EAB (paragraph 4.4.2). No evident differences between the two methods were found from the limited amount of results from Bryn and EAB. The random selection of borehole sections was the least time-consuming of the two methods. Gale and MacLeod (1995) found the geophysical logging of the boreholes, using a TV-

camera, to be useful to provide essential guidance in selecting the intervals to be stimulated and identifying the locations for the packer seals. But, according to the experiences from Bryn and EAB, the TV-logs did not show any obvious changes in fracture apertures that were produced by hydraulic fracturing. At Bryn and EAB, only a few visible changes on the borehole wall could be spotted by comparing the optical televiewer recordings before and after the hydraulic fracturing stimulations. This was also the impression from the rock stress measurements at Bryn where the attempt to orient the initiated fractures was unsuccessful (paragraph 5.2.6). The relatively high horizontal rock stresses measured in the bedrock may have caused an instant close of the fractures after pressure release.

The optical televiewer was suited for the identification on the borehole wall of geological features like the degree of fracturing, fracture patterns, rock type, large fracture openings, mineralized fractures et cetera initially appearing on the borehole wall.

Chapter 6 Economy

An economical analysis has been performed comparing the special kind of ground source heat pump system utilizing circulating groundwater in fractured crystalline bedrock, demonstrated as pilot plants at Bryn and EAB, and conventional ground source heat pump system with single U-collectors in vertical boreholes. With focus on the drilling costs, the main goal with the analysis was to find the profitability and the economical sensitivity of the ground source heat pump system at Bryn and EAB, based on groundwater, versus conventional collector systems, when varying the different construction cost.

6.1 A simple economical analysis

The main steps in the economical analysis can be summarized as follows:

- 1) Development of two equations (paragraph 6.1.1), each describing the most important construction costs for ground source heat pump system using groundwater and collectors, respectively. The construction cost for collector systems include drilling costs-only, while the hydraulic fracturing expenses were added to the construction costs for ground source heat pump system utilizing circulating groundwater in fractured crystalline bedrock. The drilling costs consist of expenses to drilling in hard rock and soils. Casing is necessary when drilling through soils.
- 2) The economical analysis is based on calculated-, and FEFLOW-modelled energy extractions from the pilot plant at EAB. Even though the operation of the plant is unsatisfactory (paragraph 5.2.14), some theoretical calculations concerning the pilot plant at Bryn are carried out using the results from the FEFLOW-modelling. The respective energy extractions were used as an input parameter in Earth Energy Designer (EED) (Hellström and Sanner, 2000), a modelling software for borehole heat exchanger design. The EED-modelling returned the effective borehole metres and the number of boreholes required in a ground source heat pump system with collectors, which is thought of as a theoretical replacement for the corresponding groundwater-based pilot plants in terms of energy extraction and geological conditions. The term effective borehole metres means the total borehole metres filled with a conducting material. According to Norwegian practice, water was used as filling medium. Both kind of ground source heat pump systems, groundwater and collectors, were designed for heating purposes only for simplicity reasons.
- 3) The final part of the analysis dealt with the profitability calculations. The construction cost for the groundwater-based, and the collector based ground source heat pump systems, were calculated and compared with basis in the EED-modelled values for the effective borehole metres, and equations 6.1 and 6.2, respectively. The profitability of the given pilot plant at EAB, and the theoretical values for Bryn, versus the conventional collector-alternative could be revealed from these results.

6.1.1 Construction costs

Equations 6.1 and 6.2 express the main construction costs for both kinds of ground source heat pump systems, based on collectors and groundwater, respectively. A detailed summary of the borehole- and cost variables are presented in table 6–1. All the cost variables are in Norwegian kroner (NOK), and value added tax (VAT) is included. The internal relation between the drilling costs, K and L, were set to be: $L(K) = 2K+100$, and the unit value M for the hydraulic fracturing with injection of sand varied with 10000, 20000 and 30000 NOK/borehole.

$$B = yK + zL \quad [6.1]$$

$$A = yK + zL + \left(\frac{y+z}{n}\right)M \quad [6.2]$$

Table 6–1: A description of variables used in equations 6.1 and 6.2.

Borehole variables	Cost variables
y = borehole metres in hard rock [m]	B = construction costs for a ground source heat pump system using collectors in vertical boreholes [NOK]
z = borehole metres in soil (with casing) [m]	A = construction costs for a ground source heat pump system based on circulating groundwater in a fractured bedrock [NOK]
n = borehole depth [m] in ground source heat pump system using groundwater	K = drilling cost in hard rock [NOK/m]
	L = casing costs [NOK/m]
	M = unit cost for hydraulic fracturing with injection of sand in one borehole. The unit cost consists of hydraulic fracturing with injection of sand in 10 borehole sections using 13 working hours. The content of the unit cost is based on the experiences from EAB.

6.1.2 Estimation of energy extraction from groundwater

In addition to the FEFLOW-modelled energy extractions, realistic energy extractions from the pilot plant at EAB can be found with basis in the measured circulation rate of approximately 14 m³/hours (figure 5–84). The method used in the determination of the energy extraction from the circulation rate is based on a linear relationship between the potential effect extraction from water at different flow rates and temperature differentials (equation 6.3) (Andersson et al., 1982). A graphical presentation of equation 6.3 can be seen in figure 6–1.

$$Effect = C_{H_2O} \times Q \times \Delta T \quad [6.3]$$

Where:

Effect is given as kW,

C_{H_2O} is the specific heat capacity of water [kWh/m³°C],

Q is the flow rate [m³/h], and

ΔT is the temperature differential, $\Delta T = T_{in} - T_{out}$ [°C].

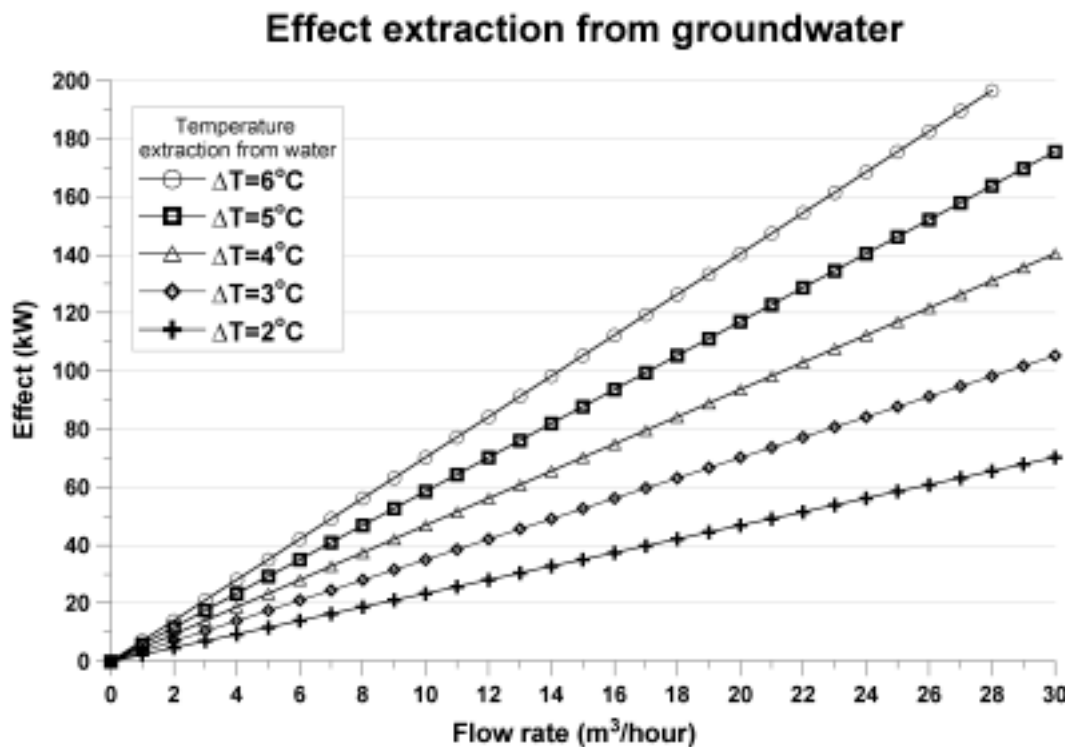


Figure 6–1: Effect extraction from water at different flow rates and temperature differentials (based on Andersson et al., 1982).

In addition to the measured circulation rate of 14 m³/hours, the estimation of the energy extraction from the circulating groundwater in the pilot plant at EAB required a value for the annual operation hours and the average temperature differential. The annual operation hours for the plant were set to 3000, which is considered to be a common value for ground source heat pump systems having an Oslo-climate (Stene, 1997), and approximate to the operation hours used in the EED-modelling. The average temperature differential through the operation period varied for the EED-modelled collector-equivalents replacing the groundwater-based pilot plant at EAB, and was in the range of 2.1 to 4°C (table 6–3). Finally, by multiplying the effect-value with the annual operation hours for the plant and by reading the actual temperature differential curve, the annual energy extraction from the pilot plant at EAB, based on the measured circulation rate, were estimated to be in the range of 105.3 to 197 MWh (figure 6–2).

The FEFLOW-modelling of the energy extraction from the groundwater-based ground source heat pump system at EAB, after an operation period of seven months, gave 92, 102 and 110 MWh for the modelling cases eab1, 2 and 3 (figure 5–95). Corresponding numbers for Bryn were 94, 135, 169, 188 and 126 MWh for cases bryn1 to 5 (figure 5–91).

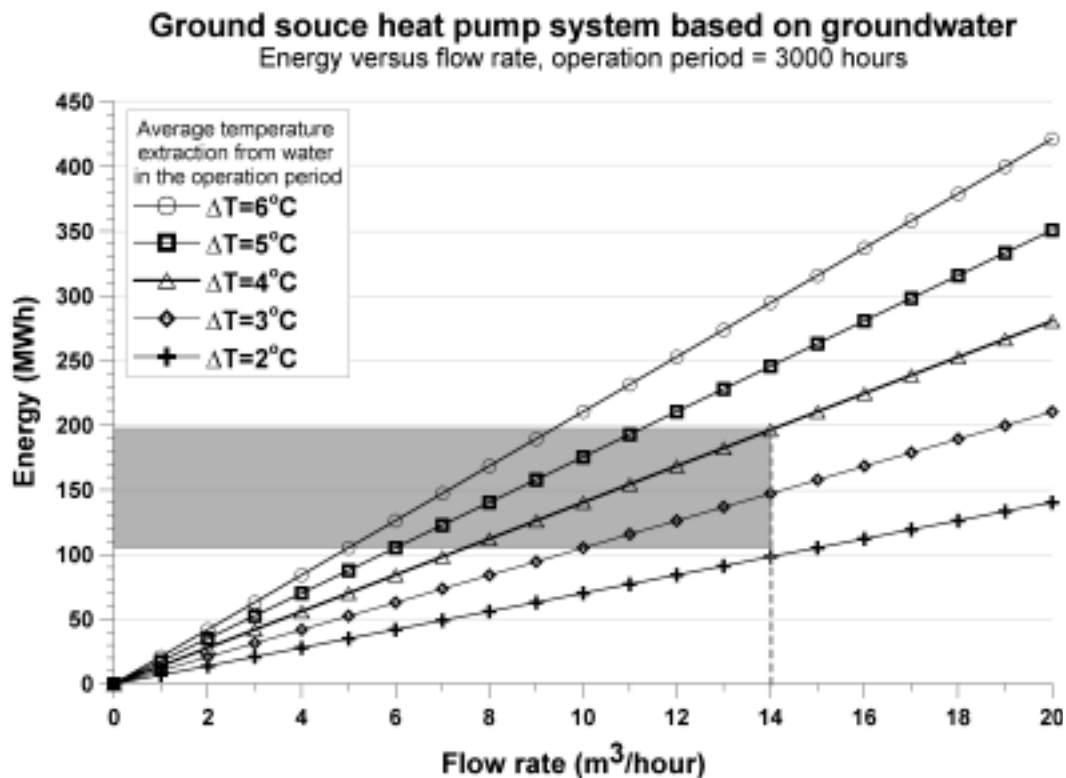


Figure 6-2: Within the grey area: Estimated annually energy extraction from the ground source heat pump system based on groundwater at EAB.

6.1.3 Calculation of effective borehole metres using EED

The EED-modelling of the collector systems, theoretically replacing the groundwater systems at EAB and Bryn, was accomplished to calculate the effective borehole metres required to meet the actual energy extraction from each modelling case. According to the seasonal performance factor of 3 for the heat pump, the values for the energy extraction from the groundwater had to be multiplied with a factor of 3/2 (tables 6-3 and 6-5). The collector systems were for simplicity reasons modelled for heating purposes-only, and a line configuration consisting of a varying number of boreholes was chosen. The boreholes had an individual spacing of 20 metres. A list of the major input parameters used in the EED-modelling is presented in table 6-2. The base load parameters in EED reflect the annual heating load and distribute it to the individual months using the given load profile (figure 6-3). Similar to the FEFLOW-modelling of the energy extraction from the circulating groundwater in the pilot plants, the operation period was set to be seven months. The determination of the effective borehole metres was based on the minimum fluid temperature after 25 years of operations, and on the fluid temperature courses. As a criterion, the minimum fluid temperature after 25 years of operation was set to be -4°C, and the fluid temperature courses should be approximate to figure 6-4 for all the modelled cases. The results from the EED-modelling of the collector-equivalents, replacing the groundwater systems at EAB and Bryn, are presented together with the borehole details used in the construction costs calculations (tables 6-3 and 6-5).

Table 6–2: Input parameters used in the EED-modelling of the collector-equivalents at EAB and Bryn.

Parameter	Value	Parameter	Value
Ground surface temp.	6 °C	U-pipe: polyethylene DN40 PN10	
Borehole spacing	20 m	U-pipe; outer diameter	0.040m
Borehole configuration	line	U-pipe; wall thickness	0.0037mm
Borehole diameter	139.7mm	U-pipe; Thermal cond.	0.42
Volumetric flow rate	0.002 m ³ /s	U-pipe; Shank spacing	0.07 m
Geothermal heat flux	0.0446 W/m ²	U-pipe; Filling thermal cond.	0.6 W/m,K
Thermal conductivity, EAB	2.7 W/m,K	Heat carrier fluid	Ethanol
Thermal conductivity, Bryn	3.3 W/m,K	Modelling period	25 years
Volumetric heat capacity, Bryn	2.1 MJ/m ³ ,K	First month of operation	September
Volumetric heat capacity, EAB	2.3 MJ/m ³ ,K	Base load, SPF	3
Contact res. outer pipe/ground	0.0	Base load	figure 6–3 (seven months)
		Peak load	0

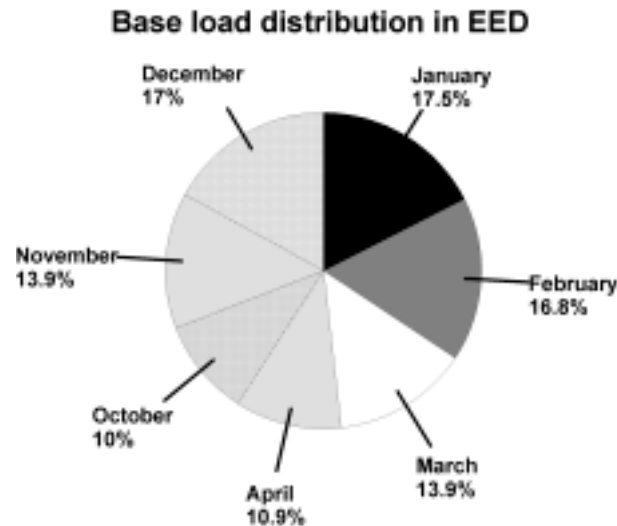


Figure 6–3: Base load distribution for the EED-modelling.

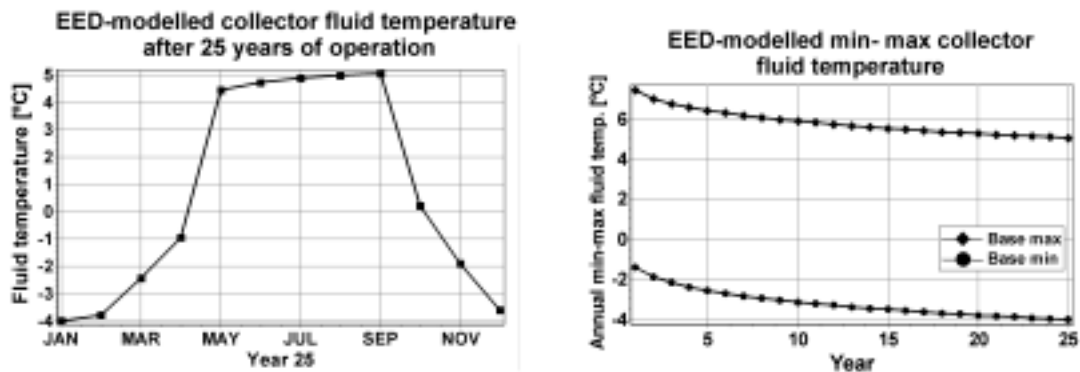


Figure 6–4: EED-modelled collector fluid temperatures.

6.1.4 Profitable pilot plant at EAB?

The profitability of the pilot plant at EAB versus a conventional ground source heat pump system with vertical collectors is the main question to be answered in this study. The EED-modelled values for the effective borehole metres, the corresponding energy extraction and all the remaining relevant variables used in the economical analysis (equation 6.1 and 6.2) are summarized in table 6–3. Using a varying number of boreholes, the borehole depths were in the range of 177 to 198 metres. The geological conditions at EAB were taken into consideration for all the modelled- and calculated cases with respect to the groundwater level and the soil cover. By using the input values in tables 6–3 and 6–4, the sensitivity of the construction costs for the pilot plant and the EED-modelled collector-equivalents replacing the groundwater system at EAB can be seen in figure 6–5. The savings by choosing a groundwater system in preference to a collector system at EAB at different construction costs can be seen in figure 6–6. Under the actual conditions (table 6–4), a reduction in the construction costs, i.e. the drilling costs for a collector system, of more than 50% were achieved for the pilot plant at EAB when the energy extraction from water is higher than 105 MWh.

Table 6–3: Borehole details for the modelled collector-equivalents at EAB.

Parametres	Modelled collector-equivalents replacing the ground source heat pump system based on circulating groundwater at EAB					
	circ197	circ147	circ105	feflow110	feflow102	feflow92
Energy water (MWh)	197	147	105	110	102	92
Energy heat pump (MWh)	295	221	158	165	153	138
Effective borehole metres (m)	2239	1675	1186	1236	1132	1031
Number of boreholes	13	10	7	7	6	6
Effective borehole depth (m)	172	168	169	177	189	172
Groundwater level (m)	9	9	9	9	9	9
Actual borehole depth (m)	181	177	178	186	198	181
Total borehole metres (y+z)	2356	1765	1249	1299	1186	1085
Total metres of drilling in soil, z (m)	87	69	48	48	42	42
Total metres of drilling in hard rock, y (m)	2269	1696	1201	1251	1144	1043
Temperture differential (°C)	4	3	2.1			

Table 6–4: Borehole details and actual construction costs for the pilot plant at EAB.

Parameter	EAB	Parameter	Actual costs
Total borehole metres (y+z)	329	K, drilling costs in hard rock (NOK/m)	200
Soil metres (z)	21	L, casing costs (NOK/m)	500
Hard rock metres (y)	308	M, unit cost for hydraulic fracturing with injection of sand (NOK/borehole)	20000
Borehole depth (m)	~110		

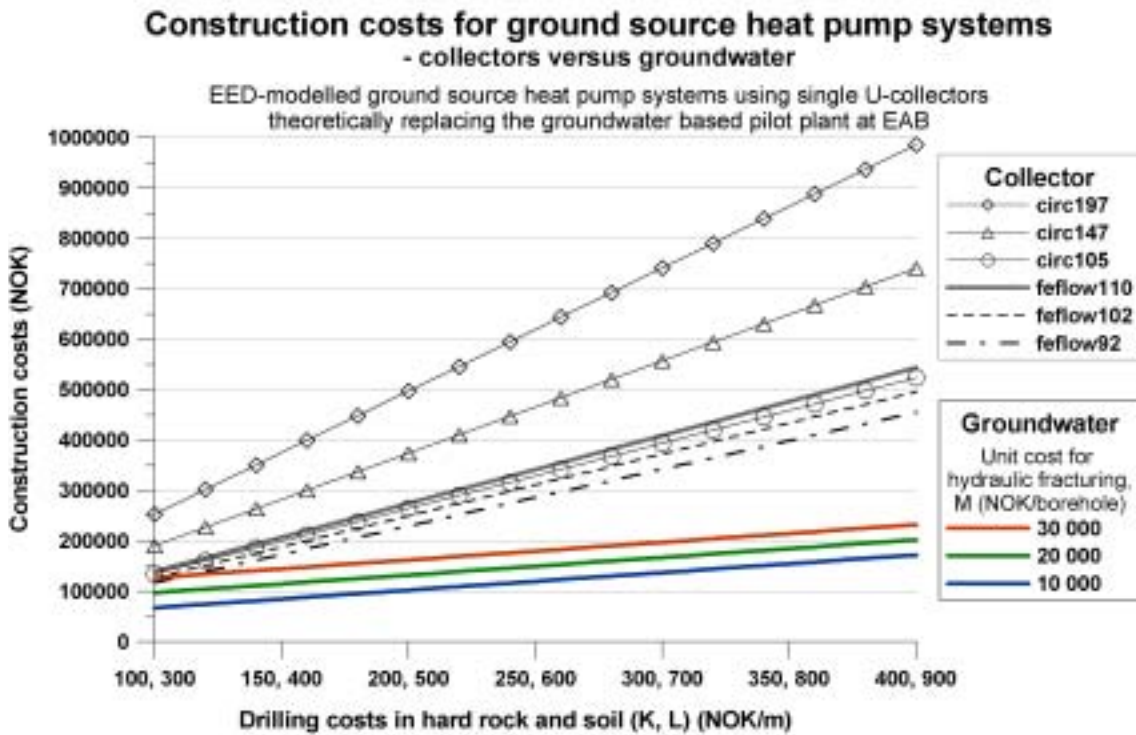


Figure 6-5: Construction costs for ground source heat pump systems at EAB. Different cost alternatives when choosing either collectors- or groundwater systems.

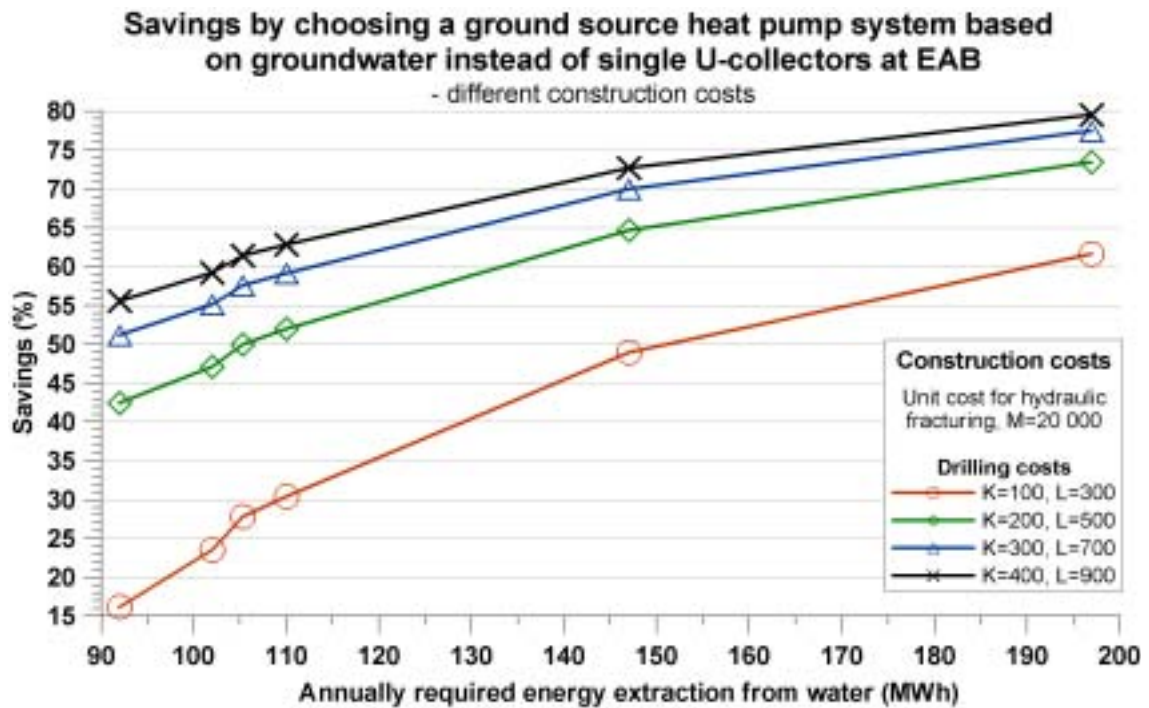


Figure 6-6: Percentage savings by choosing a groundwater system in preference to collectors at EAB at different construction costs.

6.1.5 Profitable pilot plant at Bryn? - Theoretical considerations

Due to the unsatisfactory operation of the pilot plant at Bryn (paragraph 5.2.13), the economical calculations in this paragraph is included for hypothetical reasons only, and assumes an operation of the plant according to the initial plans (figure 1–1). The EED-modelled values for the effective borehole metres, the corresponding energy extraction and all the remaining relevant variables used in the economical analysis (equation 6.1 and 6.2) are summarized in table 6–5. Using a varying number of boreholes, the borehole depths were in the range of 163 to 177 metres. The geological conditions at Bryn were taken into consideration for all the modelled cases with respect to the groundwater level and the soil cover. By using the input values in tables 6–5 and 6–6, the sensitivity of the construction costs for the pilot plant and the EED-modelled collector-equivalents replacing the groundwater system at Bryn can be seen in figure 6–7. The savings by choosing a groundwater system in preference to a collector system at Bryn at different construction costs can be seen in figure 6–8. Under the actual conditions (table 6–6), a reduction in the construction costs, i.e. the drilling costs for a collector system, of more than 50% were achieved for the pilot plant at Bryn when the energy extraction from water is higher than 188 MWh.

Table 6–5: Borehole details for the modelled collector-equivalents at Bryn.

Parametres	Modelled collector-equivalents replacing the ground source heat pump system based on circulating groundwater at Bryn				
	feflow94	feflow135	feflow169	feflow188	feflow126
Energy water (MWh)	94	135	169	188	126
Energy heat pump (MWh)	141	203	254	282	189
Effective borehole metres (m)	977	1407	1770	1987	1320
Number of boreholes	6	8	10	12	8
Effective borehole depth (m)	163	176	177	166	165
Groundwater level (m)	1	1	1	1	1
Actual borehole depth (m)	164	177	178	167	166
Total borehole metres (y+z)	983	1415	1780	1999	1328
Total metres of drilling in soil, z (m)	18	24	30	36	24
Total metres of drilling in hard rock, y (m)	965	1391	1750	1963	1304

Table 6–6: Borehole details and actual construction costs for the pilot plant at Bryn

Parameter	EAB	Parameter	Actual costs
Total borehole metres (y+z)	500	K, drilling costs in hard rock (NOK/m)	200
Soil metres (z)	21	L, casing costs [NOK/m]	500
Hard rock metres (y)	479	M, unit cost for hydraulic fracturing with injection of sand (NOK/borehole)	20000
Borehole depth (m)	100		

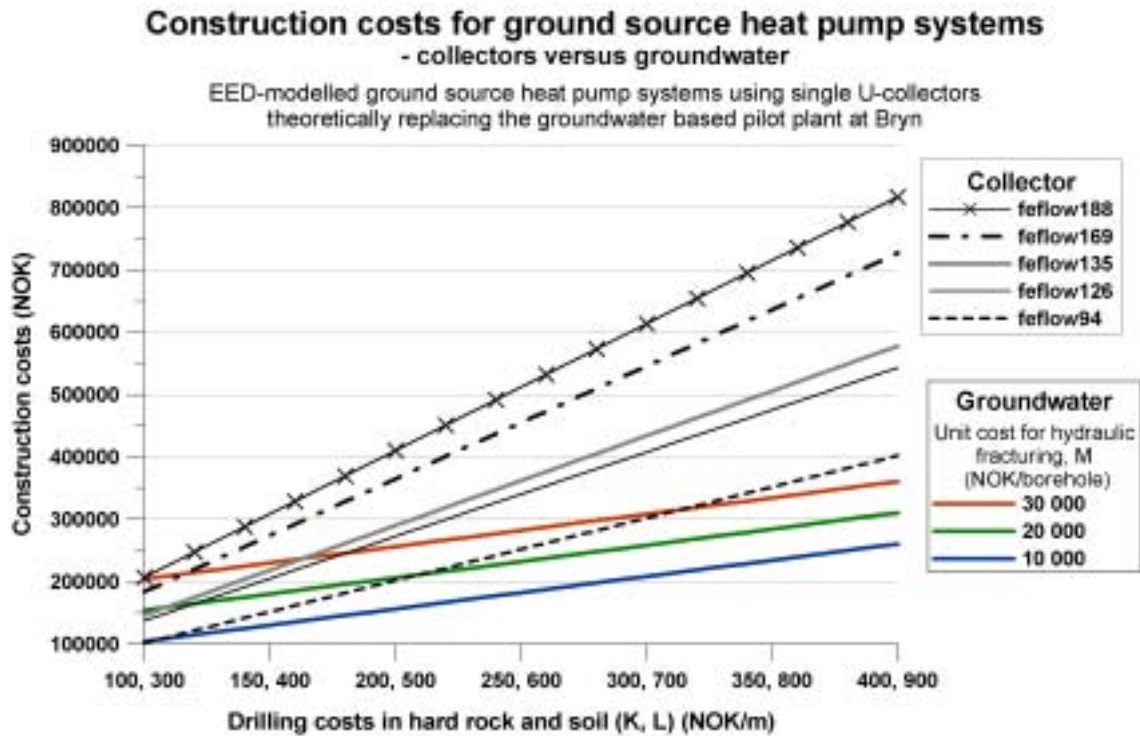


Figure 6-7: Construction costs for ground source heat pump systems at Bryn. Different cost alternatives when choosing either collectors- or groundwater systems.

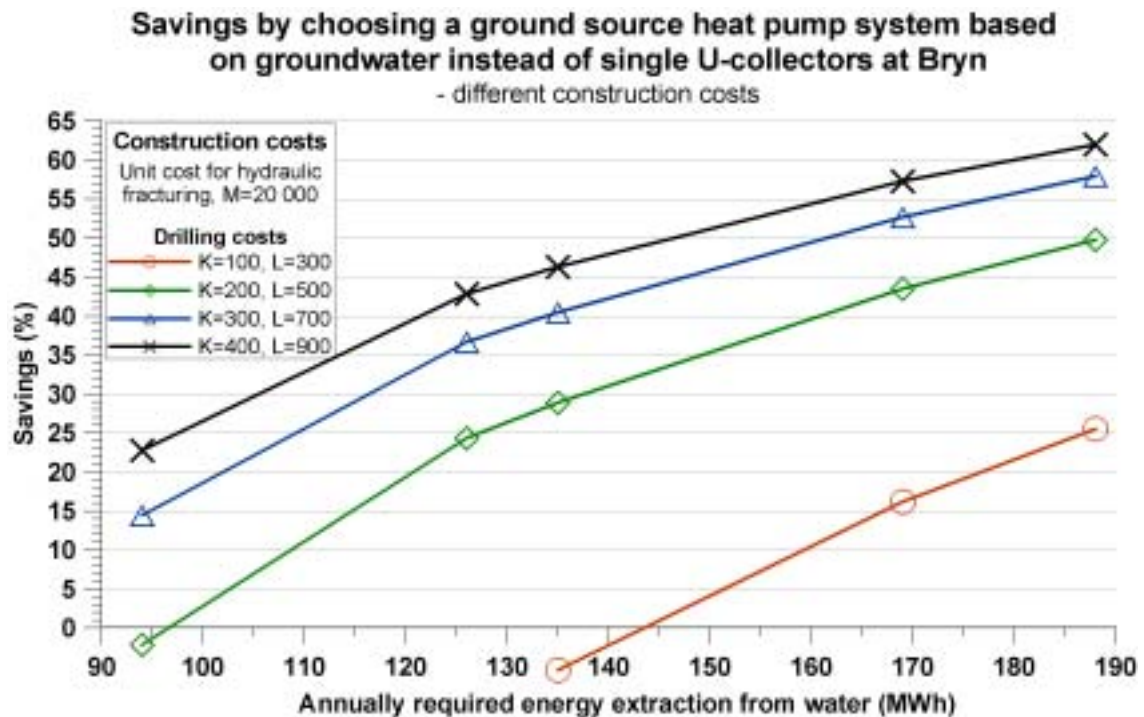


Figure 6-8: Percentage savings by choosing a groundwater system in preference to collectors at Bryn at different construction costs.

6.1.6 Construction costs at varying effect extractions at Bryn and EAB

The energy extraction from the ground and selected construction costs for the two alternative ground source heat pump systems at Bryn and EAB (figure 6–9) shows that the pilot plant at EAB achieves best profitability. In general, the profitability of groundwater systems versus collector systems increases with increasing drilling costs. The real savings related to the choice of a groundwater system in preference to a collector system at EAB can only be quantified by a full-scale operation of the plant. The calculated savings should be regarded as estimated values. A similar approach, where the plant is designed for heating- and cooling purposes, would probably improve the profitability of the pilot plant at EAB further, according to the more effective heat exchange properties of water.

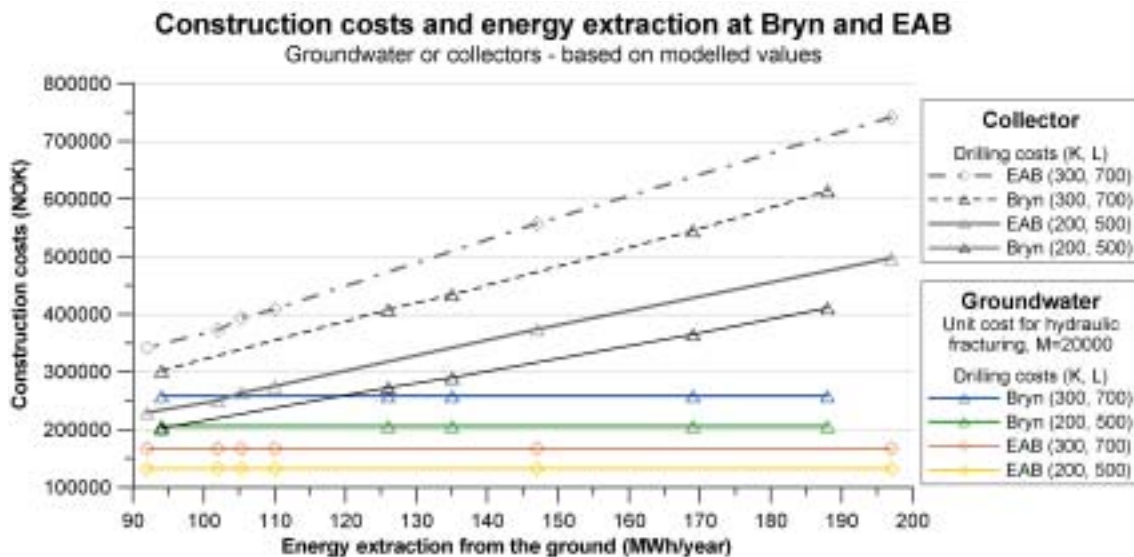


Figure 6–9: Energy extraction from the ground and selected construction costs for ground source heat pump systems at EAB and Bryn. Different cost alternatives when choosing either collectors- or groundwater systems.

6.2 Energy efficiency - energy extraction per meter borehole

A simple comparison of the energy extraction per meter borehole can be done for the different plant alternatives used in the profitability considerations (paragraphs 6.1.4 and 6.1.5). The calculation of the energy extraction per meter borehole as a measure on the energy efficiency is based on the energy extraction from the modelled collector-equivalents at EAB and Bryn, the FEFLOW-modelled energy extractions at EAB and Bryn, and the values for the energy extraction calculated from a circulation rate of 14 m³/hour and average temperature differentials of 2.1, 3 and 4°C at EAB (figure 6–2). The energy efficiency is found by dividing the energy extraction by the total borehole metres for the respective plant alternatives. The EED-modelled collector-equivalents had the lowest energy efficiency, approximately 90 kWh/meter at EAB and 95 kWh/meter at Bryn, while the median value for the FEFLOW-modelled groundwater system at EAB were 309 kWh/meter and 270 kWh/meter at Bryn. The highest energy efficiency was

obtained for the groundwater system at EAB where the calculation of the energy extraction was based on the circulation rate and the temperature differential (figure 6–10). The energy efficiency values were in the range of 320 to 600 kWh/meter according to the corresponding temperature differentials.

The high energy efficiency expressed as energy extraction per metre borehole of the groundwater system at EAB, calculated with basis in the circulation rate, can be explained by the circulating water collecting energy from a large bedrock volume outside the boreholes. On the contrary, assuming conduction to be the major heat transfer mechanism and the boreholes to have no influence on each other, the energy extraction for the collector-equivalents at Bryn and EAB are collected from a limited bedrock volume within a maximum 10-meter radius from each borehole.

The higher thermal conductivity of the bedrock at Bryn (table 6–2) is the reason why the collector-equivalents at Bryn obtained higher energy efficiency than EAB.

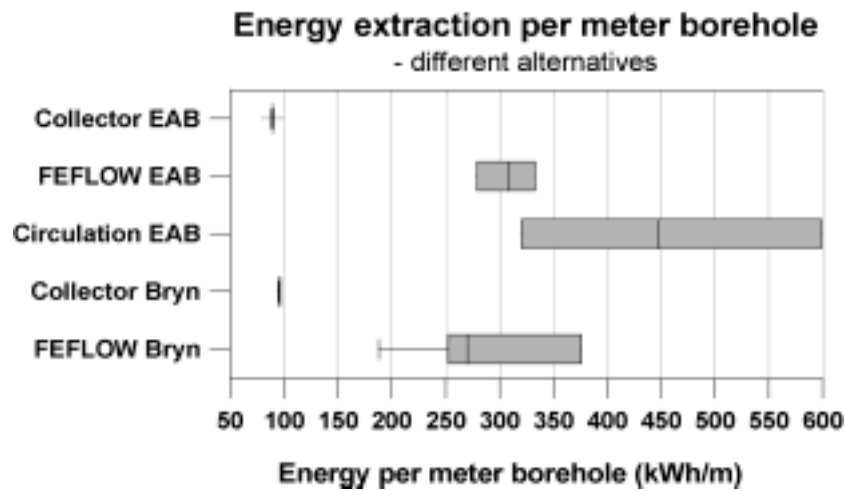


Figure 6–10: Energy extraction per meter borehole. A comparison of the different alternatives.

Chapter 7 Discussion

7.1 Cost reductions by the use of improved equipment and methodology

An economical analysis of the pilot plants at Bryn and EAB were performed to reveal the profitability of the ground source heat pump system based on groundwater versus conventional ground source heat pump system with single U-collectors in vertical boreholes. Since the operation of the pilot plant at Bryn was unsuccessful, the economical analysis using the actual construction costs was performed for hypothetical reasons only and based on the original plans. The results showed that a reduction in the construction costs, i.e. the drilling costs for a collector system, of more than 50% would have been achieved if the annual energy extraction from water was higher than 188 MWh. Corresponding number for the pilot plant at EAB, which had a successful test run, was 105 MWh. A higher annual energy extraction from the circulating groundwater and/or higher drilling costs will cause a significant improvement of the profitability of the groundwater alternative versus a conventional collector system.

A further development of the equipment for hydraulic fracturing with injection of sand to improve the efficiency and minimize the costs is required (paragraphs 5.6.3 and 7.5).

The stated hypothesis (1), that:

The development of suitable and reliable equipment and methodology for hydraulic fracturing with injection of propping agents will reduce the drilling costs for medium- to large sized ground source heat pump systems in crystalline bedrock by up to 50% has only been verified for the pilot plant at EAB. For the pilot plant at Bryn, the given hypothesis has been disproved and must be rejected due to the unsuccessful operation of the pilot plant.

7.2 Hydraulic fracturing and geological conditions

The required pressure to initiate fracturing, and the stable pressure after fracturing, were higher at Bryn compared with those at EAB (paragraph 5.5, figure 5–97). The higher degree of fracturing (97%) and the relatively lower pressure levels present at EAB, are probably caused by the stress- and strength conditions being different at the two geological sites.

The rock stress measurements carried out at Bryn showed that the minimum principal stress varied from 4.5 to 16.5 MPa (45-165 bars). The tensile strength of the rock (Ringerike sandstone) was estimated to 7-11 MPa (70-110 bars) (Jóhannsson, 2001). The relatively high rock stresses at Bryn, were also verified by the reopening pressures being above 100 bars for a majority of the borehole sections treated with hydraulic fracturing with injection of sand (figures 5–57 to 5–60).

According to equation 2.4, the magnitude of the pressure required for fracture initiation at the given conditions (paragraph 2.1.3) increases with increasing values for the horizontal principal stresses and the tensile strength of the rock. The quartzitic- and sandstone rocks, and the limestone- and clay shale/clay stone data-set in figure 2–7 can theoretically represent the rock types present at Bryn and EAB, respectively. The tensile strength of the quartzitic- and sandstone rocks are significantly higher than the corresponding value for the limestone and the clay shale/clay stone. According to this (figure 2–7), the tensile strength of the bedrock is considered to be higher at Bryn than EAB.

The initiated or reopened fractures, using hydraulic fracturing with water-only, will have its maximum extension in all directions when the water flows into the formation during the stimulation. When the water pumps are turned off and the water pressure decreases, the fracture falls back to its original state of equilibrium which is related to the rock stresses in the area. Even though a displacement in the fracture, providing a permanent opening, may occur in the closing process (Smith, 1989), a reduced borehole yield is likely to be the long-term effect of hydraulic fracturing with water-only (also mentioned in paragraph 5.2.3). Due to possible displacements in the opened fractures, the borehole yield would probably remain higher than the initial borehole yield determined before hydraulic fracturing with water-only.

A higher degree of fracturing would have been achieved at Bryn if the equipment for hydraulic fracturing had been designed to tolerate and handle higher pressures levels than the required fracture initiation pressures at the site (paragraph 7.5).

The stated hypothesis (2), that:

Independent to the geological conditions, a complete fracturing is expected to take place using the developed and improved equipment and methodology for hydraulic fracturing of boreholes in crystalline bedrock”

has been rejected.

7.3 Sufficient infiltration capacity and distributed circulation of groundwater?

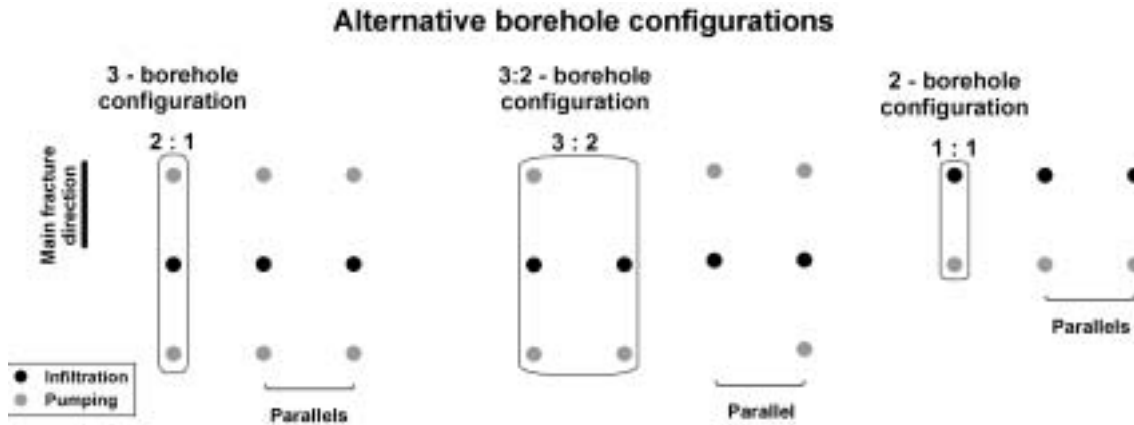
7.3.1 Hydraulic communication - preferred borehole configurations

The 5-borehole configuration, consisting of four pumping boreholes and one infiltration borehole, was chosen at Bryn (figures 1–1 and 3–3) because of uncertainties concerning the fracture propagation direction in an early phase of the study. This configuration was considered to ensure the best interconnection of the reopened- or initiated fractures, and thus the best hydraulic communication and the largest heat exchange area between the boreholes.

The best hydraulic conductivity in the bedrock at Bryn appeared to be between boreholes 1, 3 and 5 where an interconnecting and elevated response in the groundwater level was observed during hydraulic fracturing with water-only (paragraph 5.2.9). Borehole 1, 3 and 5 were located approximately north-south (figure 3–3) and parallel to

the main fracture direction (figure 5–37). The main fracture direction at Bryn, recognized in the structural geological pre-investigations (paragraph 3.2) and in the geophysical borehole inspections (paragraph 5.2.7), is likely to reflect the orientation of the maximum principal stress direction (paragraph 5.2.6). According to the basic theoretical principles regarding hydraulic fracturing and rock stresses, the fracture propagation of an initiated fracture outside the influence area of the borehole, is supposed to be parallel to the maximum principal stress direction (paragraph 2.1.3). Performing hydraulic fracturing, a reopening of existing but maybe mineralized fractures are likely to occur. Assuming the same stress regime as at the point of origin of the specific fracture, the existing fractures would probably have the same orientation as a corresponding initiated fracture only influenced by the rock stresses. The preferred direction of fracturing resulting in the best hydraulic communication between the boreholes at Bryn, suggest that a borehole configuration consisting of three boreholes, two pumping- and one infiltration borehole located on a line parallel to the main fracture direction would have been better suited than the existing 5-borehole configuration. In cases of larger energy demand, the suggested 3-borehole configuration-alternative could be extended by adding several 3-borehole parallels (figure 7–1). Still, the relative low degree of fracturing and the resulting low circulation rate achieved in the test run of the pilot plant at Bryn (paragraph 5.2.13) would have caused an unsuccessful operation of an imaginary 3-borehole configuration as well. The experiments at Bryn showed that the infiltration rate of the central borehole in the pilot plant was the limiting factor preventing a successful operation, and that the infiltration capacity of a borehole is approximately equal to the borehole yield determined from test pumping. With these results in mind, the pilot plant at EAB was chosen to have a 3-borehole configuration. The boreholes at EAB were not configured on a line due to practical adjustments (paragraph 3.3 and figure 3–6). The lack of bedrock exposure in the vicinity of the actual area, prevented structural geologic pre-investigations, and the main fracture direction was not known in advance of the drilling of the boreholes. Later a fracture analysis of the optical televiewer log for borehole 1 at EAB revealed that the main fracture direction was oriented northeast-southwest (figure 5–71). This means that boreholes 1 and 3 were located approximately parallel to the main fracture direction, but no hydraulic communication between boreholes 1 and 3, confirming a significantly preferential fracturing direction, was discovered. Independent to the fracture direction, the successful hydraulic fracturing of the boreholes at EAB made the pilot plant obtain a satisfying circulation rate (figure 5–84). According to the results from Bryn, a higher circulation rate could perhaps have been achieved at EAB if the boreholes had been configured on a line parallel to the main fracture direction. Even though a high circulation rate was achieved, the infiltration capacity of the central borehole was probably somewhat lower than the pumping capacity. The three days downtime of the pump in borehole 2 during the test run showed that the pumping capacity in borehole 3 was approximately $9 \text{ m}^3/\text{hours}$. Taking into account that borehole 3 had the lowest yield before hydraulic fracturing with injection of sand, the total pumping capacity in boreholes 2 and 3 would probably be around $18 \text{ m}^3/\text{hours}$. These observations suggest that even the 3-borehole configuration, where the relation between the number of pumping- and infiltration boreholes is 2:1, restrains the potential of the plant. As a consequence, the ideal borehole configuration to obtain the best hydraulic conditions and the maximum relative infiltration capacity, might be where the relation between the number of pumping- and

infiltration boreholes is 3:2, or 1:1 (figure 7–1). The access of a large heat exchange area within the bedrock, ensuring a satisfying heat exchange between the water and the bedrock, can be obtained by adding several parallel configurations. The exact borehole configuration should probably be determined based on the expected geological conditions at the actual construction site.



Figur 7–1: Alternative borehole configurations for ground source heat pump system based on circulating groundwater.

7.3.2 Identification of water inlets

The temperature- and conductivity logs are helpful tools to detect water inlets in the boreholes where the inflowing water has different temperature- and conductivity properties than the water in the vicinity. The results from the sectional- and columnar test pumping (figure 5–24) and the flow measurements at EAB (figure 5–69) indicate that these water inlets do not necessarily represent large water bearing fractures, but sometimes rather insignificant water inlets. For instance in the deeper part of borehole 4 (figure 5–24 and table 5–9). The visible changes in the borehole wall at 82.2 and 60.7 metres depth in borehole 2 at Bryn and EAB (figures 5–36 and 5–70), respectively, are not present on the temperature- and conductivity logs. According to their appearance, these fractures are probably yielding a significant amount of water. Even though the boreholes at EAB had higher yield than the boreholes at Bryn, fewer changes on the temperature- and conductivity logs were observed at EAB compared with Bryn.

Despite a successful fracturing (97%) when performing hydraulic fracturing with injection of sand in the boreholes at EAB, changes in the flow pattern could only be seen in borehole 2 and partly in borehole 3. All major water inlets appeared between 25 and 35 metres for all boreholes. Since a significant increase in the borehole yield was achieved as a consequence of hydraulic fracturing at Bryn, where the degree of successful fracturing was 70%, a reasonable assumption would be to expect a similar course of events for the boreholes at EAB (paragraph 5.3.9). A possible explanation why the flow pattern in the boreholes at EAB seems to be unaffected by the hydraulic fracturing with injection of sand could be that the large, and probably dominating, water bearing fractures between 25 and 35 metres in the boreholes hide the small water inlets present at a deeper level in the boreholes. This effect may be enhanced by the pump (pump D), located above the flow meter probe at 20 metres depth in the boreholes (figure

2–20), drawing water from the large fracture systems closest to the pump, following the principle of least way of resistance. Because of this, the measured inflow of water in the area close to the pump is likely to be proportionally larger compared with the measured inflow of water from other parts of the borehole at a greater distance to the pump. Consequently, the identification of new water bearing fractures in the deeper part of the boreholes requires a considerable inflow of water. It may be unrealistic to assume that the inflow of water from the new fractures will yield equally large quantities of water such as the major water inlets between 25 and 35 metres depth. As a result, the flow measurement may have been relatively unsuited to identify the new and deeper water inlets in the boreholes at EAB. This argumentation also implies that the new water inlets, recognized in borehole 2 and partly borehole 3, yield considerable quantities of water.

The stated hypothesis (3), that:

Sectional hydraulic fracturing in several levels in each borehole will ensure a distributed circulation of the groundwater and a sufficient infiltration capacity of the infiltration borehole in the ground source heat pump system based on groundwater can be rejected.

A distributed circulation of groundwater in a ground source heat pump system based on groundwater requires a complete fracturing of several borehole sections with hydraulic fracturing (hypothesis 2), and probably the use of coarser propping agents in order to create the required hydraulic conductivity of the fracture planes.

7.4 Need of sand as propping agents?

In this study, the determined improvement of the columnar- and sectional borehole yields were used as a measure of the efficiency of the hydraulic fracturing with water-only and hydraulic fracturing with injection of sand. Improved borehole yields were achieved for all the boreholes at Bryn (figure 5–26) as a result of hydraulic fracturing with water-only (figure 5–27) and of hydraulic fracturing with injection of sand (figure 7–2). The only exception was borehole 4 where the hydraulic fracturing with injection of sand caused an insignificant (12%) improvement of the yield. Values for the counter pressure or the stable minimum water pressure, immediately before the injection of sand in the desired sections of borehole 4, was in the range of 20 to 35 bars (table 5–13). These values were lower than a majority of the corresponding values from the other boreholes (figure 5–61).

A possible explanation of the relation between the low counter pressures and the minor increase of the yield in borehole 4, compared with the remaining boreholes at Bryn, might be associated with the need of sand as propping agents or spacing material in the particular fracture. Sand as spacing material may be less required in fractures having a stable and low counter pressure prior to the injection of sand, compared with fractures having a higher counter pressure. A permanent improvement of the borehole yield can possibly be achieved by injecting sand into fractures having a higher counter pressure, in this study approximately higher than 40 bars, while fractures having a lower pressure could be considered as almost permanently open fractures. With reference to the relatively higher counter pressure levels experienced at Bryn, generated by the stress-

and strength situation, sand as spacing material in the opened fractures with hydraulic fracturing should be more required at Bryn than at EAB.

As an alternative explanation, the low yield improvement in borehole 4 might also correspond to the total volume of sand injected into the three stimulated borehole sections. According to figure 7–2 the total volume of sand injected in borehole 4 is considerably lower compared with the other boreholes. The percentual- and quantitative yield improvement showed the same trend and the yield improvement for borehole 1, 2, 3 and 5 was approximately equal where borehole 1 had the best improvement. The symbols representing the total volume of injected sand and the volume of injected sand with the largest grain size, Dansand #2, displays the same pattern and corresponds to the total borehole yield after hydraulic fracturing with injection of sand.

Only Jupe et al. (1993; in Broch, 1994) reports a positive effect, in terms of improved borehole yield, as a consequence of a deep stimulation program where a small part of the program included the use of 0.2-0.4 millimetres quartz sand as propping agents (Eliasson et al., 1988). Herbert et al. (1993), using 0.5 millimetres sand as propping agents, and Williamson and Woolley (1980) in Smith (1989) achieved a reduced borehole yield after injection of propping agents. Compared with these studies, the use of coarser sand in the boreholes at Bryn, two fractions of 0.40-0.90 and 0.63-1.40 millimetres, may have contributed to the significant yield improvement. It should also be noted that the injected volume of the coarsest sand fraction shows a better correlation with the yield improvement than the smallest grain size (figure 7–2). From the oil industry, the size of the propping agents are according to the so-called *admittance criterion* which require fracture widths in the range of two to three times the largest grain diameter. The larger particles, e.g., 12/20 mesh (1.70-0.85 millimetres), provide a greater conductivity at lower stress levels than the more commonly used smaller sizes, such as 20/40 mesh (0.85-0.43 millimetres) (Anderson et al. 1989; in Gidley et al., 1989). Smith (1989) refers that the use of hard sand or plastic beads as propping agents, as coarse as possible for instance 30/50 mesh (0.60-.030 millimetres), are recommended by the groundwater industry contractors.

The yield improvement caused by two stimulations with hydraulic fracturing with water-only versus the yield improvement after hydraulic fracturing with injection of sand is not known from the Bryn-data. Two stimulations cycles with hydraulic fracturing with water-only are also expected to cause a yield improvement compared to one stimulation. However, similar to one stimulation with hydraulic fracturing with water-only, the borehole yield is expected to be reduced as a long term effect of two stimulations with water-only as well, while the injection of sand as spacing material is supposed to cause a permanent yield improvement.

The stated hypothesis (4), that:

Hydraulic fracturing with injection of propping agents will cause a further improvement of the borehole yields compared with the improved borehole yields achieved by hydraulic fracturing with water-only has not been rejected.

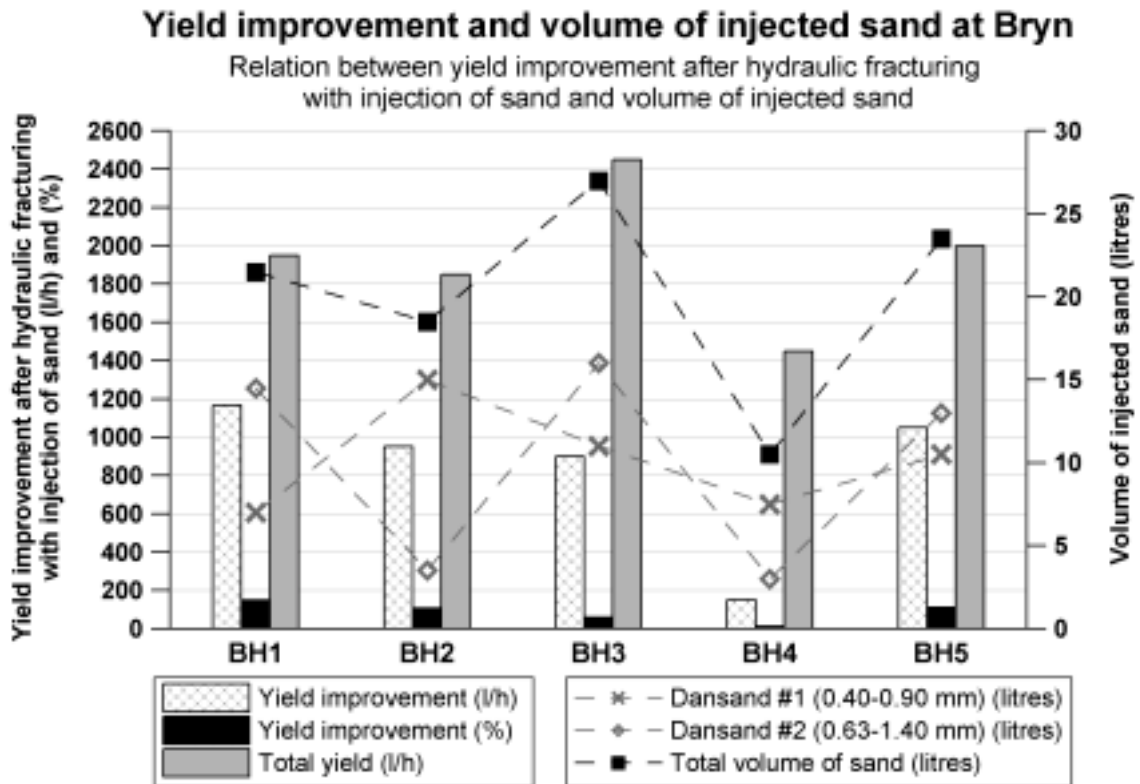


Figure 7-2: Yield improvement and volume of injected sand at Bryn.

7.5 Suggestions for further work

The equipment for hydraulic fracturing employed in this study was not capable of creating fractures in borehole sections where the required fracture initiation pressure was higher than approximately 200 bars. All the equipment used was made for a maximum working pressure of 250 bars. Further improvement of the equipment is required to achieve a higher degree of fracturing in areas with high rock stresses and high tensile strength. The first aim should be to develop low-cost equipment which can tolerate a maximum working pressure of 350 bars. The equipment improvements include the double packer, water tubes and -hoses, and high-pressure- and high-capacity pumps.

Improved equipment and procedure for mixing, filling- and injection of fluid are required for the commercialization of hydraulic fracturing with injection of propping agents. The optimal solution would be to integrate the mixer (paragraph 2.2.4) and high pressure tank (paragraph 2.2.2) with the tank lorry for hydraulic fracturing. The mixing of thickener, water and sand should be automatized. Further investigations concerning the optimal size- and volume of the use of quartz sand as propping agents are necessary.

Further research regarding the ground source heat pump system based on circulating groundwater is highly recommended. Important parameters to be optimized are:

- The borehole configuration in different geological settings,
- the distance between the pumping- and infiltration borehole, and
- the interconnecting relation between the retention time for the circulating groundwater and the temperature course during the operation periods for heating- and cooling purposes, respectively.

In addition, more sophisticated economical analyses would be required to demonstrate the economical potential of groundwater-based ground source heat pump system used for both heating- and cooling purposes.

Interesting and useful information for the use of the stimulated boreholes to drinking water purposes and ground source heat pump systems are:

- The effect, in terms of improved borehole yield, of two stimulations with hydraulic fracturing with water-only versus hydraulic fracturing with injection of sand.
- The long term effect of one and two stimulations with hydraulic fracturing with water-only, respectively, and the long term effect of hydraulic fracturing with injection of sand.

Chapter 8 Summary and conclusions

The aim of this work was to test the following hypotheses:

- 1) The development of suitable and reliable equipment and methodology for hydraulic fracturing with injection of propping agents will reduce the drilling costs for medium- to large sized ground source heat pump systems in crystalline bedrock by up to 50%.
- 2) Independent of the geological conditions, a complete fracturing is expected to take place using the developed and improved equipment and methodology for hydraulic fracturing of boreholes located in crystalline bedrock.
- 3) Sectional hydraulic fracturing in several levels in each borehole will ensure a distributed circulation of the groundwater and a sufficient infiltration capacity of the infiltration borehole in ground source heat pump systems based on groundwater.
- 4) Hydraulic fracturing using injection of propping agents will cause a further improvement of the borehole yields compared to those yields achieved by hydraulic fracturing with water-only.

Hypotheses 2 and 3 could be rejected, while hypothesis 4 was verified. Hypothesis 1 was verified for the pilot plant at EAB, but not for the pilot plant at Bryn. Together with the results that support or contradict the stated hypotheses, the main findings in this study can be summarized as follows:

- a) Comparing the results from the hydraulic fracturing performed at Bryn and EAB shows that the required pressure level, to create new fractures or reopen existing fractures, varied considerably. The maximum pressures present at Bryn were higher than the corresponding pressure at EAB. At Bryn 70% (44 out of 63) of the pressure-time curves from the hydraulic fracturing with water-only were interpreted as initiation or reopening of fractures, while the corresponding number for EAB was 97% (36 out of 37). The lower degree of fracturing at Bryn is likely caused by high rock stresses and high tensile strength of the bedrock, also confirmed by the results from the rock stress measurements. Considering the bedrock at EAB, characterized as nodular limestone and lime-rich shale, the tensile strength is assumed to be less than the corresponding values for the Ringerike sandstone at Bryn.
- b) The use of sand as propping agent seems to be more required in fractures with high counter pressure, in this study higher than approximately 40 bars, compared with fractures with lower counter pressure. The particle size of the sand should also be adjusted to the appearing counter pressure, and injection of coarser sand is recommended in fractures with lower counter pressures.
- c) The infiltration rate in the central boreholes of ground source heat pump systems based on circulating groundwater is a critical factor for the energy extraction and a successful operation. Results from the short-time circulation tests carried out at Bryn

and EAB show that the infiltration rate in borehole 3 at Bryn (approximately 2500 litres/hour) was too low to obtain a satisfactory operation of the plant, while the infiltration rate at EAB (14000 litres/hour) was sufficient. The large difference in the infiltration rate between Bryn and EAB was probably related to: (1) Large initial differences in the borehole yield prior to hydraulic fracturing (<560 litres/hour at Bryn and >6300 litres/hour at EAB). Nodular limestone or lime-rich rock types generally have high permeability, while compact sandstone rocks generally have low permeability. (2) Hydraulic fracturing was most successful at EAB. (3) The higher rock stress level present at Bryn compared with EAB will increase the tendency to close the opened fractures, even the fractures with injected sand.

- d) The extensive borehole inspection program, including logging of the temperature- and conductivity of the borehole water and the natural gamma radiation, and optical televiewer logging of the boreholes, provided useful information about the initial borehole conditions and revealed some of the changes caused by the different kinds of hydraulic fracturing. Still, the inspections did not identify as many of the actual changes as expected in advance of the investigations. For instance, new- or reopened fractures could hardly be discerned on the optical televiewer log, and probably only a limited amount of the new water inlets in the borehole related to hydraulic fracturing were revealed on the temperature- and conductivity logs. A random positioning of the double packer, to achieve the best effect from hydraulic fracturing, might be equally well suited compared with a strategic positioning based on optical televiewer inspection.
- e) Using flow measurements to document the efficiency of hydraulic fracturing in the high-yielding boreholes at EAB did not give satisfactory results. The large and dominating water inlets in the upper parts of the borehole appeared to dominate the deeper and smaller water inlets. Test pumping turned out to be the best suited method for documenting the effect of the different kinds of hydraulic fracturing. To achieve comparable results, the selection of the pump and its position in the borehole must be considered carefully.
- f) The FEFLOW-modelling of the pilot plants at Bryn and at EAB emphasized the important relation between the available heat exchange area in the bedrock, the thermal conductivity of the bedrock, and the energy potential.
- g) Hydraulic fracturing did not cause any apparent damage. Only minor changes in the terrain level, either related to measuring uncertainty or real terrain changes, were observed.
- h) The increased borehole yields achieved by hydraulic fracturing, and the improved, reliable and cost-effective hydraulic fracturing techniques in crystalline bedrock, will probably increase the interest for the use of groundwater as a domestic water supply for small- to medium sized water works.

Chapter 9 References

1. Aggson, J.R. and Kim, K. (1987): Technical Note - Analysis of hydraulic fracturing pressure histories: A comparison of five methods used to identify shut-in pressure. *Int. J. Rock Mech. Min. Sci & Geomech. Abstr.* Vol. 24, No 1 page 75-80, Pergamon Press, London.
2. Amadei, B., Stephansson, O., (1997): *Rock Stress and its Measurements*. Chapman & Hall, London. 490 pages.
3. Anderson, R.W., Cooke Jr, C.E. and Wendorff, C.L., (1989): Propping Agents and Fracture Conductivity. Chapter 6 in *Recent Advances in Hydraulic Fracturing* (Gidley et al., 1989), Monograph Volume 12, Henry L. Doherty series. Society of Petroleum Engineers. ISBN 1-55563-020-0, page 109-130.
4. Andersson, O., Johansson, I., Perers, J., (1982): Utnyttjande av överskottsvärme i grundvatten vid konstjord infiltration. Förstudie. Swedish Council for Building Research, Report R121:1982, 38 pages.
5. Andersson, O. (1992) Scaling and corrosion. Annex VI - Environmental and chemical aspects of thermal energy storage in aquifers. Swedish Council for Building Research. Document D12: 1992, 102 pages.
6. Banks, D. and Robins, N. (2002): *An Introduction to Groundwater in Crystalline Bedrock*. Geological Survey of Norway, 64 pages.
7. Banks, D. (1991): Boring og prøvepumping av hydrogeologiske testhull i en grønnstein akvifer- Østmarkneset, Tr.heim. App.: kapasitetstest av borehull i fast fjell. Geological Survey of Norway, NGU report 91.213, 107 pages.
8. Baski, H.A. (2001): Letter from Henry A. Baski to Randi Kalskin, 26th of March 2001, 1 page.
9. Baski, H. (1987): Hydrofracturing of water wells, *Water Well Journal* 41(6): Page 34-35.
10. Bredehoeft, J.D. et al. (1976): Hydraulic fracturing to determine the regional in-situ stress, Piceance Basin, Colorado. *Geol. Sco. Am. Bull.*, 87, page 250-58.
11. Brekke, E. (2003): Energiuttak fra fjell - Et studium av data fra termisk responstesting. Master thesis at the Norwegian University of Science and Technology, Faculty of Engineering Science and Technology, Department of Geology and Mineral Resources. 84 pages.
12. Broch, E. (1994): Hot Dry Rock. Report of the Evaluation of Swedish Research on Hot Dry Rock. NUTEK, Swedish National Board for Industrial and Technical Development. R 1994:57. 8 pages.

13. Broch, E., Franklin, J.A., Walton, G. (1971). Logging the mechanical character of Rock. Særtrykk av Inst. of Mining and Metall. Trans., 80A. 10 pages.
14. Driscoll, F. G., (1989): *Groundwater and wells, second edition*, publisert av Johnson Filtration Systems Inc., St. Paul, Minnesota, ISBN: 096145601, 1089 pages.
15. Eliasson, T., Sundquist, U. and Wallroth, T. (1988): Stimulation experiments with water and viscous fluid at the HDR geothermal research site in the Bohus granite, SW Sweden. HDR geothermal energy project, Department of Geology, Chalmers University of Technology and University of Göteborg. Publ. Fj-6, 69 pages.
16. Elvebakk, H., Rønning, J.S. (2003): Strømningsmåling i borehull. Påvisning av vanninnslag. Poster presentation at the 12th Seminar on Hydrogeology and Environmental Geochemistry, NGU, Trondheim 4th-5th February 2003. Abstract in NGU report 2003.015, page 61-62.
17. Elvebakk, H., Rønning, J.S. (2001): Borehullsinspeksjon. En utprøving og sammenligning av Optisk og Akustisk Televiewer. Geological Survey of Norway, NGU-rapport, 2001.011, 42 pages.
18. ETM Pacific (2003): Product data sheet for Hotbox datalogger BKT4, ElproLog. http://www.etmpacific.com.au/downloads/1-4_channel_data_loggers/hotbox_w.pdf
19. Frengstad, B. (2002): Groundwater quality of crystalline bedrock aquifers in Norway. Norwegian University of Science and Technology, Department of Geology and Mineral Resources Engineering, Dr. ing. thesis 2002:53, 389 pages.
20. Gale, J.E., and MacLeod, R. (1995): Canada-Newfoundland agreement respecting water resource management. Assessing the effectiveness of fracture stimulation for increasing well yield in Newfoundland. Government of Newfoundland and Labrador, Department of environment water resources division. Environment Canada. Environmental conservation strategies division. 48 pages.
21. Gehlin, S. (2002): Thermal Response Test. Method Development and Evaluation. Doctoral Thesis. Luleå University of Technology, Department of Environmental Engineering, Division of Water Resources Engineering. 2002: 39, 193 pages.
22. Gehlin, S. (1998): Thermal Response Test - In Situ Measurements of Thermal Properties in Hard Rock. Licentiate Thesis. Luleå University of Technology, Department of Environmental Engineering, Division of Water Resources Engineering. 1998: 37, 73 sider.
23. Gidley, J.L., Holditch, S.A., Nierode, D.E and Veatch Jr, R.W. (1989): Recent Advances in Hydraulic Fracturing. Monograph Volume 12, Henry L. Doherty series, Society of Petroleum Engineers. ISBN 1-55563-020-0, 452 pages.
24. Grundfos (2004): WebCAPS internet-based configuration tool. <http://www.grundfos.com>.
25. Gustafson, G. (1983): Brunnsystem för värmelagring och värmeutvinning i akviferer.

- Swedish Council for Building Research. Report R39:1983, 28 pages.
26. Haimson, B.C. (1968): Hydraulic Fracturing in poreous and nonporous rock and its potential for determining in situ stresses at great depth, unpublished PhD Thesis, University of Minnesota, 234 p.
 27. Hansen, S.E., Sørlokk, T. og Jóhannsson, Æ. (1998): Bergarters mekaniske egenskaper. SINTEF report. SINTEF, Civil and Environmental Engineering, department of Rock Mechanics; STF22 A98034, 6 pages + appendices.
 28. Hellström, G. and Larson, S.Å., (2001): Seasonal thermal energy storage - the HYDROCK-concept. Springer-Verlag Heidelberg. ISSN: 1435-9529. Bulletin of Engineering Geology and the Environment, Volume 60, Number 2, page 145-156.
 29. Hellström, G. and Sanner, B. (2000): EED - Earth Energy Designer, User manual, Version 2.0. Borehole heat exchangers. Electronic version on <http://www.buildingphysics.com/earth1.htm>. 43 pages.
 30. Herbert, R., Talbot, J.C. and Buckley, D.K. (1993): A study of hydraulic fracturing used on low yielding boreholes in the crystalline basement rocks of Masvingo Province, Zimbabwe. Memoires of the XXIVth Congress international association of hydrogeologists, Oslo, Norway, 28th June - 2nd July 1993, page 698-716.
 31. Herrick, D.W. (2000): Hard rock frack'n. Water well journal, July 2000, page 40-42.
 32. Hubbert, K.M. and Willis, D.B. (1957): Mechanics of hydraulic fracturing. Petrol. Trans. AIME, T.P. 4597, 210, page 153-66.
 33. Irgens, F. (1991): Fasthetlære. 4th. edition, Tapir forlag, 457 pages.
 34. ISRM (1987): Suggested Methods for Rock Stress Determination - Method 3: Suggested Method for Rock Stress Determination Using the Hydraulic Fracturing Technique. Pergamon Press. International Journal of Rock Mechanics and Mining Sciences, Volume 24, Number 1, page 59-63.
 35. Jupe, A.J., Willis-Richards, J. and Nicholls, J.D. (1993): Review of HDR projects, ETSU G 164 - P1. CSM Associates Ltd, page 229-257. Enclosure 3 in Broch (1994).
 36. Jóhannsson, Æ. (2001): Hydrauliske splittetester ved Bryn skole, Bærum. SINTEF Civil and Environmental Engineering, department of Soil and Rock Mechanics. SINTEF report STF22F01126, 5 pages.
 37. Kalskin, R. (1998): Kartlegging av potensialet for grunnvarmeuttak fra løsmasser i Elverum. Master thesis at the Norwegian University of Science and Technolgy, Faculty of Applied Earth Sciences. 61 pages.
 38. Kim, K. and Franklin (Coord.), ISRM Commision on Testing Methods (1987): Suggested Methods for Rock Stress Determination, Method 2, Suggested Method for Rock Stress Determination Using the Hydraulic Fracturing Techninque. Int. J. Rock Mech. Min. Sci. & Geomech. Abstr. Vol 24, No 1, page 59-63, Pergamon Press,

London.

39. Larsen, B. (2001): Bryn skole, Bærum. Strukturgeologiske observasjoner. Unpublished, Geological Survey of Norway. 3 pages.
40. Larson, S.Å., Fridh, B. and Haag, Ö. (1983): Hydrock - värmelager i berg. Anläggning av värmeväxlarytor med hjälp av hydraulisk uppspräckning; HYDROCK - metoden. Chalmers University of Technology/University of Göteborg, department of Geology. Publ. B 222, 118 pages.
41. Less, C. and Anderson, N., (1993): Hydrofracture: State of the art in South Africa. Memoires of the XXIVth congress international association of hydrogeologists, Oslo, Norway, 28th June - 2nd July 1993, page 717-723.
42. Lindblad-Påsse, A. (1986): Järnutfällningsproblem i grunvattenvärmesystem. Swedish Council for Building Research, Report R109:1986, 56 pages.
43. Macaulay, D. (1987): Hydro-fracturing the hard rock well, Ground Water Age 21(7): Pages 22-25, 28, 30.
44. Midttømme, K., Ramstad, R.K., Solli, A., Sjørdal, T. and Elvebakk, H. (2004): Grunnvarmekartlegging i Asker og Bærum. Geological Survey of Norway, NGU-report, 2004.013, 44 pages.
45. Midttømme, K., Hilmo, B.O., Skarphagen, H. og Nissen, A. (2000): Kartlegging av energipotensialet i berggrunnen på kartblad Bekkestua, Bærum kommune: Varmeledningsevnen til bergarter. Geological Survey of Norway, NGU-rapport, 2000.036, 105 pages.
46. Myrvang, A.M. (1996): Kompendium 1 Bergmekanikk. Norwegian University of Science and Technology, department of Geology and Mineral Resources, Trondheim. 216 pages.
47. NGU-Lab (2002a): NGU, Grunnvarme fra fast fjell - økt energiuttak v/Randi Kalskin. Prosjektnr. 277106. Geological Survey of Norway, Analysis report 2002.0032, 15 pages.
48. NGU-Lab (2002b): NGU, Grunnvarme fra fast fjell v/Randi Kalskin Ramstad. Prosjektnr. 277106. Geological Survey of Norway, Analysis report 2002.0405, 15 pages.
49. NGU-Lab (2001a): NGU, Grunnvarme fra fast fjell - økt energiuttak ved hydraulisk trykking av borebrønner v/Randi Kalskin. Prosjektnr. 277106. Geological Survey of Norway, Analysis report 2001.0003, 15 pages.
50. NGU-Lab (2001b): NGU, Grunnvarme fra fast fjell - økt energiuttak ved hydraulisk trykking av borebrønner v/Randi Kalskin. Prosjektnr. 277106. Geological Survey of Norway, Analysis report 2001.0268, 15 pages.
51. NGU Lab (2001c): Uttak av grunnvarme fra fjell -Hydraulisk trykking av brønner v/

- B.O. Hilmo. Geological Survey of Norway, Analysis report 2001.0022. 7 pages + appendices.
52. NGU-Lab (1999a): XRF-analyser. Fact sheet published by the Geological Survey of Norway, Trondheim. 1 page.
 53. NGU-Lab (1999b): XRD-analyser. Fact sheet published by the Geological Survey of Norway, Trondheim. 1 page.
 54. Nordell, B., Bjarnholt, G., Stephansson, O. and Torikka, A. (1984): Fracturing of a pilot plant for borehole heat storage in rock at Luleå, Sweden. Swedish Council for Building Research; D25:1984, 39 pages.
 55. Nordstrand, J.S. (2001): ENERGI BRØNNER I FJELL - Vurdering av forskjellige metoder for effektuttak ved et demonstrasjonsanlegg. Master thesis at the Norwegian University of Science and Technology, Department of Geology and Mineral Resources, 72 pages + appendices.
 56. Rantec Corporation (2000): LEB-H, High pH enzyme breaker. Data sheet, Rantec Corporation, P.O. Box 729, Hwy 14 West, Ranchester, WY 82839. 2 pages.
 57. Scheldt, T. (2000): Methods of In-Situ Rock Stress Measurements with Emphasis on Hydraulic fracturing. Norwegian University of Science and Technology, Department of Geology and Mineral Resources Engineering. 22 pages.
 58. Smith, S.A. (1989): Manual of hydraulic fracturing for well stimulation and geologic studies. National Water Well Association, Dublin, Ohio. 66 pages.
 59. Skarphagen, H., Hilmo, B.O. og Håbrekke, J. (1999): Grunnvarme fra fast fjell - økt energiuttak ved hydraulisk trykking av borebrønner. Prosjektbeskrivelse. Geological Survey of Norway, 11 pages.
 60. Spangelo, T. (2003): Geotermisk energi fra fast fjell - en varmeteknisk analyse av grunne og dype anlegg. Master thesis at the Norwegian University of Science and Technology, Faculty of Engineering Science and Technology, department of Energy and Process Engineering. 84 pages.
 61. Spangelo, T. (2002): Grunnvarme fra fast fjell - en varmeteknisk analyse. Project assignment at the Norwegian University of Science and Technology, Faculty of Engineering Science and Technology, department of Energy and Process Engineering. 51 pages.
 62. Stene, J. (1997): *Varmepumper: Grunnleggende varmepumpeteknikk*. SINTEF Energy Research, department of Refrigeration and Air Conditioning, STF84 A97302, Trondheim. 242 pages.
 63. Storrø, G., Elvebakk, H. og Rønning, J.S. (2002): Tunnelprosjektet: Hydraulisk testing av borehull i fjell i Gualia, Lunner kommune. Geological Survey of Norway, NGU report 2002.051. 50 pages.

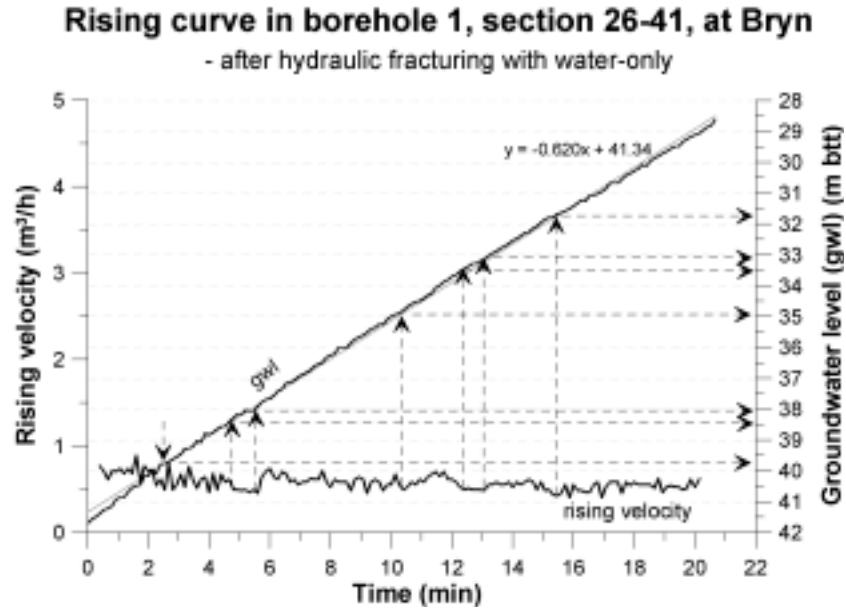
Chapter 9 References

64. Sundquist, U., Wallroth, T. (1990): Hydrock - energilager i berg. Slutrapport för etapp 1 & 2. Chalmers University of Technology/University of Göteborg, department of Geology. Publ. B 349, 37 pages.
65. Sundquist, U., Wallroth, T. and Eliasson, T. (1988): The Fjällbacka HDR geothermal energy research project: Reservoir characterisation and injection well stimulation. Chalmers University of Technology and University of Göteborg, department of Geology. Publ. Fj-9. 92 pages.
66. Waltz, J.P. (1988): Hydro-frac basics, *Ground Water Age* 22(7): Page 26-29.
67. Waterloo Hydrogeologic, (2004): FEFLOW v5.0. Internet homepage. Web address: <http://www.feflow.com/index.htm>.
68. Williamson, W.H. and Woolley, D.R. (1980): Hydraulic fracturing to improve the yield of bores in fractured rock. Australian Water Resources Council Technical Paper No. 55, Australian Government Publishing Service, Canberra, Australia.

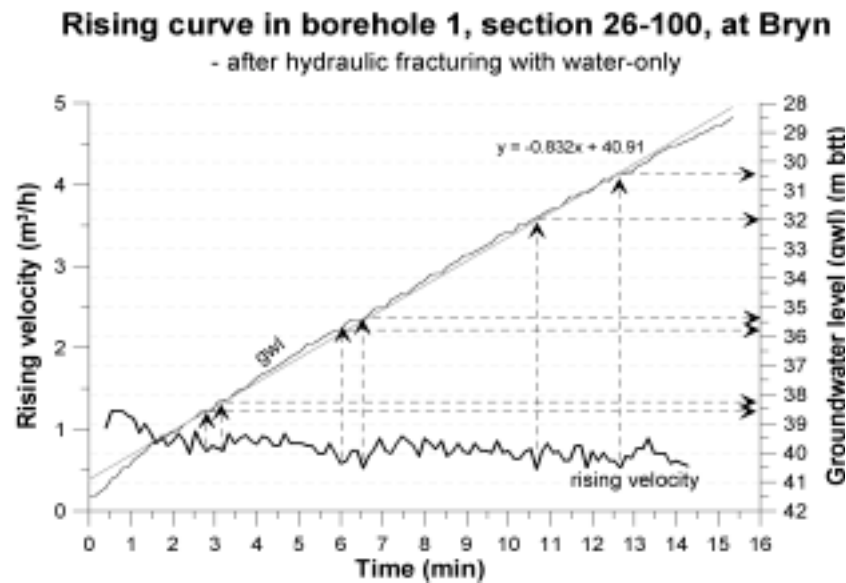
Appendix

Appendix 1 Rise data from Bryn after hydraulic fracturing with water-only

Rising curves from the sectional test pumping in the boreholes at Bryn after hydraulic fracturing with water-only are presented in figures 1–1 to 1–15. Possible water inlets are marked by arrows.

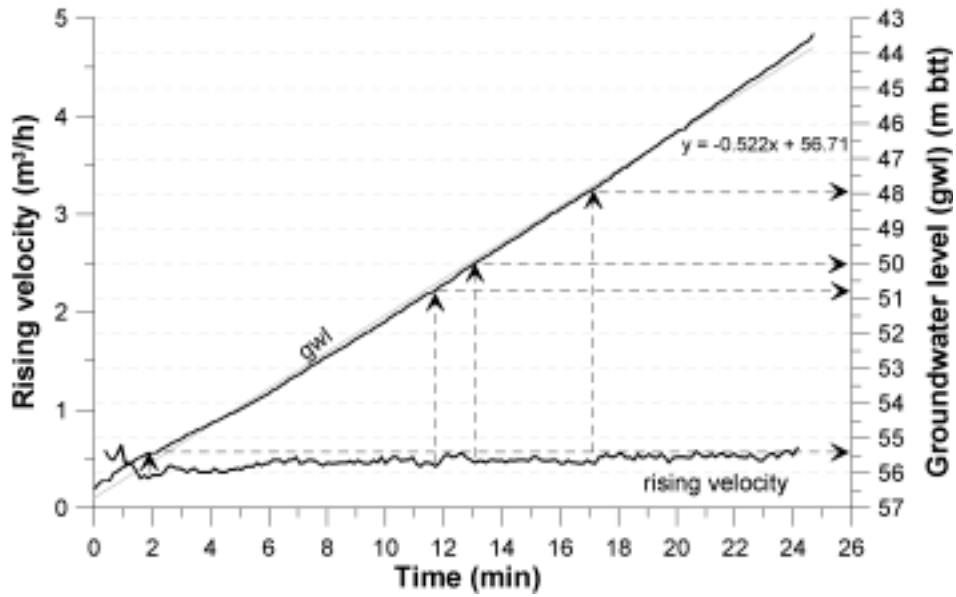


Figur 1–1: Rising curve from sectional test pumping performed after hydraulic fracturing with water-only in borehole 1, section 26-41 at Bryn.



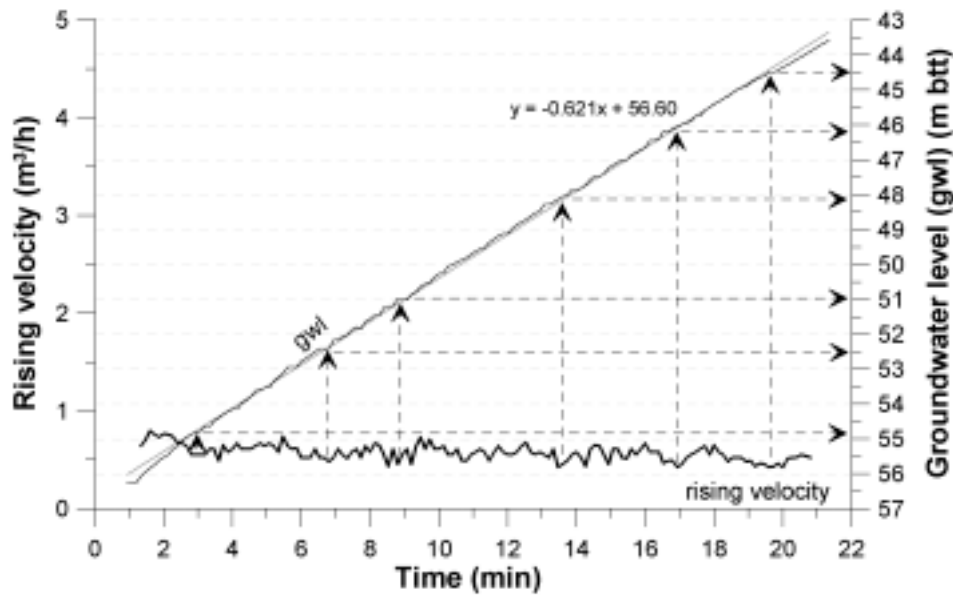
Figur 1–2: Rising curve from sectional test pumping performed after hydraulic fracturing with water-only in borehole 1, section 26-100 at Bryn.

Rising curve in borehole 1, section 41-56, at Bryn
 - after hydraulic fracturing with water-only



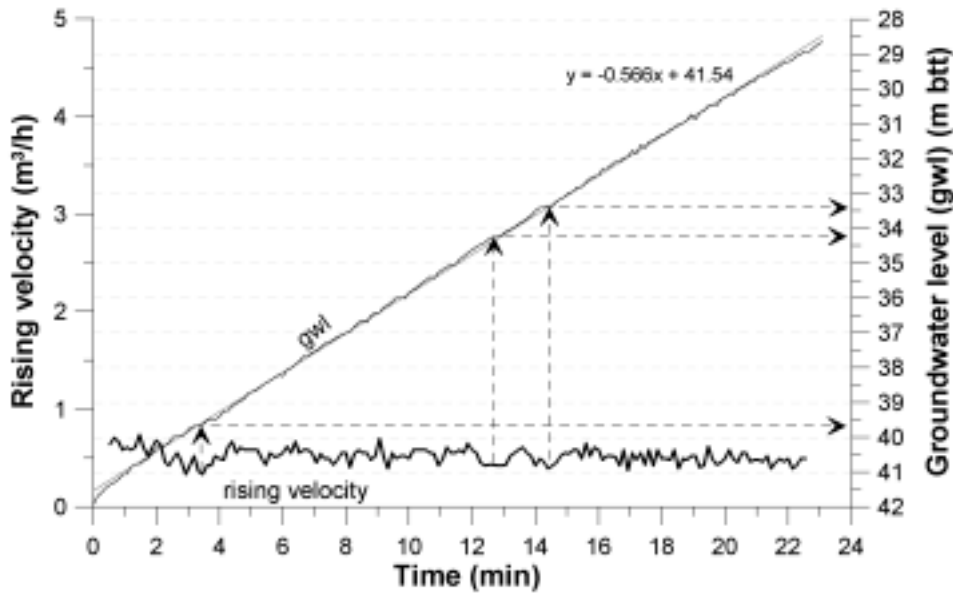
Figur 1-3: Rising curve from sectional test pumping performed after hydraulic fracturing with water-only in borehole 1, section 41-56 at Bryn.

Rising curve in borehole 1, section 41-100, at Bryn
 - after hydraulic fracturing with water-only



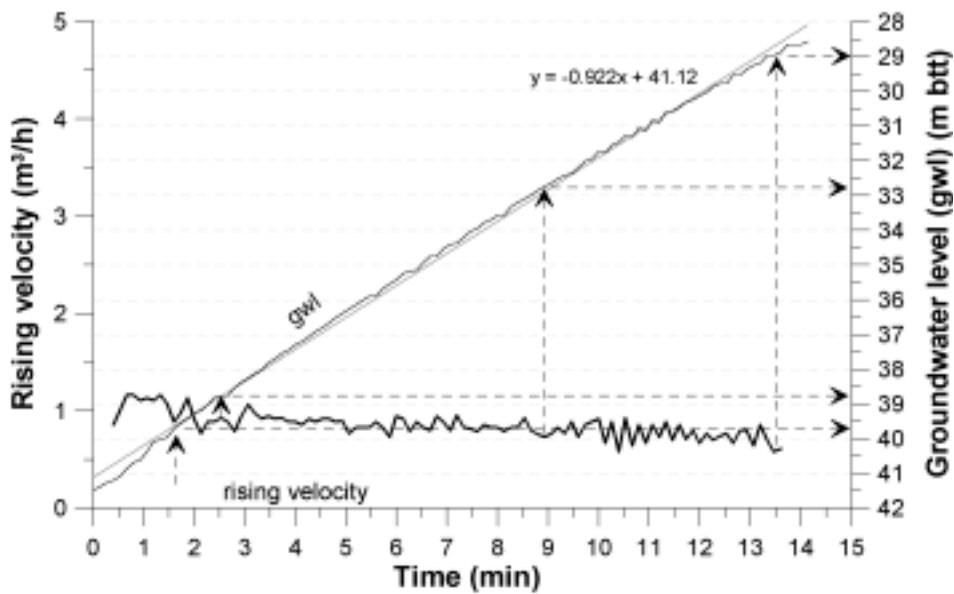
Figur 1-4: Rising curve from sectional test pumping performed after hydraulic fracturing with water-only in borehole 1, section 41-100 at Bryn.

Rising curve in borehole 2, section 26-41, at Bryn
 - after hydraulic fracturing with water-only



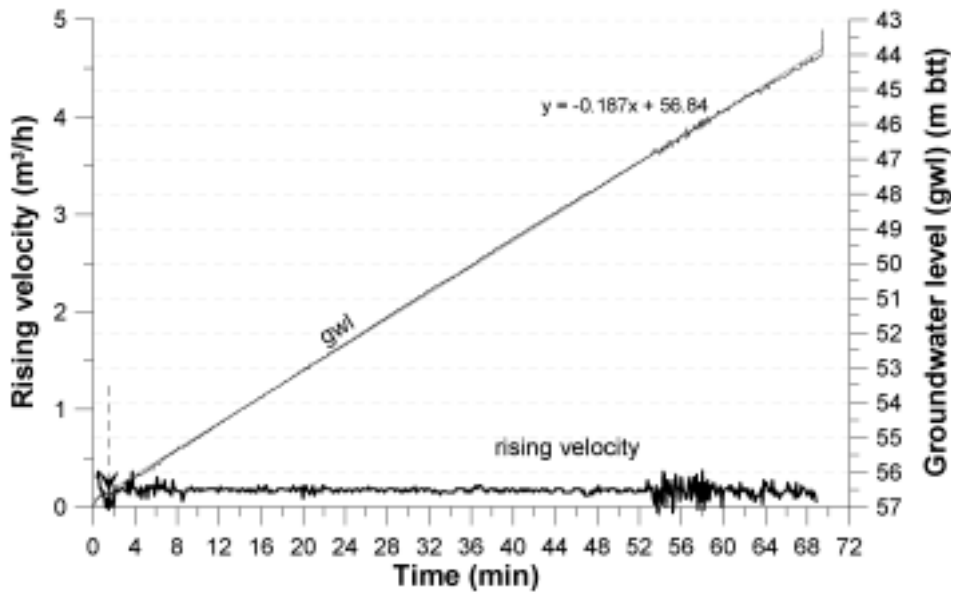
Figur 1-5: Rising curve from sectional test pumping performed after hydraulic fracturing with water-only in borehole 2, section 26-41 at Bryn.

Rising curve in borehole 2, section 26-100, at Bryn
 - after hydraulic fracturing with water-only



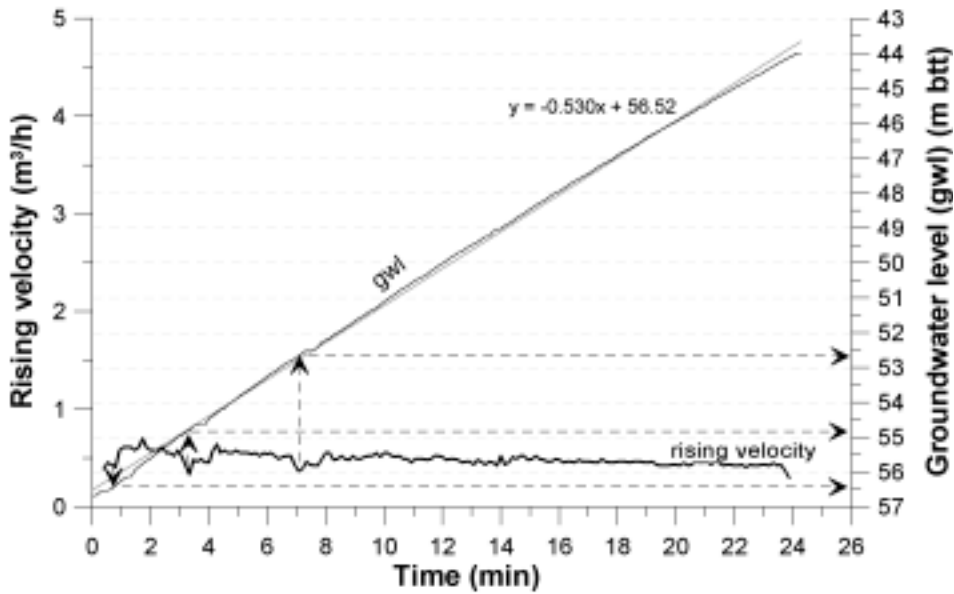
Figur 1-6: Rising curve from sectional test pumping performed after hydraulic fracturing with water-only in borehole 2, section 26-100 at Bryn.

Rising curve in borehole 2, section 41-56, at Bryn
 - after hydraulic fracturing with water-only



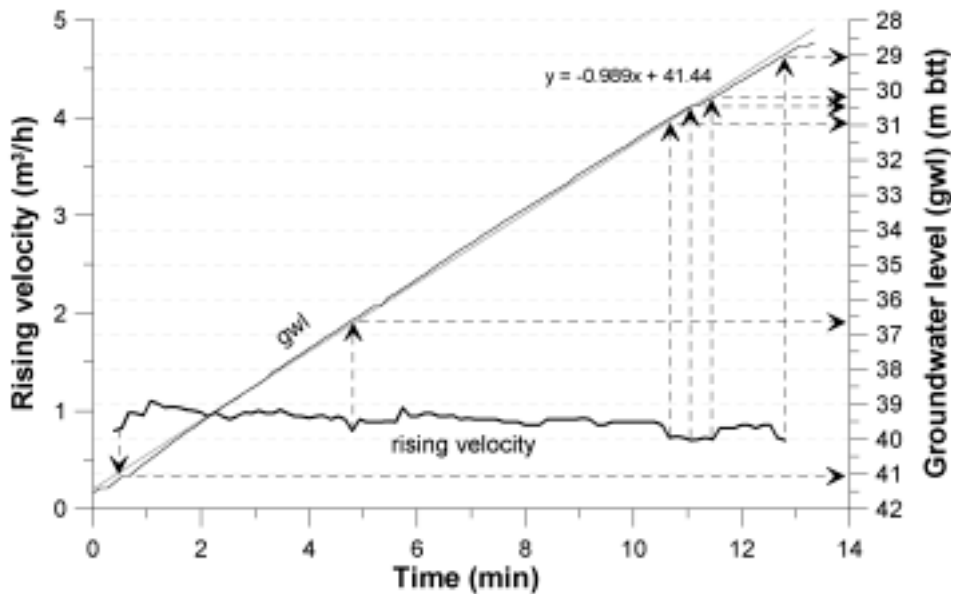
Figur 1-7: Rising curve from sectional test pumping performed after hydraulic fracturing with water-only in borehole 2, section 41-56 at Bryn.

Rising curve in borehole 2, section 41-100, at Bryn
 - after hydraulic fracturing with water-only



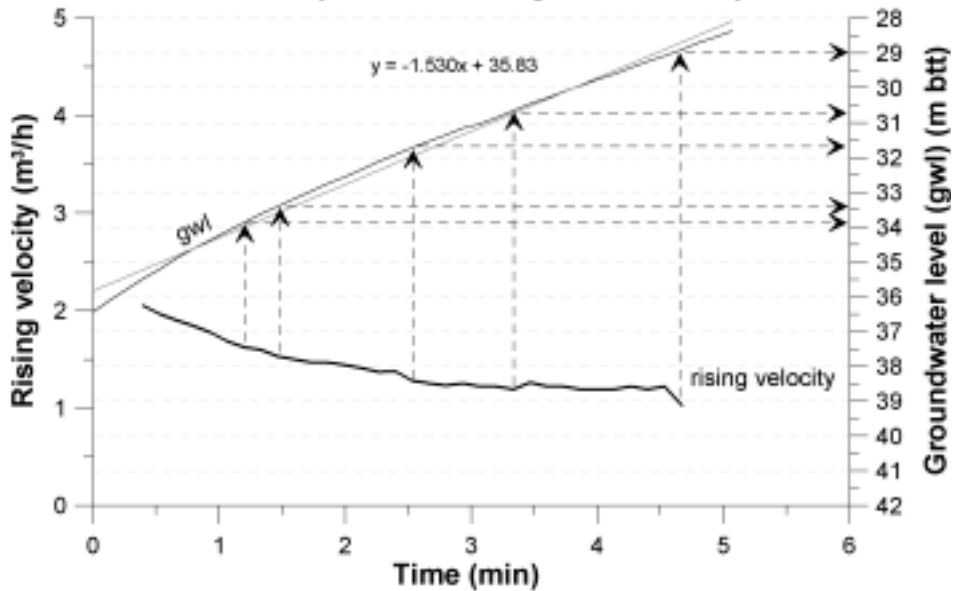
Figur 1-8: Rising curve from sectional test pumping performed after hydraulic fracturing with water-only in borehole 2, section 41-100 at Bryn.

Rising curve in borehole 3, section 26-41, at Bryn
 - after hydraulic fracturing with water-only



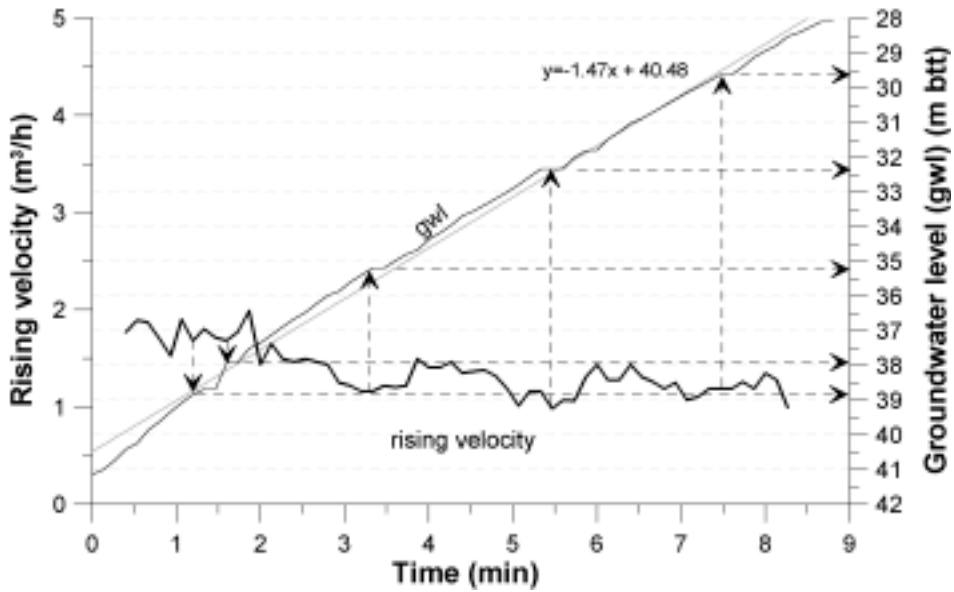
Figur 1-9: Rising curve from sectional test pumping performed after hydraulic fracturing with water-only in borehole 3, section 26-41 at Bryn.

Rising curve in borehole 3, section 26-100, at Bryn
 - after hydraulic fracturing with water-only



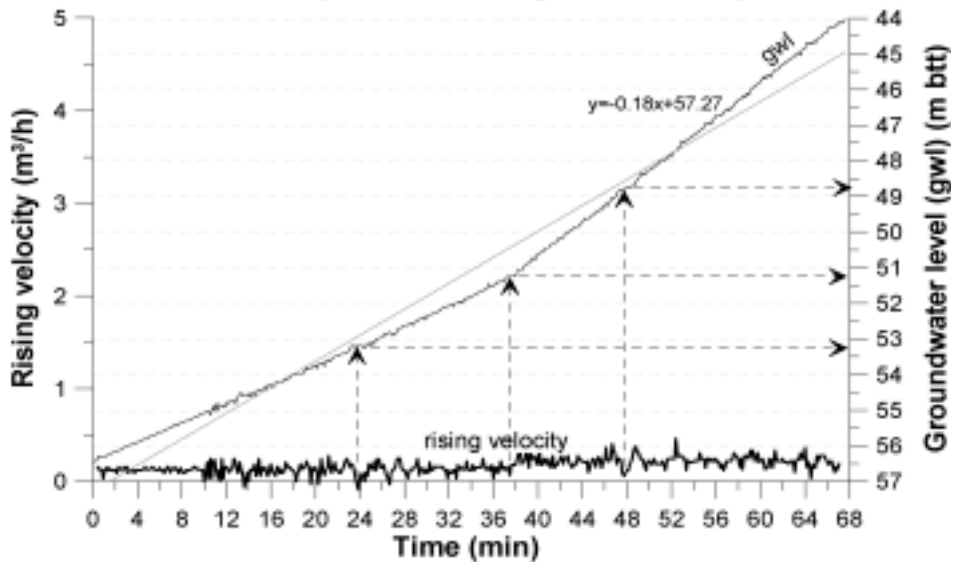
Figur 1-10: Rising curve from sectional test pumping performed after hydraulic fracturing with water-only in borehole 3, section 26-100 at Bryn.

Rising curve in borehole 4, section 26-41, at Bryn
 - after hydraulic fracturing with water-only



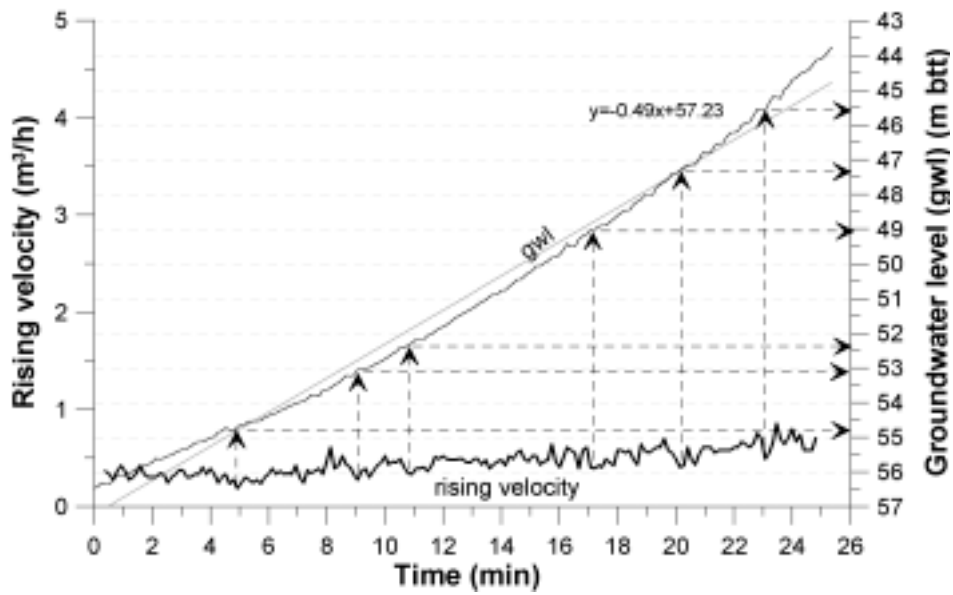
Figur 1-11: Rising curve from sectional test pumping performed after hydraulic fracturing with water-only in borehole 4, section 26-41 at Bryn.

Rising curve in borehole 4, section 41-56, at Bryn
 - after hydraulic fracturing with water-only



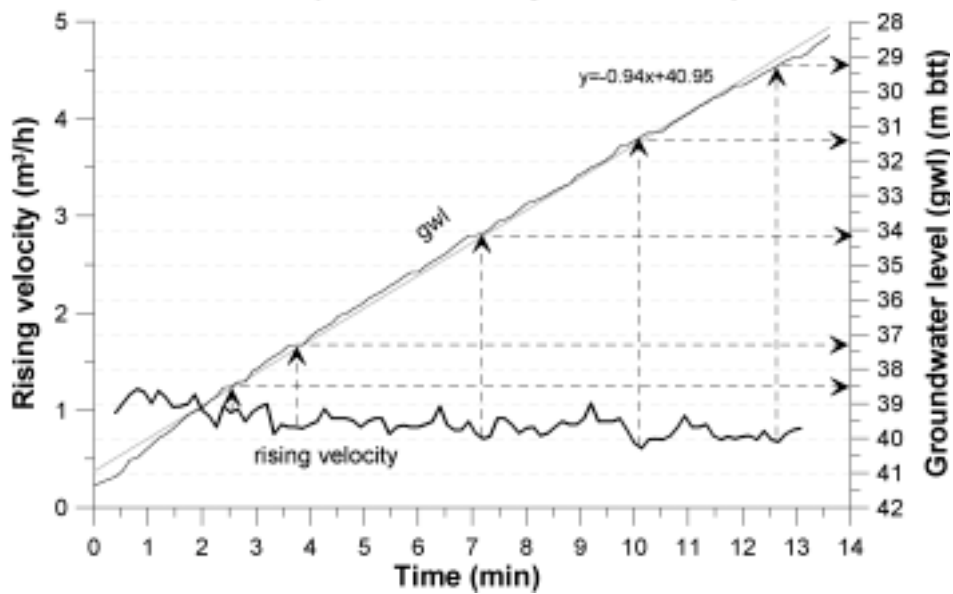
Figur 1-12: Rising curve from sectional test pumping performed after hydraulic fracturing with water-only in borehole 4, section 41-56 at Bryn.

Rising curve in borehole 4, section 41-100, at Bryn
 - after hydraulic fracturing with water-only



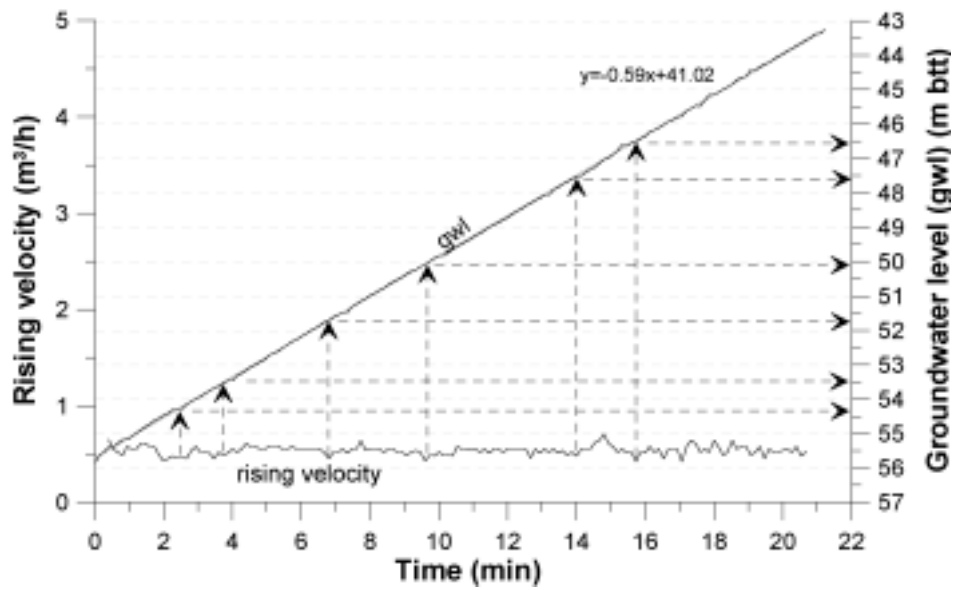
Figur 1-13: Rising curve from sectional test pumping performed after hydraulic fracturing with water-only in borehole 4, section 41-100 at Bryn.

Rising curve in borehole 5, section 26-41, at Bryn
 - after hydraulic fracturing with water-only



Figur 1-14: Rising curve from sectional test pumping performed after hydraulic fracturing with water-only in borehole 5, section 26-41 at Bryn.

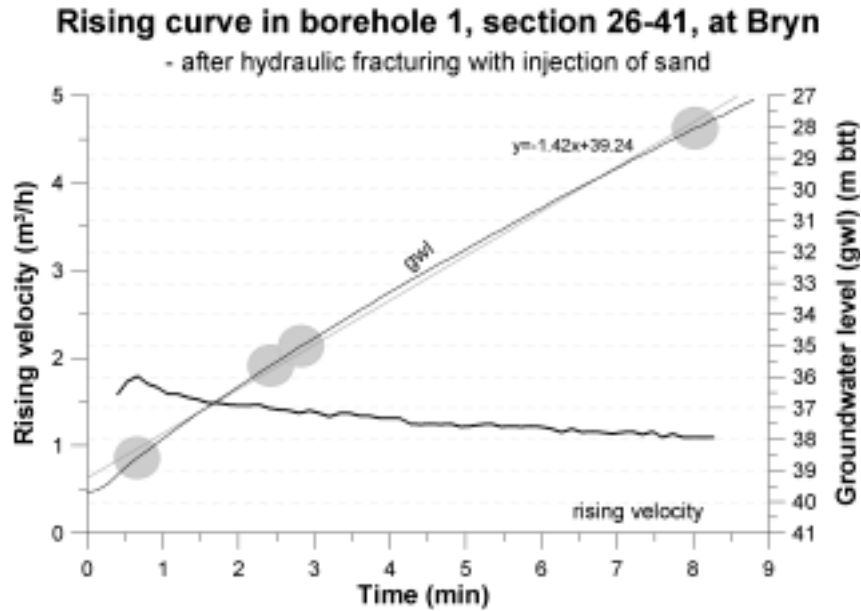
Rising curve in borehole 5, section 41-56, at Bryn
 - after hydraulic fracturing with water-only



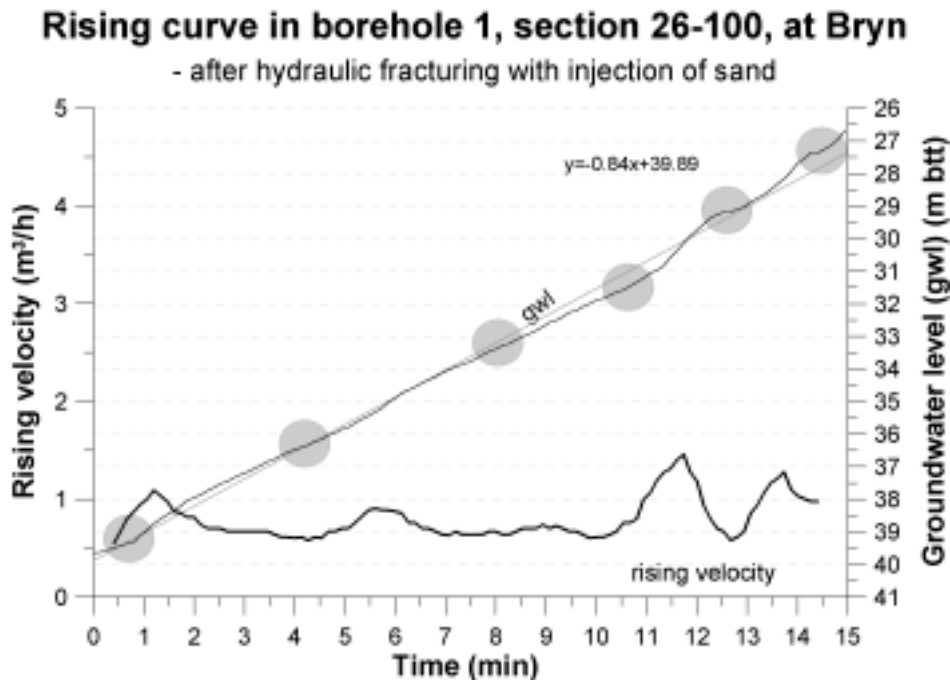
Figur 1-15: Rising curve from sectional test pumping performed after hydraulic fracturing with water-only in borehole 5, section 41-56 at Bryn.

Appendix 2 Rise data from Bryn after hydraulic fracturing with injection of sand

Rising curves from the sectional test pumping in the boreholes at Bryn after hydraulic fracturing with injection of sand are presented in figures 2-1 to 2-22. Possible water inlets are marked with shaded circles.

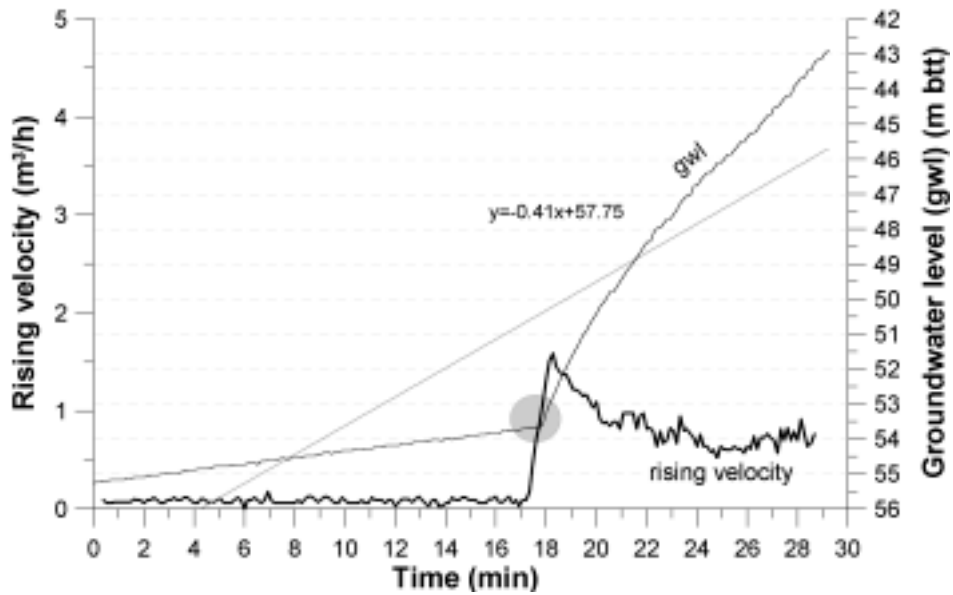


Figur 2-1: Rising curve from sectional test pumping performed after hydraulic fracturing with injection of sand in borehole 1, section 26-41 at Bryn.



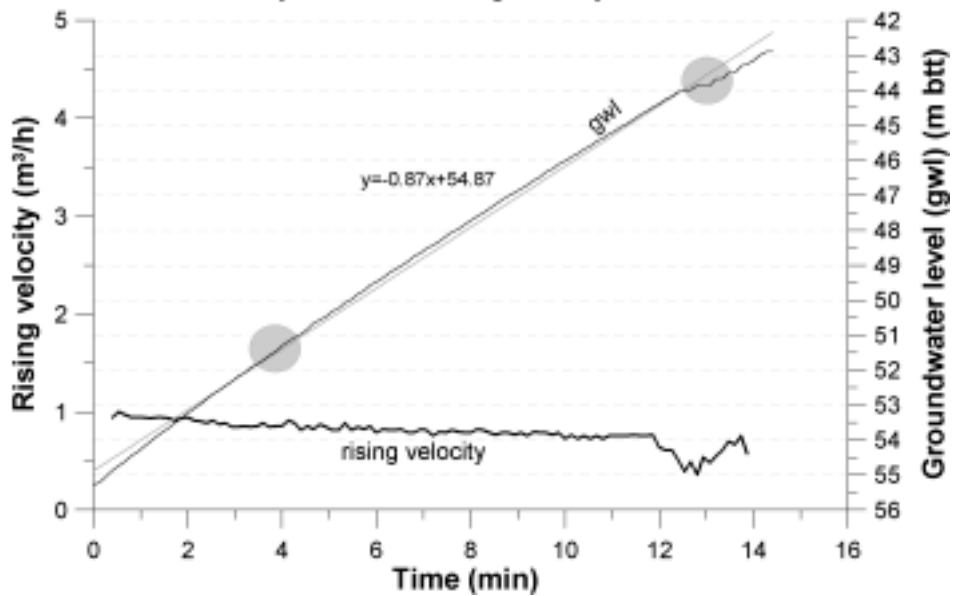
Figur 2-2: Rising curve from sectional test pumping performed after hydraulic fracturing with injection of sand in borehole 1, section 26-100 at Bryn.

Rising curve in borehole 1, section 41-56, at Bryn
 - after hydraulic fracturing with injection of sand

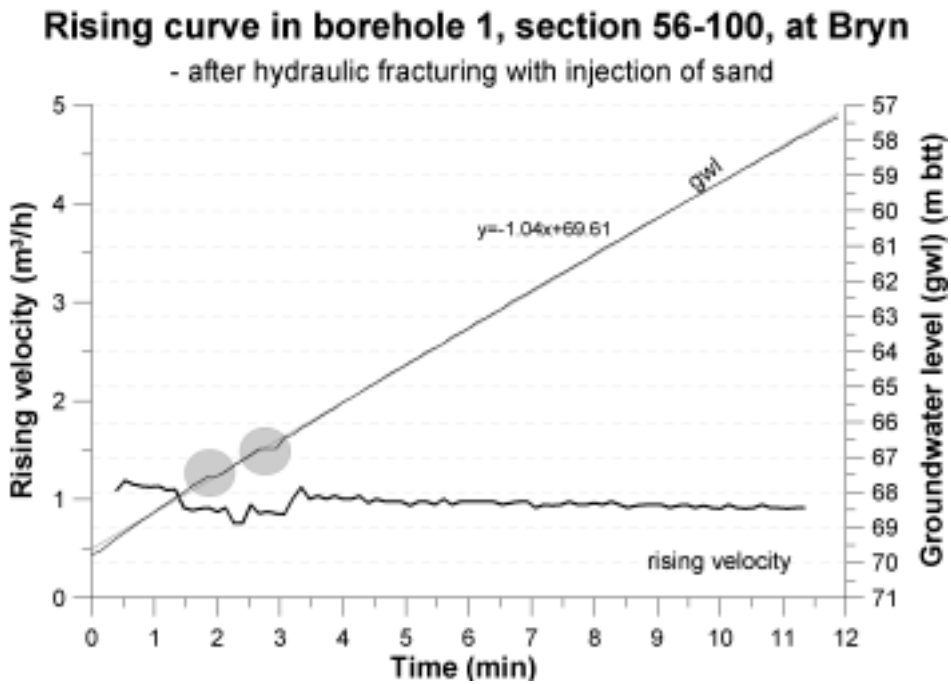


Figur 2-3: Rising curve from sectional test pumping performed after hydraulic fracturing with injection of sand in borehole 1, section 41-56 at Bryn.

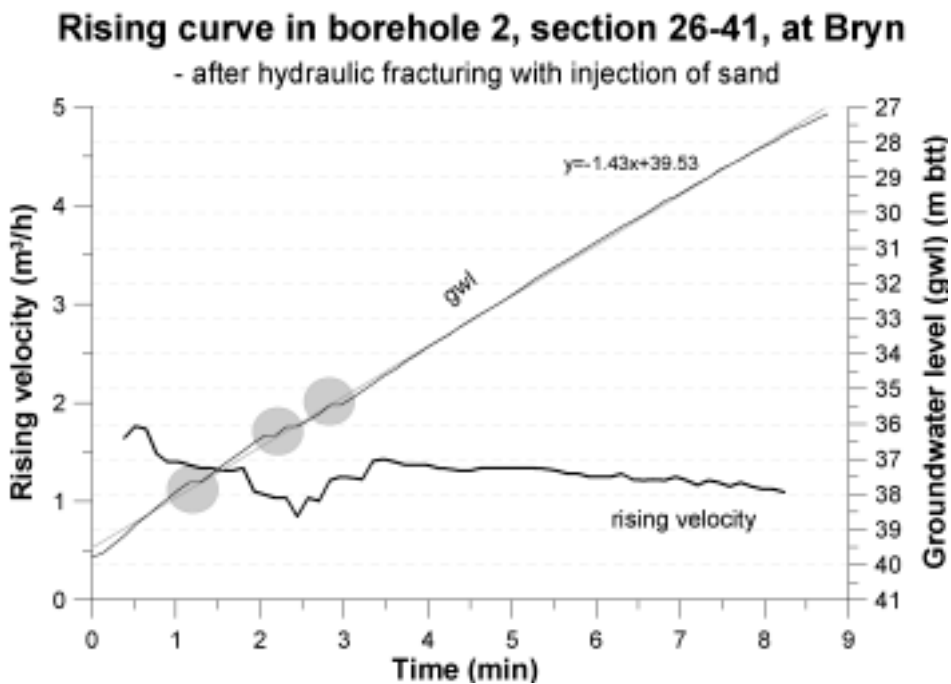
Rising curve in borehole 1, section 41-100, at Bryn
 - after hydraulic fracturing with injection of sand



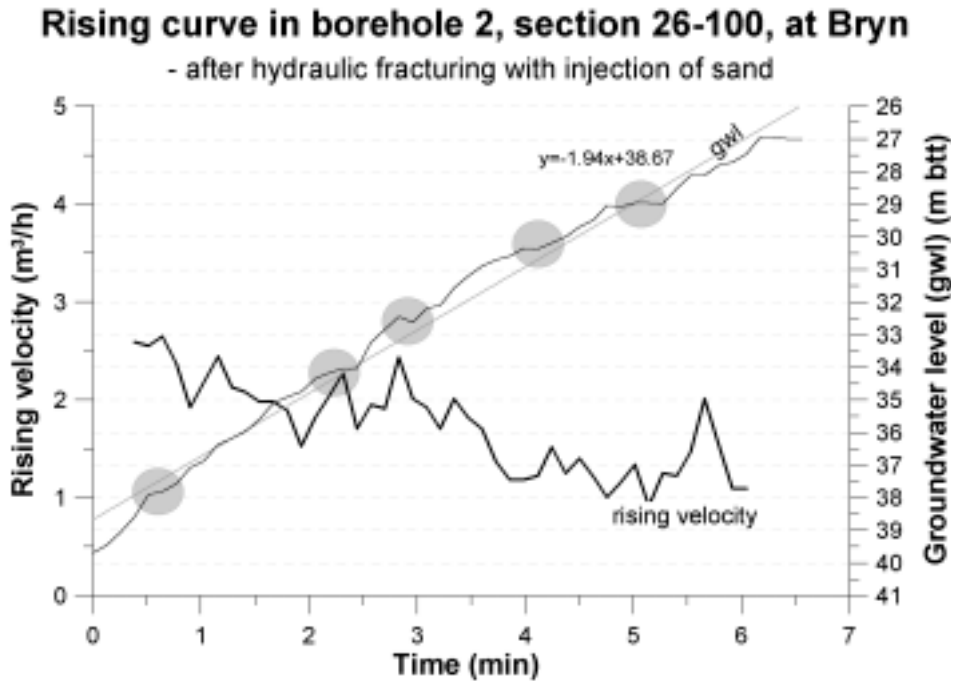
Figur 2-4: Rising curve from sectional test pumping performed after hydraulic fracturing with injection of sand in borehole 1, section 41-100 at Bryn.



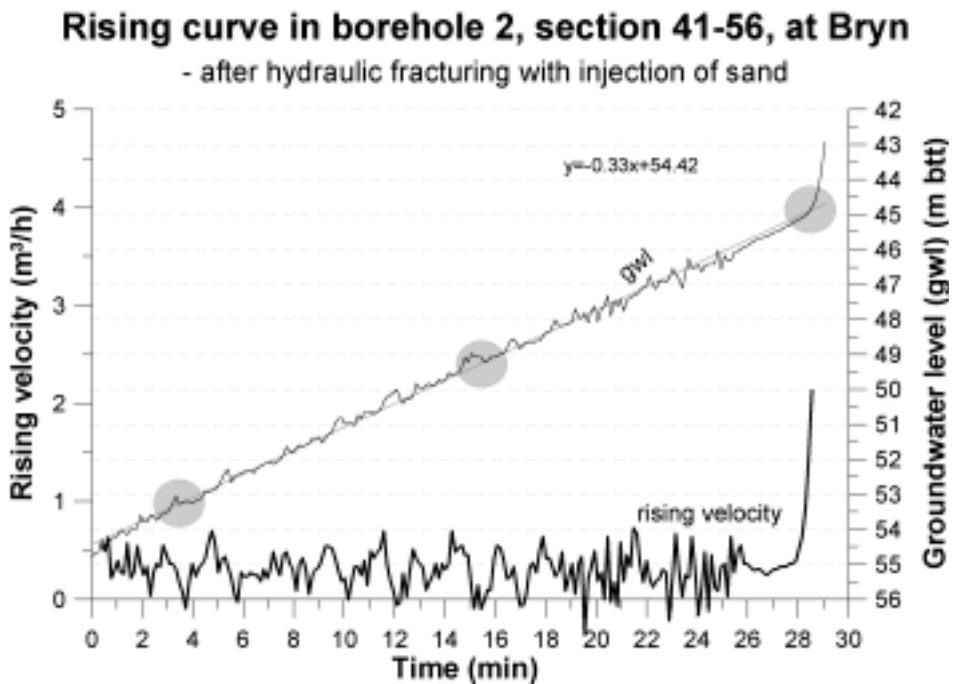
Figur 2-5: Rising curve from sectional test pumping performed after hydraulic fracturing with injection of sand in borehole 1, section 56-100 at Bryn.



Figur 2-6: Rising curve from sectional test pumping performed after hydraulic fracturing with injection of sand in borehole 2, section 26-41 at Bryn.

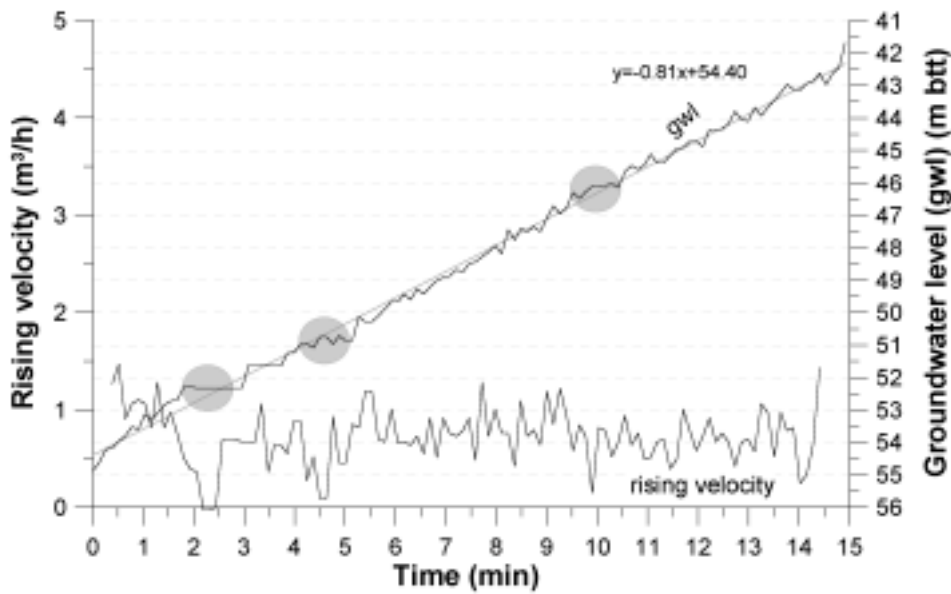


Figur 2-7: Rising curve from sectional test pumping performed after hydraulic fracturing with injection of sand in borehole 2, section 26-100 at Bryn.



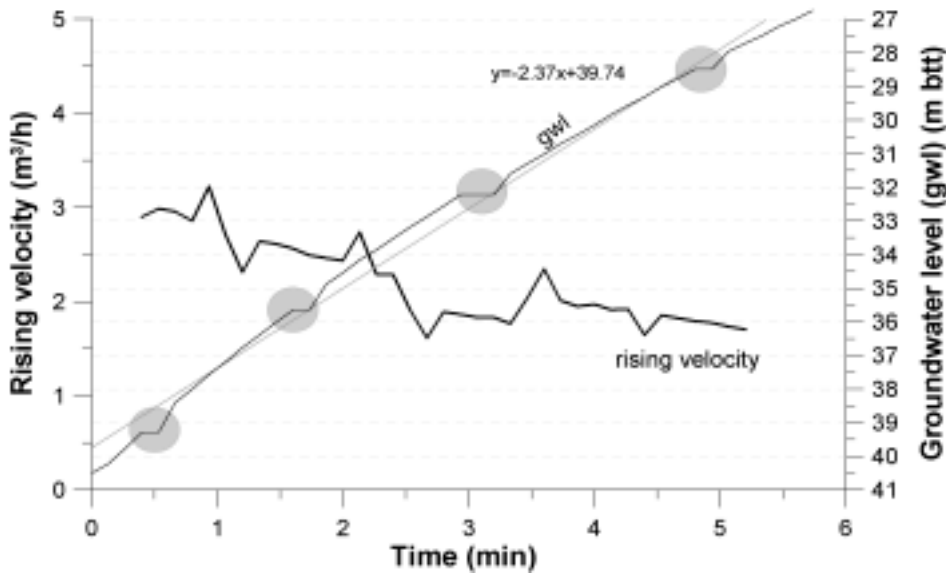
Figur 2-8: Rising curve from sectional test pumping performed after hydraulic fracturing with injection of sand in borehole 2, section 41-56 at Bryn.

Rising curve in borehole 2, section 41-100, at Bryn
 - after hydraulic fracturing with injection of sand



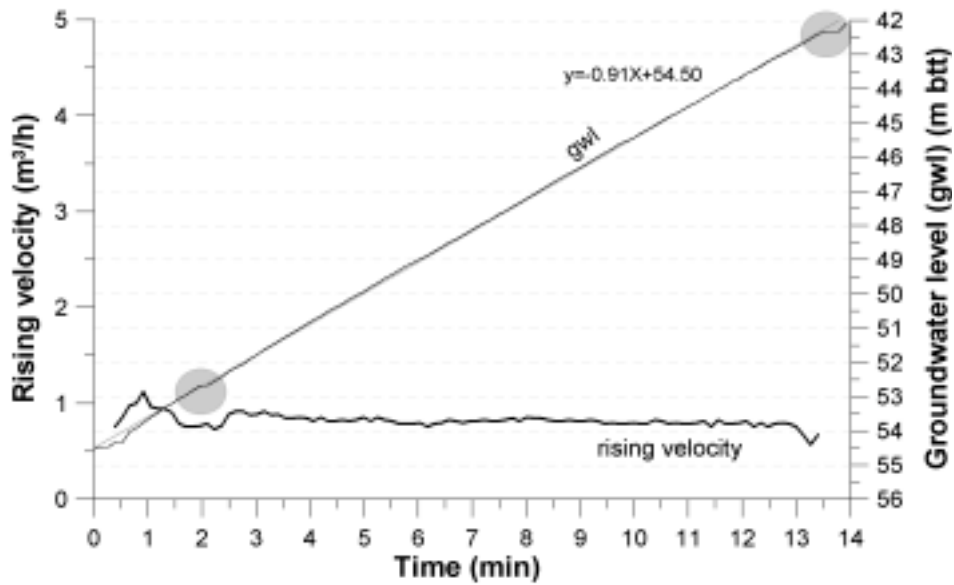
Figur 2-9: Rising curve from sectional test pumping performed after hydraulic fracturing with injection of sand in borehole 2, section 41-100 at Bryn.

Rising curve in borehole 3, section 27-42, at Bryn
 - after hydraulic fracturing with injection of sand



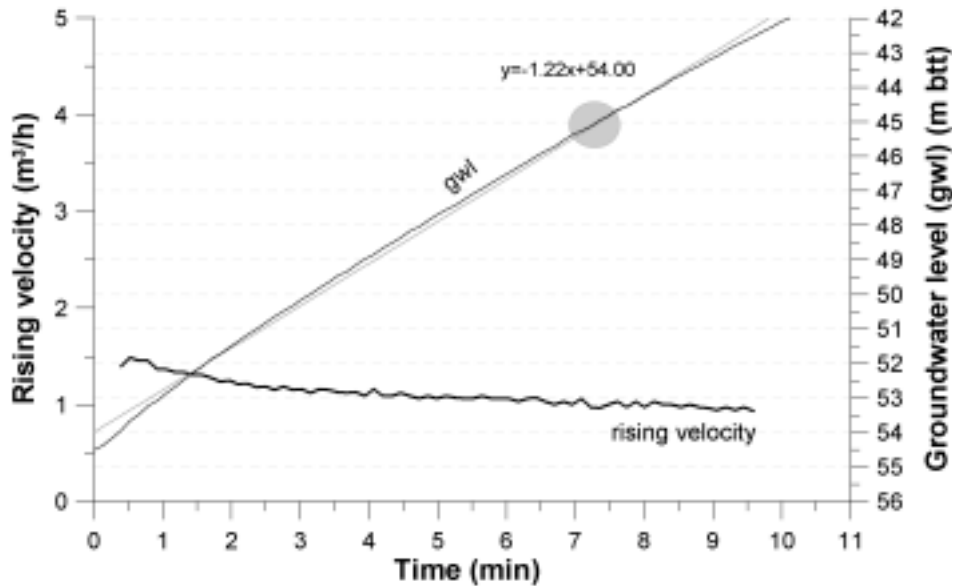
Figur 2-10: Rising curve from sectional test pumping performed after hydraulic fracturing with injection of sand in borehole 3, section 27-42 at Bryn.

Rising curve in borehole 3, section 41-56, at Bryn
 - after hydraulic fracturing with injection of sand



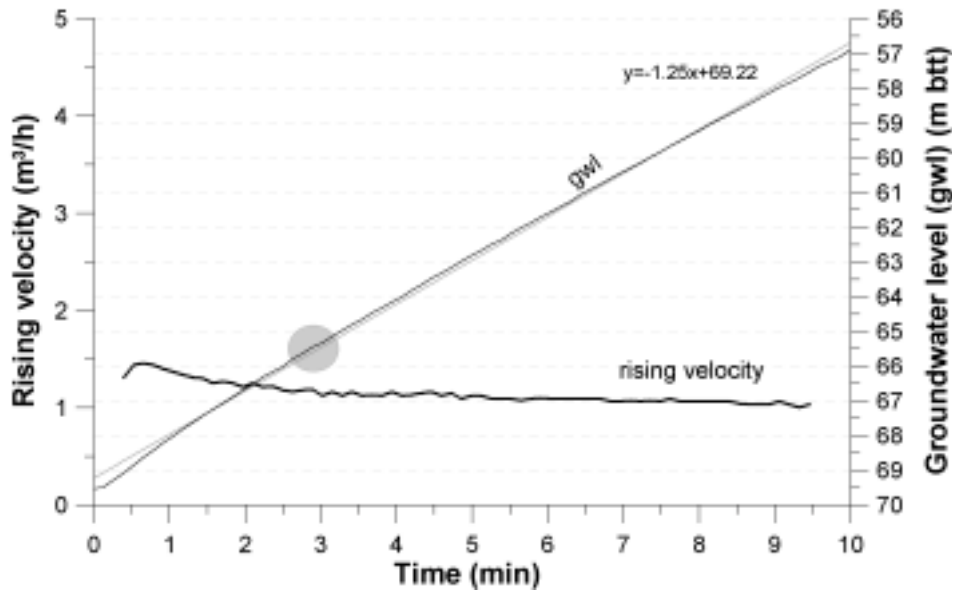
Figur 2-11: Rising curve from sectional test pumping performed after hydraulic fracturing with injection of sand in borehole 3, section 41-56 at Bryn.

Rising curve in borehole 3, section 41-100, at Bryn
 - after hydraulic fracturing with injection of sand



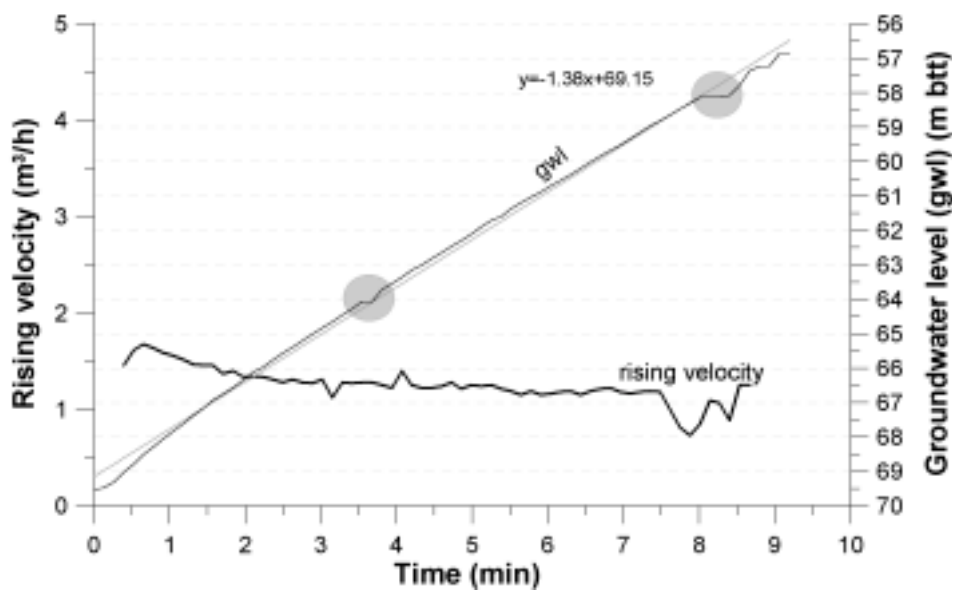
Figur 2-12: Rising curve from sectional test pumping performed after hydraulic fracturing with injection of sand in borehole 3, section 41-100 at Bryn.

Rising curve in borehole 3, section 56-71, at Bryn
 - after hydraulic fracturing with injection of sand



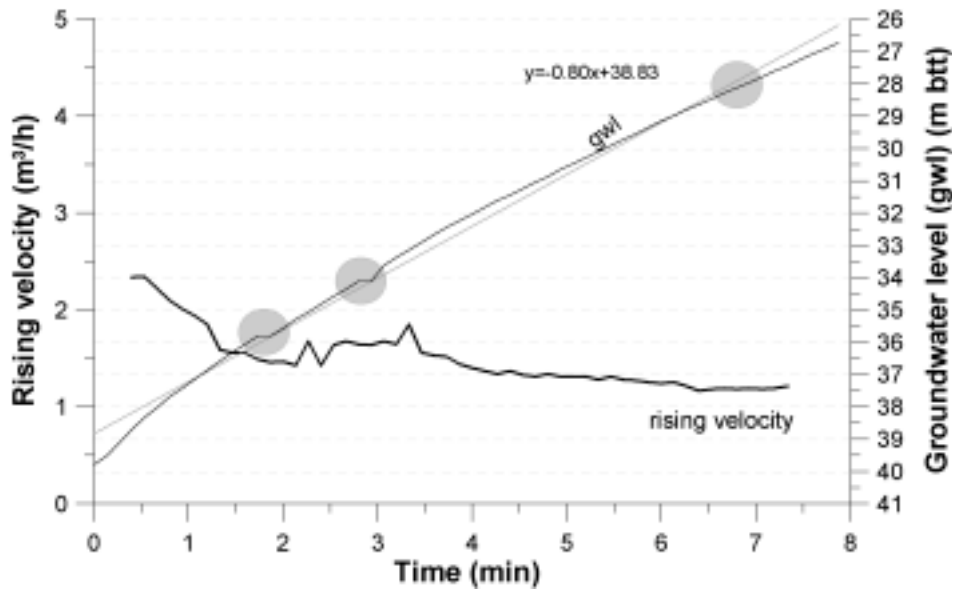
Figur 2-13: Rising curve from sectional test pumping performed after hydraulic fracturing with injection of sand in borehole 3, section 56-71 at Bryn.

Rising curve in borehole 3, section 56-100, at Bryn
 - after hydraulic fracturing with injection of sand



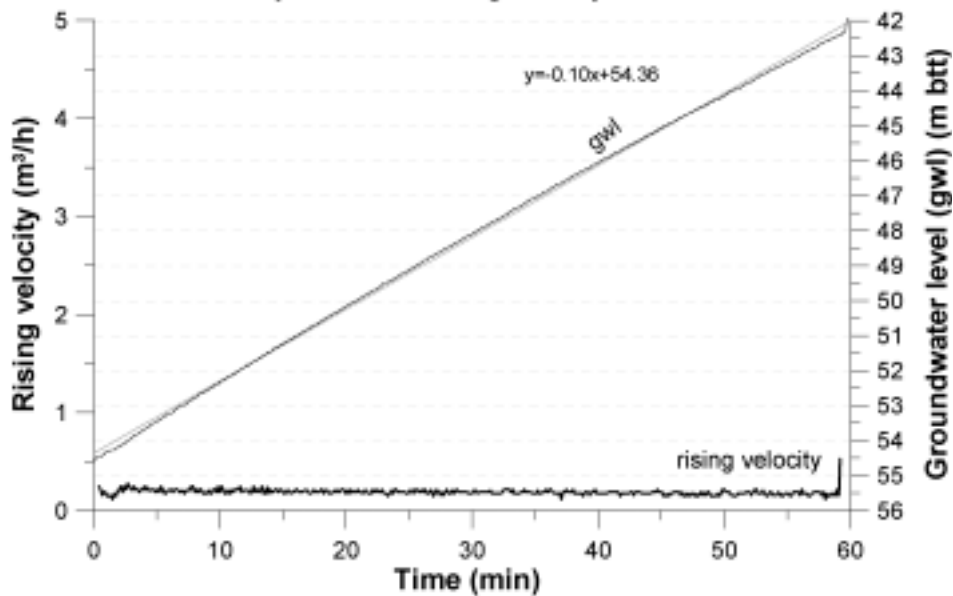
Figur 2-14: Rising curve from sectional test pumping performed after hydraulic fracturing with injection of sand in borehole 3, section 56-100 at Bryn.

Rising curve in borehole 4, section 26-41, at Bryn
 - after hydraulic fracturing with injection of sand



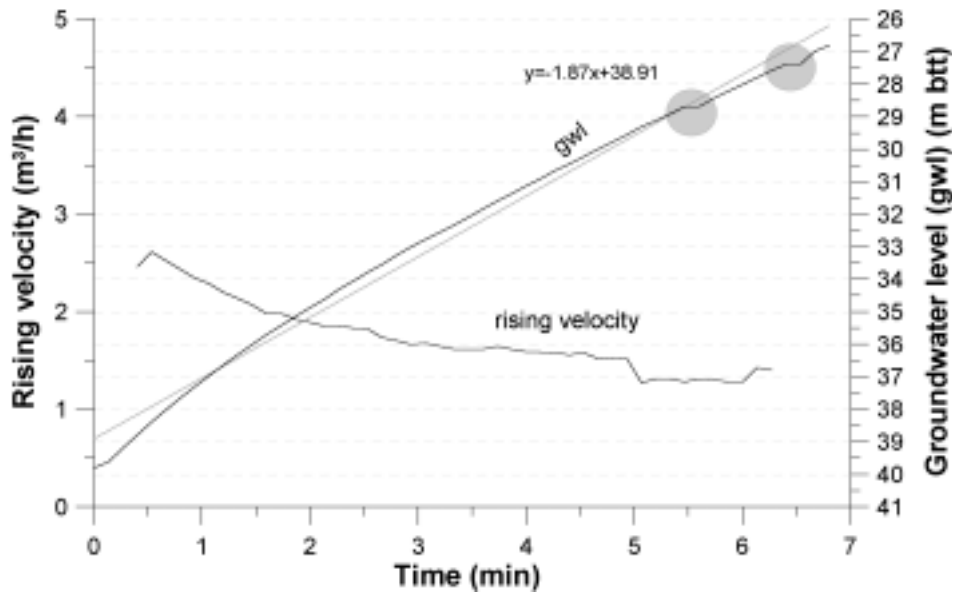
Figur 2-15: Rising curve from sectional test pumping performed after hydraulic fracturing with injection of sand in borehole 4, section 26-41 at Bryn.

Rising curve in borehole 4, section 41-100, at Bryn
 - after hydraulic fracturing with injection of sand



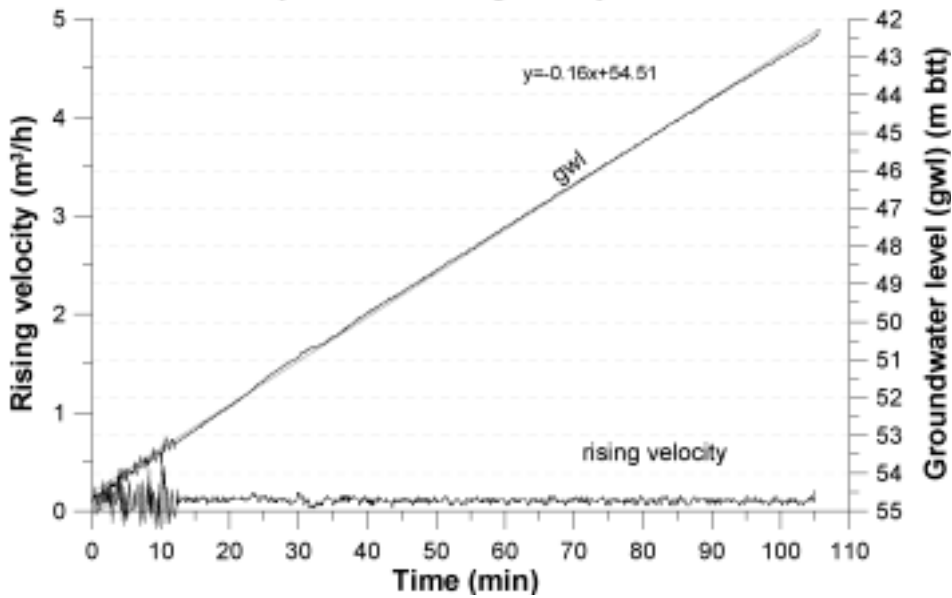
Figur 2-16: Rising curve from sectional test pumping performed after hydraulic fracturing with injection of sand in borehole 4, section 41-100 at Bryn.

Rising curve in borehole 5, section 26-41, at Bryn
 - after hydraulic fracturing with injection of sand



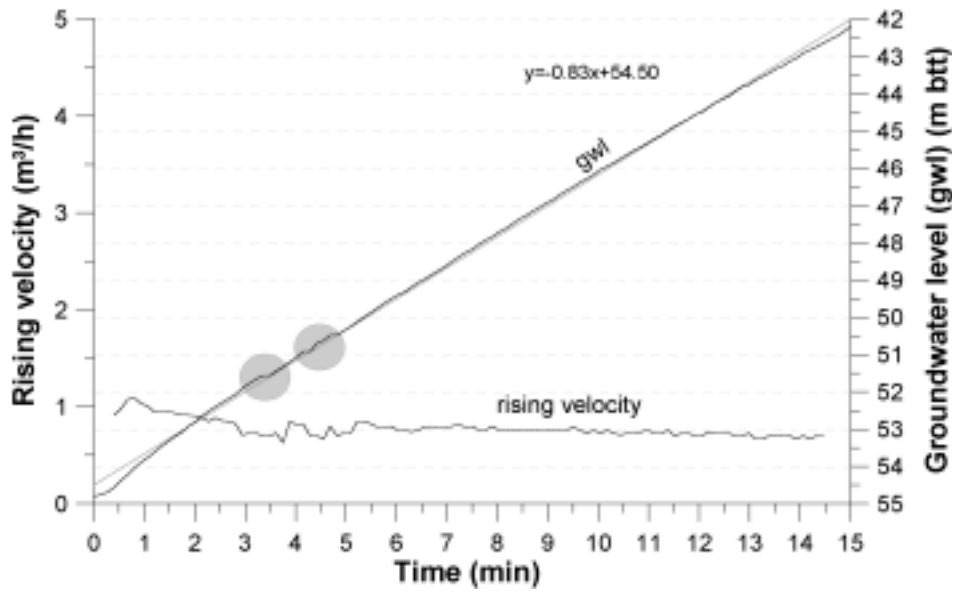
Figur 2-17: Rising curve from sectional test pumping performed after hydraulic fracturing with injection of sand in borehole 5, section 26-41 at Bryn.

Rising curve in borehole 5, section 41-56, at Bryn
 - after hydraulic fracturing with injection of sand



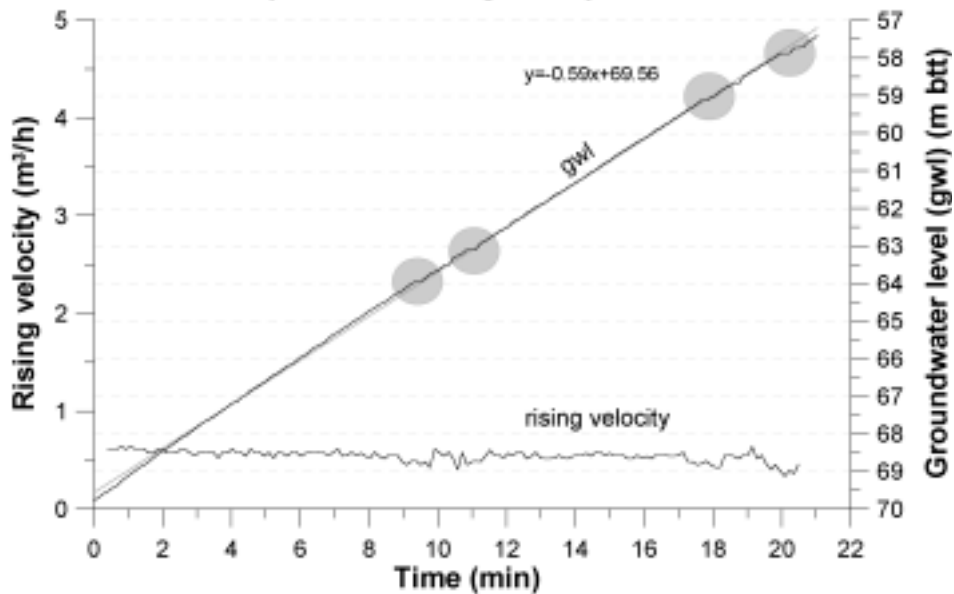
Figur 2-18: Rising curve from sectional test pumping performed after hydraulic fracturing with injection of sand in borehole 5, section 41-56 at Bryn.

Rising curve in borehole 5, section 41-100, at Bryn
 - after hydraulic fracturing with injection of sand

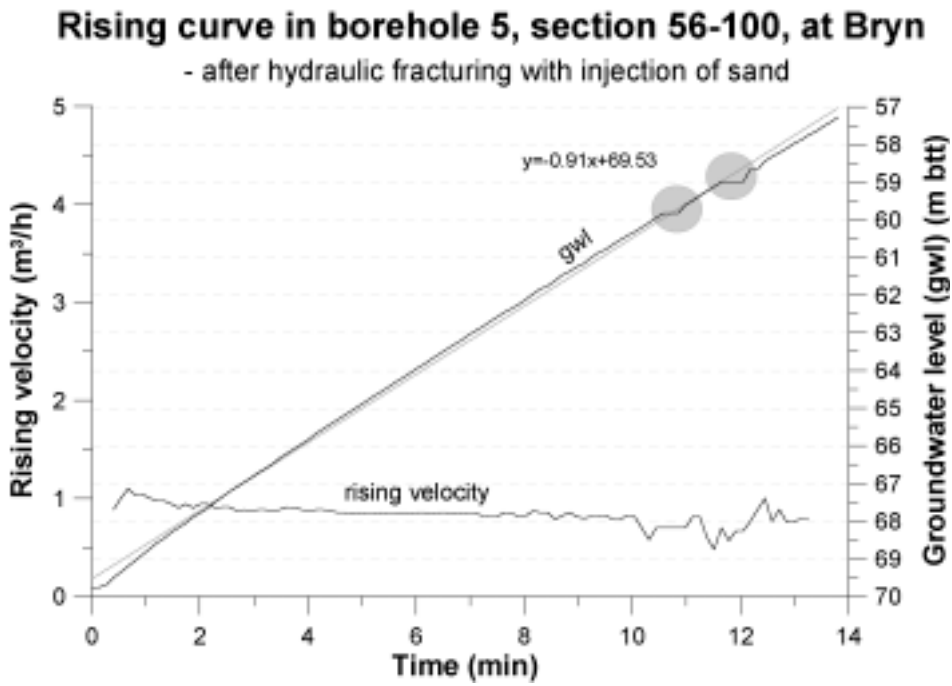


Figur 2-19: Rising curve from sectional test pumping performed after hydraulic fracturing with injection of sand in borehole 5, section 41-100 at Bryn.

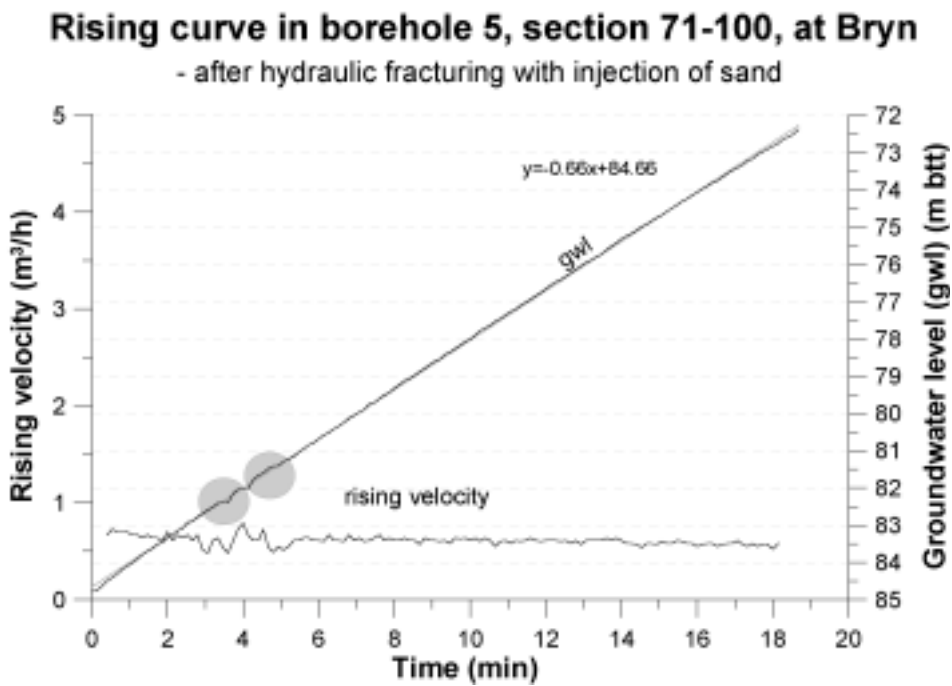
Rising curve in borehole 5, section 56-71, at Bryn
 - after hydraulic fracturing with injection of sand



Figur 2-20: Rising curve from sectional test pumping performed after hydraulic fracturing with injection of sand in borehole 5, section 56-71 at Bryn.



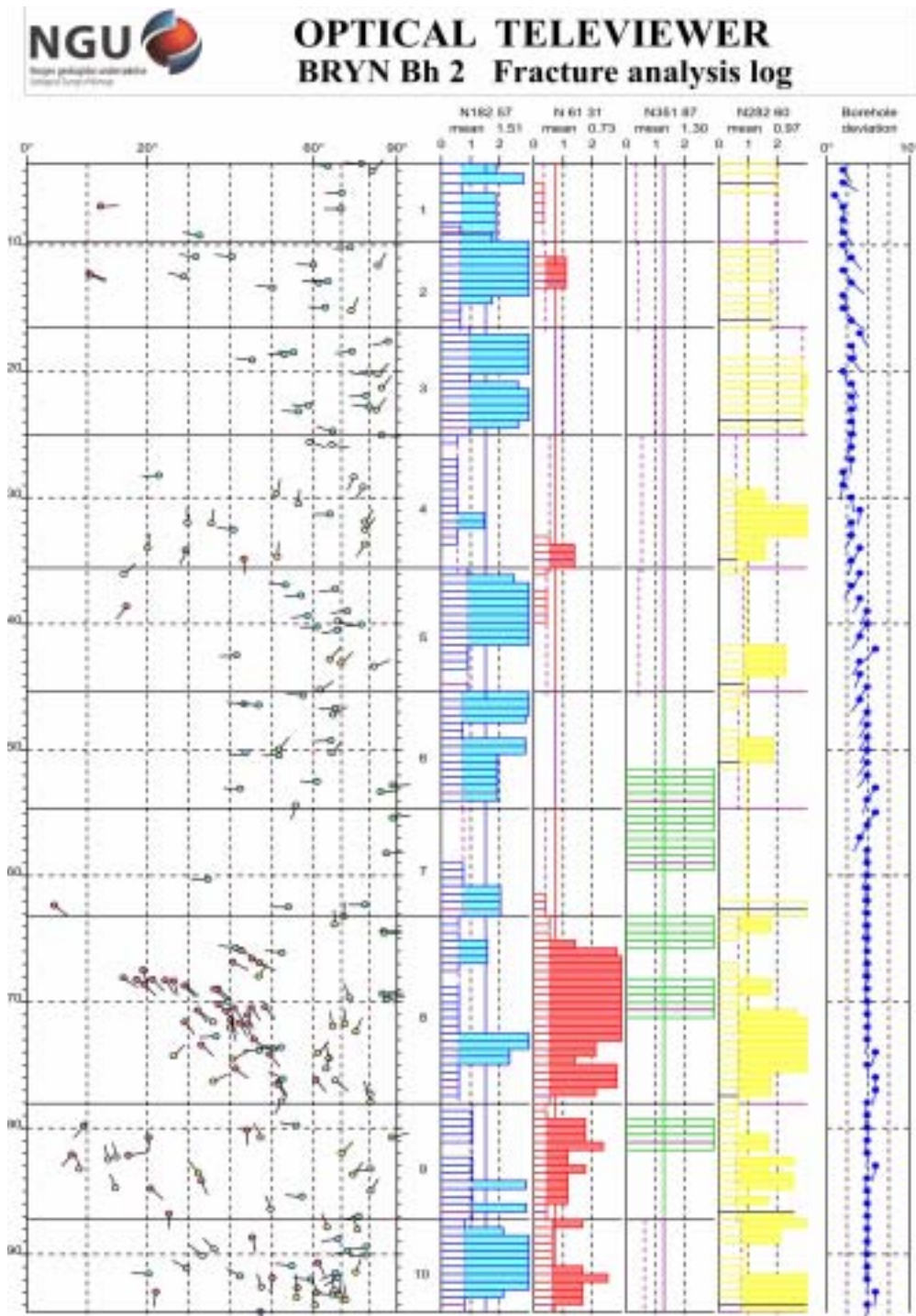
Figur 2-21: Rising curve from sectional test pumping performed after hydraulic fracturing with injection of sand in borehole 5, section 56-100 at Bryn.



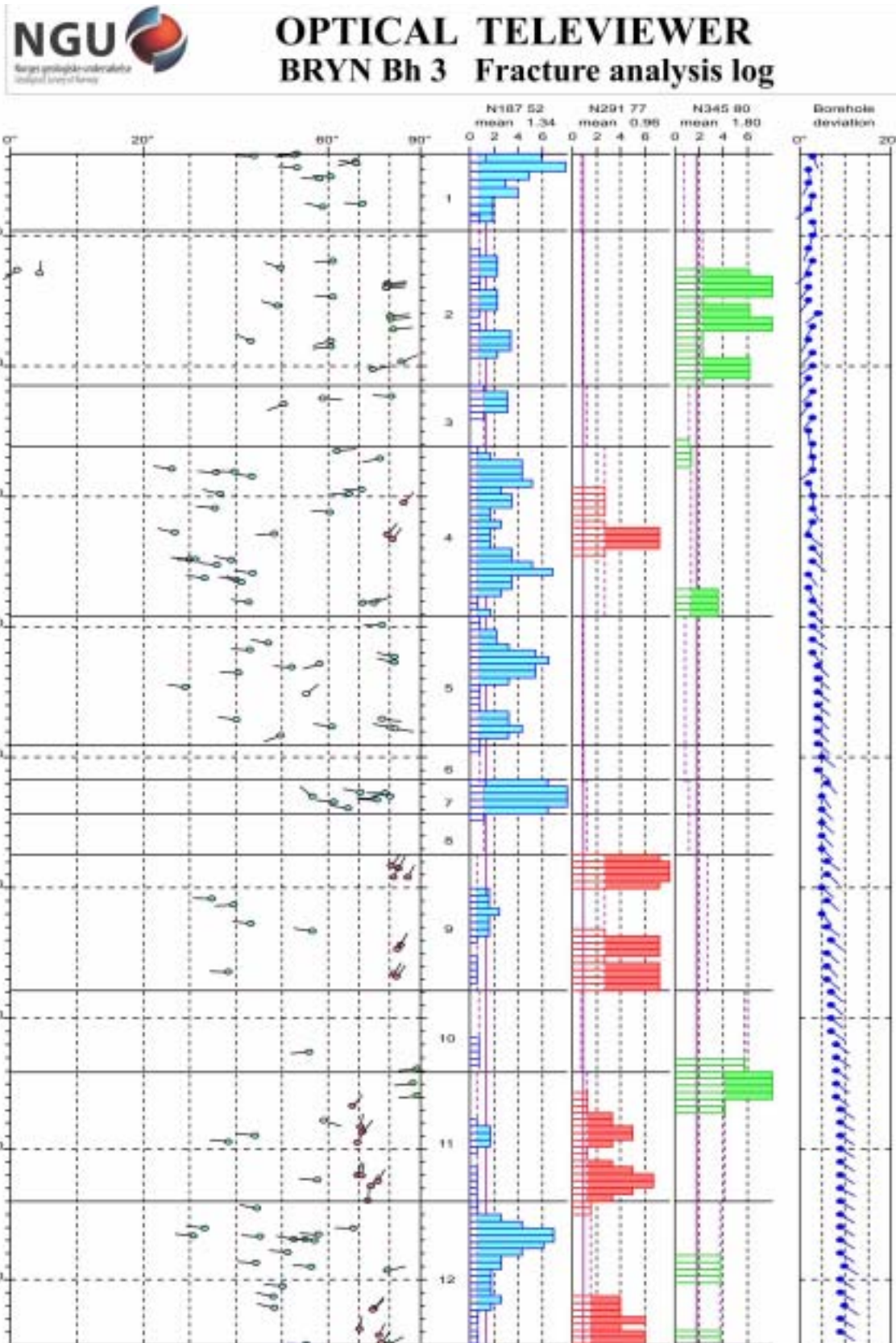
Figur 2-22: Rising curve from sectional test pumping performed after hydraulic fracturing with injection of sand in borehole 5, section 71-100 at Bryn.

Appendix 3 Fracture analysis - histograms and stereograms

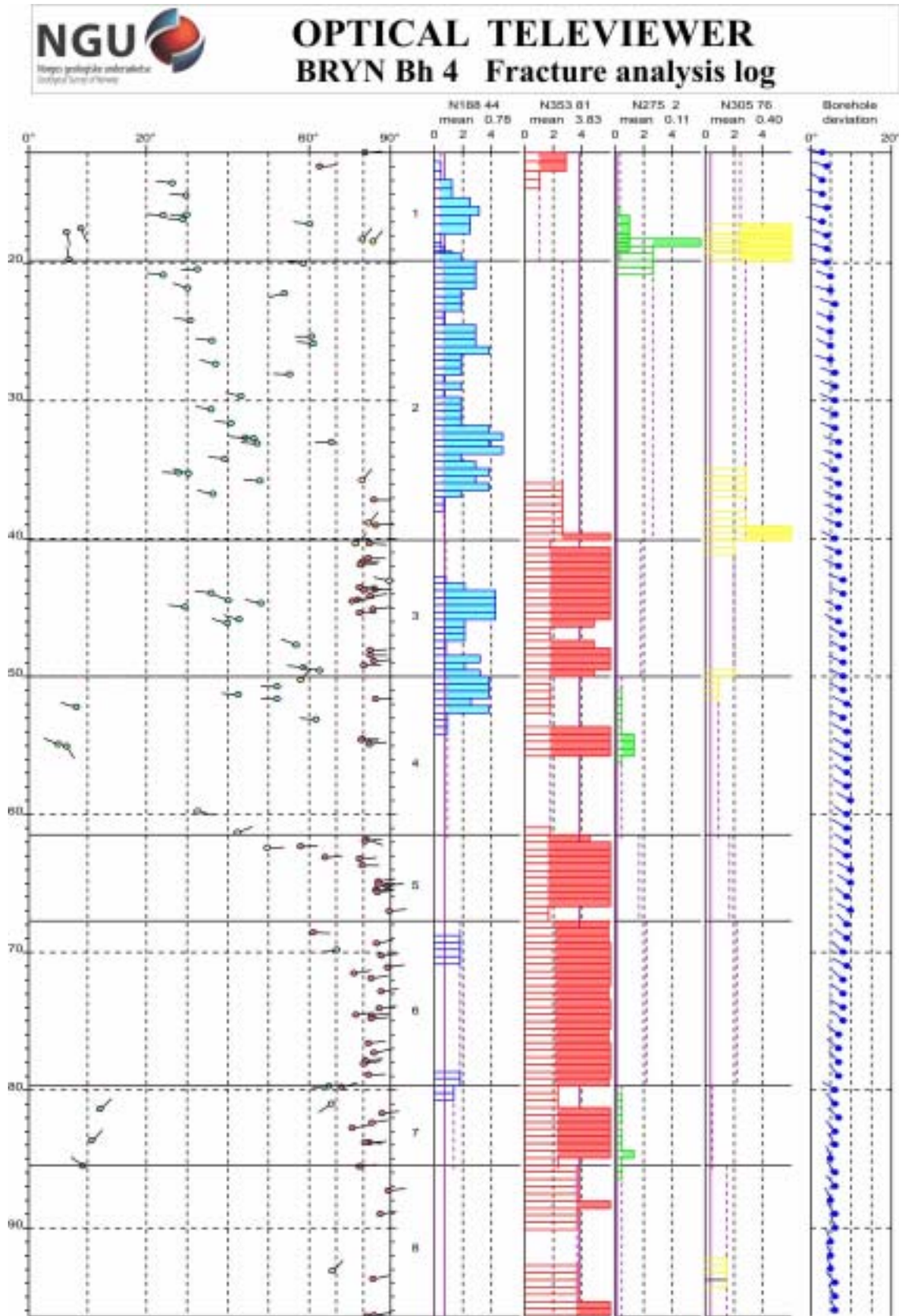
Frequency histograms and corresponding stereograms from the fracture mapping with the optical televiewer in the boreholes at Bryn and borehole 1 at EAB are presented in figures 3–1 to 3–9. Each colour represents a different fracture system.



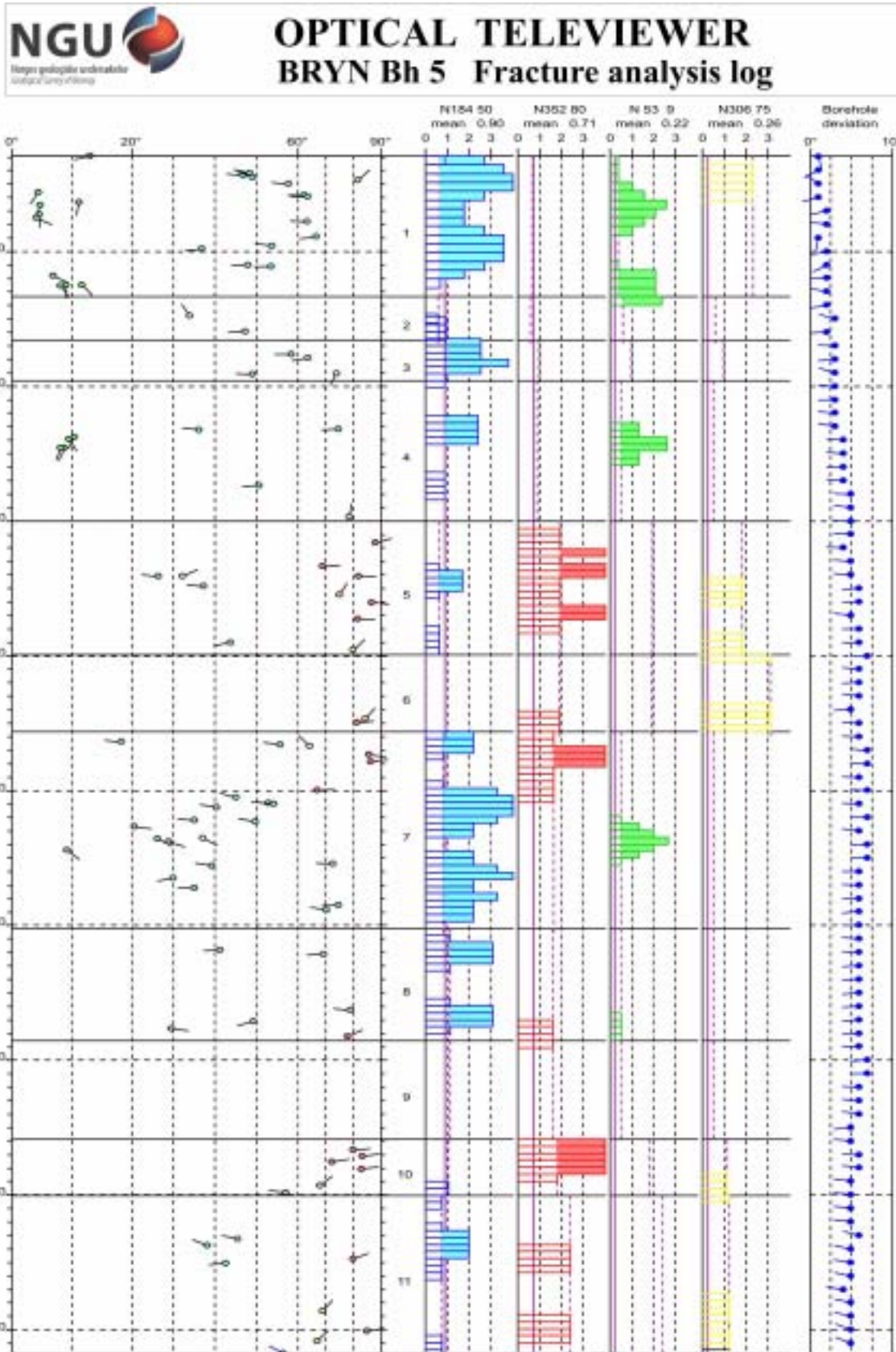
Figur 3–1: Frequency histogram for borehole 2 at Bryn.



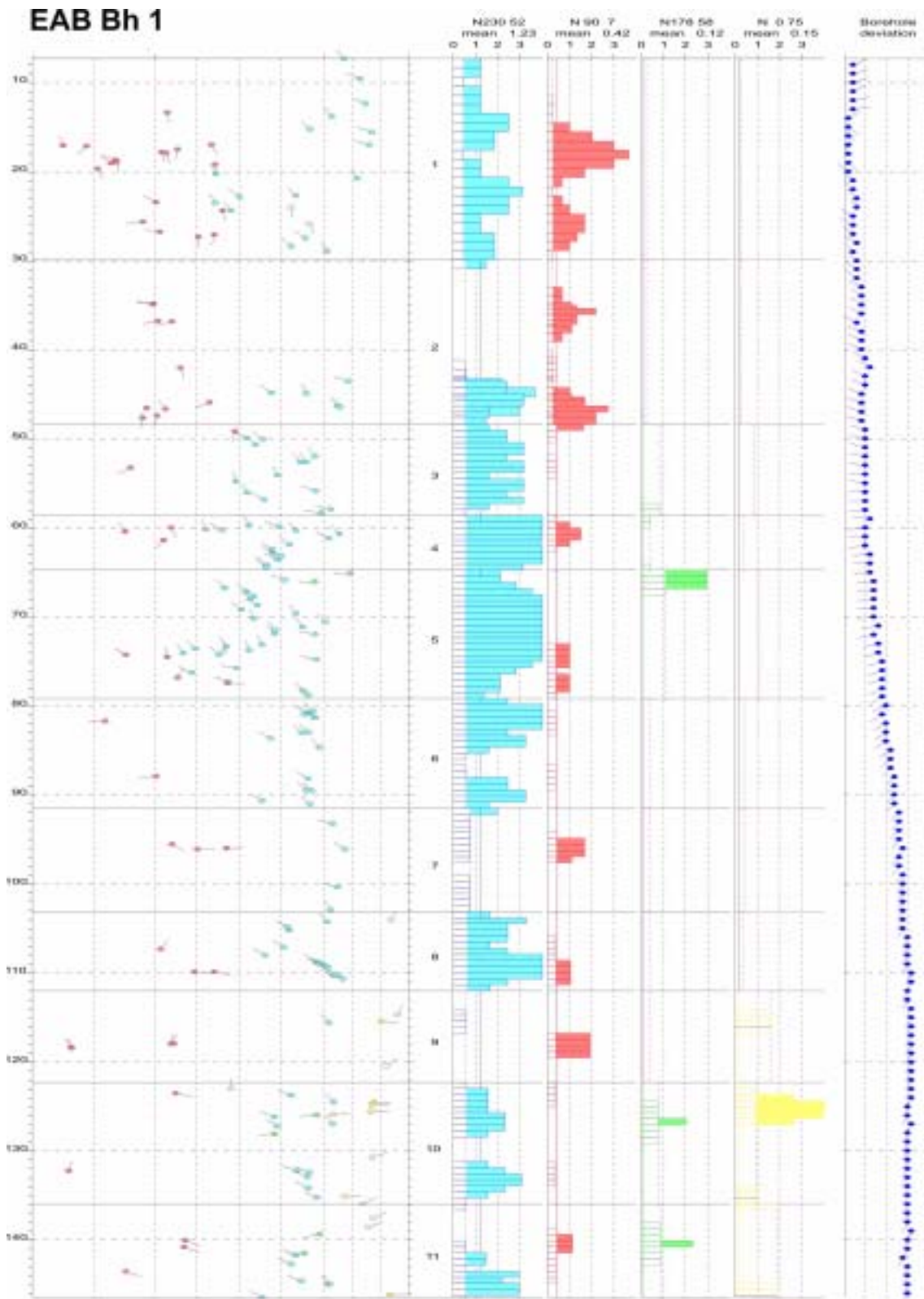
Figur 3–2: Frequency histogram for borehole 3 at Bryn.



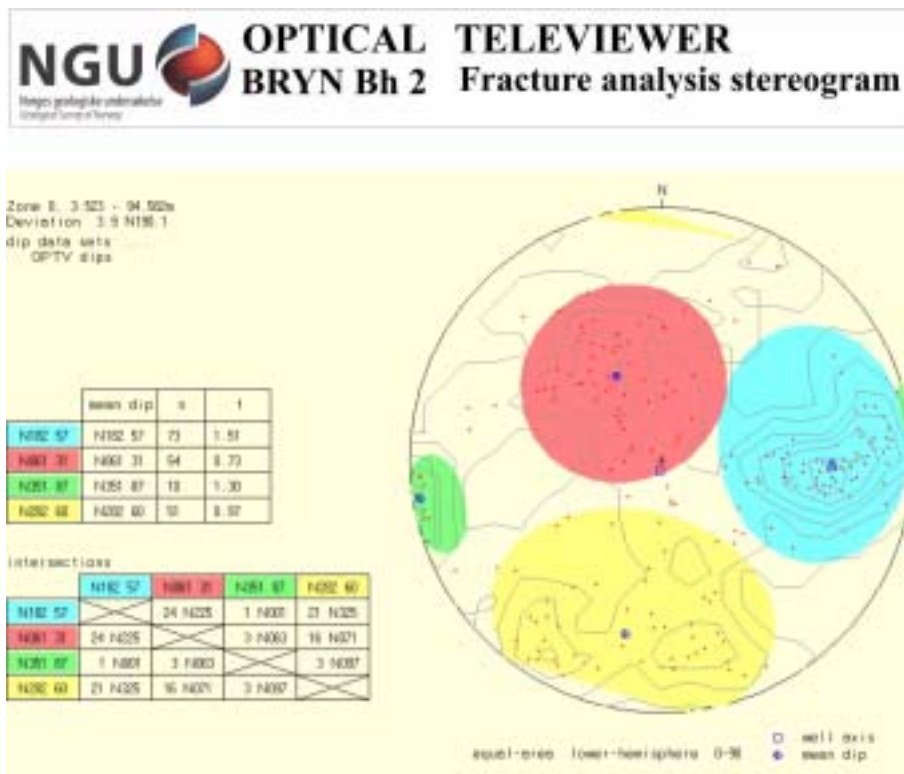
Figur 3-3: Frequency histogram for borehole 4 at Bryn.



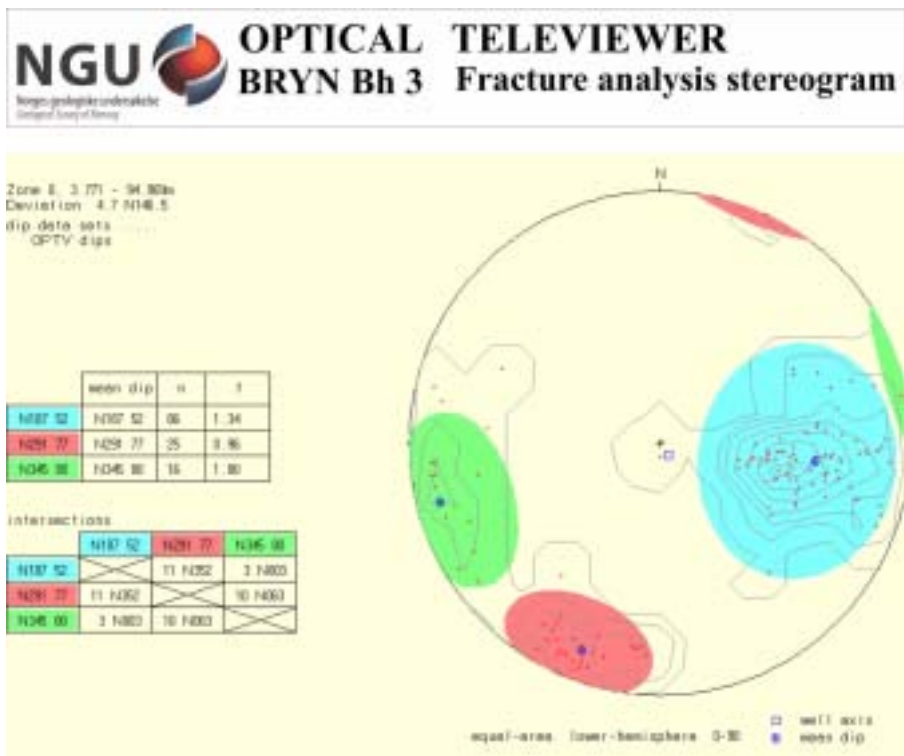
Figur 3-4: Frequency histogram for borehole 5 at Bryn.



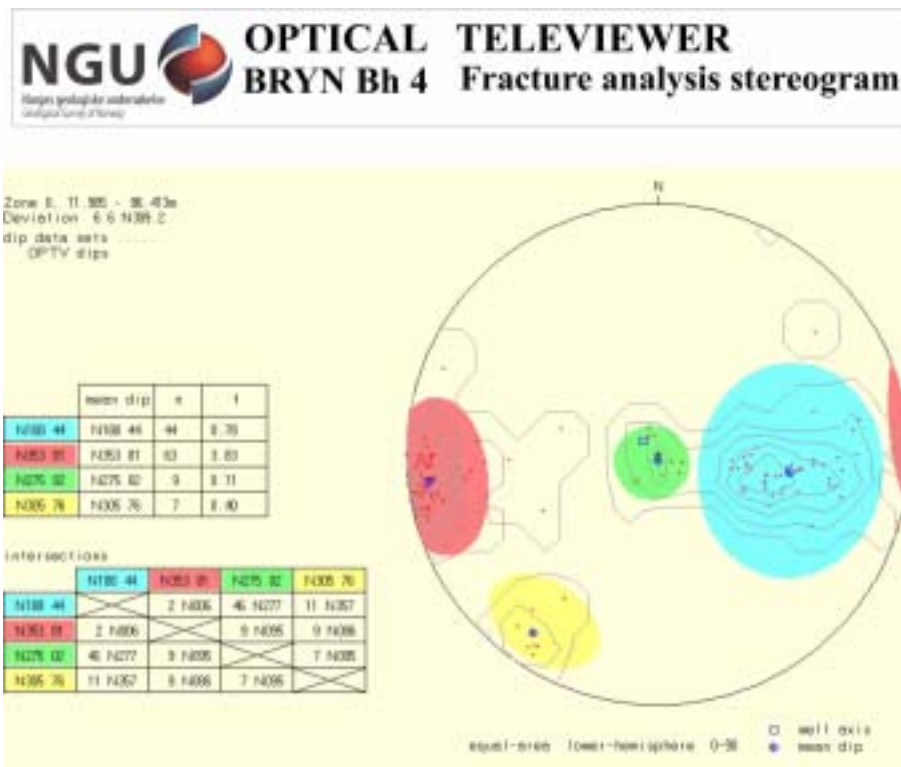
Figur 3-5: Frequency histogram for borehole 1 at EAB.



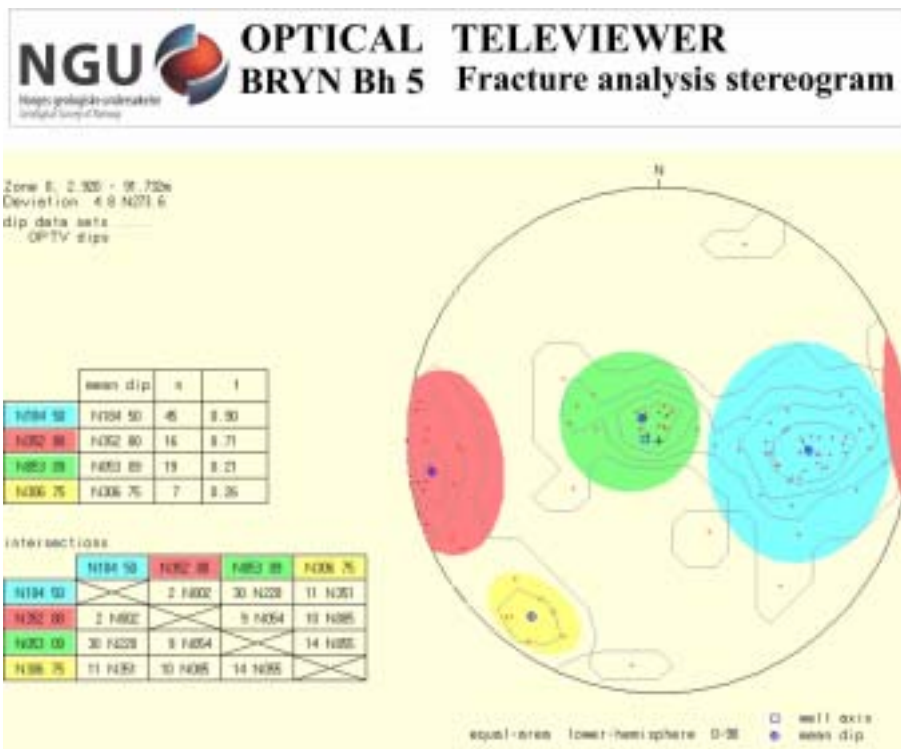
Figur 3-6: Fracture stereogram for borehole 2 at Bryn.



Figur 3-7: Fracture stereogram for borehole 3 at Bryn.



Figur 3–8: Fracture stereogram for borehole 4 at Bryn.



Figur 3–9: Fracture stereogram for borehole 5 at Bryn.

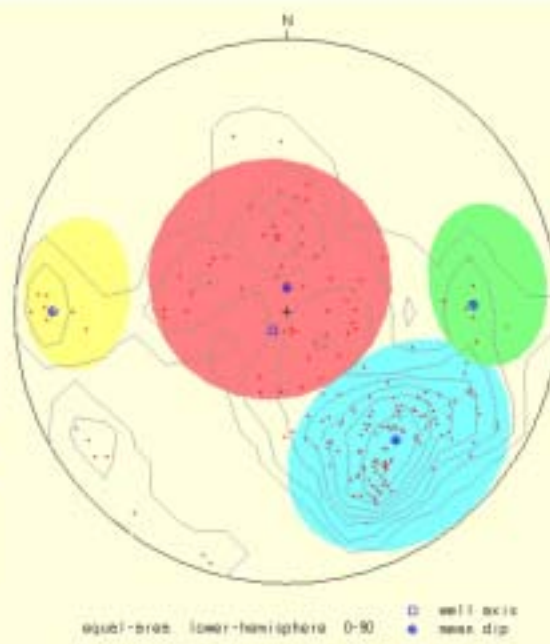
EAB Bh 1

EAB-BH
 Zone 0, 7.30 - 146.42m
 Deviation 7.4 N26.9
 dip data sets
 OPTV dips

	max dip	n	f
N230 52	N230 52	100	1.23
N090 07	N090 07	54	0.42
N176 58	N176 58	7	0.12
N000 75	N000 75	7	0.15

Intersections

	N230 52	N090 07	N176 58	N000 75
N230 52		25 N257	31 N281	8 N038
N090 07	25 N257		32 N236	15 N002
N176 58	31 N281	32 N236		8 N179
N000 75	8 N038	15 N002	8 N179	



Figur 3-10: Fracture stereogram for borehole 1 at EAB.